

Investigations into the Occurrence and Distribution of Bioturbation in
Tidally-Influenced Sedimentary Environments

by

Scott Melnyk

A thesis submitted in partial fulfillment of the requirements for the degree of
Doctor of Philosophy

Department of Earth and Atmospheric Sciences
University of Alberta

© Scott Melnyk, 2024

ABSTRACT

Tidally-influenced sedimentary environments are regions where sediment deposition is strongly influenced by the regular ebb and flow of tides. These natural processes result in distinctive and often heterogeneous patterns of sediment distribution and sedimentary structures, both physical and biological. This thesis explores the occurrence and distribution of bioturbation in these environments, with the aim of gaining a deeper understanding of the interplay between physico-chemical stressors and their impact on the ichnological record.

Chapter 1 provides a historical overview and a current analysis of the scientific field, offering essential background information for the subsequent sections of this thesis. The chapter covers the fundamental aspects of process ichnology and its relevance in the context of tidal systems. Furthermore, it explores how bioturbation distribution and intensity may be used in ichnological analysis to shed light on sedimentation dynamics and thereby paleoenvironmental conditions.

Chapter 2 demonstrates the usefulness of photogrammetry in constructing robust neoichnological datasets. Low-level drone photography allowed for the collection and analysis of visual and spatial data from photogrammetric reconstructions. This data was used to assess the relationship between shorebird track distributions and various environmental and ecological factors. The results show that the track record at each site represents a shorebird flock that traversed the tidal flats in such a way as to optimize foraging success. These findings provide context for interpretations of shorebird tracks in the rock record and illustrate the breadth of data that can be collected using photogrammetry.

Chapter 3 builds upon the techniques outlined in Chapter 2 to assess the distribution of infauna and their burrows at White Rock, British Columbia. Point counting

of burrow openings across intertidal dunes allowed the comparison of burrow distribution to elevation. A strong inverse relationship is observed, with burrows being considerably more abundant in the topographically-low interdune areas. This study shows that changes in burrow abundance can arise from local variations in pore water content and food availability, particularly in intertidal settings that experience minimal sedimentation rate or grain size variability.

Chapter 4 provides detailed documentation of a herring gull producing an unusual biodeformational structure that had not yet been reported along the west coast of North America. The resulting structure comprises a series of nested, concavo-convex sediment mounds and a terminal bowl-shaped impression. The aims of this chapter are to document the trace–tracemaker association, outline the sedimentological and ecological significance of the structure, and provide a means of comparison with similar structures.

Chapter 5 investigates the effectiveness of measuring the bioturbation intensity of a particular sedimentary deposit from bedding planes displaying vertical trace fossil assemblages (*i.e.*, piperock). Computer simulations are used to evaluate the variability associated with estimating bioturbation intensity from limited exposure. Subsequently, the results are compared to field data to evaluate the model's validity and applicability. These comparisons reveal a notable level of accuracy when attributing bioturbation intensities to piperock ichnofabrics based on bedding plane exposures.

Chapter 6 introduces a conceptual framework for the interpretation of inclined heterolithic stratification using the distribution of bioturbation at the bed scale. Core data from the Lower Cretaceous McMurray Formation was used to relate the presence of bioturbation to periods of increased marine influence. This data was used to demonstrate that in environments increasingly dominated by tides (e.g., estuaries), mud deposition is most associated with periods of elevated river discharge, while sand deposition and

redistribution is more prevalent during tidal dominance. These findings critically refine paleoenvironmental interpretations of fluvio-tidal settings that experience seasonal changes in fluvial discharge.

PREFACE

This thesis constitutes original research, a significant portion of which has been published in peer-reviewed journals. Valuable contributions were provided by the examining committee, co-authors, peer reviewers, and editors listed below.

Chapter 2 is published as: Melnyk, S., Cowper, A., Zonneveld, J-P. and Gingras, M.K., 2022. Applications of photogrammetry to neoichnological studies: The significance of shorebird trackway distributions at the Bay of Fundy. *Palaios*, 37(10), p. 606-621. M.K. Gingras, and J-P. Zonneveld and I conducted the required field work and provided interpretations. I collected, processed, and digitized the data with help from A. Cowper. I prepared the manuscript with input and edits from all authors. The manuscript was reviewed by Jon Noad and Matteo Belvedere and edited by Patrick John Orr.

Chapter 3 is currently in submission with *Sedimentology* as: Melnyk, S., Lazowski, C.N., Dashtgard, S.E., Gingras, M.K. Topographic controls on the occurrence and intensity of bioturbation in an intertidal sandflat. Field work was carried out by me, C.N. Lazowski, and M.K. Gingras. I was responsible for data processing and analysis, and developed the interpretations and prepared the manuscript with contributions from all co-authors.

Chapter 4 is published as: Melnyk, S., Lazowski, C.N. and Gingras, M.K., 2022. The sedimentological and ecological significance of an unusual biodeformational structure related to a feeding behavior in gulls (*Larus* sp.). *Ichnos*, 29(2), p. 84-92. All authors contributed to the field work, data collection, and interpretations presented in the manuscript. My role also included preparing the manuscript, with C.N. Lazowski and M.K. Gingras providing detailed revisions. The manuscript was subsequently reviewed by two anonymous reviewers and edited by L.A. Buatios.

Chapter 5 has been invited to be submitted to a Geological Society Special Publication entitled *Bedding Surfaces: True Substrates and Earth Historical Archives*

(editors: N.S. Davies and A.P. Shillito). Field work and data collection were conducted by me, B. Coutret, D. Brown. The computer simulations were performed by J.L. Kavanaugh. Conceptualization was improved through discussions with M.K. Gingras and J-P. Zonneveld.

Chapter 6 is published as: Melnyk, S. and Gingras, M.K., 2020. Using ichnological relationships to interpret heterolithic fabrics in fluvio-tidal settings. *Sedimentology*, 67(2), p. 1069-1083. I collected and analyzed the data, contributed to the interpretations, and composed the manuscript. M.K. Gingras contributed several aspects of the interpretations and provided detailed revisions. Radiographs were supplied by M.K. Gingras. The manuscript was reviewed by A.D. La Croix and F.J. Rodríguez-Tovar and edited by I. Kane.

Appendix 1 is published as: Melnyk, S., Packer, S., Zonneveld, J.P. and Gingras, M.K., 2020. A new marine woodground ichnotaxon from the Lower Cretaceous Mannville Group, Saskatchewan, Canada. *Journal of Paleontology* 95(1) 162-169. I envisaged the study based on a unique fossil specimen and prepared the manuscript. S. Packer performed the Computed Tomography scan analysis and assisted in the writing of related aspects of the Methods section. M.K. Gingras provided extant specimens which facilitated the interpretations. J-P. Zonneveld and M.K. Gingras provided expert input and edits throughout the writing process.

ACKNOWLEDGEMENTS

Thank you to Dr. Murray Gingras for teaching me that science is not solely about the pursuit of knowledge, but equally about humility, respect, and empathy. His belief in me as a young scientist gave me the courage to pursue a PhD, and I couldn't have asked for a more rewarding experience. I would also like to express my gratitude to the late Dr. George Pemberton for sparking my interest in sedimentology, Dr. John-Paul Zonneveld for being an exceptional scientific mentor, and Dr. Kurt Konhauser for his willingness to engage in lively banter over a pint.

I am fortunate to have met so many kind and intelligent people during my PhD: Scott B., Carolyn, Jared, Weiduo, Dan B., Skye, Dan S., Sara, Sheridan, Riley, Arzu, Stephen, Chundi, Anders, Kelly, Dani, Jiahui, and many others. Our shared moments in the office, lab, field, or pub have enriched my PhD experience, and for that I am grateful. Special thanks are owed to Cole Ross and Ryan Millar for countless hours of scientific discussion, Dr. Maya LaGrange and Brette Harris for their lab leadership and creating countless cherished memories, and Cody Lazowski for being a constant source of friendship and camaraderie since our undergrad days. I would also like to thank Dr. Qi Chen for being a gracious core-logging mentor, Dr. Logan Swaren for always making time for a morning coffee, Dr. Chenyang Feng for showing me the importance of boundless curiosity, and Drew Brown and Baptiste Coutret for their scientific enthusiasm that kept me motivated during the final stages of my PhD.

My sincere thanks go to my mother, Ruth, for instilling in me a sense of natural wonder and adventure, and to my father, Terry, for teaching me the value hard and honest work. These lessons form the bedrock of this thesis. Lastly, I would like to express my deepest appreciation to my loving wife, Melissa, whose selflessness has been an endless source of inspiration. I am forever enriched by her grace and presence in my life.

TABLE OF CONTENTS

Abstract.....	ii
Preface.....	v
Acknowledgements.....	vii
List of Tables.....	xii
List of Figures.....	xiii
Chapter 1 – Introduction.....	1
1.1 Sedimentological Significance of Bioturbation Intensity.....	4
1.2 Sedimentological Significance of Bioturbation Distribution.....	7
1.3 Research Objectives.....	9
1.4 References.....	10
Chapter 2 – Applications of Photogrammetry to Neoichnological Studies: The Significance of Shorebird Trackway Distributions at the Bay of Fundy.....	14
2.1 Introduction.....	14
2.2 Geological Setting.....	16
2.3 Methods and Materials.....	18
2.3.1 Photogrammetry.....	18
2.3.2 Assessing Substrate Cohesiveness.....	19
2.3.3 Statistical Analysis.....	20
2.4 Results.....	21
2.4.1 Site 1: Petitcodiac River.....	21
2.4.2 Site 2: Shepody River.....	30
2.4.3 Site 3: Selma.....	35
2.5 Discussion.....	40
2.5.1 The Influence of Substrate Cohesiveness on the Track Record.....	40
2.5.2 The Influence of Topography on Track Distribution.....	42
2.5.3 The Influence of Topography on Substrate Cohesiveness.....	42
2.5.4 The Influence of Food Distribution on Track Density.....	43
2.6 Summary.....	44
2.7 References.....	45
Chapter 3 – Topographic controls on the distribution of bioturbation in an intertidal sandflat.....	51
3.1 Introduction.....	51

3.2 Study Area	53
3.3 Methods.....	57
3.3.1 Radiography.....	57
3.3.2 Sediment Analysis.....	57
3.3.3 Photogrammetry	58
3.4 Results	60
3.4.1 Dune Characteristics and Bioturbation.....	60
3.4.2 Trace-Tracemaker Distribution	61
3.4.3 Pore Water and Organic Carbon.....	62
3.5 Topographic Controls on Intertidal Bioturbation	70
3.5.1 Shifting Substrates.....	70
3.5.2 Subaerial Exposure	71
3.5.3 Food Availability	73
3.6 Paleoenvironmental Implications	75
3.7 Summary.....	75
3.8 References.....	77
Chapter 4 – Sedimentological and Ecological Significance of a Biodeformational Structure Associated with an Unusual Feeding Behaviour in Gulls (<i>Larus</i> sp.).....	85
4.1 Introduction	85
4.2 Study Area	86
4.3 Methods.....	88
4.4 An Unusual Feeding Trace	89
4.5 Discussion	90
4.6 Summary.....	100
4.7 References.....	101
Chapter 5 – Drawing Interpretations of Bioturbation Intensity from Bedding Planes of Vertical Trace Fossil Assemblages	104
5.1 Introduction	104
5.2 Geological Context.....	105
5.3 Methods.....	108
5.3.1 Monte Carlo Methods	108
5.3.2 Field Methods.....	109
5.4 Results	109

5.4.1 Monte Carlo Results.....	109
5.4.2 Piperock Descriptions	110
5.5 Discussion	111
5.6 Summary.....	121
5.7 References.....	122
Chapter 6 – Using Ichnological Relationships to Interpret Heterolithic Fabrics in Fluvio-Tidal Settings.....	127
6.1 Introduction	127
6.2 Study Area and Dataset	129
6.3 Methods.....	132
6.4 Results	132
6.4.1 Sand-Dominated IHS with Bioturbated Siltstone	136
6.4.2 Mud-Dominated IHS with Bioturbated Sandstone	139
6.5 Interpretation and Discussion	143
6.5.1 Fabric A Interpretation	143
6.5.2 Fabric B Interpretation	144
6.5.3 Depositional Setting.....	146
6.5.4 Refinement of the Sedimentary Environment	147
6.6 Summary.....	153
6.7 References.....	154
Chapter 7 – Conclusions.....	160
7.1 Contributions to Process Ichnology	160
7.2 Research Horizons.....	161
7.3 References.....	164
Bibliography	167
Appendix 1 – A New marine woodground ichnotaxon from the lower cretaceous manville group, saskatchewan, canada.....	190
S1.1 Introduction	190
S1.2 Geologic Setting.....	191
S1.3 Materials and Methods	191
S1.3.1 Specimens.....	191
S1.3.2 Computed Tomography.....	193
S1.3.3 Institutional Abbreviations	195

S1.4 Systematic Ichnology	196
S1.5 Discussion.....	199
S1.6 Summary	203
S1.7 References	204
Appendix 2 – Supplemental Material for Chapter 6.....	211

LIST OF TABLES

Table 2.1. Overview of the physical characteristics and trackways at each site.	22
Table 2.2. Summary of the proportion of substrate types and their effect on shorebird track distributions at each site.	26
Table 2.3. Relationship between nereid burrow density and elevation.	40
Table 3.1. Key features of the examined dunes within 5-meter wide transects perpendicular to the dune crests.	63
Table 3.2. Summary of pore water content and organic matter content from various stations across the study area	69
Table 5.1. Summary of Monte Carlo results for examined Plan View Bioturbation Intensities.	113
Table 5.2. Description of the sedimentological and ichnological characteristics of each piperock ichnofabric.	116
Table 6.1. Summary of studied well bore locations.	135
Table 6.2. Summary of results for fabrics A and B.	137
Table 6.3. List of occurrences for each endmember fabric.	138
Table 6.4. Summary of interpretations for fabrics A and B.	141
Table S1.1. Summary of formally recognized woodground ichnospecies.	202

LIST OF FIGURES

Figure 1.1. Schematic diagram depicting the loosely defined relationship between depositional energy and the preservation of bioturbation	3
Figure 1.2. Plot illustrating the time required for different population densities of suspension feeders and deposit feeders to rework a specific volume of sediment.....	6
Figure 1.3. Schematic representation of the bioturbation distributions that arise from different sedimentation regimes	8
Figure 2.1. Overview of the study area, Bay of Fundy	17
Figure 2.2. Overview of the study sites, Bay of Fundy	18
Figure 2.3. Incumbent anisodactyl shorebird tracks emplaced in the different substrate types at Site 1	23
Figure 2.4. Palmate shorebird tracks emplaced in the different substrate types at Site 2.	24
Figure 2.5. Semipalmate tridactyl shorebird tracks emplaced in the different substrate types at Site 3	25
Figure 2.6. Orthomosaic of Site 1 illustrating the distribution of shorebird tracks	27
Figure 2.7. Elevation and orientation data for Site 1	28
Figure 2.8. Substrate data for Site 1	29
Figure 2.9. Orthomosaic of Site 2 illustrating the distribution of shorebird tracks.	32
Figure 2.10. Elevation and orientation data for Site 2.....	33
Figure 2.11. Substrate data for Site 2	34
Figure 2.12. Orthomosaic of Site 3 illustrating the distribution of shorebird tracks and nereid polychaete burrows	37
Figure 2.13. Elevation and orientation data for Site 3.....	38
Figure 2.14. Substrate data for Site 3	39
Figure 3.1. Overview of the study area.....	54

Figure 3.2. Historical imagery from Google Earth depicting migration patterns through time of the landward dune.....	55
Figure 3.3. Historical imagery from Google Earth depicting the migration patterns through time of the seaward dune	56
Figure 3.4. Grain size distributions acquired through sieving	63
Figure 3.5. Orthographic projections of the landward dune and seaward dune transects showing the variation in surface features along the dune profiles.....	64
Figure 3.6. Assessment of burrow abundance along the cross-sectional profile of the landward dune	65
Figure 3.7. Assessment of burrow abundance along the cross-sectional profile of the seaward dune	66
Figure 3.8. X-ray radiographs and schematic interpretations of sediment cores from the landward end of East Beach	67
Figure 3.9. A) Box-and-whisker plot showing the estimated percentage of void filled by pore water for dune crest versus interdune sediment samples. B) Plot illustrating the correlation between pore water and organic matter content in surficial sediment samples collected from various stations within the study area.....	68
Figure 4.1. Geographic location of the study area at White Rock, East Beach, with an inset showing the site of observation (49°0'35.22"N; 122°46'55.06"W).	87
Figure 4.2. Photos of the <i>Larus</i> sp. tracemaker and resulting biodeformational structure.	91
Figure 4.3. Varnish clam (<i>Nuttallia obscurata</i>) collected from directly below the examined biodeformational structure.....	92
Figure 4.4. Additional examples of the <i>Larus</i> sp. feeding trace from White Rock Beach.	93
Figure 4.5. Drone image of a cluster of <i>Larus</i> sp. feeding traces near the margin of standing water.....	94
Figure 4.6. Accumulation of organic material in a trough between sediment mounds of the examined biodeformational structure	94

Figure 4.7. Illustration of the foraging technique employed by <i>Larus</i> sp. and a schematic interpretation of the cross-sectional view of the resulting biodeformational structure. .	97
Figure 4.8. Examples of incipient <i>Piscichnus</i>	98
Figure 4.9. Unusual sedimentary structures produced by foraging shorebirds	99
Figure 5.1. Schematic stratigraphic column and geologic map of the study area.....	107
Figure 5.2. Two-dimensional representations of the models for each plan view bioturbation intensity (PVBI).....	114
Figure 5.3. Summary of the seven probability distributions of Elevation View Bioturbation Intensity (EVBI) for each Plane View Bioturbation Intensity (PVBI).....	115
Figure 5.4. Photographs of both plan and elevation views of piperocks 1 to 6 (left) and their corresponding interpreted bioturbation intensity as depicted by the black polygons (right).....	117
Figure 5.5. Outcrop occurrence of Piperock 7.....	118
Figure 5.6. Interpretations of two-dimensional bioturbation intensity for Piperock 7....	119
Figure 5.7. Plot showing a strong correlation between plan view and elevation view bioturbation intensities for all examined piperock.....	120
Figure 6.1. (A) Map of Alberta, Canada, outlining the distribution of oil sands deposits. (B) Location of the 24 cores logged for this study. (C) Schematic stratigraphy of the study area.....	131
Figure 6.2. Examples of Fabric A from various core.....	140
Figure 6.3. Examples of Fabric B from various core.....	142
Figure 6.4. Schematic distribution of sediments in a tide-dominated estuary as a function of fluvial flux	145
Figure 6.5. Comparison of suspended load concentration in estuary <i>versus</i> delta settings as a function of river discharge.....	150
Figure 6.6. Modern examples bioturbated IHS.....	151
Figure 6.7. Location map for examples from (A) the Fraser River and (B) Willapa Bay.	152

Figure S1.1. Stratigraphic occurrence of the holotype and hypodigm of <i>Apectoichnus lignummasticans</i> in west-central Saskatchewan, Canada, from well-bore 16-15-44-20W3M. 52°47'45.0"N, 108°48'55.6"W	192
Figure S1.2. <i>Apectoichnus lignummasticans</i> assemblage in fossil wood.....	194
Figure S1.3. Micro-CT images of UAI080	195
Figure S1.4. Extant <i>Limnoria lignorum</i> borings. Scale bars = 1 cm.....	201
Figure S2.1. Legend of symbols used in figures S2.2 to S2.25.....	211
Figure S2.2. Litholog for UWI AA-03-14-092-08W4.....	212
Figure S2.3. Litholog for UWI AA-03-25-092-08W4.....	213
Figure S2.4. Litholog for UWI AA-04-06-092-08W4.....	214
Figure S2.5. Litholog for UWI AA-04-34-092-08W4.....	215
Figure S2.6. Litholog for UWI AA-05-13-092-08W4.....	216
Figure S2.7. Litholog for UWI AA-06-10-092-08W4.....	217
Figure S2.8. Litholog for UWI AA-07-24-092-08W4.....	218
Figure S2.9. Litholog for UWI AA-07-27-092-08W4.....	219
Figure S2.10. Litholog for UWI AA-10-15-092-08W4.....	220
Figure S2.11. Litholog for UWI AA-10-22-092-08W4.....	221
Figure S2.12. Litholog for UWI AA-10-23-092-08W4.....	222
Figure S2.13. Litholog for UWI AA-10-35-092-08W4.....	223
Figure S2.14. Litholog for UWI AA-10-36-092-08W4.....	224
Figure S2.15. Litholog for UWI AA-11-03-092-08W4.....	225
Figure S2.16. Litholog for UWI AA-11-04-092-08W4.....	226
Figure S2.17. Litholog for UWI AA-11-33-092-08W4.....	227
Figure S2.18. Litholog for UWI AA-12-11-092-08W4.....	228
Figure S2.19. Litholog for UWI AA-12-12-092-08W4.....	229
Figure S2.20. Litholog for UWI AA-12-30-092-08W4.....	230

Figure S2.21. Litholog for UWI AA-13-02-092-08W4.....	231
Figure S2.22. Litholog for UW AA-15-09-092-08W4.....	232
Figure S2.23. Litholog for UWI AA-16-16-092-08W4.....	233
Figure S2.24. Litholog for UWI AA-16-19-092-08W4.....	234
Figure S2.25. Litholog for UWI AA-16-21-092-08W4.....	235

CHAPTER 1 – INTRODUCTION

Bioturbation, which refers to any form of disturbance of sediment and soil caused by biological activities, is crucial for understanding sedimentary environments and their ecological contexts. The interactions between burrowing organisms and their surroundings are influenced primarily by physico-chemical stresses related to salinity, oxygen, food, sedimentation, and substrate consistency. An important application of ichnology relies on constraining these parameters by using a process ichnological framework within which the magnitude of these stressors can be constrained (Gingras et al., 2011). To that end, this thesis examines how bioturbation intensity and distribution can be used to infer local changes in substrate consistency and the relative rates of sediment deposition.

The influence of substrate consistency on the character and distribution of bioturbation is well-recognized. This relationship has led to the development of substrate-controlled ichnofacies, which are theoretical models that represent recurring spatial and temporal patterns of ethological assemblages of biogenic sedimentary structures, reflecting specific environmental settings (Seilacher, 1964; MacEachern et al., 2007). While much research has focused on semi-consolidated firmgrounds and their association with the *Glossifungites* ichnofacies (e.g., Pemberton and Frey, 1984; Gingras et al., 2000, 2001; Abdel-Fattah et al., 2016), local variations in substrate consistency that arise from subtle differences in sediment texture or pore water content are less understood.

Sedimentation rate has also long been recognized for its marked influence on bioturbation distributions within sediment layers (van Straaten, 1954; Moore and Scruton, 1957; Schäfer, 1962; Reineck, 1963, 1967; Rhoads, 1967). This is based on the concept of

the colonization window and posits an inverse relationship between sedimentation rate and bioturbation intensity (Wheatcroft, 1990) (Figure 1.1). Heightened sedimentation rates and/or shifting substrates reduce the time available for infauna to rework the sediment, thereby precluding bioturbation in environments that would otherwise support infaunal activity.

Despite the importance of neoichnological investigations in informing paleoenvironmental interpretations, the methods employed in these studies have undergone only incremental changes since the 1960s. The emergence and affordable use of drone technology represent a significant leap forward in enhancing both empirical and numerical data. Chapter 2 demonstrates this progress by showcasing innovative techniques to assess local variations substrate consistency and other environmental factors on an intertidal flat.

Intertidal settings exhibit heterogeneous bioturbation distributions owing to the spatio-temporal variability of these settings and the resulting effects on different physical and chemical stressors (Swinbanks and Murray, 1981). While sedimentation rate is often cited as a key factor (Dashtgard, 2011; Yang et al., 2009), a detailed analysis of local-scale burrow distributions is lacking. Chapter 3 explores the impact that topography has on bioturbation in an intertidal sandflat, considering factors such as shifting substrates, subaerial exposure, and food availability.

The distribution of infaunal bioturbation in intertidal settings in turn plays a key role in determining the distribution of shorebird traces. This is because shorebirds rely on infaunal food sources, and sometimes exploit the inability of infaunae to escape predators in liquefied sediment. This foraging technique is utilized by herring gulls, which employ paddling to liquefy sand substrates. Chapter 4 offers an in-depth exploration of the relationship between these traces and their makers, extending the documented

occurrences of such interactions to the western coast of North America (Müller, 1985; Cadee, 1990; Gregory et al., 1999).

Existing methods for estimating bioturbation intensity from bedding planes (Miller and Smail, 1997; Marenco and Bottjer, 2010) are much less developed than their cross-sectional counterparts (Droser and Bottjer, 1986; Taylor and Goldring, 1993). For the bioturbation intensity of both perspectives to be interpreted within a single framework, the relationship between these two approaches must be interrogated. Chapter 5 takes steps towards this goal, using Monte Carlo simulations and outcrops of the Lower Cambrian Gog Group to demonstrate the relationship between bioturbation intensity observed on bedding planes and in elevation view.

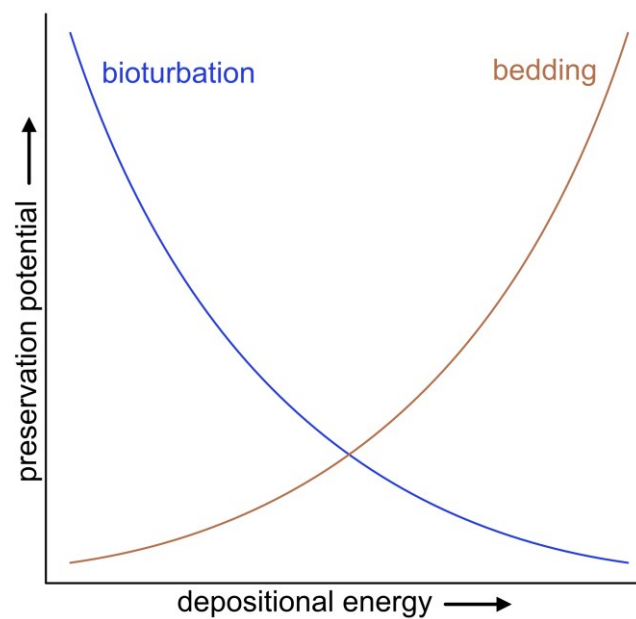


Figure 1.1. Schematic diagram depicting the loosely defined relationship between depositional energy and the preservation of bioturbation, showing that higher depositional energies tend to favor the preservation of primary physical bedding over bioturbation.

Interpretations of Inclined Heterolithic Stratification (IHS) in fluvio-tidal environments have remained largely unchanged since they were formally recognized in Thomas et al. (1987). As such, bioturbation distributions in IHS have generally been ignored when interpreting paleogeographic aspects of fluvio-tidal settings. This gap is addressed in Chapter 6, wherein a conceptual framework is proposed to relate the distribution of bioturbation to paleogeographic position within the fluvio-tidal zones of estuaries and deltas. The framework is underpinned by the notion that infaunal colonization and thereby bioturbation distribution is controlled by brackish-water colonization windows that are influenced by seasonal variations in river discharge.

1.1 Sedimentological Significance of Bioturbation Intensity

The occurrence and intensity of bioturbation has been used in a variety of ways to assess the rate, frequency, and magnitude of erosional and depositional processes (e.g., Reineck et al., 1967; Howard, 1978; Goldring, 1962, 1964; Wetzel and Aigner, 1986). However, it remains challenging to precisely determine the timescales associated with these events. Wheatcroft (1990) built a model relating transit time (time required to bury an event bed past the reach of burrowing fauna) to dissipation time (time required to rework the entire event bed) (Equation 1). Earlier modeling efforts defined transit time simply as the thickness of the mixing zone divided by sedimentation rate, whereas Wheatcroft (1990) emphasized the importance of event bed thickness by defining transit time as:

$$T_m = [L_b - L_s/2]/w \quad (\text{Equation 1})$$

where L_b = the thickness of the biogenic mixing zone; L_s = the thickness of the event layer; and w = sedimentation rate. Dissipation time, on the other hand, is difficult to assess because it depends on a myriad of factors, both biological (e.g., population density, animal size, ethology) and environmental (e.g., food distribution, substrate cohesiveness, lithologic contrast between layers, time available for colonization).

Ethology plays a crucial role in determining the rate at which invertebrates burrow (Thayer 1979; 1983). Indeed, infaunal composition plays a more significant role than infaunal density when determining bioturbation intensity (Rhoads, 1967). Mobile-deposit feeders (“bulldozers”) are much more efficient at mixing sediment than tube dwellers that construct and maintain a single burrow throughout their life cycle. Using X-ray analysis of thin-walled aquaria, Gingras et al. (2008) found that suspension feeders exhibited volumetric burrowing rates of 0.01 to 0.15 $\text{cm}^3 \text{h}^{-1}$, whereas deposit feeders burrowed at a rate of 1 to 10 $\text{cm}^3 \text{h}^{-1}$. Dafoe et al. (2008) showed that deposit-feeding opheliid polychaetes were capable of reworking aquaria sediment at a rate of 1.77 $\text{cm}^3 \text{h}^{-1}$ per adult. These studies culminated in a matrix for estimating the rate at which different ethological groupings rework a certain volume of sediment (Figure 1.2). These findings suggest time scales of several months to years to produce bioturbated media. Similar timescales have been estimated in studies framed in a more oceanographic context (e.g., Bentley et al 2006).

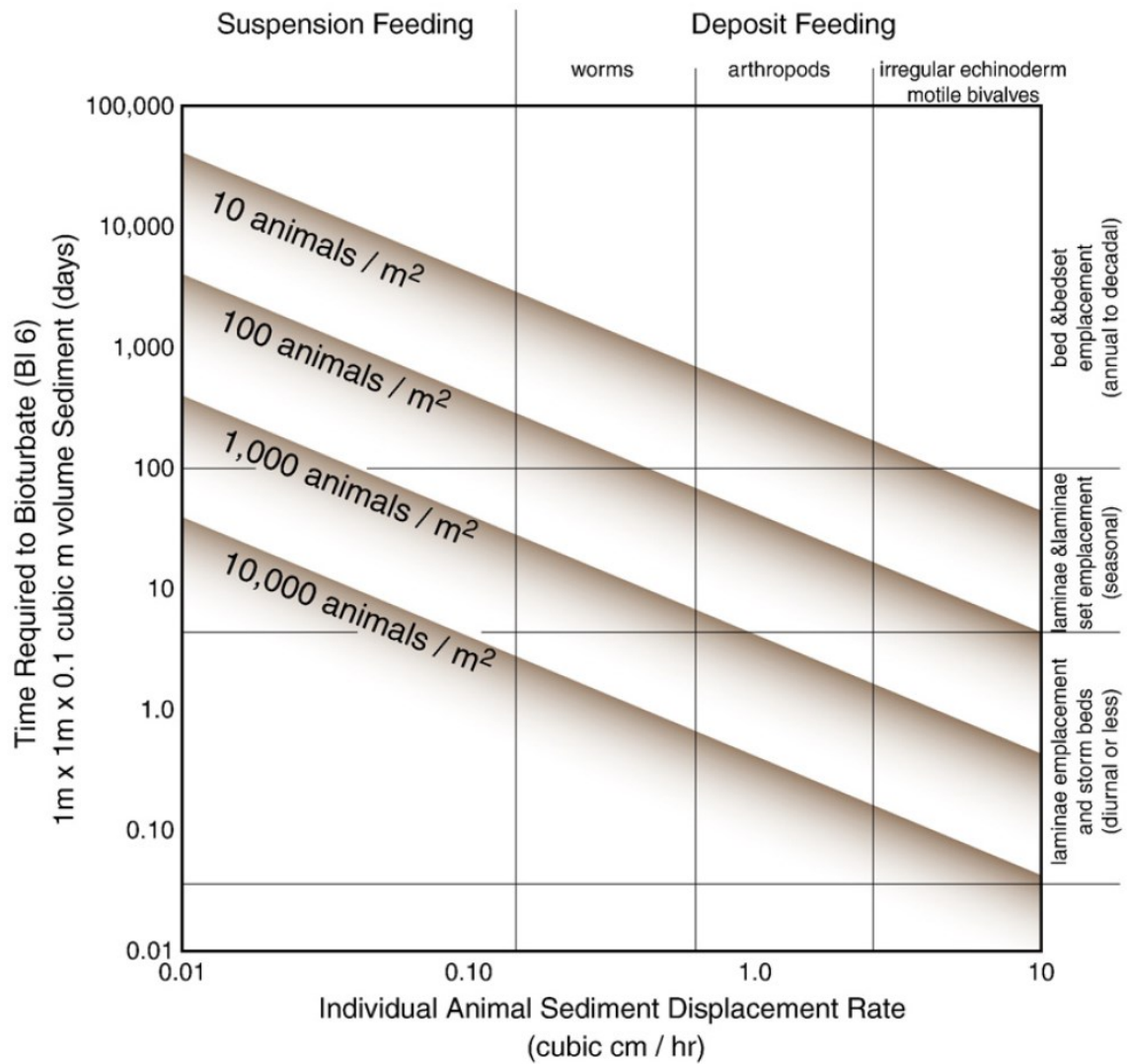


Figure 1.2. Plot illustrating the time required for different population densities of suspension feeders and deposit feeders to rework a specific volume of sediment. Taken from Gingras et al. (2008, 2011).

1.2 Sedimentological Significance of Bioturbation Distribution

Interpretations of past depositional conditions are improved by assessments of vertical changes in bioturbation intensity and the delineation of omission surfaces indicated by burrow truncations (Bromley, 1975; Howard et al., 1978; Gingras et al., 2011). Careful analysis of bioturbation patterns can therefore significantly enhance the recognition of common sedimentation regimes in the rock record (Figure 1.3). For example, in settings where dissipation time exceeds transit time, the sedimentary layers generally exhibit complete and homogeneous bioturbation (Wheatcroft, 1990) (Figure 1.3A). Such conditions are found in areas dominated by pelagic settling, as well as those characterized by sedimentary stasis punctuated by infrequent deposition of thin sediment layers. Conversely, in settings where sedimentation is predominantly driven by episodic events, bioturbation is typically not preserved or reflects escape or equilibrium behaviour. Following deposition, renewed infaunal colonization may lead to the emplacement of burrows in the upper part of the event bed (Figure 1.3B). Consequently, in environments with recurring alternations of erosion and deposition, bioturbation tends to be sporadically distributed and generally increases upwards within event beds that are bounded by erosive contacts (Gingras et al., 2011) (Figure 1.3C).

In the absence of significant erosional processes, alternations between event-style deposition and fairweather sedimentation result in the development of heterolithic stratification. These conditions arise from periodic changes in the influence of rivers, waves, or tides, and are thus linked to a wide range of depositional environments. In cases where both lithosomes exhibit bioturbation, it can be inferred that the time between the deposition of each was sufficient to allow infaunal colonization (Figure 1.3D). Differences

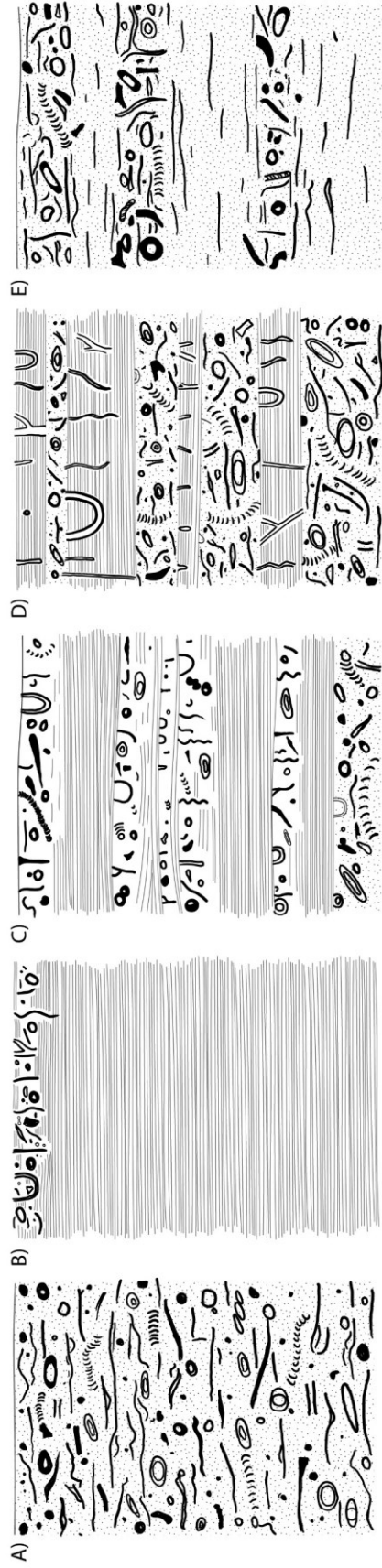


Figure 1.3. Schematic representation of the bioturbation distributions that arise from different sedimentation regimes. Originally drafted by Howard et al. (1978).

in trace fossil types between lithosomes reflect infaunal sensitivity to grain size variations (Howard, 1978). Should either lithosome lack bioturbation, it may be inferred that deposition either occurred too rapidly or was concomitant with additional environmental stressors, such as salinity fluctuations or diminished oxygen levels. Settings characterized by truly cyclic deposition often exhibit a regular heterogeneous burrow distribution (Gingras et al., 2011) (Figure 1.3E). This is most common in areas that experience seasonal fluctuations in river discharge as well as settings that are strongly influenced by tidal periodicities. These dynamics give rise to a pattern of alternating depositional states that place temporal constraints infaunal colonization.

1.3 Research Objectives

In this thesis, neoichnological and paleoichnological investigations are combined to explore the significance of bioturbation in tidally-influenced sedimentary environments. The selection of these environments was based primarily on their high infaunal biomass, spatio-temporal variability, and accessibility. The aim of these studies is to enhance our understanding of the factors that affect bioturbation intensity and distribution within the rock record, offering insights that can refine interpretations of ancient environments.

1.4 References

- Abdel-Fattah, Z. A., Gingras, M. K., Caldwell, M. W., Pemberton, S. G., & MacEachern, J. A. (2016). The *Glossifungites* ichnofacies and sequence stratigraphic analysis: A case study from Middle to Upper Eocene successions in Fayum, Egypt. *Ichnos*, *23*, 157–179.
- Bentley, S. J., Sheremet, A., & Jaeger, J. M. (2006). Event sedimentation, bioturbation, and preserved sedimentary fabric: Field and model comparisons in three contrasting marine settings. *Continental Shelf Research*, *26*, 2108–2124.
- Cadée, G. C. (1990). Feeding traces and bioturbation by birds on a tidal flat, Dutch Wadden Sea. *Ichnos*, *1*, 23–30.
- Dafoe, L. T., Gingras, M. K., & Pemberton, S. G. (2008). Determining *Euzonus mucronata* burrowing rates with application to ancient *Macaronichnus segregatis* trace-makers. *Ichnos*, *15*, 78–90.
- Dashtgard, S. E. (2011). Linking invertebrate burrow distributions (neoichnology) to physicochemical stresses on a sandy tidal flat: Implications for the rock record: Tidal-flat ichnology. *Sedimentology*, *58*, 1303–1325.
- Droser, M. L., & Bottjer, D. J. (1986). A semiquantitative field classification of ichnofabric. *Journal of Sedimentary Research*, *56*, 558–559.
- Gingras, M. K., George Pemberton, S., & Saunders, T. (2001). Bathymetry, sediment texture, and substrate cohesiveness; their impact on modern *Glossifungites* trace assemblages at Willapa Bay, Washington. *Palaeogeography, Palaeoclimatology, Palaeoecology*, *169*, 1–21.
- Gingras, M. K., MacEachern, J. A., & Dashtgard, S. E. (2011). Process ichnology and the

- elucidation of physico-chemical stress. *Sedimentary Geology*, 237, 115–134.
- Gingras, M. K., Pemberton, S. G., Dashtgard, S., & Dafoe, L. (2008). How fast do marine invertebrates burrow? *Palaeogeography, Palaeoclimatology, Palaeoecology*, 270, 280–286.
- Gingras, M. K., Pemberton, S. G., & Saunders, T. (2000). Firmness profiles associated with tidal-creek deposits: The temporal significance of *Glossifungites* assemblages. *Journal of Sedimentary Research*, 70, 1017–1025.
- Goldring, R. (1964). Trace-Fossils and the Sedimentary Surface in Shallow-Water Marine Sediments. In L. M. J. U. van Straaten (Ed.), *Developments in Sedimentology* (pp. 136–143). Elsevier.
- Goldring, Roland. (1962). The trace fossils of the Baggy Beds (Upper Devonian) of North Devon, England. *Paläontologische Zeitschrift*, 36, 232–251.
- Gregory, M. R. (1999). Unusual “paddling” trails left by gulls and “aviturbation” in Rarawa and Mangawhai Estuaries, Northland, New Zealand. *New Zealand Natural Sciences*, 24, 27–34.
- Howard, J. D. (1975). The sedimentological significance of trace fossils. In R. W. Frey (Ed.), *The Study of Trace Fossils: A Synthesis of Principles, Problems, and Procedures in Ichnology* (pp. 131–146). Berlin, Heidelberg: Springer.
- Howard, J. D. (1978). Sedimentology and Trace Fossils. *SEPM Trace Fossil Concepts*.
- MacEachern, J. A., Bann, K. L., Pemberton, S. G., & Gingras, M. K. (2007). The Ichnofacies Paradigm: High-Resolution Paleoenvironmental Interpretation of the Rock Record. In J. A. MacEachern, K. L. Bann, M. K. Gingras, & S. G. Pemberton (Eds.), *Applied Ichnology* (Vol. 52). SEPM Society for Sedimentary Geology.
- Marenco, K. N., & Bottjer, D. J. (2010). The intersection grid technique for quantifying the extent of bioturbation on bedding planes. *Palaios*, 25, 457–462.

- Miller, M. F., & Smail, S. E. (1997). A semiquantitative field method for evaluating bioturbation on bedding planes. *PALAIOS*, 12, 391–396.
- Moore, D. G., & Scruton, P. C. (1957). Minor internal structures of some recent unconsolidated sediments. *Bulletin of the American Association of Petroleum Geologists*, 41, 2723–2751.
- Müller, A. H. (1985). *Rhizocorallium*-artige lebensspuren (ichnia) vom litoral der Ostsee. *Freiberger Forschungshefte*, 400, 77–79.
- Pemberton, S. G., & Frey, R. W. (1984). The *Glossifungites* Ichnofacies: Modern Examples from The Georgia Coast, U. S. A. *Special Publications of SEPM*.
- Reineck, H.-E. (1963). Sedimentgefüge im Bereich der südlichen Nordsee. *Abhandlungen der senckenbergische naturforschende Gesellschaft*, 505, 1–138.
- Reineck, H.-E. (1967). Parameter von Schichtung und Bioturbation. *Geologische Rundschau*, 56, 420–438.
- Rhoads, D. C. (1967). Biogenic reworking of intertidal and subtidal sediments in Barnstable Harbor and Buzzards Bay, Massachusetts. *The Journal of Geology*, 75, 461–476.
- Schafer, W. (1962). *Aktuo-Palaontologie nach Studien in der Nordsee*. Frankfurt am Main: Kramer.
- Seilacher, A. (1964). Biogenic sedimentary structures. *Approaches to Paleoecology*, 296–316.
- Swinbanks, D. D., & Murray, J. W. (1981). Biosedimentological zonation of Boundary Bay tidal flats, Fraser River Delta, British Columbia. *Sedimentology*, 28, 201–237.
- Taylor, A. M., & Goldring, R. (1993). Description and analysis of bioturbation and ichnofabric. *Journal of the Geological Society*, 150, 141–148.
- Thayer, C. W. (1979). Biological bulldozers and the evolution of marine benthic

- communities. *Science*, *203*, 458–461.
- Thayer, Charles W. (1983). Sediment-mediated biological disturbance and the evolution of marine benthos. In M. J. S. Tevesz & P. L. McCall (Eds.), *Biotic Interactions in Recent and Fossil Benthic Communities* (pp. 479–625). Boston, MA: Springer US.
- Thomas, R. G., Smith, D. G., Wood, J. M., Visser, J., Calverley-Range, E. A., & Koster, E. H. (1987). Inclined heterolithic stratification—Terminology, description, interpretation and significance. *Sedimentary Geology*, *53*, 123–179.
- van Straaten, L. M. J. U. (1954). Composition and structure of recent marine sediments in the Netherlands. *Leidse Geologische Mededelingen*, *19*, 1–108.
- Wetzel, A., & Aigner, T. (1986). Stratigraphic completeness: Tiered trace fossils provide a measuring stick. *Geology*, *14*, 234–237.
- Wheatcroft, R. A. (1990). Preservation potential of sedimentary event layers. *Geology*, *18*, 843–845.
- Yang, B., Dalrymple, R. W., Gingras, M. K., & Pemberton, S. G. (2009). Autogenic occurrence of *Glossifungites Ichnofacies*: Examples from wave-dominated, macrotidal flats, southwestern coast of Korea. *Marine Geology*, *260*, 1–5.

CHAPTER 2 – APPLICATIONS OF PHOTOGRAMMETRY TO NEOICHOLOGICAL STUDIES: THE SIGNIFICANCE OF SHOREBIRD TRACKWAY DISTRIBUTIONS AT THE BAY OF FUNDY

2.1 Introduction

Vertebrate tracks potentially contain information about the trackmaker's behaviour and environmental conditions at the time of emplacement (Lockley, 1986). Sources of morphological variation include the anatomy and behaviour of the trackmaker, the substrate conditions during emplacement, and post-emplacement processes (Cohen et al., 1991; Milàn and Bromley, 2007; Marty et al., 2009; Scott et al., 2010; Falkingham, 2014; Zonneveld, 2016; Marchetti et al., 2019). As such, for anatomically similar vertebrates exhibiting similar behaviours, variations in track morphology are most commonly associated with differences in substrate conditions (Padian and Olsen, 1984; Brand, 1996; Gatesy et al., 1999; Milàn, 2006; Razzolini et al., 2014; Gatesy and Falkingham, 2017). Substrate consistency can also affect limb dynamics. Indeed, these two variables are intrinsically linked (Razzolini and Klein, 2018). Environmental factors such as irregular terrain or changes in slope may also influence the track record (e.g., Razzolini and Klein, 2018).

Several ornithological studies have assessed the relationship between shorebirds and their prey (e.g., Hicklin and Smith, 1984; Wilson, 1990; Colwell and Landrum, 1993; Kalejta and Hockey, 1991; Pérez-Vargas et al., 2016). These efforts have shown that the degree to which invertebrate prey abundance (or biomass) influences the distribution of

shorebirds varies with spatial scale. Wilson (1990) noted a critical density threshold below which shorebirds will not occupy a foraging site at the Bay of Fundy. Apart from that only a weak relationship exists between Semipalmated Sandpiper density and prey density at intermediate (102 m) spatial scales (Wilson, 1990). This relationship is generally much stronger at the kilometre scale (e.g., Hicklin and Smith, 1984).

An important aspect of this paper is that it explores the use of Structure-from-Motion photogrammetry (SfM). Although other ichnological studies have used similar techniques to assess ichnological characteristics of ichnofossils (Petti et al., 2018; Razzolini and Klein, 2018; Mujal et al., 2020), the use of SfM in neoichnological analysis remains relatively unexplored (e.g., Kopcinski, 2017). Structure-from-Motion photogrammetry is a useful tool in a wide range of geological research. In addition to providing visual datasets, georeferenced orthographic models (orthomosaics) permit spatial measurements such as distance, area, and volume. They are also useful for performing point counts, constructing elevation models, and determining the orientation of bedding planes and other geographic features. Such analyses can be carried out in the rock record, but only if there is adequate bedding plane exposure. Modern intertidal settings thus provide an ideal testing ground for neoichnological applications of photogrammetry owing to their accessibility and relatively high abundance of animals.

Using three sites across the Bay of Fundy, this study evaluates the relationship between the distribution and orientation of shorebird tracks, surface topography, substrate cohesiveness and macrobenthic prey density at a local scale. The range of topographic expressions and substrate cohesiveness at each site provides an opportunity to assess their influence on modern shorebird trackways. These insights will provide context to the paleoecological (e.g., Anfinson et al., 2009; Lockley et al., 2009; Zonneveld et al., 2011; 2012; Contessi and Fanti, 2012; Kim et al., 2012; Falk et al., 2014; Serrano-

Brañas et al., 2022) and paleoenvironmental significance (e.g., Lockley et al., 1992; Brand, 1996; Diaz-Martinez et al., 2015; Melchor, 2015) of fossilized trackways.

2.2 Geological Setting

The Bay of Fundy is a megatidal estuary that borders the provinces of New Brunswick and Nova Scotia, Canada. Field work was conducted in partly cloudy, low-wind conditions in early September 2019, shortly after the height of autumn migration. Shorebird trackways were examined from upper intertidal flats at three sites across the Bay of Fundy (Figure 2.1). Trackways at each site are reworked during high tide. The data was collected at approximately low tide and thus represents an approximately 5- to 6-hour neoichnological record. The sites were chosen based on accessibility and represent a range of tidal flat environments. Site 1 consists of a tidal flat next to a salt marsh at the confluence of a tributary with the Petitcodiac River (A). Site 2 is situated along the Shepody River and represents an east-west transition from a bar top to the laterally accreting margin of the tidally dominated channel (Figure 2.2B). Site 3 consists of a gently dipping tidal flat near Selma, Nova Scotia that is adjacent to a forested area and thus has a higher predation risk (Beauchamp, 2012) (Figure 2.2C). Although the track sites were made by flocks of unknown size and identity, tentative identifications are provided based on observations of shorebirds near each site in conjunction with anatomical details of the footprints.

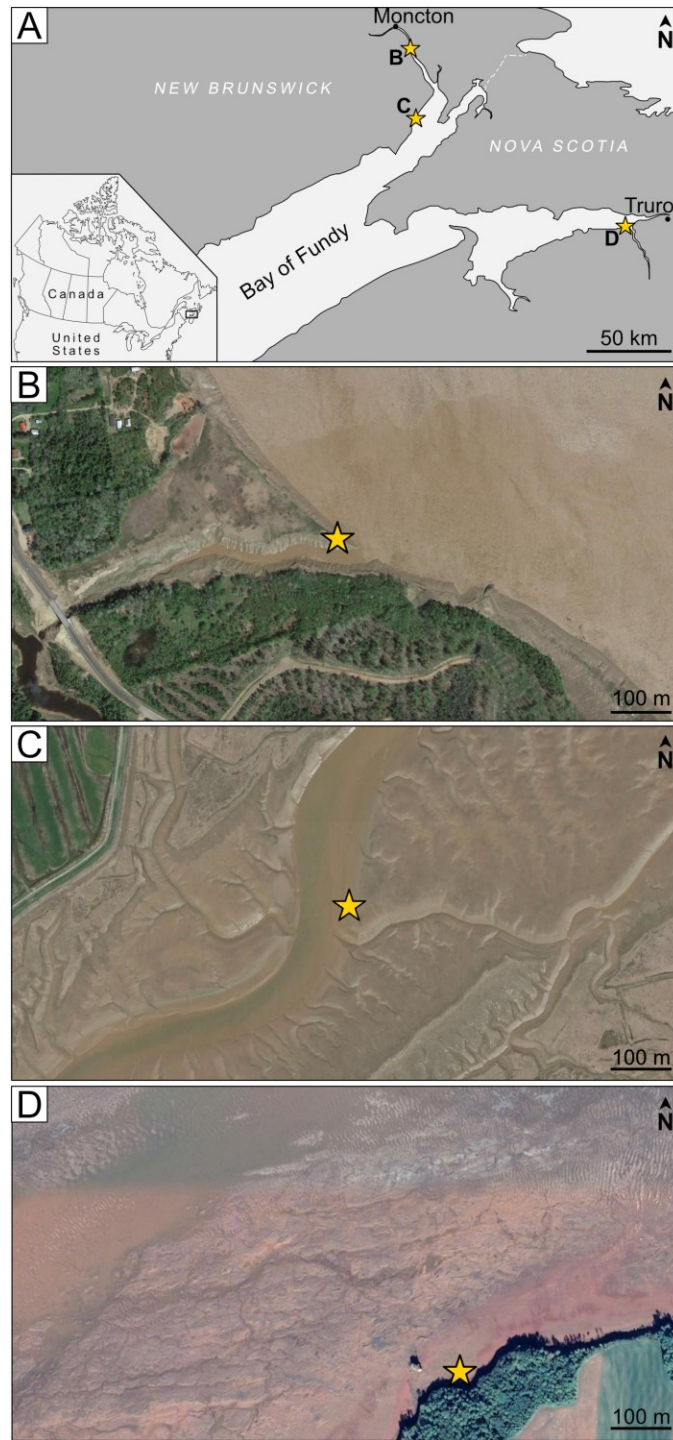


Figure 2.1. Overview of the study area. (A) Map of the Bay of Fundy indicating the locations of the study sites. (B) Google Earth image of Site 1: Petitcodiac River, (C) Google Earth image of Site 2: Shepody River, and D) Google Earth image of Site 3: Selma.



Figure 2.2. Overview of the study sites. (A) View looking to the west from Site 1 (Petitcodiac River). Notice the increase in water content towards the salt marsh to the right. (B) View looking to the south from Site 2 (Shepody River), showing the transition from the uppermost tidal flat to the channel margin. (C) View looking to the North at Site 3 (Selma). Note the drone in flight and the pieces of firmground at the bottom of the photograph.

2.3 Methods and Materials

2.3.1 Photogrammetry

Structure-from-motion photogrammetry was used to generate three-dimensional (3D) dense point clouds and meshes for each study area. Images were taken 3-5 m above the tidal flat with a DJI Mavic 2 Pro quadrotor drone equipped with a Hasselblad L1D-20c

camera (4000 x 3000 pixels; 72 dpi). The error of the spatial data points collected from each model are as follows: Site 1 average = 0.003 mm, maximum = 0.161 mm; Site 2 average = 0.005 mm, maximum = 0.032 mm; Site 3 average = 0.002 mm, maximum = 0.072. The number of images used at sites 1 to 3 were 57, 113, and 55, respectively. The images were used to build photogrammetry-based models using Agisoft Metashape Professional v.1.5.5. The dataset for each site consists of an orthomosaic and corresponding Digital Elevation Model (DEM) that were used to examine the avian tracks. The datum (elevation = 0 m) chosen for each site corresponds to the highest elevation in each photogrammetric model. Markers were placed on the centre of each track to represent their locations using a 3D spatial coordinate system. Individual tracks were grouped into trackways and numbered sequentially within their trackway. A similar technique was used to demarcate the location of the invertebrate burrow openings at Site 3. Information regarding the distribution of invertebrates at sites 1 and 2 is limited to field observations because the burrow openings were too small to be resolved in the orthomosaics.

2.3.2 Assessing Substrate Cohesiveness

Each study site consists of parallel-laminated muddy tidal flats that exhibit significant variability in water content. Three substrate types were empirically identified at each site based on anatomical fidelity of the shorebird tracks: soupy, very soft, and soft substrates (Figure 2.3 to Figure 2.5). Polygons were used to illustrate the distribution of each substrate type. The surface area of the polygons was determined using ImageJ software. The relative groupings were chosen to appropriately represent the range of water saturation at each individual site. Accordingly, each substrate type exhibits variability and does not necessarily have the same properties between sites. For instance,

some of the soft substrate at Site 1 was microbially mediated whereas others were simply well drained, but these properties lead to a similar track expression. The substrate at Site 2 displayed the highest overall water content. At Site 3, a veneer of water-saturated mud several centimeters thick overlies a firm substrate which provided support for the shorebirds.

2.3.3 Statistical Analysis

The spatial data collected from the photogrammetric dataset was used to calculate various parameters of the shorebird tracks. The following parameters were examined: elevation, slope, trackway orientation and stride length. Elevation is simply the altitude relative to the datum. The remaining metrics are presented in relation to strides taken by the shorebirds as defined by two successive steps. Accordingly, trackway orientations were determined using the angle of a line connecting every second track in a trackway. Stride relief is defined as the change in altitude between strides, whereas stride inclination takes into consideration stride length. Stride length (d) is defined herein as the horizontal distance between the two steps as determined by the Haversine formula (Robusto, 1957) (Equation 1):

$$d = 2r \arcsin \left(\sqrt{\sin^2((\Phi_2 - \Phi_1) \div 2) + \cos(\Phi_1) \cdot \cos(\Phi_2) \cdot \sin^2((\lambda_2 - \lambda_1) \div 2)} \right) \quad (\text{Equation 1})$$

where r = the earth's radius, Φ_1 = the latitude of the initial step, Φ_2 = the latitude of the final step, λ_1 = the longitude of the initial step, and λ_2 = the longitudes of the final step. When separating these metrics based on substrate type, only the strides that did not cross substrate types were considered in the analysis.

2.4 Results

Empirical observations and statistical analysis were used to evaluate the association between various ichnological and environmental parameters. Each site exhibits a unique set of environmental conditions that influence the shorebird tracks' distribution and fidelity. These parameters are discussed below within the context of surface topography, drainage, and substrate conditions. The impact of various environmental factors on substrate cohesiveness is also addressed.

2.4.1 Site 1: Petitcodiac River

Site 1 (68.3 m²; Table 2.1) is a tidal flat that lies between a salt marsh to the north and a tributary of the Petitcodiac River to the south (Figure 2.2A). It contains 1549 incumbent anisodactyl footprints grouped into 39 trackways commonly displaying a meandering to looping course (Table 2.1; Figure 2.5). Potential trackmakers include the dunlin (*Calidris alpina*) or the ruddy turnstone (*Arenaria interpres*). The site is relatively flat but there is a break in the slope to the southwest associated with the tributary channel margin (Figure 2.6). Track density generally increases away from the channel margin. The predominant trackway orientation is southwest indicating that most of the flock traversed in a gently sloping downhill direction oblique to the tributary channel axis (Figure 2.6D).

The shorebird tracks at Site 1 are grouped into three categories based on the anatomical fidelity of the tracks. The first category exhibits crudely defined outlines and conspicuous toe III drag marks (Figure 2.3A). The substrates that host these tracks are used to delineate soupy substrates. The second group of tracks is similar, but their outer margins are more clearly defined (Figure 2.3B). This indicates that they were emplaced in more cohesive substrates, herein classified as very soft substrates. The final grouping of tracks consists of well-defined footprints that lack drag marks and show a broad

resemblance to the anisodactyl tracemaker's foot (Figure 2.3C). Substrates in which these tracks are found are referred to as soft.

Soft substrates predominate at Site 1, comprising nearly half of its surface area (Table 2.2; Figure 2.1). Very soft and soupy substrates have approximately equal surface areas. Substrate cohesiveness is loosely related to elevation, with water content generally increasing upslope. Whereas water-saturated (soupy) substrates are more common in the topographic highs, more cohesive (soft) substrates tend to occur closer to the channel margin. One exception is the topographic high near the salt marsh, which is characterized as a soft substrate due to a thin biofilm binding the sediment and perhaps withdrawing pore water. Substrate cohesiveness tends to be lower where the topography is flat (Figure 2.7C). Track density is highest where soupy substrates predominate (Table 2.2. Summary of the proportion of substrate types and their effect on shorebird track distributions at each site.). Stride length is generally longer in more cohesive substrates (Figure 2.7D). It is also worth noting that trackways in microbially-mediated soft substrates exhibit a significantly longer stride (mean = 15.87 cm; median = 12.50 cm) than the well-drained soft substrates near the tributary channel (mean = 11.77 cm; median = 11.68 cm).

Table 2.1. Overview of the physical characteristics and trackways at each site.

Study location	Area [m ²]	Topographic relief [m]	Number of tracks	Number of trackways	Track density [tracks/m ²]
Site 1	68.3	1.8	1549	39	22.7
Site 2	557.7	4	1848	106	3.3
Site 3	63.2	1	4538	212	71.8



Figure 2.3. Incumbent anisodactyl shorebird tracks emplaced in the different substrate types at Site 1. (A) Soupy substrate. (B) Very soft substrate. (C) Soft substrate. Note the pronounced toe III drag marks in the tracks emplaced in soupy and very soft substrates, and the barely perceptible toe III drag mark present in front of only one of the tracks emplaced in soft substrate. Also note the mud-drop impact mark in the very soft substrate. Scale bars = 5 cm.

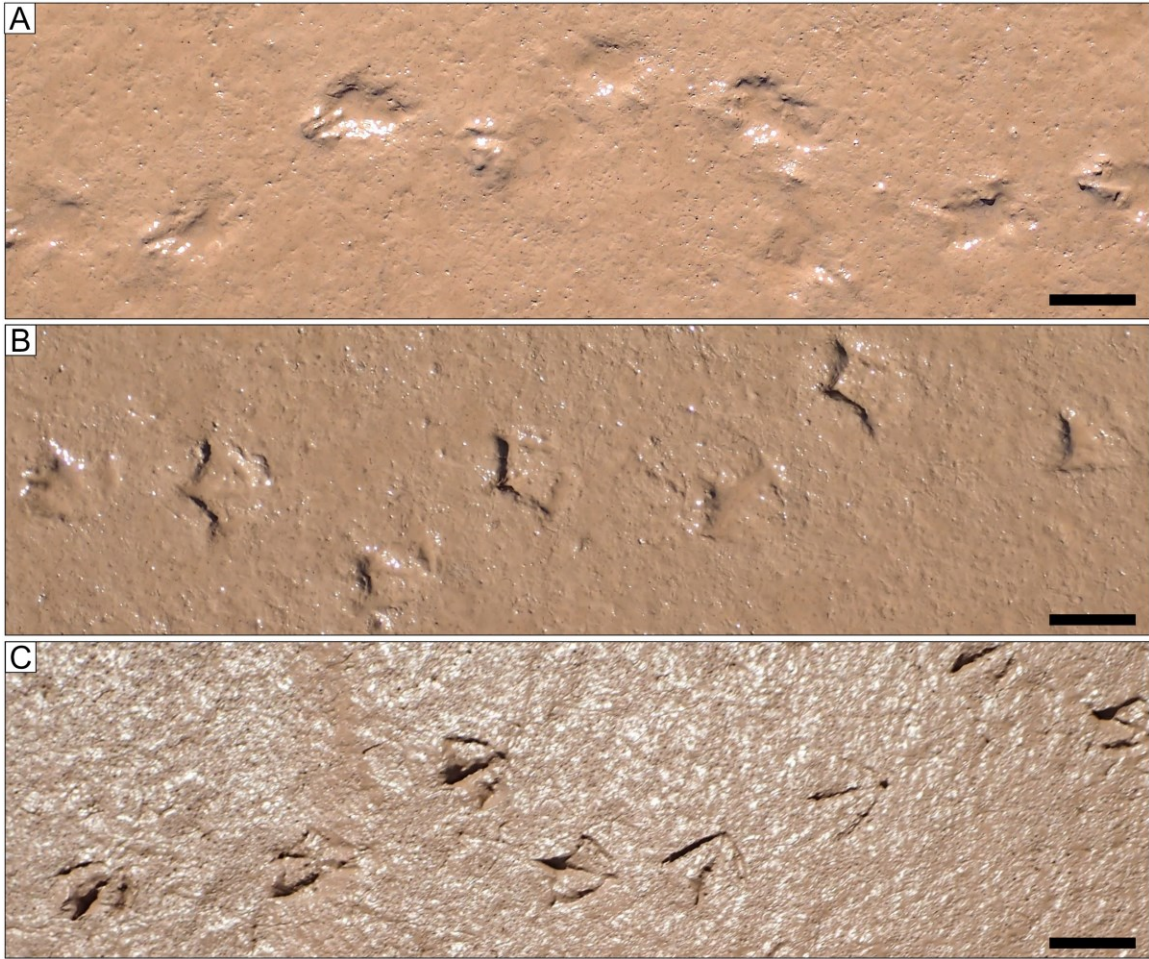


Figure 2.4. Palmate shorebird tracks emplaced in the different substrate types at Site 2. (A) Soupy substrate. (B) Very soft substrate. (C) Soft substrate. Note the intra-trackway variability in the sharpness of the outer margin of tracks emplaced in very soft substrates, and the distinct digit impressions in tracks associated with soft substrates. Scale bars = 5 cm.

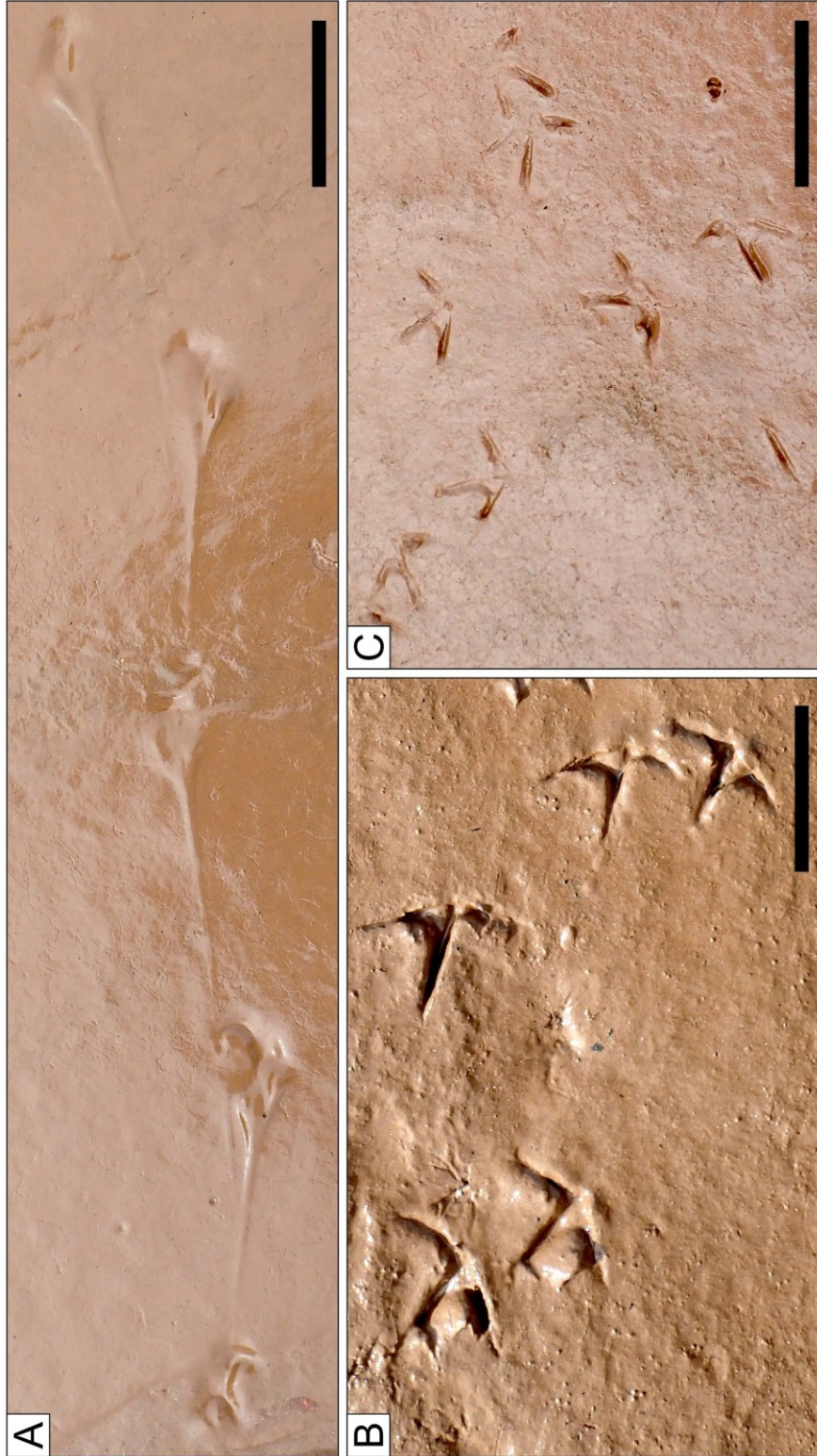


Figure 2.5. Semipalmate tridactyl shorebird tracks emplaced in the different substrate types at Site 3. (A) Soupy substrate. (B) Very soft substrate. (C) Soft substrate. Note the pronounced drag mark in the soupy substrate and the probe mark in the soft substrate. Scale bars = 5 cm.

Table 2.2. Summary of the proportion of substrate types and their effect on shorebird track distributions at each site.

	Surface area [m ²]	Proportion of surface area [%]	Number of tracks	Track density [tracks/m ²]	Proportion of tracks [%]	Mean track elevation [m]	Median track elevation [m]	Mean stride length [cm]	Median stride length [cm]	Mean inclination [°]	Median inclination [°]	
<u>Site 1</u>												
Soupy substrate	18	26.4	454	25.2	29.3	-0.86	-0.97	13.2	11.3	0.11	0.1	
Very soft substrate	18.3	26.8	427	23.3	27.6	-0.55	-0.49	13.5	12.4	0.08	0.07	
Soft substrate	31.9	46.8	668	20.9	43.1	-0.74	-0.66	12.6	12.1	0.13	0.09	
<u>Site 2</u>												
Soupy substrate	326.6	58.6	971	3	52.5	-2.72	-1.44	44.7	28.5	0.11	0.1	
Very soft substrate	195.3	35	632	3.2	34.2	-2.28	-1.29	39	27.4	0.12	0.11	
Soft substrate	35.8	6.4	245	6.8	13.3	-2.63	-0.81	28	19.9	0.11	0.11	
<u>Site 3</u>												
Soupy substrate	3	4.8	518	172.1	11.5	-0.21	-0.16	26.1	13.3	0.06	0.04	
Very soft substrate	34.8	55	2263	65.1	50.1	-0.26	-0.24	17.9	12.3	0.05	0.05	
Soft substrate	25.4	40.2	1731	68.1	38.4	-0.35	-0.36	21.1	11.7	0.07	0.06	

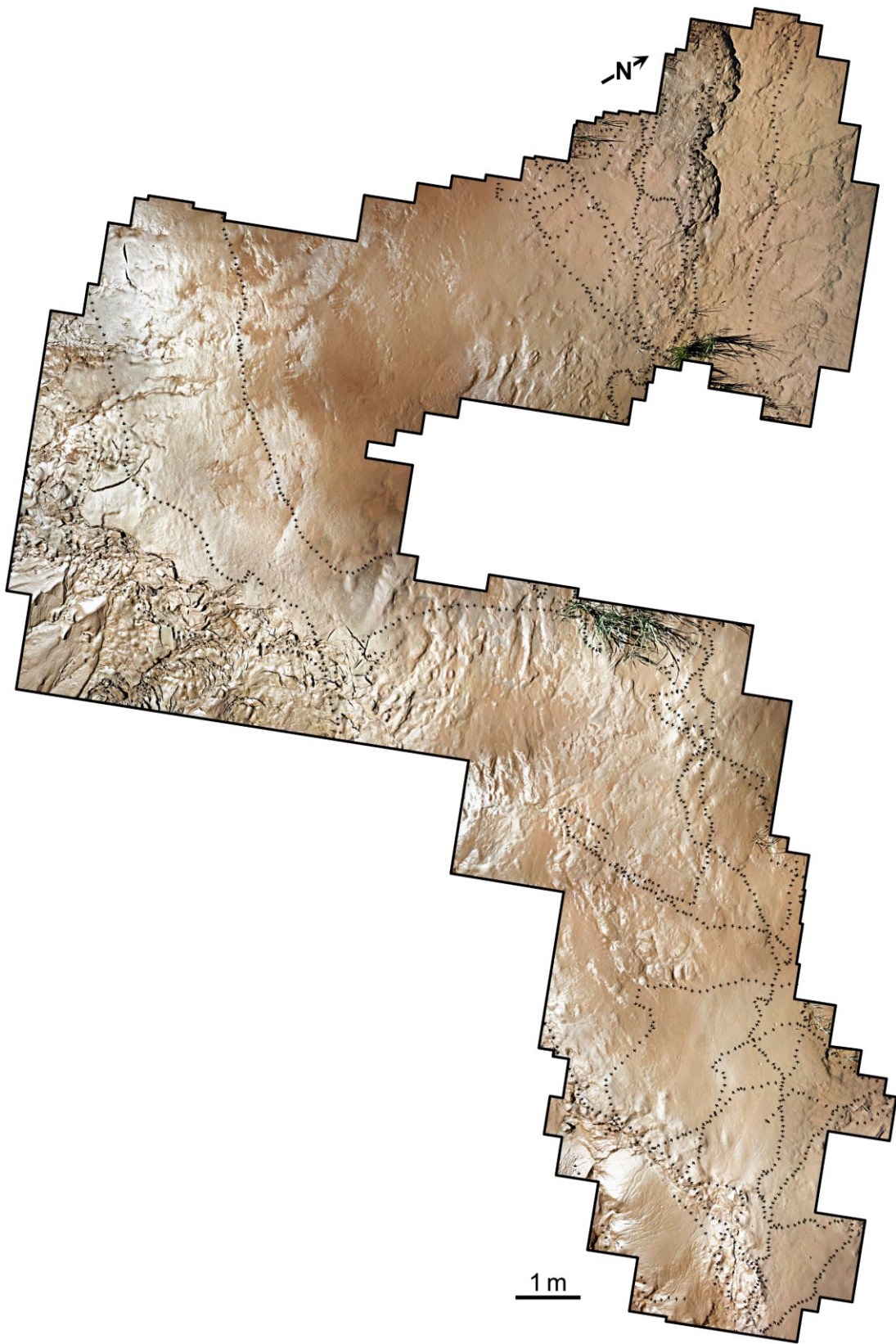


Figure 2.6. Orthomosaic of Site 1 illustrating the distribution of shorebird tracks.

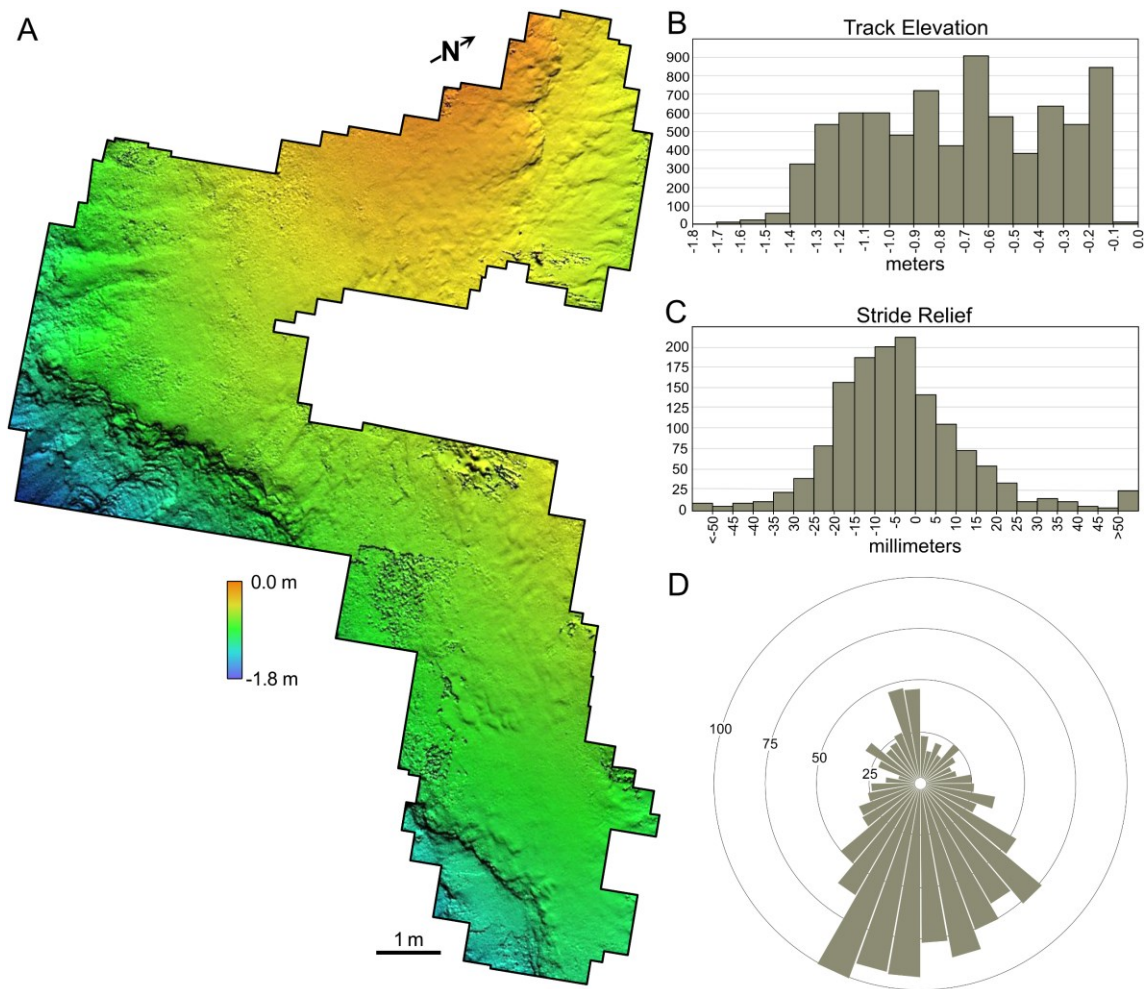


Figure 2.7. Elevation and orientation data for Site 1. (A) Digital Elevation Model. (B) Histogram of the elevation of the shorebird tracks. (C) Histogram of the stride relief of the shorebird tracks. (D) Rose diagram showing the directionality of the shorebird trackways.

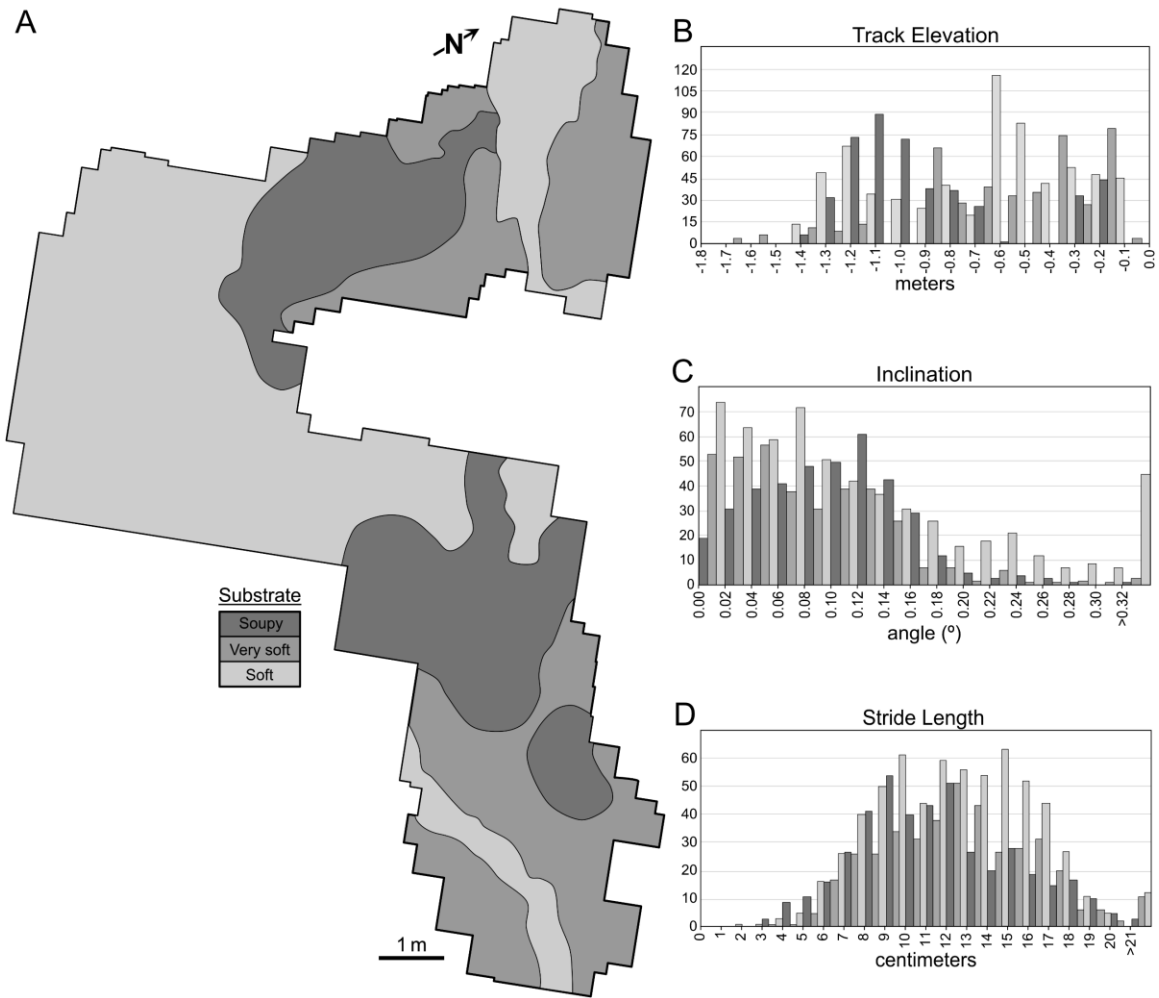


Figure 2.8. Substrate data for Site 1. (A) Spatial distribution of substrate types. (B) Histogram of the elevation of the shorebird tracks separated by substrate type. (C) Histogram of the inclination of shorebird strides separated by substrate type. (D) Histogram of the stride length separated by substrate type.

2.4.2 Site 2: Shepody River

Site 2 (557.7 m²; Table 2.1) is a bar top that is strongly influenced by drainage into the Shepody River (Figure 2.1B). It has a comparably low track density, containing 1848 palmate tracks organized into 106 trackways (Table 2.1; Figure 2.8). The tracks are believed to be footprints of great black-backed gulls (*Larus marinus*). Individual trackways are straight to clustered. The site displays an overall east-dipping trend across the study area, with local small-scale changes in topography associated with conspicuous rills (Figure 2.9). Tracks are notably more abundant at higher elevations. Most of the trackways are oriented parallel to the drainage rills, especially those at lower elevations (Figure 2.8). The tracks found in soupy substrates are characterized by indistinct depressions that bear only subtle similarities to an avian foot (Figure 2.4A). In very soft substrates the palmate outline of the tracks is apparent, but the margins are poorly defined and internal features are not preserved. In contrast, tracks emplaced in soft substrates have well-defined digit impressions and, in some areas, the full outline of the track is observed (Figure 2.4C).

As with Site 1, three morphological categories of shorebird tracks are recognized at Site 2. The first is characterized by indistinct impressions that bear only subtle similarities to an avian foot (Figure 2.4A). We associate these tracks to soupy substrates. The second category of tracks has poorly defined margins and lacks internal features (Figure 2.4B). In this group, the palmate outline of the tracks is apparent, indicating a more cohesive substrate than those found in soupy substrates. Accordingly, the substrates that host these tracks are classified as very soft. The third group of tracks recognized at Site 2 have well-defined digit impressions and, in some areas, the full outline of the track is observed (Figure 2.4C). These tracks are emplaced in substrates referred to here as soft.

Over half of the surface area of Site 2 consists of soupy substrates (Table 2.2; Figure 2.9). Water content is generally higher at low elevations and decreases upslope, thus soft substrates are restricted to the topographic highs to the east. Additionally, drainage rills become more pronounced downslope leading to intervening soupy substrates within the areas of very soft substrate. The soft substrates have a larger slope than the more water-saturated substrates (Figure 2.10C). They also display an average track density that is over twice that of soupy or very soft substrates (Table 2.2). Stride length increases with decreasing substrate cohesiveness (Figure 2.10D), with soupy substrates displaying a mean stride length that is 16.7 cm longer than that of soft substrates (Table 2.2).



Figure 2.9. Orthomosaic of Site 2 illustrating the distribution of shorebird tracks.

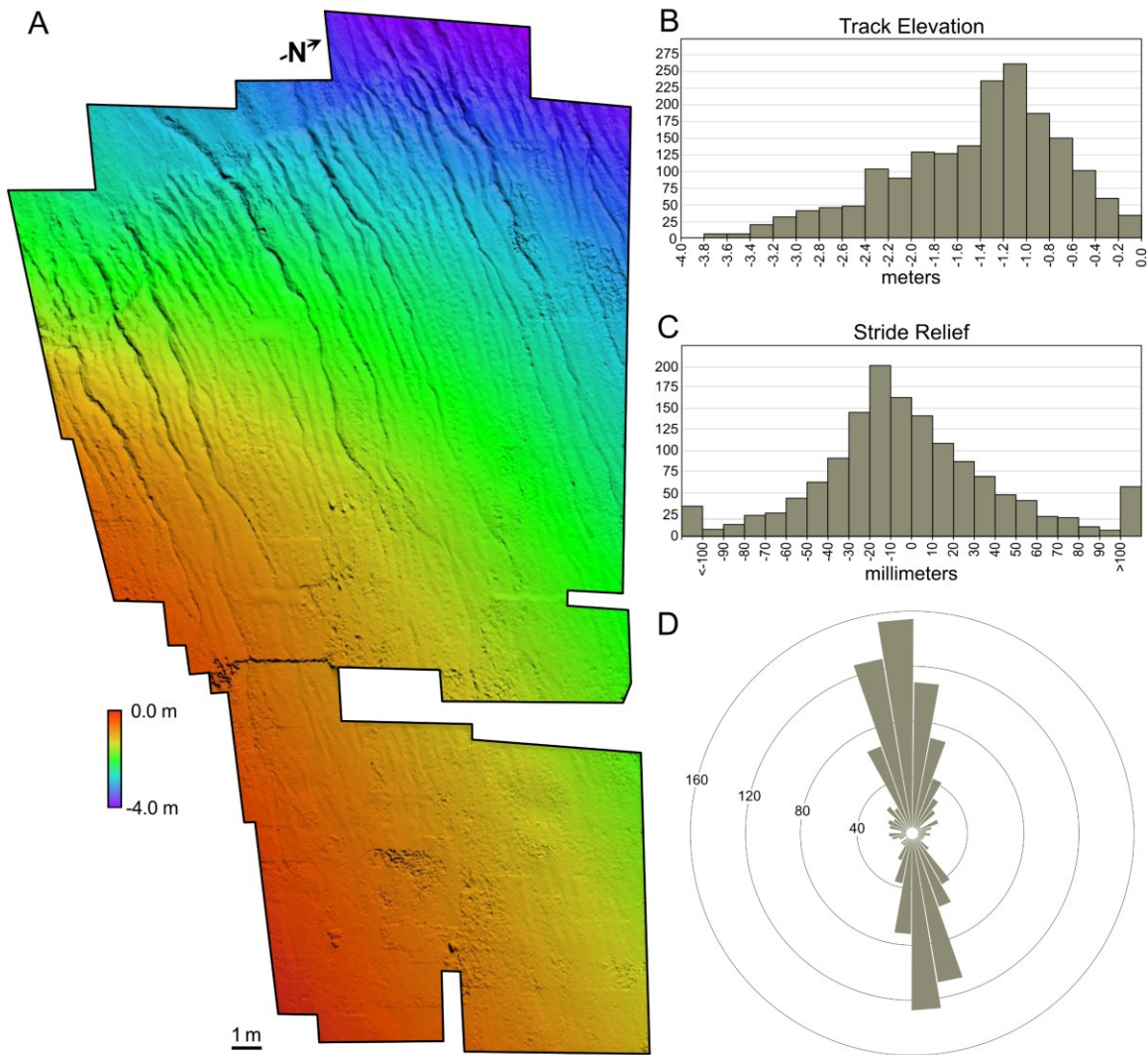


Figure 2.10. Elevation and orientation data for Site 2. (A) Digital Elevation Model. (B) Histogram of the elevation of the shorebird tracks. (C) Histogram of the stride relief of the shorebird tracks. (D) Rose diagram showing the directionality of the shorebird trackways.

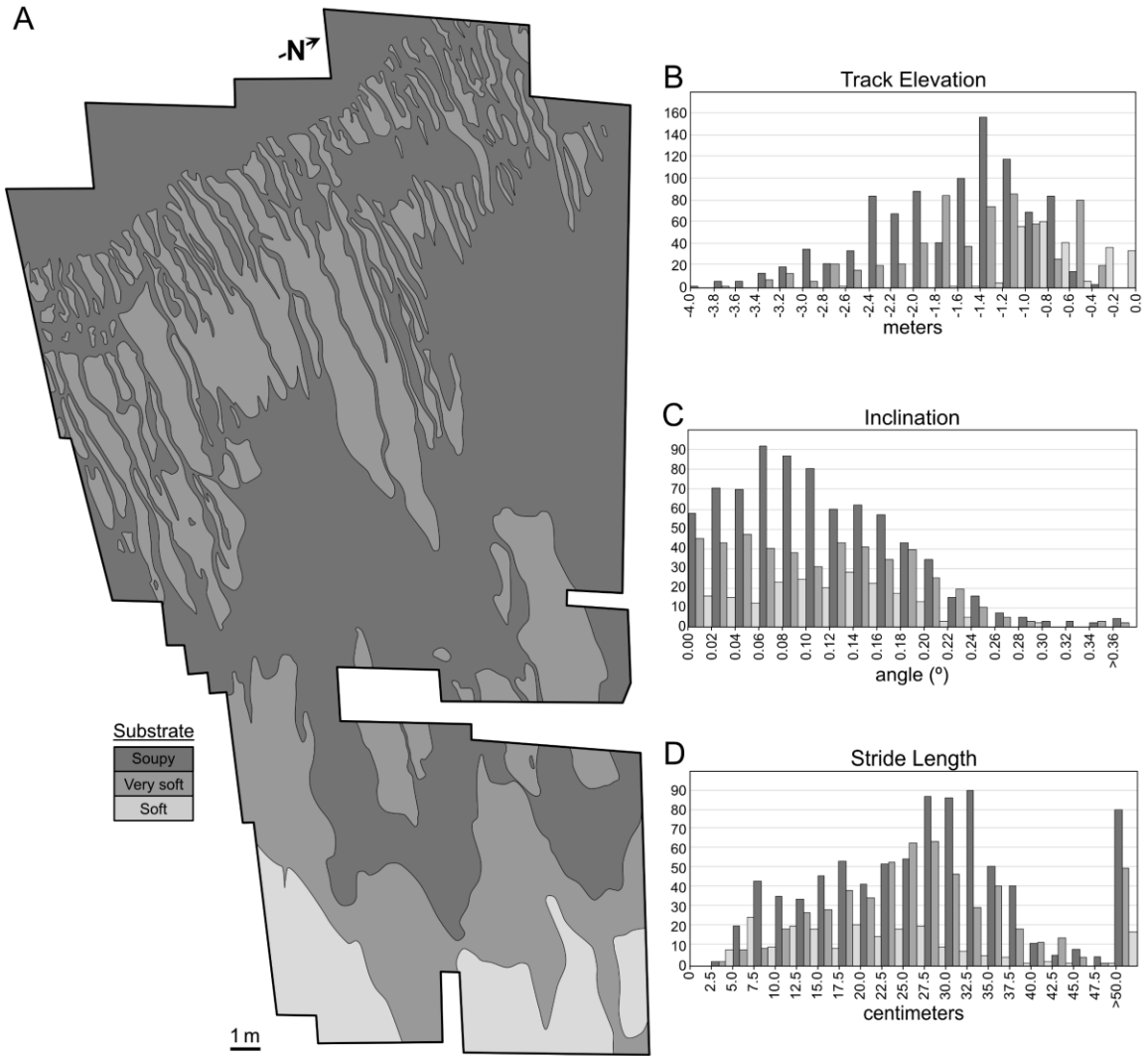


Figure 2.11. Substrate data for Site 2. (A) Spatial distribution of substrate types. (B) Histogram of the elevation of the shorebird tracks separated by substrate type. (C) Histogram of the inclination of shorebird strides separated by substrate type. (D) Histogram of the stride length separated by substrate type.

2.4.3 Site 3: Selma

Site 3 (63.2 m²; Table 2.1) is a gently dipping tidal flat near the community of Selma, Nova Scotia (Fig. 2C). The dataset comprises 4538 semipalmate tridactyl shorebird footprints grouped into 212 trackways that exhibit a meandering to looping course similar to that of Site 1 (Table 2.2; Figure 2.11). The trackways are tentatively assigned to the semipalmated plover (*Charadrius semipalmatus*). Additionally, the locations of 1103 nereid polychaete burrow openings are shown in Figure 2.11. The DEM shows only minor topographic relief across the site (Table 2.1; Figure 2.12). The tracks and burrows have a slight affinity for higher elevations, and both display locally clustered distributions. Trackway orientation is less consistent than at the other sites (Figure 2.13D). The dominant orientation of the trackways is bimodal from southeast to northwest or vice versa, which is sub-parallel to the depositional slope and roughly perpendicular to the dominant tidal current direction. The tracks emplaced in the soupy substrates at Site 3 consist of an indistinct impression with a pronounced toe III drag mark (Figure 2.5A). Very soft substrates are associated with tracks that exhibit well-defined digits and soles and have moderately sharp margins (Figure 2.5B). Tracks found in soft substrates are shallower than those found in very soft substrates, and many examples lack an imprint of the sole of the foot (Figure 2.5C).

The variation in anatomical fidelity of the tracks at Site 3 are again separated into three morphological categories (Figure 2.14). Sediment containing tracks that consist of an indistinct impression with a pronounced toe III drag mark are classified as soupy substrates (Figure 2.5A). Well-defined digits and soles displaying moderately sharp margins are attributed to very soft substrates (Figure 2.5B). The third group of tracks are comparably shallow, and many lack an imprint of the sole of the foot (Figure 2.5C), which are used to delineate soft substrates.

The soupy substrates at Site 3 are associated exclusively with minor rills and the topographic lows into which they drain (Figure 2.13). Much more common are soft and very soft substrates, which are only loosely related to elevation. On average, soft substrates exhibit the steepest slopes (Figure 2.13C). Despite comprising only 5% of the total surface area, soupy substrates exhibit the highest track density, whereas soft and very soft substrates have comparatively lower track densities (Table 2.2). Stride length increases noticeably with decreasing substrate cohesiveness (Figure 2.13D). Invertebrate burrows show a strong visual correlation with track density (Figure 2.11) and occur in higher abundance in more cohesive substrates (Table 2.3).

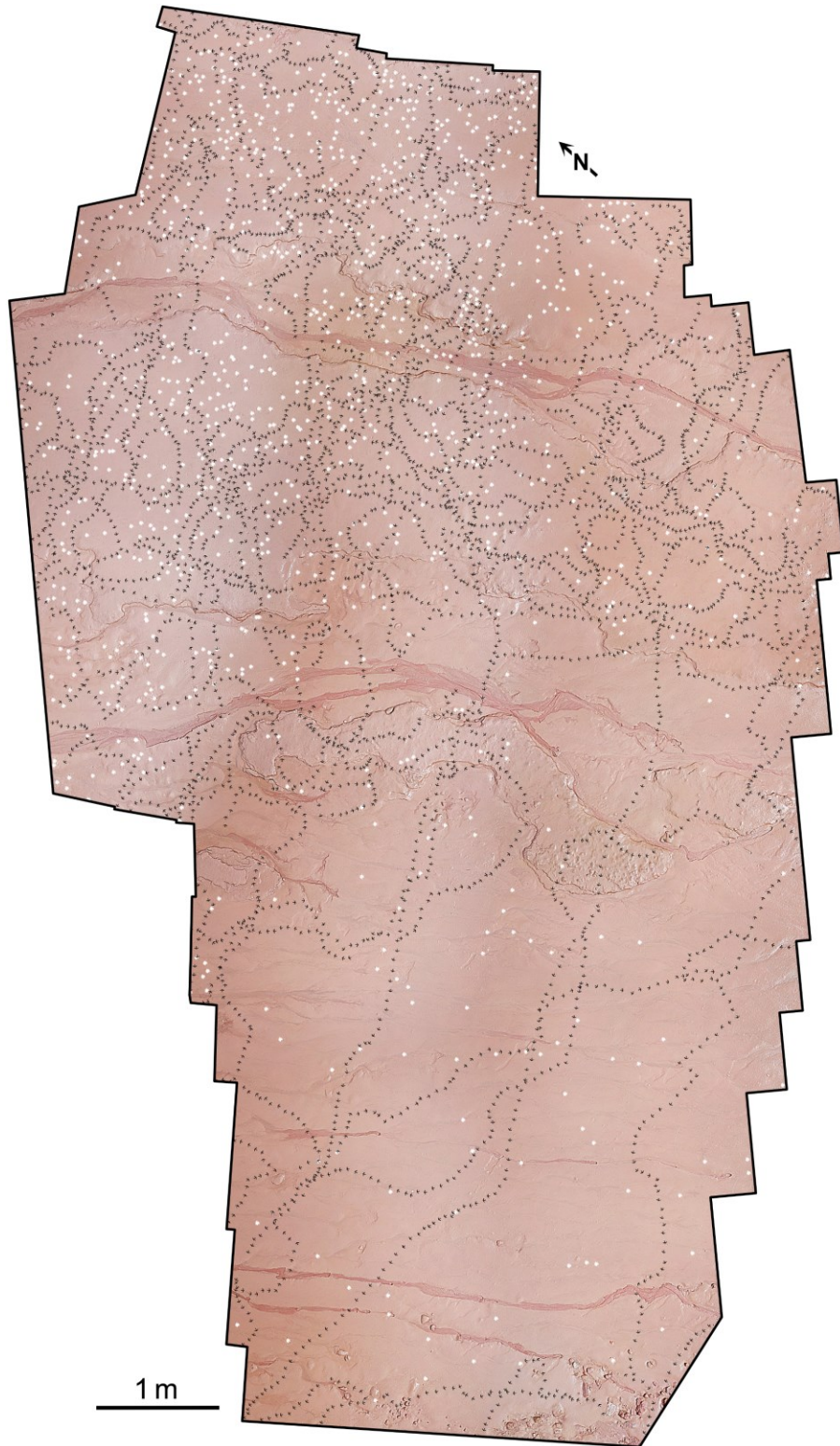


Figure 2.12. Orthomosaic of Site 3 illustrating the distribution of shorebird tracks (black) and nereid polychaete burrows (white).

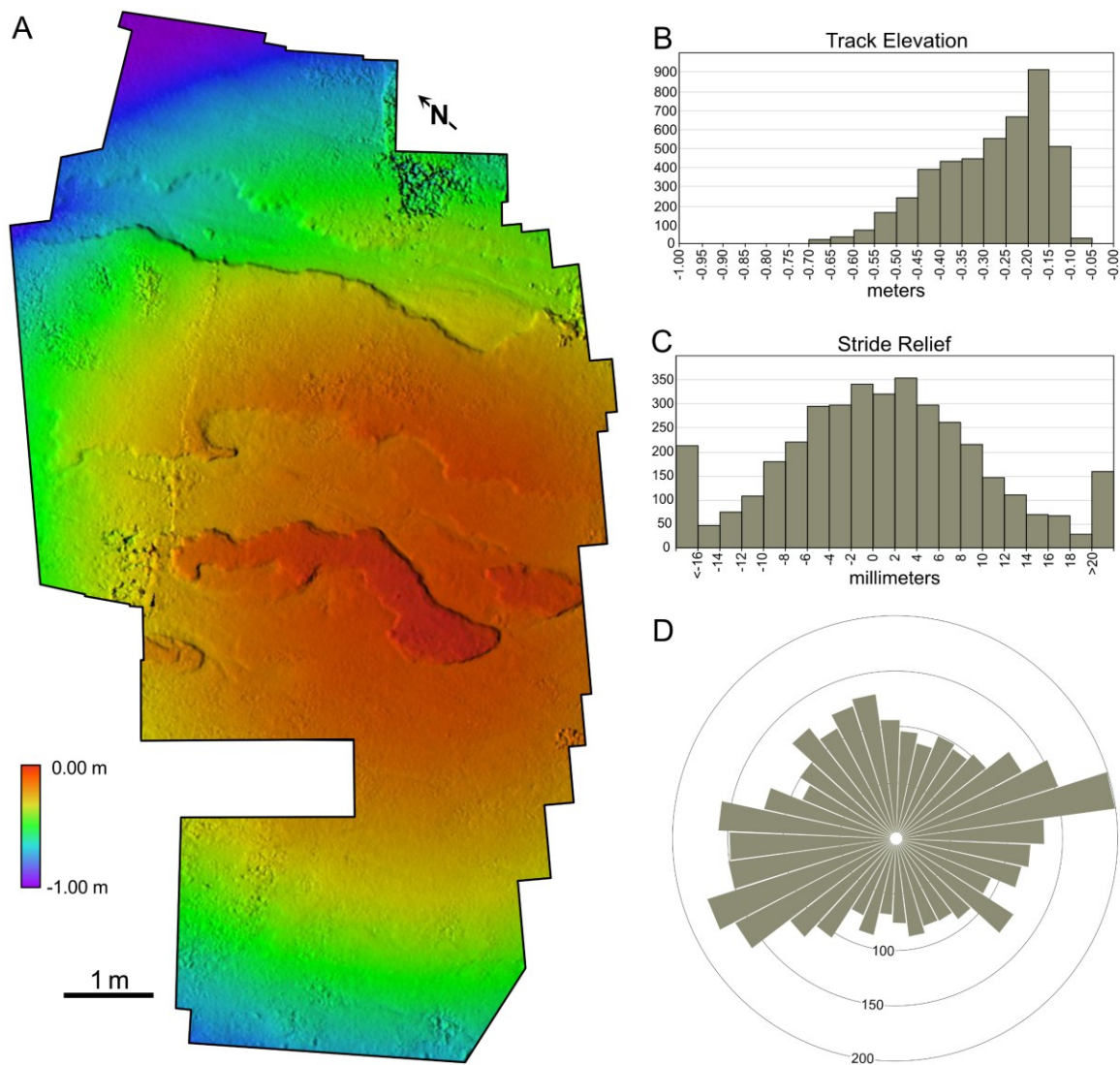


Figure 2.13. Elevation and orientation data for Site 3. (A) Digital Elevation Model. (B) Histogram of the elevation of the shorebird tracks. (C) Histogram of the stride relief of the shorebird tracks. (D) Rose diagram showing the directionality of the shorebird trackways.

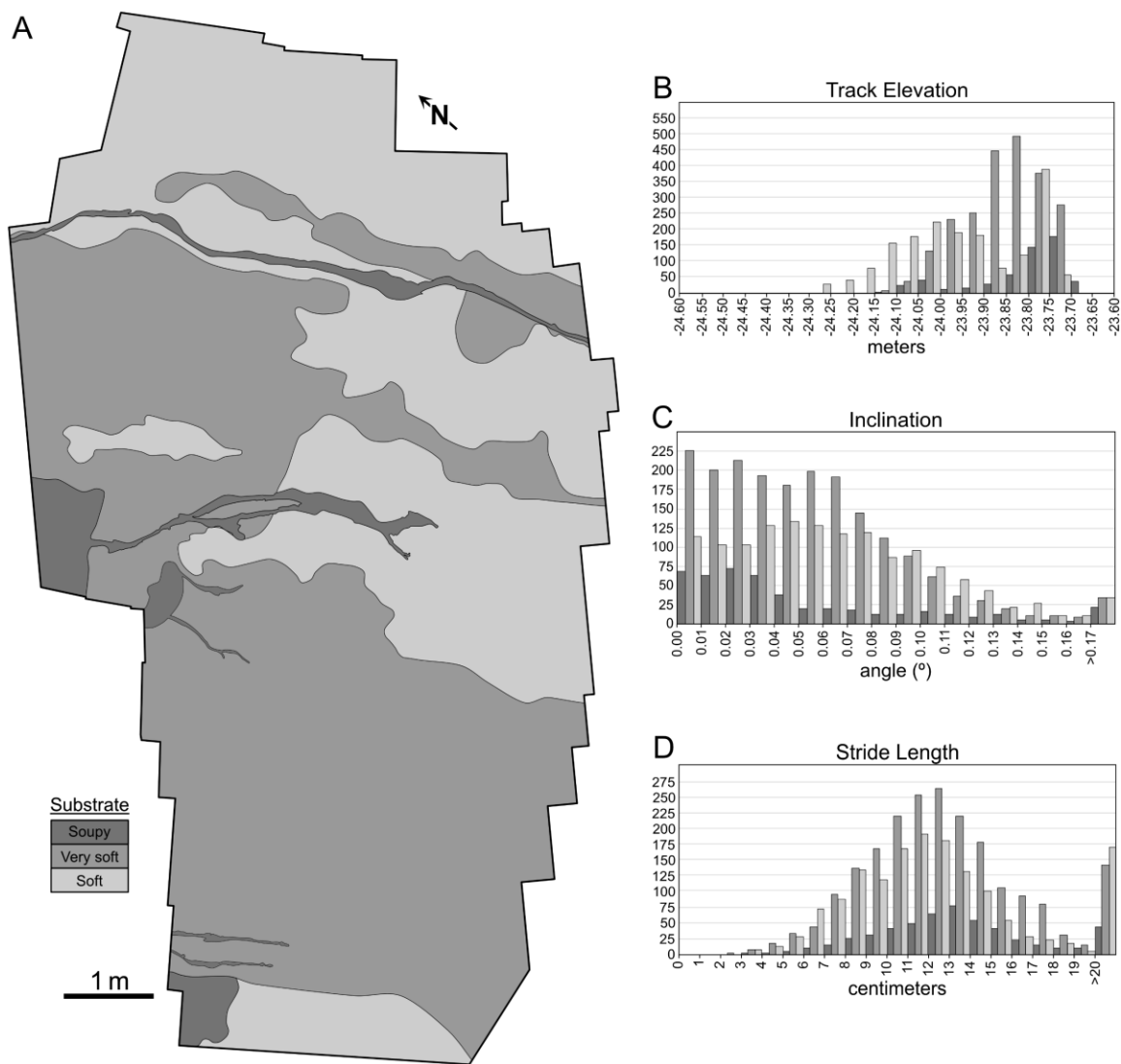


Figure 2.14. Substrate data for Site 3. A) Spatial distribution of substrate types at Site 3. B) Histogram of the elevation of the shorebird tracks separated by substrate type. C) Histogram of the inclination of shorebird strides separated by substrate type. D) Histogram of the stride length separated by substrate type.

Table 2.3. Relationship between nereid burrow density and elevation.

	Number of burrows	Proportion of burrows [%]	Burrow density [burrows/m ²]	Mean elevation [m]	Median elevation [m]
Soupy substrate	29	3	10	-0.4	-24
Very soft substrate	488	44	14	-0.3	-23.9
Soft substrate	586	53	23	-0.2	-23.8

2.5 Discussion

2.5.1 The Influence of Substrate Cohesiveness on the Track Record

The recency with which the shorebird tracks were emplaced suggests that not enough time had passed for significant taphonomic alteration to occur. As a result, variation in track morphology is determined by the interplay of anatomy, limb dynamics and substrate conditions (Falkingham, 2014). Considering that the trackways at each site were made by the same species displaying a similar foraging behaviour, it stands to reason that substrate cohesiveness is the primary factor influencing track morphology. This interpretation is supported by intra-trackway morphological variation whereby trackways pass through different substrate zones resulting in morphological variations without substantial changes in direction or stride length (cf. Razzolini et al., 2014).

Assigning each track to a substrate type provides an opportunity to assess how substrate cohesiveness influences the track record. Interestingly, the relationship between track density and substrate cohesiveness varies between sites. Track density decreases with increasing substrate cohesiveness at Site 1, whereas the opposite trend is observed at the steeply dipping Site 2 where birds tended to forage in areas less affected by the tidal channel. The slightly higher track densities in soft substrates compared to very soft substrates at Site 3 may indicate that the shorebirds preferred to walk on more cohesive substrates. It is notable, however, that burrow density is also higher in the more cohesive substrates (Figure 2.11), so this may be an indirect relationship.

Variations in stride length as a function of substrate cohesiveness are also unique to each site. At Site 1, strides taken in soft substrates tend to be longer. This is largely due to the microbially-mediated sediment adjacent to the salt marsh which provided a more cohesive substrate. This would suggest that stride length increases as substrate cohesiveness increases. However, the trackways at sites 2 and 3 display longer strides in soupy substrates, so relating stride length to substrate cohesiveness may be untenable. Variations in stride length may instead be linked to behavioral changes. One possible explanation is that the shorebirds must lift their legs higher when traversing through less cohesive substrates, which could result in longer steps. Alternatively, burrows in such substrates are less visible thus the shorebirds may move through these areas more efficiently. The relationship between stride length and substrate cohesiveness is less apparent at Site 3, however, the firmer substrate at a few centimeters' depth may alter the limb dynamics of the trackmaker (Razzolini and Klein, 2018).

2.5.2 The Influence of Topography on Track Distribution

The distribution of shorebird tracks is dependent on the local environment and behavioural patterns, which are unique to each site studied. The distribution at Site 1 is primarily influenced by the adjacent tidal channel; the shorebirds generally foraged along the top of the channel's bank and avoided the steep channel margin. In contrast, a large majority of the trackways at Site 2 are oriented perpendicular to the tidal channel axis (i.e., parallel to the drainage rills). This relationship is less pronounced away from the rills at higher elevations where the tracks become more sporadically distributed. Importantly, both sites 1 and 2 display an increase in track density away from the tidal channels. At Site 1 this is owing to the shorebirds avoiding the steep slope, whereas for Site 2 it is most likely due to an increase in exposure time towards the bar top. Razzolini and Klein (2018) showed that strides taken on sloped surfaces tend to be slightly shorter than those on flat surfaces. The drainage at Site 3 is less prominent owing to its gentle slope. As a result, trackway orientation is more variable (Figure 2.12D). Nonetheless, a preference for foraging sub-parallel to depositional dip is observed across all sites, with the down-dip direction being preferred (especially at Site 1; Figure 2.6D). This may be caused by shorebirds landing when a portion of the site was still underwater and following the tide out as it receded.

2.5.3 The Influence of Topography on Substrate Cohesiveness

The impact that topographic elevation has on water content and in turn substrate cohesiveness is complex and dependent on local factors. At Site 1, an increase in water saturation at higher elevations is presumably due to poor drainage associated with a shallow slope. The drainage at Site 2 is much more prominent, and as such there is lower water content at higher elevations. Although local trends can be observed, the relationship

between substrate cohesiveness to elevation may not be brought under a general rule. Rather, it is dependent upon a complex interplay of local factors including exposure time, grain size, drainage, microbial stabilization, and vegetation.

2.5.4 The Influence of Food Distribution on Track Density

Shorebirds walking on the upper parts of the tidal flats exhibit a foraging behaviour, feeding on locally abundant polychaetes (*Nereididae*) or amphipods (*Corophium volutator*) (Beauchamp, 2007, 2009). Field observations indicate a strong empirical relationship between macrobenthic prey abundance and track density at the studied sites (Figure 2.12). Our findings suggest that visible prey abundance has a greater direct influence on the track density than substrate cohesiveness or other environmental factors. However, factors such as topography indirectly influence track densities through their effect on macrobenthic communities (VanDusen et al., 2012). Macrobenthic invertebrate distributions are also influenced by other environmental factors such as substrate cohesiveness, salinity, exposure time, sediment grain size and sediment composition (Yates et al., 1993; Finn et al., 2008). Of these factors, substrate cohesiveness varies most appreciably across the studied sites. Foraging success is generally lower in more resistant substrates owing to a decrease in prey density and penetrability (Finn et al., 2008). However, for the water-saturated substrates in this study, this is less of a concern. Instead, burrowing organisms are limited by their ability to stabilize and maintain their burrows (Gingras et al., 2000; Bromley, 2012). An increase in substrate cohesiveness is therefore favourable for macrobenthic colonization, which in turn gives rise to higher shorebird track densities.

2.6 Summary

Three-dimensional photogrammetry using low-level drone photography permits the construction of spatially realized orthomosaics. This method provides an aerial perspective that allows for a visual appraisal and assessment of geographic features. The accessibility, lack of aerial obstructions, and high biological activity make tidal flats an ideal setting for experimenting with neoichnological applications of this technique. Neoichnological features (traces) observed from the drone imagery can be evaluated spatially and compared with potential influencing factors, such as topography, substrate cohesiveness, tidal current direction, and invertebrate prey abundance. These factors were assessed for their influence on the distribution of shorebird tracks using parameters including track density, stride length and stride orientation. The strongest correlation was between shorebird track density and prey abundance. The dominant foraging direction indicates that the shorebirds preferred to follow the tide out as it receded. The studied sites are characterized by water-saturated sediments that exhibit variable substrate cohesiveness. Three substrate types were defined at each site using track morphology as a proxy for substrate cohesiveness. The relationship between topography and substrate cohesiveness at each site shows that substrate distributions are unpredictable and based on local environmental conditions. The environmental and ecological considerations discussed in this paper provide insight into the significance of shorebird track distributions in the rock record and contribute to paleogeographic interpretations of shorebird trackways.

2.7 References

- Anfinson, O. A., Lockley, M. G., Kim, S. H., Kim, K. S., & Kim, J. Y. (2009). First report of the small bird track *Koreanaornis* from the Cretaceous of North America: Implications for avian ichnotaxonomy and paleoecology. *Cretaceous Research*, *30*, 885–894.
- Beauchamp, G. (2007). Competition in foraging flocks of migrating semipalmated sandpipers. *Oecologia*, *154*, 403–409.
- Beauchamp, G. (2009). Functional response of staging semipalmated sandpipers feeding on burrowing amphipods. *Oecologia*, *161*, 651–655.
- Beauchamp, G. (2012). Foraging speed in staging flocks of semipalmated sandpipers: Evidence for scramble competition. *Oecologia*, *169*, 975–980.
- Brand, L. R. (1996). Variations in salamander trackways resulting from substrate differences. *Journal of Paleontology*, *70*, 1004–1010.
- Bromley, R. G. (2012). *Trace Fossils: Biology, Taxonomy and Applications*. Routledge.
- Cohen, A., Lockley, M. G., Halfpenny, J., & Michel, A. E. (1991). Modern vertebrate track taphonomy at Lake Manyara, Tanzania. *Palaios*, *6*, 371–389.
- Colwell, M. A., & Landrum, S. L. (1993). Nonrandom shorebird distribution and fine-scale variation in prey abundance. *The Condor*, *95*, 94–103.
- Contessi, M., & Fanti, F. (2012). First record of bird tracks in the Late Cretaceous (Cenomanian) of Tunisia. *Palaios*, *27*, 455–464.
- Diaz-Martinez, I., Suarez-Hernando, O., Martinez-Garcia, B., Hernandez, J. M., Fernandez, S. G., Perez-Lorente, F., & Murelaga, X. (2015). Early Miocene shorebird-like footprints from the Ebro Basin, La Rioja, Spain: Paleoecological and paleoenvironmental significance. *Palaios*, *30*, 424–431.

- Elnor, R. W., Beninger, P. G., Jackson, D. L., & Potter, T. M. (2005). Evidence of a new feeding mode in western sandpiper (*Calidris mauri*) and dunlin (*Calidris alpina*) based on bill and tongue morphology and ultrastructure. *Marine Biology*, *146*, 1223–1234.
- Falk, A. R., Lim, J.-D., & Hasiotis, S. T. (2014). A behavioral analysis of fossil bird tracks from the Haman Formation (Republic of Korea) shows a nearly modern avian ecosystem. *Vertebrata Palasiatica*, *52*, 129–152.
- Falkingham, P. L. (2014). Interpreting ecology and behaviour from the vertebrate fossil track record: Ecology and behaviour from fossil track record. *Journal of Zoology*, *292*, 222–228.
- Finn, P. G., Catterall, C. P., & Driscoll, P. V. (2008). Prey versus substrate as determinants of habitat choice in a feeding shorebird. *Estuarine, Coastal and Shelf Science*, *80*, 381–390.
- Gatesy, S. M., & Falkingham, P. L. (2017). Neither bones nor feet: Track morphological variation and 'preservation quality.' *Journal of Vertebrate Paleontology*, *37*, e1314298.
- Gatesy, S. M., Middleton, K. M., Jenkins Jr, F. A., & Shubin, N. H. (1999). Three-dimensional preservation of foot movements in Triassic theropod dinosaurs. *Nature*, *399*, 141–144.
- Gingras, M. K., Pemberton, S. G., & Saunders, T. (2000). Firmness profiles associated with tidal-creek deposits: The temporal significance of *glossifungites assemblages*. *Journal of Sedimentary Research*, *70*, 1017–1025.
- Hamilton, D. J., Barbeau, M. A., & Diamond, A. W. (2003). Shorebirds, mud snails, and *Corophium volutator* in the upper Bay of Fundy, Canada: Predicting bird activity on intertidal mud flats. *Canadian Journal of Zoology*, *81*, 1358–1366.

- Hicklin, P. W., & Smith, P. C. (1984). Selection of foraging sites and invertebrate prey by migrant Semipalmated Sandpipers, *Calidris pusilla* (Pallas), in Minas Basin, Bay of Fundy. *Canadian Journal of Zoology*, *62*, 2201–2210.
- Kalejta, B., & Hockey, P. A. R. (1991). Distribution, abundance and productivity of benthic invertebrates at the Berg River Estuary, South Africa. *Estuarine, Coastal and Shelf Science*, *175–191*, 17.
- Kim, J. Y., Lockley, M. G., Seo, S. J., Kim, K. S., Kim, S. H., & Baek, K. S. (2012). A paradise of Mesozoic birds: The world's richest and most diverse Cretaceous bird track assemblage from the Early Cretaceous Haman Formation of the Gajin Tracksite, Jinju, Korea. *Ichnos*, *19*, 28–42.
- Kopcznski, K., Buynevich, I., Curran, H. A., Caris, J., & Nyquist, J. (2017). Imaging bioturbation in supratidal carbonates: Non-invasive field techniques enhance neoichnological and zoogeomorphological research, San Salvador, The Bahamas. *Bollettino Della Società Paleontologica Italiana*, *289–297*.
- Lockley, M., Chin, K., Houck, K., Matsukawa, M., & Kukiwara, R. (2009). New interpretations of Ignotornis, the first-reported Mesozoic avian footprints: Implications for the paleoecology and behavior of an enigmatic Cretaceous bird. *Cretaceous Research*, *30*, 1041–1061.
- Lockley, M. G. (1986). The paleobiological and paleoenvironmental importance of dinosaur footprints. *Palaios*, *1*, 37–47.
- Lockley, M. G., Yang, S. Y., Matsukawa, M., Fleming, F., & Lim, S. K. (1992). The track record of Mesozoic birds: Evidence and implications. *Philosophical Transactions of the Royal Society of London. Series B: Biological Sciences*, *336*, 113–134.
- Marchetti, L., Belvedere, M., Voigt, S., Klein, H., Castanera, D., Díaz-Martínez, I., ... Farlow, J. O. (2019). Defining the morphological quality of fossil footprints. Problems and

- principles of preservation in tetrapod ichnology with examples from the Palaeozoic to the present. *Earth-Science Reviews*, 193, 109–145.
- Marty, D., Strasser, A., & Meyer, C. A. (2009). Formation and taphonomy of human footprints in microbial mats of present-day tidal-flat environments: Implications for the study of fossil footprints. *Ichnos*, 16, 127–142.
- Melchor, R. N. (2015). Application of vertebrate trace fossils to palaeoenvironmental analysis. *Palaeogeography, Palaeoclimatology, Palaeoecology*, 439, 79–96.
- Milan, J. (2006). Variations in the morphology of emu (*dromaius novaehollandiae*) tracks reflecting differences in walking pattern and substrate consistency: Ichnotaxonomic implications. *Palaeontology*, 49, 405–420.
- Milàn, J., & Bromley, R. G. (2007). True tracks, undertracks and eroded tracks, experimental work with tetrapod tracks in laboratory and field. *Palaeogeography, Palaeoclimatology, Palaeoecology*, 231, 253–264.
- Mujal, E., Marchetti, L., Schoch, R. R., & Fortuny, J. (2020). Upper Paleozoic to Lower Mesozoic Tetrapod ichnology revisited: Photogrammetry and relative depth pattern inferences on functional prevalence of autopodia. *Frontiers in Earth Science*, 8, 248.
- Padian, K., & Olsen, P. K. (1984). The fossil trackway *Pteraichnus*: Not pterosaurian, but crocodylian. *Journal of Paleontology*, 58, 178–184.
- Pérez-Vargas, A. D., Bernal, M., Delgadillo, C. S., González-Navarro, E. F., & Landaeta, M. F. (2016). Benthic food distribution as a predictor of the spatial distribution for shorebirds in a wetland of central Chile. *Revista de Biología Marina y Oceanografía*, 51, 147–159.
- Petti, F., Petruzzelli, M., Conti, J., Spalluto, L., Wagensommer, A., Lamendola, M., ... Tropeano, M. (2018). The use of aerial and close-range photogrammetry in the

- study of dinosaur tracksites: Lower Cretaceous (upper Aptian/lower Albian) Molfetta ichnosite (Apulia, southern Italy). *Palaeontologia Electronica*.
<https://doi.org/10.26879/845>
- Razzolini, N. L., & Klein, H. (2018). Crossing slopes: Unusual trackways of recent birds and implications for tetrapod footprint preservation. *Ichnos*, *25*, 252–259.
- Razzolini, N. L., Vila, B., Castanera, D., Falkingham, P. L., Barco, J. L., Canudo, J. I., ... Galobart, À. (2014). Intra-Trackway Morphological Variations Due to Substrate Consistency: The El Frontal Dinosaur Tracksite (Lower Cretaceous, Spain). *PLoS ONE*, *9*, e93708.
- Robusto, C. C. (1957). The Cosine-Haversine Formula. *The American Mathematical Monthly*, *64*, 38–40.
- Scott, J. J., Renaut, R. W., & Owen, R. B. (2010). Taphonomic controls on animal tracks at Saline, Alkaline Lake Bogoria, Kenya Rift Valley: Impact of salt efflorescence and clay mineralogy. *Journal of Sedimentary Research*, *80*, 639–665.
- Serrano-Brañas, C. I., Espinosa-Chávez, B., Ventura, J. F., Barrera-Guevara, D., Torres-Rodríguez, E., & Vega, F. J. (2022). New insights on the avian trace fossil record from NE Mexico: Evidences on the diversity of latest Maastrichtian web-footed bird tracks. *Journal of South American Earth Sciences*, *113*, 15.
- VanDusen, B. M., Fegley, S. R., & Peterson, C. H. (2021). Prey distribution, physical habitat features, and guild traits interact to produce contrasting shorebird assemblages among foraging patches. *PLoS ONE*, *7*, e52694.
- Wilson, W. H., Jr. (1990). Relationship between prey abundance and foraging site selection by semipalmated sandpipers on a bay of fundy mudflat. *Journal of Field Ornithology*, *61*, 9–19.
- Yates, M. G., Goss-Custard, J. D., McGroarty, S., Lakhani, K. H., Durell, S. E. A., Clarke, R. T.,

- ... Frost, A. J. (1993). Sediment characteristics, invertebrate densities and shorebird densities on the inner banks of the wash. *The Journal of Applied Ecology*, *30*, 599–614.
- Zonneveld, John-Paul. (2016). Applications of experimental neoichnology to paleobiological and evolutionary problems. *Palaios*, *31*, 275–279.
- Zonneveld, J.-P., Zaim, Y., Rizal, Y., Ciochon, R. L., Bettis, E. A., Aswan, & Gunnell, G. F. (2011). Oligocene shorebird footprints, Kandi, Ombilin Basin, Sumatra. *Ichnos*, *18*, 221–227.
- Zonneveld, J.-P., Zaim, Y., Rizal, Y., Ciochon, R. L., Bettis, E. A., Aswan, & Gunnell, G. F. (2012). Ichnological constraints on the depositional environment of the Sawahlunto Formation, Kandi, northwest Ombilin Basin, west Sumatra, Indonesia. *Journal of Asian Earth Sciences*, *45*, 106–113.

CHAPTER 3 – TOPOGRAPHIC CONTROLS ON THE DISTRIBUTION OF BIOTURBATION IN AN INTERTIDAL SANDFLAT

3.1 Introduction

Intertidal flats are characterized by patchy infaunal distributions that reflect the dynamic nature of intertidal settings (Dashtgard, 2011a,b). At the local scale, these distributions are linked to the presence and intensity of physico-chemical stressors (Gingras et al., 2011; Dashtgard and Gingras, 2012). However, the distribution of these stressors is complex due to the combination of wave and tidal processes and biological overprinting (Swinbanks, 1981; Swinbanks and Murray, 1981). In addition, interactions between infauna and their local environment can be difficult to disentangle, particularly in the rock record. What remains evident is that the distribution and abundance of infauna reflects their responses to physico-chemical stressors (La Croix et al., 2022).

Sedimentation rate is often regarded as the primary limiting factor of bioturbation intensity in the rock record (Wheatcroft, 1990; Gingras et al., 2011; Tipper et al., 2015; Bhattacharya et al., 2020; Allport et al., 2021; Miguez-Salas et al., 2022), and this includes both substrate mobility (rate at which sediment shifts across the sediment surface) and sediment accumulation rate. The decrease in bioturbation with an increase in sedimentation rate and substrate mobility was originally documented in studies of modern intertidal environments (Reineck, 1967; Howard, 1978), and has been further emphasized in more recent efforts. Research conducted by Dashtgard (2011) in Boundary Bay, British Columbia, suggested that burrow distributions were most strongly influenced by substrate mobility and grain size, with secondary influence by subaerial exposure. Yang

et al. (2009) documented pronounced variability in bioturbation intensity across intertidal berm profiles that corresponded to relative sedimentation rates. Patel and Desai (2009) analyzed infaunal distributions in the Gulf of Kachchh, Western India, noting their correlation with various dynamic landforms.

Other research has highlighted the importance of sediment characteristics affecting infaunal distributions in intertidal flats, including grain size (Gingras et al., 1999; Dashtgard et al., 2008), substrate firmness (Gingras et al., 2000; Yang et al., 2009; Tovar et al., 2014), and the distribution of food resources (Hauck et al., 2008, 2009). At larger spatial scales, salinity plays an increasing role, particularly in areas with high fluvial input (Gingras et al., 1999; Hauck et al., 2009; La Croix et al., 2015; Melnyk and Gingras, 2020). The significance of current energy has also been assessed (Grant, 1981).

In the context of the aforementioned studies, understanding the full range of factors contributing to infaunal distributions in intertidal zones is challenging. This paper aims to address this by investigating the factors that influence infaunal distributions at East Beach in White Rock, British Columbia, Canada. The study area consists of low-relief dunes that give rise to two predominant subenvironments: current-rippled dune crests and heavily burrowed interdunes. With the exception of major storms, substrate mobility and the sedimentation rate are negligible in both subenvironments presenting an opportunity to assess how factors such as subaerial exposure and food availability affect burrow distributions within intertidal settings.

3.2 Study Area

Semiahmoo Bay is located south of the Fraser River Delta and straddles the border between Canada and the United States (Figure 2.1). Tides in Semiahmoo Bay follow a mixed semi-diurnal pattern, with the M1 tide being weaker than M2. The maximum spring tidal range is approximately 4.5 m. This study was conducted at East Beach, which is a sandy intertidal flat located at the north end of Semiahmoo Bay in White Rock, British Columbia, Canada. The sandflat broadens to the southeast and extends 6.5 km along strike, covering an area of approximately 4.2 km². There is minimal freshwater influence, with local drainage from the Campbell River representing the only appreciable fluvial input. Dykes that extend the entire length of the shoreline help maintain the overall geometry of the sandflat.

This study focuses on the upper and middle intertidal flats of East Beach, which consist of gently undulating sand dunes (*sensu* Ashley, 1990) that vary in geometry from symmetrical to slightly asymmetrical. Individual bedforms display wavelengths that range from 30 to 40 m and heights of up to 1 m. They are aligned sub-parallel to the shoreline and are laterally continuous except where they are interrupted by shore-normal run-off channels (Figure 3.1B). The dunes remain relatively fixed in their position between storm events resulting in multi-year colonization windows in the interdunes (Figure 3.2 and Figure 3.3).

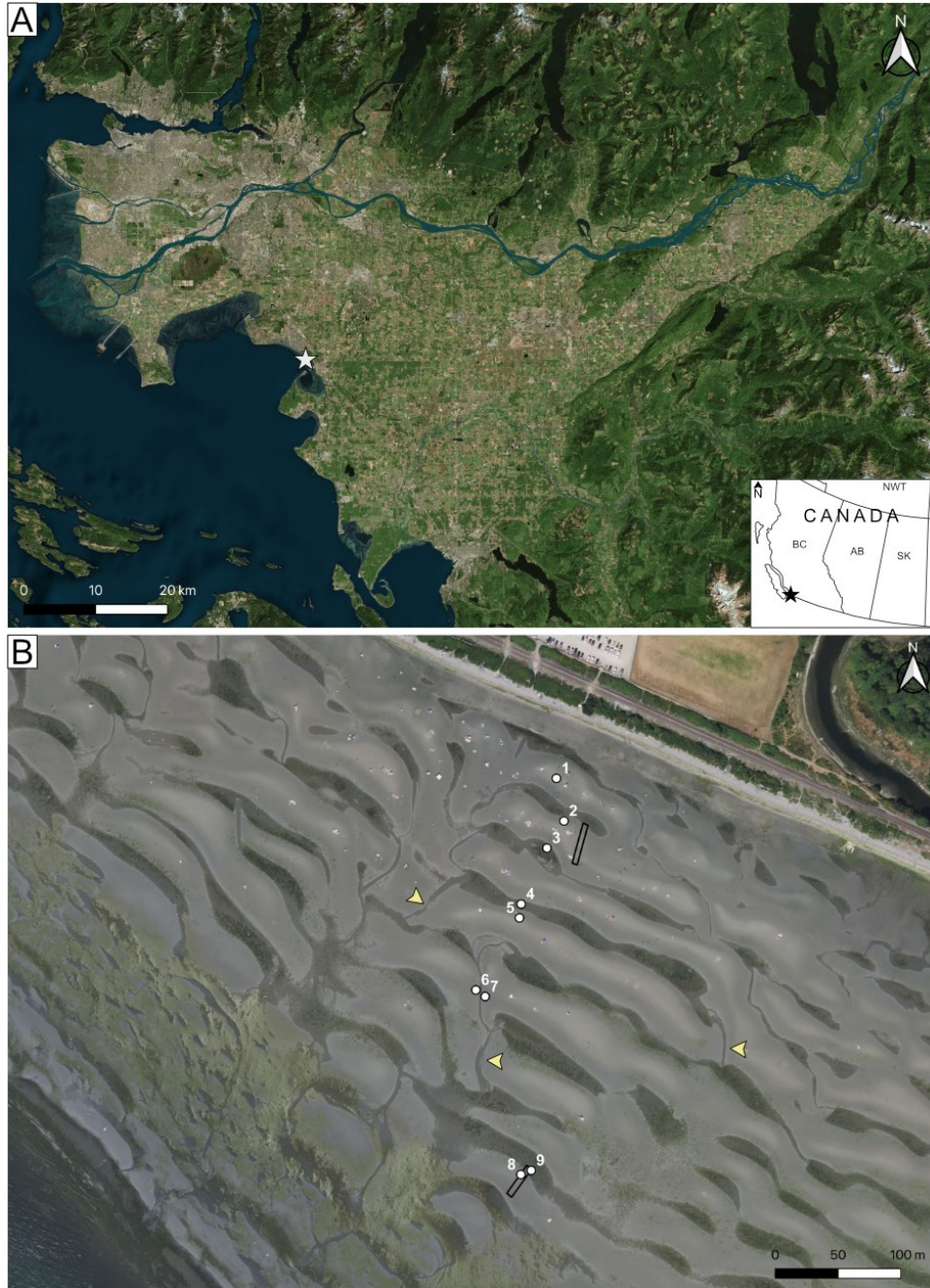


Figure 3.1. Overview of the study area. (A) Satellite image of the Fraser River Delta along the southwestern coast of British Columbia, Canada. The location of the study area is denoted by the white star. (B) Inset of the study area showing the locations of the dune transects (black outlines) and stations where sediment samples were collected (white dots). The coordinates for each station are provided in Table 3.2. Note that the position of the dunes (delineated by pools of standing water) and run-off channels (indicated by yellow arrows) shown in this image may differ slightly from when data collection occurred 13 months prior (image captured on July 20, 2020). This discrepancy is due to sediment redistribution and bedform migration over time. Both images sourced from Bing Maps.

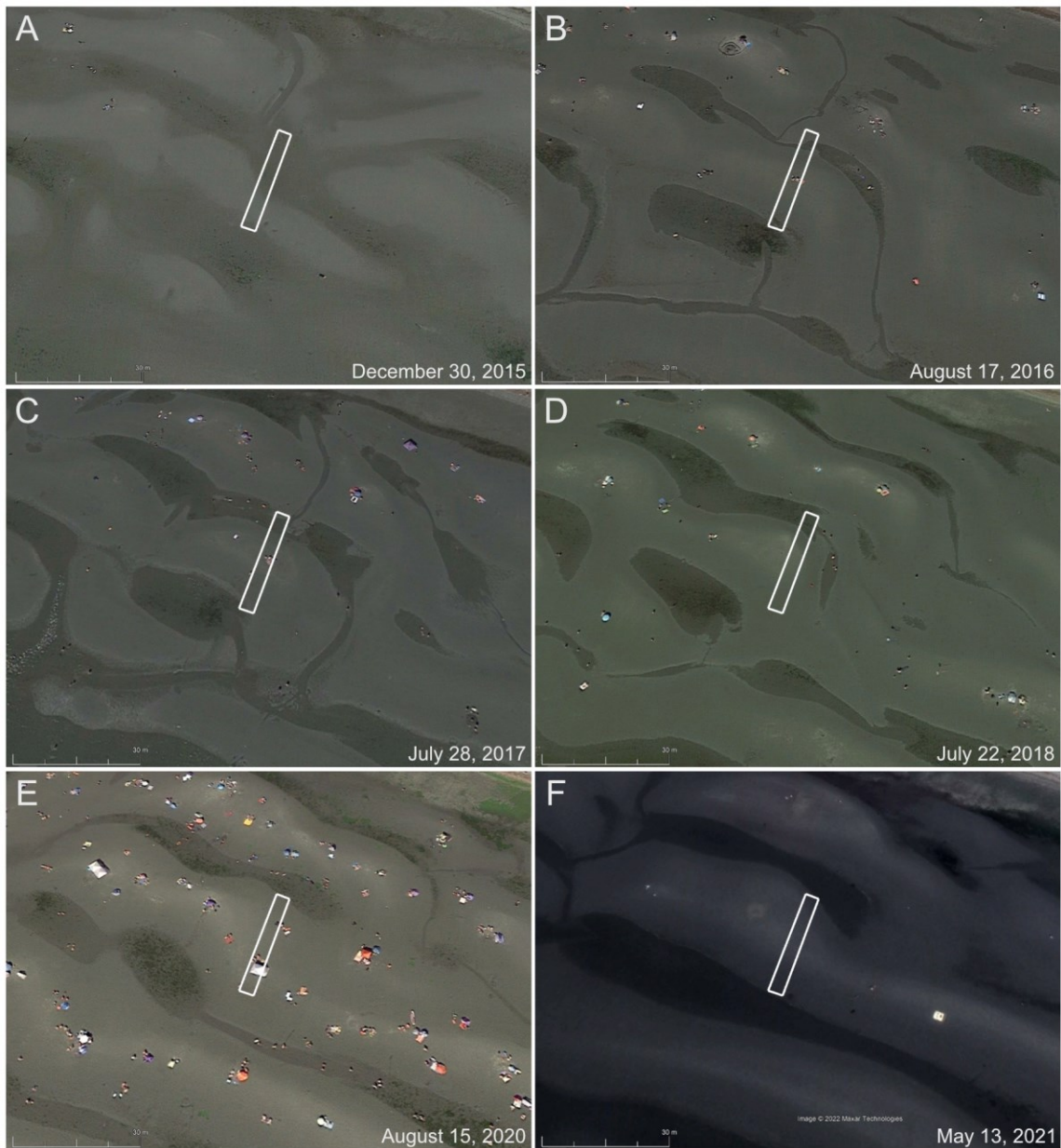


Figure 3.2. Historical imagery from Google Earth depicting migration patterns through time of the landward dune. The white rectangle indicates the location of the dune transect. The imagery shows that the overall position of the dunes remains relatively stable over the course of several years, indicating that substrate mobility is low to negligible at the time scale of infaunal life cycles.

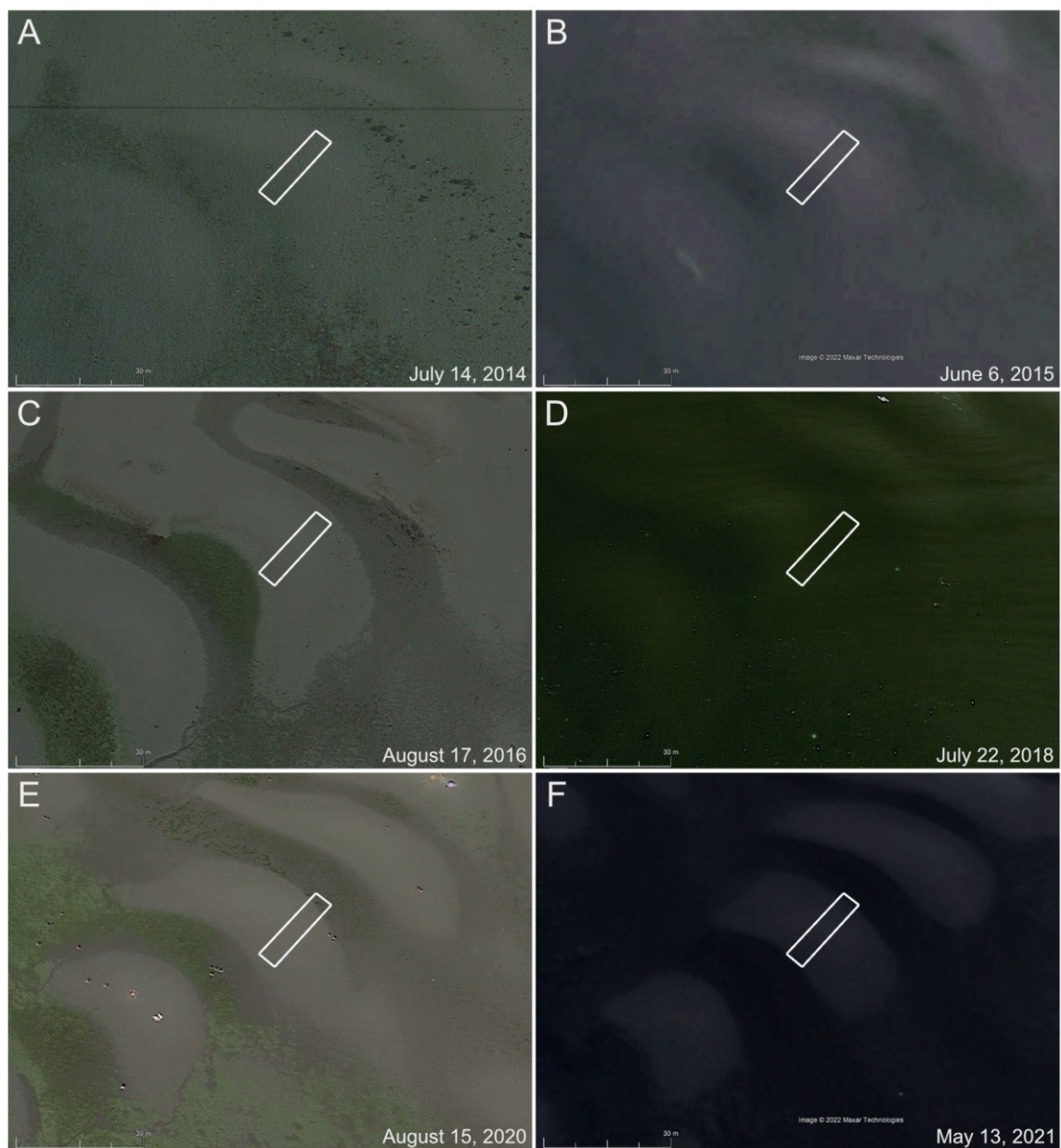


Figure 3.3. Historical imagery from Google Earth depicting the migration patterns through time of the seaward dune. The white rectangle indicates the location of the dune transect. Note that the dunes are underwater in some images, but their positions are still discernible. As with the landward site, the position of the dunes remains relatively fixed for several years.

3.3 Methods

3.3.1 Radiography

Polyvinyl chloride (PVC) sediment cores of the upper 34 cm of sediment were collected from various locations across the sandflat to compare the sedimentary fabric of interdune and dune crest sediments. The cores were cut in half using a circular saw and subsequently impressed into 24-gauge sheet metal channels (34 cm x 9 cm with 1.5 cm flanges on each side). The resulting sediment slabs were X-radiographed. Density differences within the slabs result in radiographs that display varying darkness according to the amount of radiation reaching each area. This darkness is related to the density of the material, with lighter zones (coarser-grained sediment) being more dense than darker zones (void space and finer-grained sediment). The density changes permit the identification of the sedimentary fabric, discrete burrows and the overall intensity of bioturbation. Field observations and x-rays of sediment cores were used to establish trace–tracemaker associations and measure bioturbation intensity. Although it is not advised to assign an ichnotaxon to modern traces (Bertling et al., 2006, 2022), we adopt this approach for the purpose of brevity and facilitating comparisons to paleoenvironmental analyses.

3.3.2 Sediment Analysis

Surficial sediment samples (upper 3 cm) were collected from various dune crests and interdunes shortly after the tide receded. Dune crest samples were taken from the highest point on the dune, whereas samples chosen to represent the interdune areas were collected roughly 1 m from the standing water pools. Nine stations were selected from across the study area for sediment analysis, with two samples being taken from each

station (Figure 2.1. Overview of the study area. (A) Map of the Bay of Fundy indicating the locations of the study sites. (B) Google Earth image of Site 1: Petitcodiac River, (C) Google Earth image of Site 2: Shepody River, and D) Google Earth image of Site 3: Selma. Figure 2.1B). The sediment was weighed prior to and following drying to determine the amount of pore water present in each sample.

Pore water content was determined for the sediment samples by determining weight percent (wt%) water of the bulk sample. The proportion of pore space filled by water was then estimated using the following steps. First, the volume of dry sand was calculated by dividing its mass by dry bulk density. In this calculation the dry bulk density is assumed to be 1.6 g/cm^3 (Bosboom and Stive, 2023). Next, total pore volume was then determined by multiplying the sand volume by the porosity fraction, assuming a consistent porosity value of 42% (Beard and Weyl, 1973). Finally, the total volume of pore water determined during the drying process was divided by the calculated total pore volume to determine the pore water content for each sample. The sediment samples were collected shortly after the tide receded at each station. As such the reported values presumably represent the maximum pore water content during subaerial exposure.

Seven samples were analyzed further to determine the respective weights of inorganic sediment, interstitial pore water, and organic matter. Organic matter content was determined via combustion elemental analysis (Thermo Scientific FLASH 2000 Organic Elemental Analyzer). In addition, grain size distributions were determined for four stations (eight samples), with grain sizes being classified according to Udden (1914) and Wentworth (1922) and reported in wt%.

3.3.3 Photogrammetry

Low-level drone photography was carried out using a DJI Mavic 2 Pro equipped with a Hasselblad L1D-20c camera. Photographs of the sandflat were taken roughly 4 m above the ground surface and with at least 60% overlap (James and Robson, 2012). The images were georeferenced, allowing for photogrammetry-based models to be built using Agisoft Metashape Professional software (version 1.7.4). Image alignment was facilitated by Structure-from-Motion algorithms (Ullman, 1979) whereby feature points were used to confirm geolocations (Verhoeven, 2011). The sparse clouds of georeferenced data points were processed using a Multi-View Stereo algorithm to improve the resolution of the model (Scharstein and Szeliski, 2002). Triangular meshes were generated from the dense point clouds, revealing the three-dimensional relief of the sandflats. The drone imagery was ultimately overlain onto the meshed models via texture maps generated by photostitching.

Photogrammetric models were used to generate orthographic projections of 5 m-wide dune transects that were aligned parallel to the direction of migration. The ends of each transect are demarcated by the edge of the standing water. Examination of the pooled areas was not feasible due to the disruption of water caused by the drone's propellers. The relationship between dune morphology and burrow distributions was assessed using photogrammetric techniques outlined in Melnyk et al. (2022a). Point counts of burrow openings were conducted at equidistant intervals across the transects, with each count representing an average of two 1 m² plots. To account for limitations in the resolution of the orthographic projection, only burrow apertures with a diameter greater than 1 mm were counted.

3.4 Results

The East Beach intertidal sandflat displays locally dense infaunal populations that are strongly influenced by the position of shore-parallel dunes. Grain size does not vary significantly, with very fine sand being the predominant grain size throughout the study area (Figure 3.4). Dune crest sediments display slightly higher sorting and are generally current-ripple laminated with locally occurring sheet sands. The uppermost sediments on the dune crests are mobile, thus wave ripples formed during high tide are likely reformed into current ripples during falling tide. The interdune areas consist of bioturbated sand with only locally preserved laminae. The topographic lows are characterized by the presence of biofilm, which appears to be an accumulation of planktonic biomass that is captured during falling and low tides.

3.4.1 Dune Characteristics and Bioturbation

The abundance of burrows was quantitatively assessed across two sand dunes: one located in the upper intertidal zone (landward dune), and the other in the middle intertidal zone (Figure 3.5; Table 3.1). The lower intertidal zone is heavily colonized by eelgrass and therefore was excluded from the study. The landward dune is located near the high-water mark (Figure 3.1B) and displays a symmetrical geometry (Figure 3.6). It has a wavelength of 33.8 m, is 0.9 m high, and has a volume of approximately 74.3 m³ of sediment within a 5-m wide transect (Table 3.1). The abundance of burrows varies markedly, ranging from 579 per m² in the seaward interdune to 11 per m² on the dune crest. Interestingly, changes in burrow abundance roughly correspond to the elevation profile of the dune (Figure 3.6).

The seaward dune differs from its landward counterpart by its smaller size and asymmetrical shape, displaying a steeper slope on the landward side (Figure 3.7). It has a

wavelength of 26.0 m, is 0.6 m high, containing 47.8 m³ of sediment within a 5 m-wide transect (Table 3.1). The distribution of burrows exhibits a similar trend to the landward dune. However, burrows are slightly more abundant, reaching a maximum of 709 burrow openings per m² in the interdune (Figure 3.7). The dune crests exhibit a more notable increase in burrow abundance, with a minimum of 118 burrow openings per m². Throughout the entire study area, bioturbation intensity is strongly correlated with the abundance of biodeformational structures made by foraging shorebirds, which were not examined in this study (see Melnyk et al., 2022b).

3.4.2 Trace-Tracemaker Distribution

The distribution of infauna and their traces was assessed using field observations supplemented by radiographs (Figure 3.8). The dominant tracemaker observed in the study area is the varnish clam *Nuttallia obscurata*, which produces equilibrium structures best described as *Siphonichnus*. These burrows typically penetrate the sediment to depths of 10 – 20 cm, although shallower depths are observed for juvenile tracemakers (Figure 3.8C,D). The lower portions of these traces consist of 1) the body cavity, 2) spreite produced as the tracemaker adjusts its position in the sediment, and 3) any disturbances caused by pedal feeding activities. The upper portion comprises two vertically oriented siphon traces and any downwarping of laminae that result from the continuous reaming of the burrow by the tracemaker. The most efficient sediment mover in the study area is the thalassinid shrimp *Neotrypaea californiensis*, which excavates interconnected burrow networks referable to *Thalassinoides*. These burrows generally range in diameter from 1 to 2 cm and have been reported to reach depths of up to 50 cm (Swinbanks & Murray, 1981). Lastly, the study area harbors a diverse range of polychaetes, including *Arenicola* sp., *Abarenicola pacifica*, *Nereis* sp., *Heteromastus filiformis*, and *Saccoglossus* sp..

These organisms produce a range of burrows referable to *Skolithos*, *Arenicolites*, *Polykladichnus* and *Planolites*, displaying highly variable lengths and diameters spanning from mm to cm scale.

The distribution of burrows is qualitatively assessed across the study area. The interdunes display comparably high ichnodiversity characterized by abundant *Skolithos* and *Siphonichnus* and lesser *Arenicolites*, *Polykladichnus* and *Thalassinoides*. The transition from interdune to dune crest is marked by a decrease in polychaete abundance that corresponds to a reduction in vertical to inclined (cf. *Skolithos*) and U-shaped burrows (cf. *Arenicolites*). As such, dune crest bioturbation is largely characterized by sparse *Siphonichnus-Thalassinoides* assemblages, along with sporadic occurrences of diminutive *Skolithos* and *Polykladichnus* produced by juvenile *Nereis* (Figure 3.8A,B). The disparity between dune crests and interdunes is consistent throughout the study area, but is less distinct in the seaward reaches, where burrows are more abundant. This is manifested by a progressive extension of polychaetes further up the dune profile, with minor amounts of *Skolithos* and *Arenicolites* being observed in the most distal dunes (e.g., the seaward dune).

3.4.3 Pore Water and Organic Carbon

A total of 18 sediment samples were collected from nine stations across the study area (Figure 2.1B). The pore water content ranges from 25.0 to 33.1 wt% in the interdunes and from 22.4 to 22.7 wt% on the dune crests (Table 3.2). Based on the assumptions discussed in the Methods section, the average volumetric pore water content for dune crest and interdune sediments are estimated to be 67% and 90%, respectively (Figure 3.9A; Table 3.2). The organic matter content of the dry sediment ranges from 0.16 to 0.26 wt% in the interdunes and from 0.15 to 0.19 wt% on the dune crests. Despite the relatively low

amount of organic matter and the considerably variable pore water content, these two parameters exhibit a strong positive correlation ($R^2 = 0.901$; Figure 3.9B).

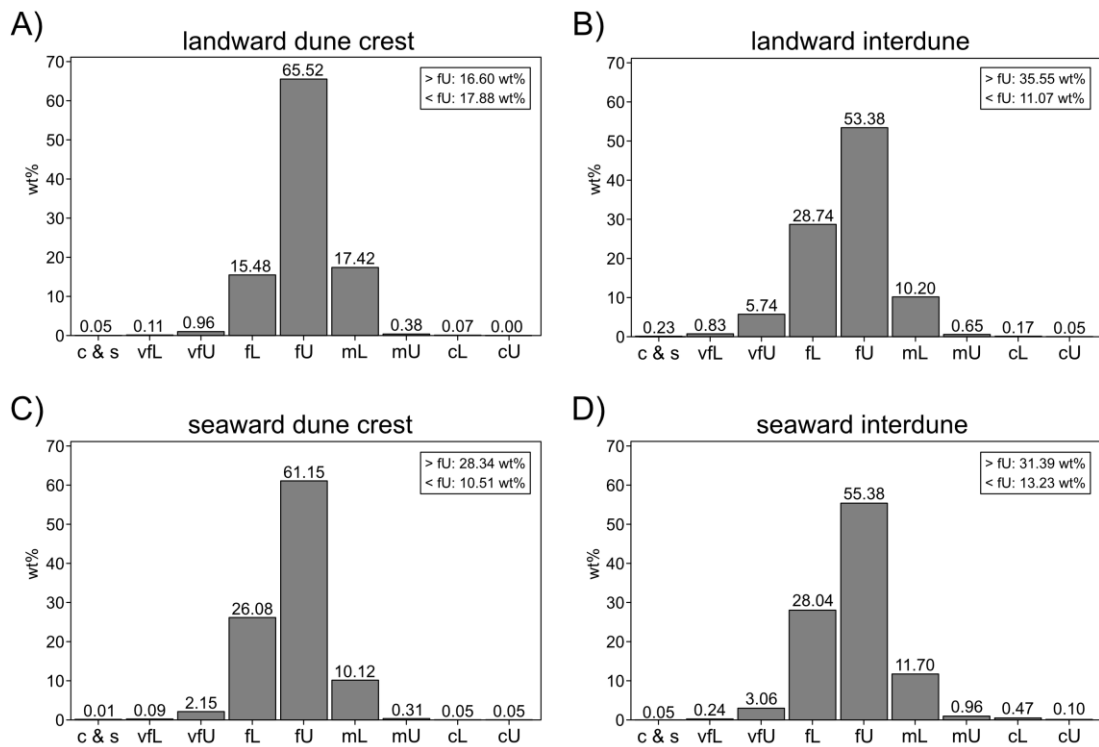


Figure 3.4. Grain size distributions acquired through sieving. (A) Dune crest sediments from the landward dune (station 2). (B) Interdune sediments from nearby the landward dune (station 1). (C) Dune crest sediments from the seaward dune (station 8). (D) Interdune sediments from the seaward dune (station 9). Grain sizes follow the Udden-Wentworth scale: c & s = clay and silt; vf = very fine sand; f = fine sand; m = medium sand; c = coarse sand. The modifiers U and L designate upper and lower subdivisions, respectively.

Table 3.1. Key features of the examined dunes within 5-meter wide transects perpendicular to the dune crests.

	Length [m]	Height [m]	Sediment volume [m ³]	Burrow density [burrows m ⁻²]
Landward dune	33.8	0.9	74.5	11-579
Seaward dune	26.0	1.0	61.8	118-709

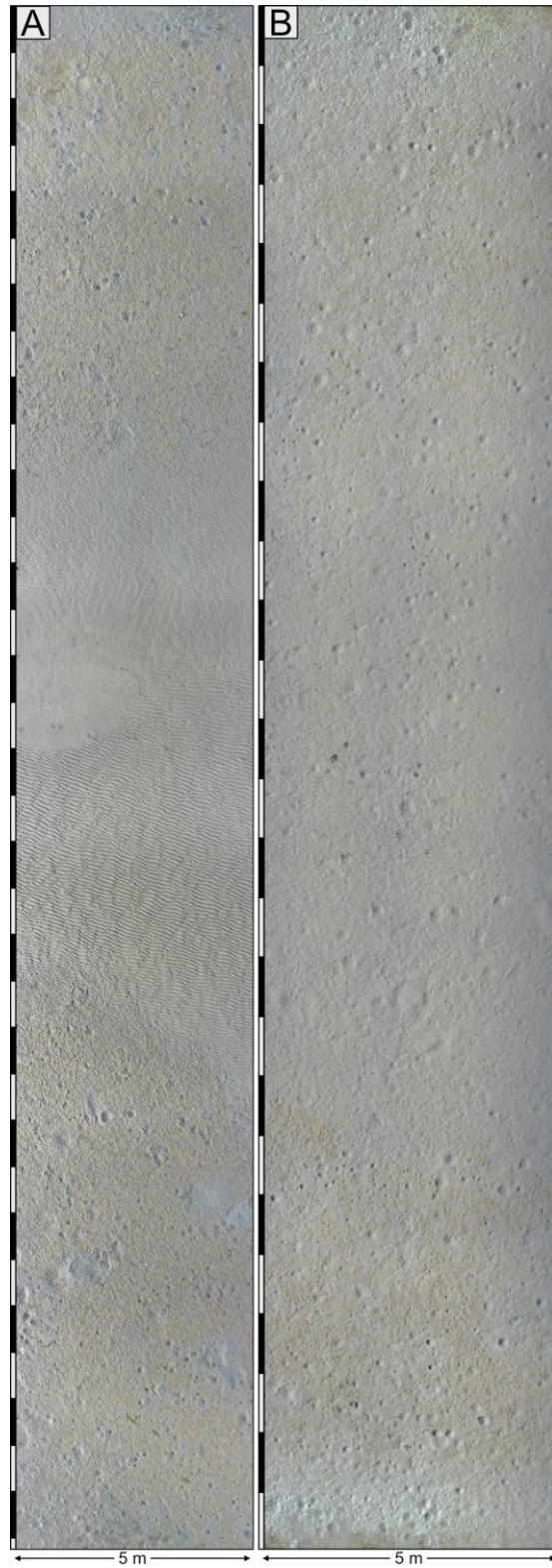


Figure 3.5. Orthographic projections of the (A) landward dune and (B) seaward dune transects showing the variation in surface features along the dune profiles. The landward direction is towards the bottom of the page.

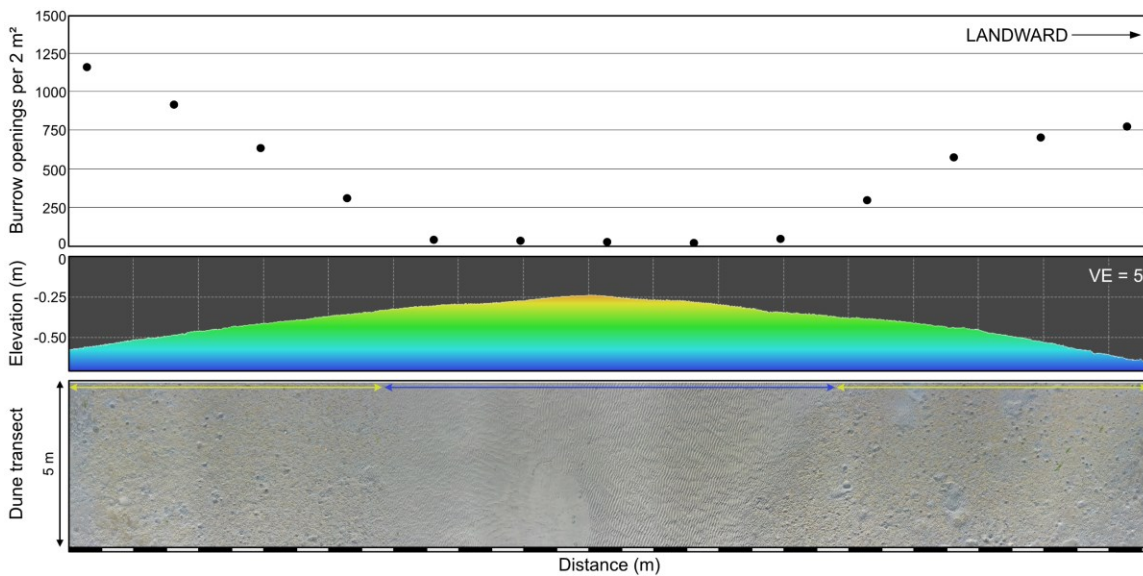


Figure 3.6. Assessment of burrow abundance along the cross-sectional profile of the landward dune. Plotted data illustrates the average count of burrow openings per two square meters along the profile (top). The dune profile is shown with a 5x vertical exaggeration (middle) and the orthographic projection from Figure 3A facilitates the comparison of burrow abundance to surface features (bottom). Note the development of ripples on the dune crest (blue arrow) and presence of biofilm in the interdune areas (yellow arrows).

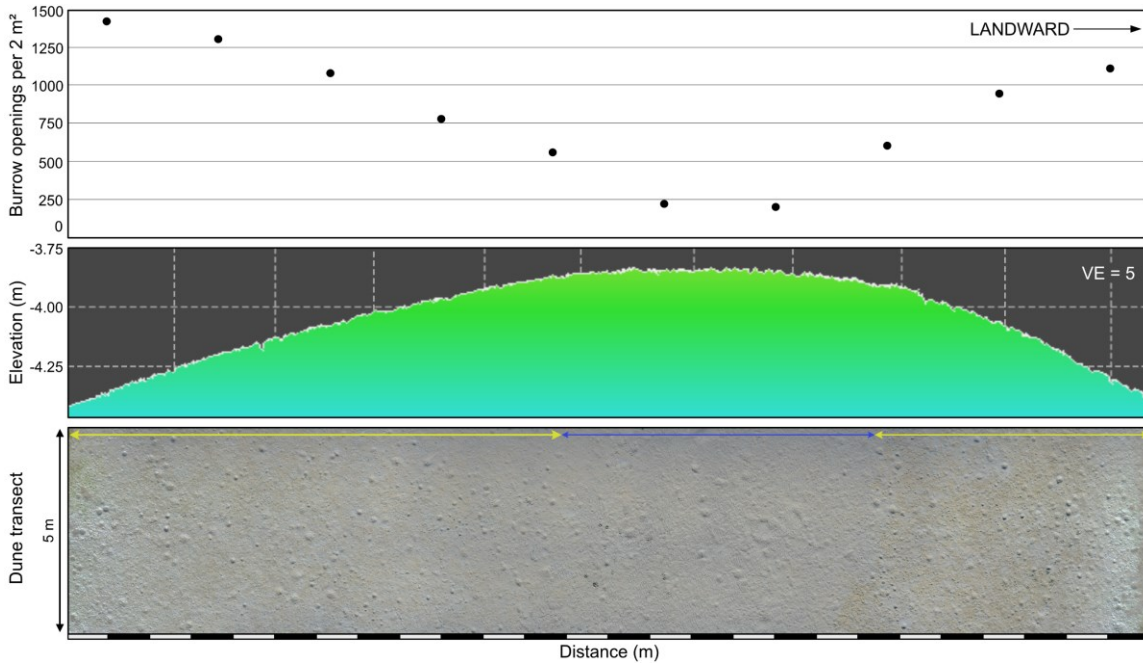


Figure 3.7. Assessment of burrow abundance along the cross-sectional profile of the seaward dune. Plotted data illustrates the average count of burrow openings per square meter at each respective position along the profile (top), which is presented with a vertical exaggeration of 5 (middle). Incorporating the orthographic projection from Figure 3B facilitates the comparison of burrow abundance to surface features (bottom). Note the development of patchy, poorly formed ripples on the dune crest (blue arrow) and increased abundance of biofilm in the interdune areas (yellow arrows).

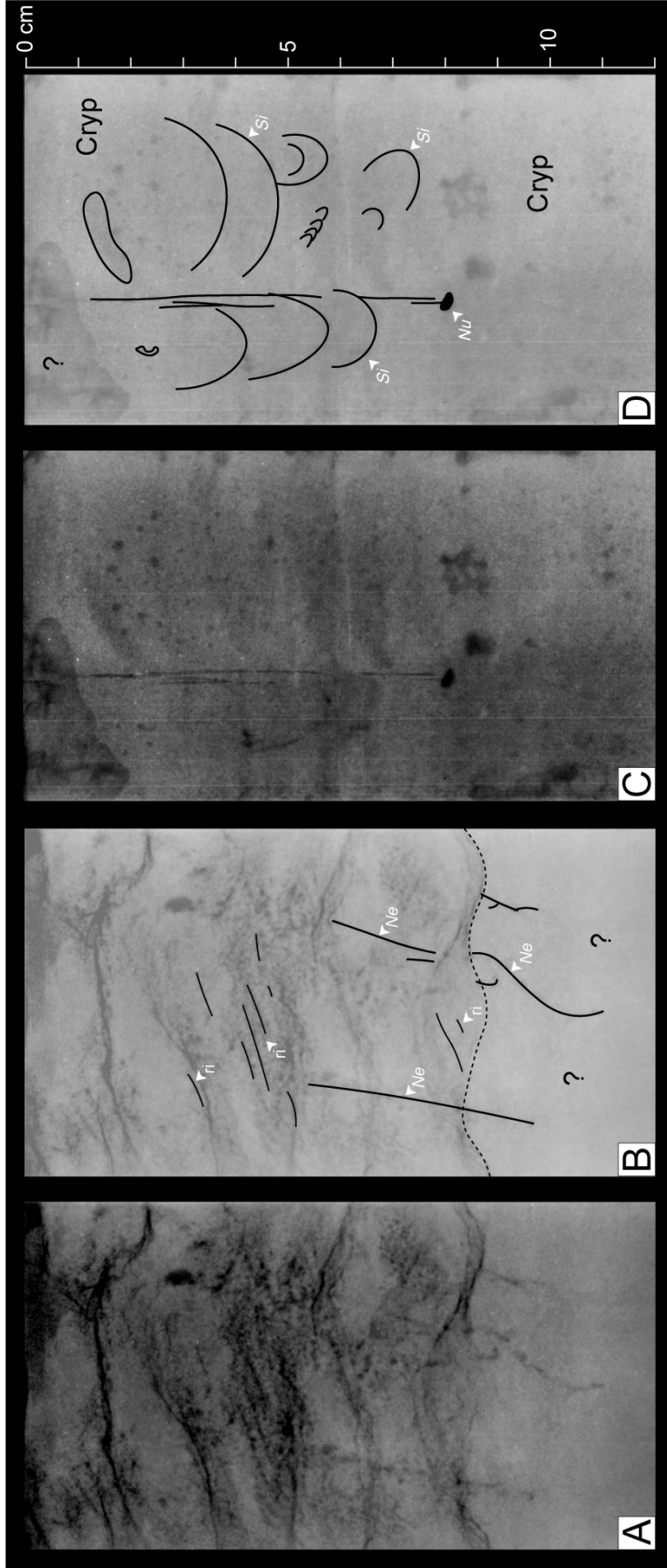


Figure 3.8. X-ray radiographs and schematic interpretations of sediment cores from the landward end of East Beach. A,B) Sediment core from a dune crest (station 2) showing current-ripples (ri) and locally observed juvenile *Mereis* burrows (Ne) that are best described as *Skolithos* and *Polykladichnus*. The dashed line marks the lower limit of observable lamination, beneath which the sediment exhibits a homogeneous appearance. C,D) Sediment core from an interdune area (station 1) showing the overall disruption of physical structure primarily by *Siphonichnus* (Sj) and cryptic bioturbation (cryp). The core also reveals a juvenile *Nuttallia obscurata* (Nu) producing an incipient *Siphonichnus*.

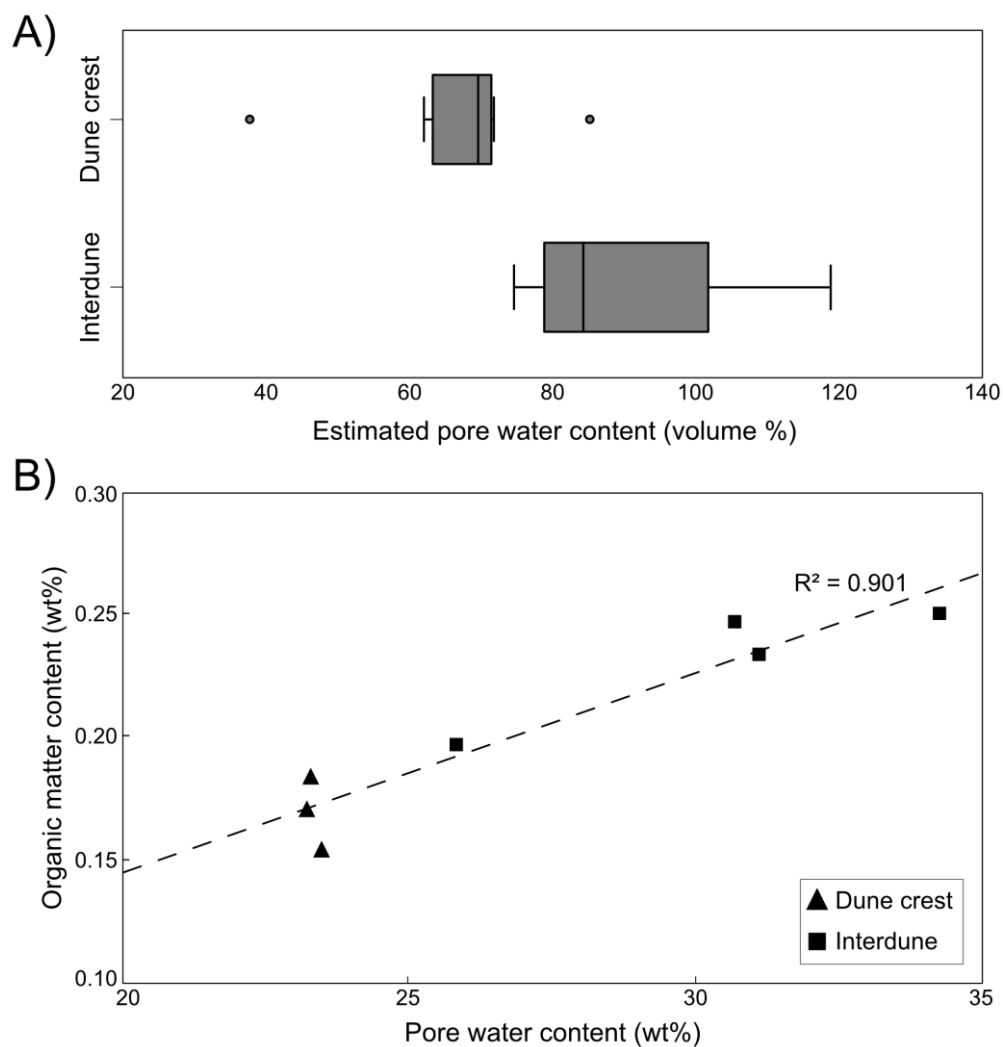


Figure 3.9. A) Box-and-whisker plot showing the estimated percentage of void filled by pore water for dune crest versus interdune sediment samples. B) Plot illustrating the correlation between pore water and organic matter content in surficial sediment samples collected from various stations within the study area. Reported weight percentages are based on the combined weight of the detrital sediment, organic matter, and pore water. The pore water content was determined once per sample, and the organic matter values represent the average of three replicates (see Table 3.2).

Table 3.2. Summary of pore water content (PWC) and organic matter content (OMC) from various stations across the study area.

Station	Sample #	Subenvironment	Latitude	Longitude	Wet sample mass [g]	Dry sample mass [g]	PWC [wt%]	PWC [volume %]*	OMC 1 [wt%]	OMC 2 [wt%]	OMC 3 [wt%]
1	1a	interdune	49.01430	-122.78567	40.0	29.9	25.3	81	-	-	-
1	1b	interdune	49.01430	-122.78567	39.9	26.7	33.1	119	0.26	0.26	0.23
2	2a	crest	49.01399	-122.78559	40.0	31.0	22.4	69	0.18	0.16	0.17
2	2b	crest	49.01399	-122.78559	40.0	34.6	13.6	38	-	-	-
3	3a	interdune	49.01380	-122.78577	39.9	27.9	30.1	103	0.24	0.22	0.24
3	3b	interdune	49.01380	-122.78577	39.9	29.2	26.7	88	-	-	-
4	4a	crest	49.01340	-122.78606	39.9	29.5	26.2	85	-	-	-
4	4b	crest	49.01340	-122.78606	40.0	31.8	20.5	62	-	-	-
5	5a	interdune	49.01330	-122.78608	40.1	28.2	29.7	101	0.24	0.24	0.26
5	5b	interdune	49.01330	-122.78608	40.0	29.0	27.5	91	-	-	-
6	6a	crest	49.01278	-122.78655	39.9	30.7	23.0	72	-	-	-
6	6b	crest	49.01278	-122.78655	40.0	31.0	22.5	70	0.18	0.19	0.18
7	7a	interdune	49.01274	-122.78645	40.1	30.6	23.7	75	-	-	-
7	7b	interdune	49.01274	-122.78645	40.0	30.1	24.7	79	-	-	-
8	8a	crest	49.01146	-122.78607	40.0	31.3	21.8	67	-	-	-
8	8b	crest	49.01146	-122.78607	40.0	30.9	22.7	70	0.15	0.16	0.15
9	9a	interdune	49.01149	-122.78596	40.0	30.0	25.0	80	0.20	0.20	0.19
9	9b	interdune	49.01149	-122.78596	40.0	30.1	24.7	79	-	-	-

*Values are estimated based on the assumptions of a dry bulk density of 1.6 g cm^{-3} and a porosity of 42%.

3.5 Topographic Controls on Intertidal Bioturbation

The spatial relationship between the dunes and burrow distributions at East Beach provides an opportunity to assess the influence of topography on the colonization of infaunal organisms. The distribution of burrows is highly influenced by the position of the dunes, with burrows being significantly more abundant in topographically low interdune areas. The factors that influence infaunal colonization and thereby burrow abundance across the study area are discussed below.

3.5.1 Shifting Substrates

Sedimentation stress at East Beach can be categorized according to timescales: there is short-term movement of near-surface sediments by currents during high tide, medium-term sediment mobilization caused by dune movement during storms, and potentially long-term sediment accumulation caused by an increase in accommodation space. The burrow distributions observed at East Beach are ostensibly linked to the short- and medium-term processes. Dunes are activated by major storms, subjecting all infauna to temporary but significant sedimentation stress. The newly formed dune surfaces are presumably unburrowed but colonized by infauna after the storm subsides. During these interstorm colonization windows, wave and tidal currents may mobilize the near-surface sediments. This sediment shifting can lead to the redistribution of sediments from the dune crests into the interdune regions, gradually reducing the dune's amplitude over time. While this daily sediment movement has a less pronounced impact compared to the sediment shifts caused by storms, it may still impede larval settlement (Butman, 1986), increase the energy needed for burrow maintenance (Gingras et al., 2011), and lead to lower levels of particulate organic matter (Miller and Suess, 1979).

Some studies have linked the occurrence of bioturbation to sediment supply and bedform migration in tidal settings (e.g., Pollard et al., 1993; Desjardins et al., 2010, 2012; Dashtgard, 2011a; Olariu et al., 2012), and over the long-term, higher rates of bedform migration should result in lower preservation of bioturbated strata. However, on shorter timeframes as measured in this study, there is pronounced infaunal zonation despite negligible sediment input and dune migration rates during fairweather conditions. This results in colonization windows that seemingly remain open for multiple years (Figure 3.2Figure 3.3). Based on current estimates, the time required to produce fully bioturbated media spans from seasonal to yearly timescales (Bentley et al., 2006; Gingras et al., 2008; Melnyk and Gingras, 2020). Considering these timescales, along with the infrequent occurrence of storm events in the study area, it can be inferred that sedimentation does not limit infaunal colonization at East Beach.

3.5.2 Subaerial Exposure

Subaerial exposure is detrimental to infaunal organisms due to physiological stresses related primarily to temperature changes, reduced pore water content, and potentially oxygen limitations. These stresses are more pronounced on the dune crests, where drainage and infiltration lead to desiccation during low tide. The interdunes are less affected at low tide due to the presence of standing water. This is significant because even a partial decrease in pore water content can impede bioirrigation processes, which play a critical role in supporting respiration and facilitating solute exchange (e.g., Thompson and Pritchard, 1969; Aller and Aller, 1998; Meysman et al. 2006; Wrede et al., 2019). Our pore water estimations suggest that the near-surface pore spaces in the interdune sediments ranged from 48.9% to 110.5% in the dune crest and 96.7% to 154.0% in the interdune (Figure 3.9A; Table 3.2). The values exceeding 100% are most likely

attributed to errors in the estimation of bulk density and porosity. Nonetheless, the relative difference in pore water content between the dune crest and interdune areas may explain the patterns of burrow distribution, especially during the late stages of exposure when pore water content is presumably lower than the values reported herein.

Data obtained from sediment samples indicate that the pore water content remains relatively stable on the dune crests, whereas the interdunes display higher but fluctuating values (Figure 3.9A; Table 3.2). At the dune scale, reductions in pore water content from interdunes to dune crest range from 9.2 – 32.2%, without a discernible trend along the intertidal gradient. This suggests that topography has a greater influence on pore water content during low tide compared to intertidal position. Importantly, the sediment samples were collected shortly after the tide receded, thus the reported pore water content approximates the maximum pore water present during exposure. Thus, our results should be considered in a relative sense as opposed to considering the reported value as a limiting factor.

Local variations in pore water content throughout East Beach are strongly correlated with tracemaker distributions. The water-saturated interdune sediments are inhabited by all locally observed tracemakers, leading to relatively high ichnodiversities compared to the dune crests. Polychaetes are notably absent on upper intertidal dune crests and occur only in small numbers on middle intertidal dune crests. The presence of *N. obscurata* on the exposed dune crests may be partially attributed to their ability to retreat into their shell during low tide to avoid desiccation in water-depleted sediment. Clams mitigate the effects of oxygen deficiency by closing their valves and utilizing anaerobic metabolism, which substantially reduces their metabolic rate (Grieshaber et al., 1994; Ortmann and Grieshaber, 2003). The deeply burrowing *Neotrypaea californiensis* may retreat into water-saturated sediment during low tide to avoid desiccation and utilize

hydraulic activity to facilitate the transport of oxygenated water into their burrows and surrounding sediment (Volkenborn et al., 2012). Moreover, *N. californiensis* can survive for up to 5.7 days under anoxic conditions when required (Thompson and Pritchard, 1969).

In addition to providing a source of pore water, seawater coverage also reduces harmful exposure to ultraviolet radiation and provides a buffer for diurnal temperature fluctuations. However, evaluating thermal stress in intertidal environments is complex due to variations in space and time (Helmuth and Hofmann, 2001). This is because the magnitude of stress depends on several factors, including but not limited to seawater temperature, atmospheric temperature, duration of exposure, and sediment depth (Johnson, 1965; Roberts et al. 1997, Feder and Hofmann 1999). For example, sediments at higher elevations experience greater diurnal temperature fluctuations due to increased exposure to direct sunlight. There is also a significant reduction in thermal variability at a depth of 10 cm in the sediment column of sandy tidal flats (Johnson, 1965). This may explain why infauna living in subaerially exposed dune crest sediments (*e.g.*, *N. obscurata* and *N. californiensis*) generally burrow to depths greater than 10 cm. At these depths the pore water content is greater in comparison to the surface, further reducing the physiological stress experienced by the relatively large tracemakers on the dune crests.

3.5.3 Food Availability

Field observations indicate that surficial biofilms and detrital organic matter are regularly exploited by interface feeders at East Beach. Not surprisingly, invertebrates that rely more heavily on this mode of feeding (*i.e.*, polychaetes) are exclusively found in areas with biofilm. In contrast, the persistence of *N. obscurata* on dune crests is likely due to its ability to employ diverse feeding strategies. In addition to being effective filter feeders, they use pedal-sweep movements to deposit feed during times of exposure. *Nuttallia*

obscurata has also been reported to interface feed on particulate organic matter (Tsuchiya and Kurihara, 1980). The presence of sediment mounds around burrow openings of *Neotrypaea californiensis* suggests that these tracemakers primarily deposit feed on buried organic matter, however they may also obtain nutrients through filter/suspension feeding or drift catching (Griffis and Suchanek, 1991).

The diversity of feeding strategies employed by resident tracemakers suggests that food may be readily available despite the low concentration of particulate organic matter in the sediment (e.g., suspended organic matter; Gingras and MacEachern, 2012). Nonetheless, the empirical relationship between biofilms and burrow abundance suggests that its relevance should be considered. One possible explanation for the minimal variation observed in organic matter along dune profiles is that the biofilms are only present at the surface, resulting in their underrepresentation in a wt% analysis of sediment collected at a depth of 3 cm.

Microorganisms inhabiting intertidal sand and mudflats serve as significant sources of food within intertidal environments (e.g., Decho, 1990; Decho and Lopez, 1993; Herman et al., 2000; Hoskins et al., 2003; Nagarkar et al., 2004). These microbial communities are predominantly composed of prokaryotes and microbial eukaryotes (particularly cyanobacteria and diatoms) (Decho, 2000). The structure and functioning of these communities are directly influenced by the environmental factors discussed herein. For example, sediment redistribution caused by ripple migration hinders the accumulation of biofilms. Furthermore, prolonged subaerial exposure imposes stress related to desiccation (Coelho et al., 2009), ultraviolet radiation (Mouget et al., 2008; Waring et al., 2007), and salinity and temperature fluctuations (Rijstenbil, 2005; Hořtacká et al., 2010). The effective reduction of one or more of these stresses may promote the development of biofilms in the interdune areas of East Beach.

3.6 Paleoenvironmental Implications

Research on bioturbation intensity often considers the concept of the colonization window, whereby a lack of sediment accumulation promotes larval recruitment and the bioturbation of near-surface sediments (Wheatcroft et al., 1990). This implies that, under otherwise similar conditions, sediment layers deposited under slower sedimentation rates should exhibit greater bioturbation intensities. Although the inverse relationship between sedimentation rate and bioturbation intensity remains a useful framework (Reineck et al., 1967; Howard, 1978; Gingras et al., 2011; Allport et al., 2021), this study emphasizes the importance of sedimentological context when interpreting sedimentary rocks.

The cross-beds produced by dune migration in East Beach are largely reworked by bioturbation, providing evidence that the bedforms are not exceedingly mobile. As such, integrated sedimentological and ichnological analyses of comparable rock record examples would indicate subdued sedimentation rates. The more accurate depiction as discerned through field observations is as follows: general sedimentary stasis and periodic subaerial exposure, punctuated by storm events during which the dunes reactivate, form a new cross-bedded sedimentary fabric that stratigraphically overlies the previously adjacent bioturbated sediment. Over time, this primary sedimentary fabric becomes overprinted by bioturbation.

3.7 Summary

The shoreline-parallel dunes at East Beach present a unique opportunity to assess the influence of topographically-controlled factors on the distribution of intertidal invertebrates and their burrows. This study shows that burrow abundance correlates strongly with topography, with the lower elevations (interdunes) displaying a markedly

higher abundance of burrows compared to higher elevations (dune crests). The preference for infauna to colonize the interdunes is putatively ascribed to the interrelated factors of subaerial exposure, food availability, and shifting substrates. Among these factors, subaerial exposure appears to exert the primary influence, largely owing to its impact on pore water content and consequential effects on bioirrigation processes (e.g., respiration and solute exchange). The presence of surficial biofilms in the interdune sediments may favour colonization, however many of the tracemakers are known suspension feeders and thus may obtain additional food from the water column during high tide. Moreover, the low net dune migration rates suggest that near-surface sediment shifting during high tide constitutes the only sedimentation stress between storm events. Although additional work is needed to assess the relative influence of each factor, this study provides a detailed assessment of heterogeneous bioturbation distribution that is complementary to intertidal studies conducted on more regional scales (Swinbanks, 1981; Dashtgard 2011a,b).

3.8 References

- Aller, R. C., & Aller, J. Y. (1998). The effect of biogenic irrigation intensity and solute exchange on diagenetic reaction rates in marine sediments. *Journal of Marine Research*, *56*, 905–936.
- Allport, H. A., Davies, N. S., Shillito, A. P., Mitchell, E. G., & Herron, S. T. (2022). Non-palimpsested crowded *Skolithos* ichnofabrics in a Carboniferous tidal rhythmite: Disentangling ecological signatures from the spatio-temporal bias of outcrop. *Sedimentology*, *69*, 1028–1050.
- Ashley, G. M. (1990). Classification of large-scale subaqueous bedforms: A new look at an old problem. *Journal of Sedimentary Research*, *60*, 160–172.
- Beard, D. C., & Weyl, P. K. (1973). Influence of Texture on Porosity and Permeability of Unconsolidated Sand. *AAPG Bulletin*, *57*, 349–369.
- Bentley, S. J., Sheremet, A., & Jaeger, J. M. (2006). Event sedimentation, bioturbation, and preserved sedimentary fabric: Field and model comparisons in three contrasting marine settings. *Continental Shelf Research*, *26*, 2108–2124.
- Bertling, M., Braddy, S. J., Bromley, R. G., Demathieu, G. R., Genise, J., Mikuláš, R., ... Uchman, A. (2006). Names for trace fossils: A uniform approach. *Lethaia*, *39*, 265–286.
- Bertling, M., Buatois, L. A., Knaust, D., Laing, B., Mángano, M. G., Meyer, N., ... Wisshak, M. (2022). Names for trace fossils 2.0: Theory and practice in ichnotaxonomy. *Lethaia*, *55*, 1–19.
- Bosboom, J., & Stive, M. J. F. (2023). Coastal Dynamics. In *TU Delft OPEN Textbooks*. TU Delft Open Textbooks.
- Butman, C. A. (1986). Larval settlement of soft-sediment invertebrates: Some predictions

- based on an analysis of near-bottom velocity profiles. In J. C. J. Nihoul (Ed.), *Marine Interfaces Ecohydrodynamics* (Vol. 42, pp. 487–513).
- Coelho, H., Vieira, S., & Serôdio, J. (2009). Effects of desiccation on the photosynthetic activity of intertidal microphytobenthos biofilms as studied by optical methods. *Journal of Experimental Marine Biology and Ecology*, *381*, 98–104.
- Dashtgard, S. E. (2011a). Linking invertebrate burrow distributions (neoichnology) to physicochemical stresses on a sandy tidal flat: Implications for the rock record: Tidal-flat ichnology. *Sedimentology*, *58*, 1303–1325.
- Dashtgard, S. E. (2011b). Neoichnology of the lower delta plain: Fraser River Delta, British Columbia, Canada: Implications for the ichnology of deltas. *Palaeogeography, Palaeoclimatology, Palaeoecology*, *307*, 98–108.
- Dashtgard, S. E., & Gingras, M. K. (2012). Chapter 10—Marine Invertebrate Neoichnology. In D. Knaust & R. G. Bromley (Eds.), *Developments in Sedimentology* (pp. 273–295). Elsevier.
- Dashtgard, S. E., Gingras, M. K., & Pemberton, S. G. (2008). Grain-size controls on the occurrence of bioturbation. *Palaeogeography, Palaeoclimatology, Palaeoecology*, *257*, 224–243.
- Decho, A. W. (1990). Microbial exopolymer secretions in ocean environments: Their role(s) in food webs and marine processes. In H. Barnes (Ed.), *Oceanography and Marine Biology: An Annual Review* (Vol. 28, pp. 73–153).
- Decho, Alan W. (2000). Microbial biofilms in intertidal systems: An overview. *Continental Shelf Research*, *20*, 1257–1273.
- Decho, Alan W., & Lopez, G. R. (1993). Exopolymer microenvironments of microbial flora: Multiple and interactive effects on trophic relationships. *Limnology and Oceanography*, *38*, 1633–1645.

- Desjardins, P. R., Buatois, L. A., Pratt, B. R., & Mángano, G., M. (2012). Sedimentological-ichnological model for tide-dominated shelf sandbodies: Lower Cambrian Gog Group of western Canada: Subtidal compound cross-stratified sandstone architecture. *Sedimentology*, *59*, 1452–1477.
- Desjardins, P. R., Mángano, M. G., Buatois, L. A., & Pratt, B. R. (2010). *Skolithos* pipe rock and associated ichnofabrics from the southern Rocky Mountains, Canada: Colonization trends and environmental controls in an early Cambrian sand-sheet complex. *Lethaia*, *43*, 507–528.
- Feder, M. E., & Hofmann, G. E. (1999). Heat-shock proteins, molecular chaperones, and the stress response: Evolutionary and ecological physiology. *Annual Review of Physiology*, *61*, 243–282.
- Gingras, M. K., & MacEachern, J. A. (2012). Tidal Ichnology of Shallow-Water Clastic Settings. In R. A. Davis Jr. & R. W. Dalrymple (Eds.), *Principles of Tidal Sedimentology* (pp. 57–77). Dordrecht: Springer Netherlands.
- Gingras, M. K., MacEachern, J. A., & Dashtgard, S. E. (2011). Process ichnology and the elucidation of physico-chemical stress. *Sedimentary Geology*, *237*, 115–134.
- Gingras, M. K., Pemberton, S. G., Dashtgard, S., & Dafoe, L. (2008). How fast do marine invertebrates burrow? *Palaeogeography, Palaeoclimatology, Palaeoecology*, *270*, 280–286.
- Gingras, M. K., Pemberton, S. G., & Saunders, T. (2000). Firmness Profiles Associated with Tidal-Creek Deposits: The Temporal Significance of Glossifungites Assemblages. *Journal of Sedimentary Research*, *70*, 1017–1025.
- Gingras, M. K., Pemberton, S. G., Saunders, T., & Clifton, H. E. (1999). The ichnology of modern and Pleistocene brackish-water deposits at Willapa Bay, Washington; variability in estuarine settings. *Palaios*, *14*, 352–374.

- Grant, J. (1981). Sediment Transport and Disturbance on an Intertidal Sandflat: Infaunal Distribution and Recolonization. *Marine Ecology Progress Series*, 6, 249–255.
- Grieshaber, M. K., Hardewig, I., Kreutzer, U., & Pörtner, H.-O. (1994). Physiological and Metabolic Responses to Hypoxia in Invertebrates. In S. H. F. Pedersen (Ed.), *Reviews of Physiology, Biochemistry and Pharmacology* (Vol. 125, pp. 43–147). Berlin, Heidelberg: Springer.
- Griffis, R. B., & Suchanek, T. H. (1991). A model of burrow architecture and trophic modes in thalassinidean shrimp (Decapoda: Thalassinidea). *Marine Ecology Progress Series*, 79, 171–183.
- Hauck, T. E., Dashtgard, S. E., & Gingras, M. K. (2008). Relationships between organic carbon and Pascichnia morphology in intertidal deposits: Bay of Fundy, New Brunswick, Canada. *Palaios*, 23, 336–343.
- Helmuth, B. S. T., & Hofmann, G. E. (2001). Microhabitats, Thermal Heterogeneity, and Patterns of Physiological Stress in the Rocky Intertidal Zone. *The Biological Bulletin*, 201, 374–384.
- Herman, P. M. J., Middelburg, J. J., Widdows, J., Lucas, C. H., & Heip, C. H. R. (2000). Stable isotopes as trophic tracers: Combining field sampling and manipulative labelling of food resources for macrobenthos. *Marine Ecology Progress Series*, 204, 79–92.
- Hoskins, D. L., Stancyk, S. E., & Decho, A. W. (2003). Utilization of algal and bacterial extracellular polymeric secretions (EPS) by the deposit-feeding brittlestar *Amphipholis gracillima* (Echinodermata). *Marine Ecology Progress Series*, 247, 93–101.
- Hošťacká, A., Čižnár, I., & Štefkovičová, M. (2010). Temperature and pH affect the production of bacterial biofilm. *Folia Microbiologica*, 55, 75–78.
- Howard, J. D. (1978). Sedimentology and Trace Fossils. In P. B. Basan (Ed.), *Trace Fossil*

Concepts (Vol. 5, p. 0). SEPM Society for Sedimentary Geology.

- James, M. R., & Robson, S. (2012). Straightforward reconstruction of 3D surfaces and topography with a camera: Accuracy and geoscience application. *Journal of Geophysical Research: Earth Surface*, 117. Retrieved from <http://agupubs.onlinelibrary.wiley.com/doi/abs/10.1029/2011JF002289>
- Johnson, R. G. (1965). Temperature variation in the infaunal environment of a sand flat. *Limnology and Oceanography*, 10, 114–120.
- Melnyk, S., Cowper, A., Zonneveld, J.-P., & Gingras, M. K. (2022). Applications of photogrammetry to neoichnological studies: The significance of shorebird trackway distributions at the bay of fundy. *Palaios*, 37, 606–621.
- Melnyk, S., & Gingras, M. (2020). Using ichnological relationships to interpret heterolithic fabrics in fluvio-tidal settings. *Sedimentology*, 67. <https://doi.org/10.1111/sed.12674>
- Melnyk, S., Lazowski, C. N., & Gingras, M. K. (2022). Sedimentological and ecological significance of a biodeformational structure associated with an unusual feeding behavior in gulls (*Larus* sp.). *Ichnos*, 29, 84–92.
- Meysman, F. J. R., Galaktionov, O. S., Gribsholt, B., & Middelburg, J. J. (2006). Bioirrigation in permeable sediments: Advective pore-water transport induced by burrow ventilation. *Limnology and Oceanography*, 51, 142–156.
- Mouget, J.-L., Perkins, R., Consalvey, M., & Lefebvre, S. (2008). Migration or photoacclimation to prevent high irradiance and UV-B damage in marine microphytobenthic communities. *Aquatic Microbial Ecology*, 52, 223–232.
- Müller, P. J., & Suess, E. (1979). Productivity, sedimentation rate, and sedimentary organic matter in the oceans—I. Organic carbon preservation. *Deep Sea Research Part A. Oceanographic Research Papers*, 26, 1347–1362.

- Nagarkar, S., Williams, G. A., Subramanian, G., & Saha, S. K. (2004). Cyanobacteria-Dominated Biofilms: A High Quality Food Resource for Intertidal Grazers. In P. O. Ang (Ed.), *Asian Pacific Phycology in the 21st Century: Prospects and Challenges* (pp. 89–95). Dordrecht: Springer Netherlands.
- Ortmann, C., & Grieshaber, M. K. (2003). Energy metabolism and valve closure behaviour in the Asian clam *Corbicula fluminea*. *Journal of Experimental Biology*, *206*, 4167–4178.
- Patel, S. J., & Desai, B. G. (2009). Animal-sediment relationship of the crustaceans and polychaetes in the intertidal zone around Mandvi, Gulf of Kachchh, Western India. *Journal of the Geological Society of India*, *74*, 233–259.
- Pollard, J. E., Goldring, R., & Buck, S. G. (1993). Ichnofabrics containing *Ophiomorpha*: significance in shallow-water facies interpretation. *Journal of the Geological Society*, *150*, 149–164.
- Reineck, H.-E. (1967). Parameter von Schichtung und Bioturbation. *Geologische Rundschau*, *56*, 420–438.
- Rijstenbil, J. W. (2005). UV- and salinity-induced oxidative effects in the marine diatom *Cylindrotheca closterium* during simulated emersion. *Marine Biology*, *147*, 1063–1073.
- Roberts, D. A., Hofmann, G. E., & Somero, G. N. (1997). Heat-Shock Protein Expression in *Mytilus californianus*: Acclimatization (Seasonal and Tidal-Height Comparisons) and Acclimation Effects. *The Biological Bulletin*, *192*, 309–320.
- Rodríguez-Tovar, F. J., Seike, K., & Allen Curran, H. (2014). Characteristics, Distribution Patterns, and Implications for Ichnology of Modern Burrows of *Uca* (*Leptuca*) *Speciosa*, San Salvador Island, Bahamas. *Journal of Crustacean Biology*, *34*, 565–572.

- Scharstein, D., & Szeliski, R. (2002). A taxonomy and evaluation of dense two-frame stereo correspondence algorithms. *International Journal of Computer Vision*, 47, 7–42.
- Swinbanks, D. D. (1981). Sediment reworking and the biogenic formation of clay laminae by *Abarenicola pacifica*. *Journal of Sedimentary Research*, 51, 1137–1145.
- Swinbanks, D. D., & Murray, J. W. (1981). Biosedimentological zonation of Boundary Bay tidal flats, Fraser River Delta, British Columbia. *Sedimentology*, 28, 201–237.
- Taylor, A. M., & Goldring, R. (1993). Description and analysis of bioturbation and ichnofabric. *Journal of the Geological Society*, 150, 141–148.
- Thompson, R. K., & Pritchard, A. W. (1969). Respiratory adaptations of two burrowing crustaceans, *Callinassa californiensis* and *Upogebia pugettensis* (decapoda, thalassinidea). *The Biological Bulletin*, 136, 274–287.
- Tsuchiya, M., & Kurihara, Y. (1980). Effect of the feeding behaviour of macrobenthos on changes in environmental conditions of intertidal flats. *Journal of Experimental Marine Biology and Ecology*, 44, 85–94.
- Uchman, A. (2003). Trends in diversity, frequency and complexity of graphoglyptid trace fossils: Evolutionary and palaeoenvironmental aspects. *Palaeogeography, Palaeoclimatology, Palaeoecology*, 192, 123–142.
- Udden, J. A. (1914). Mechanical composition of clastic sediments. *GSA Bulletin*, 25, 655–744.
- Ullman, S. (1979). The interpretation of motion from structure. *Proceedings of the Royal Society of London Series B, Biological Sciences*, 203, 405–426.
- Verhoeven, G. (2011). Taking computer vision aloft – archaeological three-dimensional reconstructions from aerial photographs with photostan. *Archaeological Prospection*, 18, 67–73.
- Volkenborn, N., Polerecky, L., Wetthey, D., DeWitt, T., & Woodin, S. (2012). Hydraulic

- activities by ghost shrimp *Neotrypaea californiensis* induce oxic–anoxic oscillations in sediments. *Marine Ecology Progress Series*, 455, 141–156.
- Waring, J., Baker, N. R., & Underwood, G. J. C. (2007). Responses of estuarine intertidal microphytobenthic algal assemblages to enhanced ultraviolet B radiation. *Global Change Biology*, 13, 1398–1413.
- Wentworth, C. (1922). A scale of grade and class terms for clastic sediments. *The Journal of Geology*, 30, 337–424.
- Wheatcroft, R. A. (1990). Preservation potential of sedimentary event layers. *Geology*, 18, 843–845.
- Wrede, A., Andresen, H., Asmus, R., Wiltshire, K. H., & Brey, T. (2019). Macrofaunal irrigation traits enhance predictability of nutrient fluxes across the sediment–water interface. *Marine Ecology Progress Series*, 632, 27–42.
- Yang, B., Dalrymple, R. W., Gingras, M. K., & Pemberton, S. G. (2009). Autogenic occurrence of *Glossifungites Ichnofacies*: Examples from wave-dominated, macrotidal flats, southwestern coast of Korea. *Marine Geology*, 260, 1–5.

CHAPTER 4 – SEDIMENTOLOGICAL AND ECOLOGICAL SIGNIFICANCE OF A BIODEFORMATIONAL STRUCTURE ASSOCIATED WITH AN UNUSUAL FEEDING BEHAVIOUR IN GULLS (*LARUS* SP.)

4.1 Introduction

Biogenic sedimentary structures are disruptions of sedimentary substrates that are produced by organisms such as animals, microbes, and plants. Biodeformational structures are a subset of biogenic sedimentary structures characterized by poorly defined outlines and geometries (Schäfer, 1956; Wetzel, 1983, 1991). Additionally, biodeformational structures tend to be relatively large and associated with relatively high degrees of bioturbation, so they are less commonly preserved in full relief than discrete ichnofossils. Poorly preserved examples may be indistinguishable from soft-sediment deformation because they are commonly associated with soupy to soft substrates (e.g., Wetzel & Uchman, 1998; Lobza & Schieber, 1999; Miguez-Salas & Rodríguez-Tovar, 2019).

In addition to their indistinct architectures and poor preservation potential, the enigmatic nature of biodeformational structures is due in part to a lack of understanding of how they are formed, which can be difficult to assess from rock-record examples. This study describes an unusual biodeformational structure produced by a gull (*Larus* sp.) on an intertidal sand flat near White Rock, British Columbia, Canada. These structures have been documented at various locations worldwide, however they have received little attention since the 1990s (e.g., Müller, 1985; Cadée, 1990; Gregory, 1999; Martin, 2013, p. 479). This study uses field observations of the tracemaker actively liquifying the sediment to provide a unique insight into the significance of these biogenic sedimentary structures.

We provide the first formal documentation of the feeding structures from the Pacific Coast of North America and refine earlier interpretations of the structures.

4.2 Study Area

Semiahmoo Bay is located south of the Fraser River Delta in southwestern British Columbia (BC). It is partly split by the Canada–United States border and is bounded by the city of Delta, BC to the north, cities of White Rock, BC and Blaine, Washington to the east, and the Tsawwassen Peninsula to the west. The mouth of the bay is approximately 19 km wide and opens into the Strait of Georgia to the south.

The bay is a relatively shallow water setting (up to approximately 10 m depth) with an intertidal zone that extends over a kilometer into the bay during low tide and covers an area of approximately 4.2 km² along the East Beach of White Rock, BC. The tidal range is upper microtidal to lower mesotidal with a mean tidal range of 1.9 m. The bay is dominated by well sorted, fine-grained sand with minor amounts of silt and clay. The sediment forms straight to sinuous crested dunes with heavily bioturbated interdune areas. The only nearby source of continental sediment comes from the relatively small Little Campbell River (drainage area 75 km²) (Wiberg & Jackson, 2017).

The study area was accessed by driving south down Highway 99, exiting onto 8th Avenue west and continuing to Marine Drive in the city of White Rock. City parking to East Beach is available at the corner of Finlay Street and Marine Drive where the tidal flat was entered via footpath (Figure 4.1). Notably, Semiahmoo Bay was designated as a wildlife management area in 1995, deemed critical for the conservation of migrating and wintering waterfowl and shorebird populations (British Columbia MFLNRO, 2021). No permits were required to access the study area.

4.3 Methods

Field work was carried out on September 6, 2021, at approximately low tide. Field photography and videography was conducted using an Olympus Tough TG-6 digital camera and a DJI Mavic 2 Pro drone equipped with a Hasselblad L1D-20c camera. The photos taken with the Olympus Tough were captured with the following settings: 4000 x 3000 pixels, 314 dpi, ISO 100, aperture f/2.8, exposure time 1/800 seconds, focal length 4 mm. The camera settings for videos were 1920 x 1080 pixels (FHD) and 30 frames/second. Additional video was taken with the drone in an attempt to get closer to the trace maker; the camera settings for the video were the same as for the TG-6. The photographic settings of the Hasselblad were as follows: 960 x 544 pixels, 96 dpi, ISO 100, aperture f/4.5, exposure time 1/160 seconds, focal length 10 mm.

The photogrammetric model of the sedimentary structure was built using Agisoft Metashape Professional software (v 1.7.4). Photographs were aligned using Structure-from-Motion (SfM; Ullman, 1979) algorithms. Feature points that could be distinctly recognized were used to confirm 3D locations (Verhoeven, 2011). Following photo alignment, intrinsic and extrinsic orientation parameters were computed using the location where the photograph was captured (Javernick et al., 2014). The output was a sparse point cloud which was then processed using a Multi-View Stereo (MVS; Scharstein & Szeliski, 2002; Seitz et al., 2006) algorithm to increase the reliability of the model. The SfM algorithm relied on distinctive features points to obtain spatial information, whereas MVS matches the values of individual pixels of the previously aligned photographs. This step can improve the resolution of the model by up to three orders of magnitude (Scharstein & Szeliski, 2002; Seitz et al. 2006). Next, a triangular mesh was generated from the dense point cloud, revealing the 3D relief of the trace. Each vertex of the triangular

mesh was assigned two coordinates, both of which were determined from a texture map that is generated by photo stitching (Tavani et al., 2014). Each triangle in the mesh is georeferenced and the corresponding textured triangle is projected onto the mesh surface, generating a complete 3D model. Finally, the raw imagery was overlain onto the surface of the model.

4.4 An Unusual Feeding Trace

The tracemaker, *Larus* sp., was observed kneading the sediment while slowly moving backwards and probing intermittently in search of food (Figure 4.2A-B). Iterative stepping in place and moving its feet back and forth caused the tracemaker to sink into the sediment; this continued until its belly nearly touched the sediment. The gull would stop momentarily to probe the sediment for food, then move backward slightly and repeat the process of kneading the sediment.

The varnish clam (*Nuttallia obscurata*) is the most common prey of *Larus* sp. in the study area (Figure 4.3). The majority of *N. obscurata* live 5–20 cm below the sediment surface with their siphons maintaining connection to the sediment–water interface. In some cases, particularly in less water-saturated substrates, their burrow apertures can be observed within the shallow foraging structures (Figure 4.4). This indicates that several individuals escaped the efforts of the sediment-convecting avian tracemaker.

The examined structure is approximately 180 cm long and 30 to 40 cm wide (Figure 4.2C,D). It is the longest example observed during the field work; most examples are less than 100 cm long (Figure 4.4). They are commonly organized into a series of nested, concavo-convex mounds of sediment that mimic the shape of the nearly circular terminal depression. Altitude data show that the full relief of the surficial expression (from

the base of the depression to the top of the mounds) is approximately 4.5 cm. Some examples lack the nested form (Figure 4.5). Such occurrences are nearly indistinguishable from *Piscichnus*. The distribution of the foraging traces across the sand flat is sporadic, but they occur in higher abundance in water-saturated substrates, particularly near the margins of standing water (Figure 4.5; cf. Gregory, 1999). Several examples occur in algae-rich sediment that is biogenically stabilized and thus have a higher preservation potential (Figure 4.2C and Figure 4.4; Marty et al., 2009). Organic debris and fecal material commonly accumulate between the sediment mounds and in the depression (Figure 4.6).

4.5 Discussion

Gull feeding traces of comparable size and shape to those examined in this study have been documented from the Baltic Sea (Müller, 1985), the Wadden Sea (Cadée, 1990), the coast of Northland, New Zealand (Gregory, 1999), and the coast of Georgia, United States (Martin, 2013). Müller (1985) likened the structures to *Rhizocorallium*, a comparison regarded by Gregory (1999) as an erroneous comparison due to the irregularity of the outer margin, absence of a U-shaped tube, and generally larger size. Gregory (1999) noted some similarities between the gull feeding traces and *Climactichnites*, which is thought to have been produced by muscular contractions of a slug-like animal as it moved across damp sand (Yochelson & Fedonkin, 1993). However, the feeding traces differ from *Climactichnites* in morphology, mode of formation, ecological significance, and amount of sediment disruption. In these regards, the gull-manufactured structure is more comparable to *Piscichnus*, which is a steep-sided, circular, bowl-shaped structure associated with ray feeding behaviors or nesting behaviors in fishes (e.g., Feibel, 1987; Gregory, 1991; Gingras et al., 2007; Kotake, 2007;

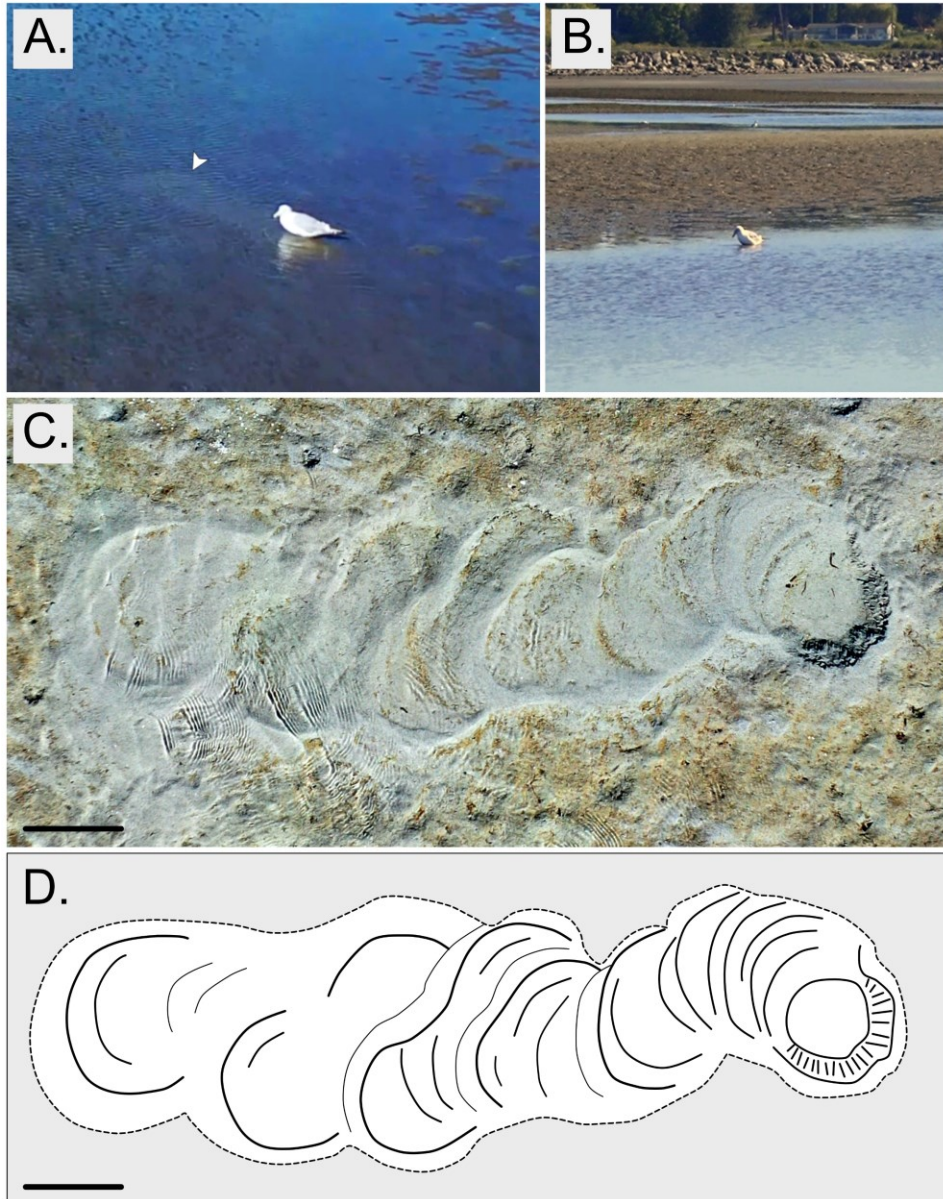


Figure 4.2. Photos of the *Larus* sp. tracemaker and resulting biodeformational structure. (A) Screen capture of a drone video showing the *Larus* sp. tracemaker systematically liquifying the sediment. Note the outline of the structure in front of the tracemaker (white arrow). (B) Screen capture of a video taken with an Olympus Tough TG-6 camera showing the tracemaker near the margin of standing water in the topographic low of a sand flat. The videos that correspond to B and C can be found in the supplementary material. (C) Plan-view orthomosaic of the biodeformational structure showing nested impressions resulting from the tracemaker iteratively stepping in place. Scale bar = 20 cm. (D) Schematic representation of C depicting the surficial expression of the nested sediment mounds.

Belvedere et al., 2011; Uchman, 2018).

Examples of the *Larus* sp. feeding traces that lack the nested, concavo-convex mounds of sediment may be indiscernible from *Piscichnus* in the rock record (Figure 4.5), particularly in cross-section. Well-preserved examples may be distinguished in that *Piscichnus* generally exhibits steeper margins, a higher relief, and a slightly more distinct outline (Figure 4.8). Although both traces commonly occur in intertidal areas, *Piscichnus* is also found in subtidal environments. Subtidal indicators such as wave-generated sedimentary structures could therefore be used to justify attributions of bowl-shaped structures to *Piscichnus*. Another type of bowl-shaped structure was revealed using side-scan sonar along the shelf of the Bering Sea (Oliver & Kvitek, 1984; Oliver et al., 1985; Nelson et al., 1987). These excavations, made by the California gray whale (*Eschrichtius robustus*) suction feeding on infaunal amphipods, are easily distinguishable by their large size (roughly 40 cm deep) and oval shape.



Figure 4.3. Varnish clam (*Nuttallia obscurata*) collected from directly below the examined biodeformational structure.

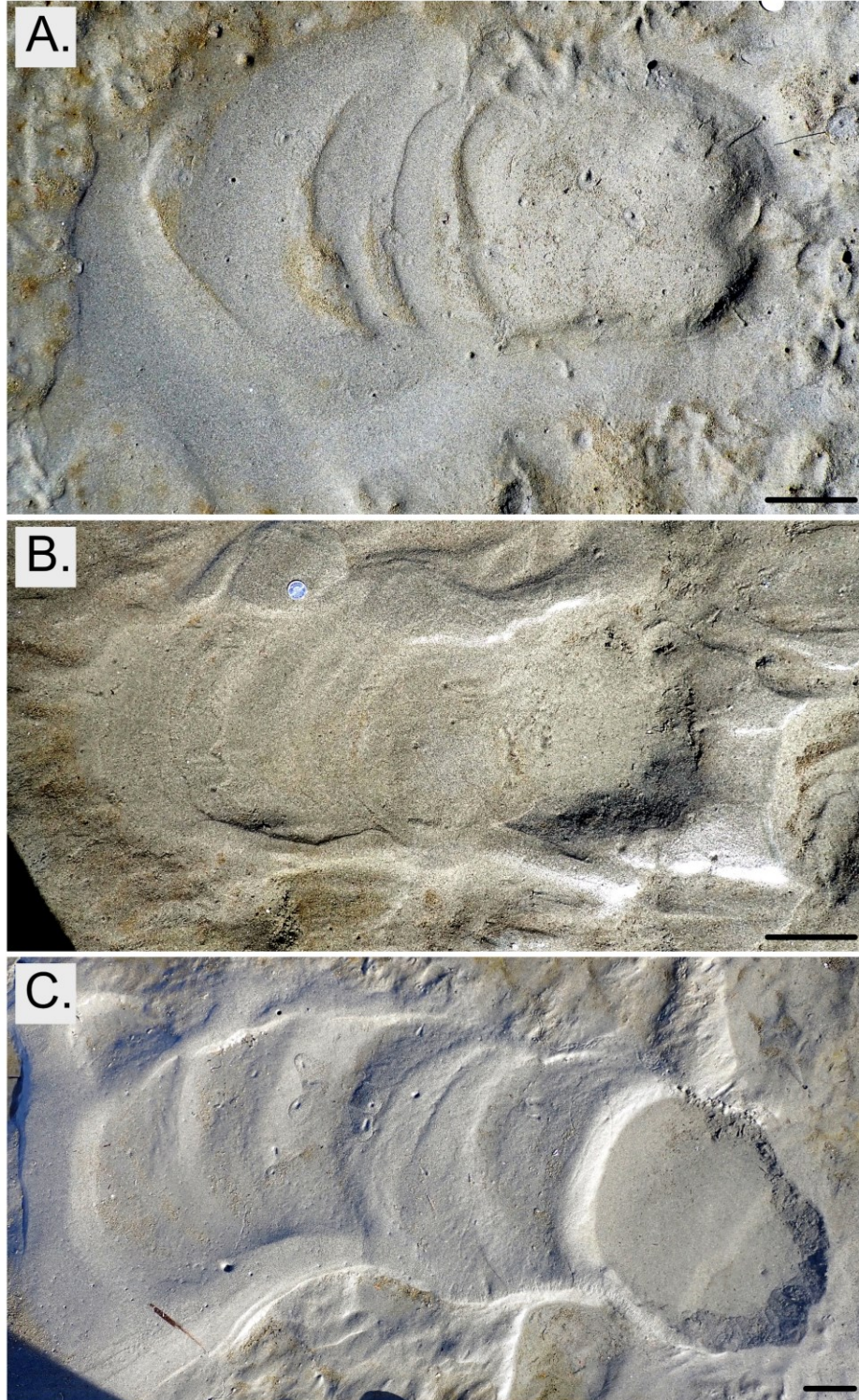


Figure 4.4. Additional examples of the *Larus* sp. feeding trace from White Rock Beach. Note the *Nuttallia obscurata* burrow apertures and organic debris and fecal material that accumulates in the troughs between the concavo-convex mounds. Scale bars = 5 cm.



Figure 4.5. Drone image of a cluster of *Larus* sp. feeding traces near the margin of standing water. Some examples show a single, shallow depression. Scale bar = 50 cm.



Figure 4.6. Accumulation of organic material in a trough between sediment mounds of the examined biodeformational structure.

The examined biodeformational structure was produced by the tracemaker liquifying the sediment below its feet, making it easier to probe the sediment and causing infaunal organisms to advect upward through the sediment (Figure 4.7; e.g., Cadée, 1990; Gregory, 1999). This is in contrast to related techniques whereby shorebirds use their beaks to stir or liquify the sediment (Figure 4.9A,B). Foraging behaviors that rely on their beaks in this way are perhaps more common in highly water-saturated substrates because of the ease with which the sediments become liquified. These behaviors also produce distinctive biodeformational structures, all of which are formed by the tracemaker digging and dragging its beak through the sediment in search of food (Figure 4.9). For example, one such trace was produced by an individual *Egretta caerulea* (little blue heron; Figure 4.9C) dragging a beak back and forth (side to side) in sediment while walking forward (Figure 4.9A,B). Other shallow drag marks or scoops made by bird beaks have been documented at the Bay of Fundy in eastern Canada (Figure 4.9D,E,F). In both of these cases, the abundant food available in the sediment were amphipods and, to a lesser degree, small polychaetes. These systematic beak drag marks may be preferred strategies in areas where the dominant prey are larger or live closer to the sediment surface.

The technique employed by the gull also benefits from water-saturated substrates that are easily liquified and appears to be an effective strategy for reaching deeper-seated prey. In the case of deep-burrowing siphonate bivalves such as *Nuttallia obscurata*, liquifying the sediment causes them to advect upwards through the substrate, making them more susceptible to predation in a manner similar to some *Piscichnus* feeding behaviors (Figure 4.7; Gingras et al., 2007). Previous studies have estimated that the avian tracemaker disrupts the upper 2–6 cm of sediment during its foraging efforts (Cadée, 1990; Gregory, 1999), whereas our observations suggest that the sediment is liquified to

greater depths than can be observed from the surficial expression (Figure 4.7). Most invertebrate prey live deeper than 5 cm below the sediment–water interface, so reaching greater depths would significantly improve foraging success.

Although these gull-manufactured biodeformational structures share a resemblance globally, the variations in morphology reported are notable. The lengths of the gull-feeding structures vary markedly across all sites, ranging from a single depression that is approximately 10-20 cm in diameter to multiple nested depressions with a total length that locally exceeding 3 m (Cadée, 1990; Gregory, 1999). Another source of variability within the sites is the shape of the terminal impression, and, to a lesser degree, the nested sediment mounds (Figure 4.2A,B). Many examples show well-developed, W-shaped impressions (Cadée, 1990; Gregory, 1999; Martin, 2013, p. 479). This taphonomic expression gives rise to a kind of bilateral symmetry in which the two footprints of the gull become distinct. Other examples, such as those that are common at White Rock Beach, display a nearly circular terminal impression, although a W-shaped impression can be faintly observed in some cases (Figure 4.4A). The W-shaped impression is most likely related to a higher abundance of fine-grained sediment and increased substrate cohesiveness. Despite their subtle differences in surface expression, these two taphonomic endmembers should exhibit a similar cross-sectional appearance (Figure 4.7).

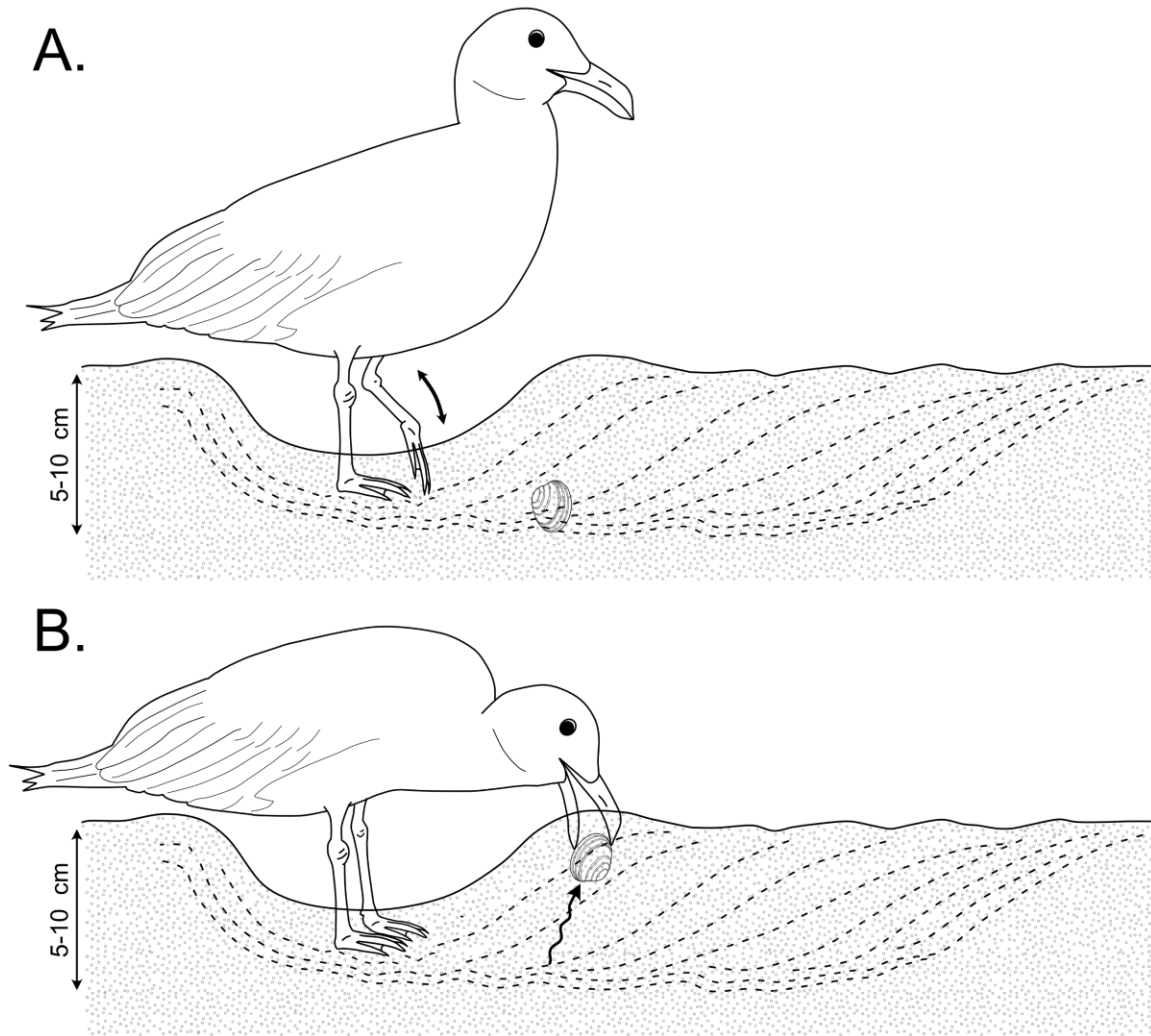


Figure 4.7. Illustration of the foraging technique employed by *Larus* sp. and a schematic interpretation of the cross-sectional view of the resulting biodeformational structure. (A) The tracemaker uses its feet to knead the sediment in an effort to liquify the substrate. As it moves backward and repeats this process, the newly displaced sediment is pushed up against previously exploited areas, resulting in nested mounds of sediment that exhibit a crude, sigmoidal pattern in cross-section. (B) The liquefaction process causes invertebrate prey such as *Nuttallia obscurata* to advect upward, making them susceptible to predation through sediment probing.



Figure 4.8. Examples of incipient *Piscichnus*. (A) Underwater example (~40 cm in diameter) from Taino Beach, Grand Bahama Island. Photo courtesy of Robert W. Boessenecker. (B) Intertidal example from Nannygoat Beach, Sapelo Island, Georgia, USA. Photo courtesy of Anthony J. Martin.

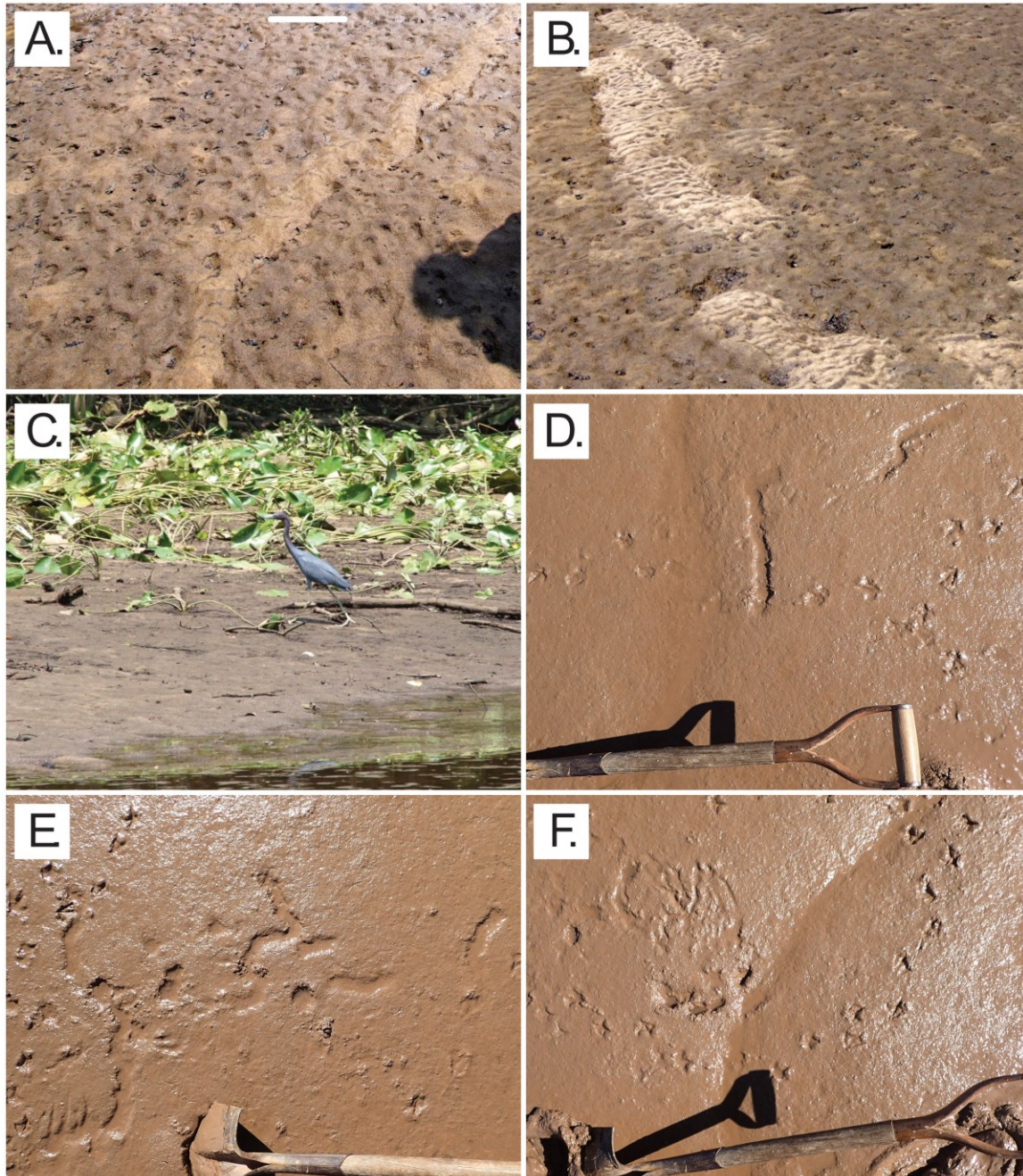


Figure 4.9. Unusual sedimentary structures produced by foraging shorebirds. (A–B) Biodeformational structures produced by the tracemaker digging and dragging its beak back and forth through the sediment in search of food. Scale bar in A = 30 cm. The field of view in B is approximately 1.4 m. (C) Photo of a little blue heron (*Egretta caerulea*) taken near the Ogeechee River, Georgia. This species is the tracemaker of the structures in A and B. (D–F) Feeding structures of varying complexity produced by an unidentified shorebird believed to be employing a dragline technique whereby it systematically digs its beak into the sediment and drags it back towards its body.

4.6 Summary

Although most shallow, bowl-shaped biogenic sedimentary structures are broadly morphologically similar, they differ greatly in how they are formed. Previously described forms have been interpreted to represent nesting behaviors in fishes, hydraulic jetting behaviors in foraging ray fishes, and suction feeding behaviors in gray whales. This study presents a fourth type, produced by a foraging gull (*Larus* sp.). The tracemaker was observed kneading the sediment by moving its feet back and forth, thereby liquifying the sediment and causing invertebrate prey to advect upward toward the sediment surface. This observation sheds light on the sedimentological, ecological, and environmental significance of these biodeformational structures and provides context for the interpretation of related structures in the rock record.

4.7 References

- Belvedere, M., Franceschi, M., Morsilli, M., Zoccarato, P. L., & Mietto, P. (2011). Fish feeding traces from middle Eocene limestones (Gargano Promontory, Apulia, southern Italy). *Palaios*, *26*, 693–699.
- Cadée, G. C. (1990). Feeding traces and bioturbation by birds on a tidal flat, Dutch Wadden Sea. *Ichnos*, *1*, 23–30.
- Feibel, C. S. (1987). Fossil fish nests from the Koobi Fora Formation (Plio-Pleistocene) of northern Kenya. *Journal of Paleontology*, *61*, 130–134.
- Gingras, M. K., Armitage, I. A., Pemberton, S. G., & Clifton, H. E. (2007). Pleistocene walrus herds in the Olympic Peninsula area: Trace-fossil evidence of predation by hydraulic jetting. *Palaios*, *22*, 539–545.
- Gregory, M. R. (1991). New trace fossils from the Miocene of Northland, New Zealand: *Rorschachichnus amoeba* and *Piscichnus waitemata*. *Ichnos*, *1*, 195–205.
- Gregory, M. R. (1999). Unusual “paddling” trails left by gulls and “aviturbation” in Rarawa and Mangawhai Estuaries, Northland, New Zealand. *New Zealand Natural Sciences*, *24*, 27–34.
- Javernick, L., Brasington, J., & Caruso, B. (2014). Modeling the topography of shallow braided rivers using Structure-from-Motion photogrammetry. *Geomorphology*, *213*, 166–182.
- Kotake, N. (2007). *Macaronichnus* isp. Associated with *Piscichnus waitemata* in the Miocene of Yonaguni-jima Island, Southwest Japan. In W. Miller (Ed.), *Trace Fossils* (pp. 492–501). Amsterdam: Elsevier.
- Lobza, V., & Schieber, J. R. (1999). Biogenic sedimentary structures produced by worms

- in soupy, soft muds: Observations from the Shattanooga Shale (Upper Devonian) and experiments. *Journal of Sedimentary Research*, 69, 1041–1049.
- Martin, A. (2013). *Life Traces of the Georgia Coast: Revealing the Unseen Lives of Plants and Animals*. Bloomington: Indiana University Press.
- Marty, D., Strasser, A., & Meyer, C. A. (2009). Formation and taphonomy of human footprints in microbial mats of present-day tidal-flat environments: Implications for the study of fossil footprints. *Ichnos*, 16, 127–142.
- Miguez-Salas, O., & Rodríguez-Tovar, F. J. (2019). Ichnofacies distribution in the Eocene–Early Miocene Petra Tou Romiou outcrop, Cyprus: Sea level dynamics and palaeoenvironmental implications in a contourite environment. *International Journal of Earth Sciences*, 108, 2531–2544.
- Müller, A. H. (1985). *Rhizocorallium*-artige lebensspuren (ichnia) vom litoral der Ostsee. *Freiberger Forschungshefte*, 400, 77–79.
- Nelson, C. H., Johnson, K. R., & Barber, J. H. (1987). Gray whale and walrus feeding excavation on the Bering Shelf, Alaska. *Journal of Sedimentary Petrology*, 57, 419–430.
- Oliver, J. S., & Kvitek, R. G. (1984). Side-scan sonar records and diver observations of the gray whale (*Eschrichtius robustus*) feeding grounds. *The Biological Bulletin*, 167, 264–269.
- Oliver, J. S., Kvitek, R. G., & Slattery, P. N. (1985). Walrus feeding disturbance: Scavenging habits and recolonization of the Bering Sea benthos. *Journal of Experimental Marine Biology and Ecology*, 91, 233–246.
- Scharstein, D., & Szeliski, R. (2002). A taxonomy and evaluation of dense two-frame stereo correspondence algorithms. *International Journal of Computer Vision*, 47, 7–42.
- Tavani, S., Granado, P., Corradetti, A., Girundo, M., Iannace, A., Arbués, P., ... Mazzoli, S.

- (2014). Building a virtual outcrop, extracting geological information from it, and sharing the results in Google Earth via OpenPlot and Photoscan: An example from the Khaviz Anticline (Iran). *Computers & Geosciences*, 63, 44–53.
- Uchman, A., Torres, P., Johnson, M. E., Berning, B., Ramalho, R. S., Rebelo, A. C., ... Ávila, S. P. (2018). Feeding traces of recent ray fish and occurrences of the trace fossil *Piscichnus waitemata* from the Pliocene of Santa Maria Island, Azores (northeast Atlantic). *Palaios*, 33, 361–375.
- Ullman, S. (1979). The interpretation of motion from structure. *Proceedings of the Royal Society of London Series B, Biological Sciences*, 203, 405–426.
- Verhoeven, G. (2011). Taking computer vision aloft – archaeological three-dimensional reconstructions from aerial photographs with photoscan. *Archaeological Prospection*, 18, 67–73.
- Wetzel, A. (1983). Biogenic Structures in Modern Slope Deep-Sea Sediments in the Sulu Sea Basin (Philippines). *Palaeogeography, Palaeoclimatology, Palaeoecology*, 42, 285–304.
- Wetzel, A. (1991). Ecologic interpretation of deep-sea trace fossil communities. *Palaeogeography, Palaeoclimatology, Palaeoecology*, 85, 47–69.
- Wetzel, A., & Uchman, A. (1998). Biogenic sedimentary structures in mudstones: An overview. In J. Schieber, W. Zimmerle, & S. S. Parvinder (Eds.), *Shales and Mudstones I: Basin studies, sedimentology, and paleontology* (Vol. 1, pp. 351–369). E. Schweizerbart.
- Yochelson, E. L., & Fedonkin, M. A. (1993). *Paleobiology of Climactichnites, an Enigmatic Late Cambrian Fossil*. Washington, D. C.: Smithsonian Institution Press.

CHAPTER 5 – DRAWING INTERPRETATIONS OF BIOTURBATION INTENSITY FROM BEDDING PLANES OF VERTICAL TRACE FOSSIL ASSEMBLAGES

5.1 Introduction

Bioturbation intensity, defined as the proportion of a sedimentary unit that has been reworked by biological processes, is an important element of ichnological datasets owing to its capacity to reveal paleoenvironmental details. For instance, the distribution of bioturbation in sedimentary successions has long been used to make inferences regarding variations in sedimentation rate (Middlemiss, 1962; Piper and Marshall, 1969; Howard, 1975; Bhattacharya et al., 2020; Miguez-Salas et al., 2022), bottom-water oxygenation (Savrda et al., 1984; Savrda and Bottjer, 1986, 1987, 1989), and salinity (La Croix et al., 2019; Melnyk and Gingras, 2020). Despite its widespread application, uncertainty remains regarding the efficacy of estimating true bioturbation intensity from two-dimensional (2D) views (Eltom et al., 2022). This uncertainty is heightened when evaluating bedding planes, which are less studied than cross-sectional perspectives.

Various methods are used to measure bioturbation intensity, ranging from qualitative descriptions to quantitative percentages derived through computer-based techniques (see Dorador and Rodríguez-Tovar, 2018 for detailed review). The most common approaches are semi-quantitative classification schemes whereby bioturbation intensities are partitioned based on percentage-based categories. Currently, two ordinal indices are widely employed: the Bioturbation Index (Reineck, 1963; Taylor and Goldring, 1993) and the Ichnofabric Index (Droser and Bottjer, 1986). Both schemes utilize flashcards to facilitate data collection and are most effectively applied when examining

core slabs or outcrop faces in elevation view. In contrast, techniques for assessing bioturbation intensity on bedding planes are less developed and therefore more seldom applied (Miller and Smail, 1997; Marenco and Bottjer, 2010).

While it has been acknowledged that there are constraints associated with estimating the bioturbation intensity from 2D perspectives (Timmer et al., 2016; Rodríguez-Tovar et al., 2018), these constraints have not been thoroughly quantified. Preliminary computer modeling suggests that errors in assigning bioturbation intensities from 2D views depend on the true bioturbation intensity, the orientation of the plane, and burrow morphology (Eltom et al. 2022). Within the context of simple vertical burrows (*Skolithos*), this research demonstrated that 2D views tend to overestimate bioturbation intensity at lower true intensities and to underestimate it at higher intensities—a pattern consistent across both bedding planes and elevation views. The present study extends previous work by comprehensively analyzing the relationship between bioturbation intensities on bedding planes and those in elevation view. Monte Carlo simulations are used to explore the range and frequency of cross-sectional bioturbation intensities over a range of bedding plane intensities (2-50%). The resulting data are compared to vertical trace fossil assemblages (e.g., piperock) from the Lower Cambrian Gog Group to validate the model's predictions.

5.2 Geological Context

Piperock, first documented in the early 19th century, is one of the earliest ichnofabrics in the literature. The term was initially applied to early Paleozoic cross-bedded sandstone (quartzite) containing dense assemblages of vertical shafts referable to *Skolithos*. Remarkably, interpretations of piperock have endured little change for more

than two centuries (cf. Ekdale and Lewis, 1993). In its first written account, MacCulloch (1814) compared the rod-like structures to the remnants of annelid worms. Nicols (1857) later coined the term 'pipes' to characterize these structures, leading to the naming of the Pipe Rock Member of the Lower Cambrian Eriboll Formation (Lapworth, 1883; Preach et al., 1907). Today, there is a consensus that these deposits were formed in high-energy nearshore environments (Droser and Bottjer, 1989, Droser, 1991, McIlroy and Garton, 2010, Desjardins et al., 2010). The current depositional model suggests that sedimentation was linked to compound dune migration, with bioturbation being most associated with areas with low sediment accumulation rates (Desjardin et al., 2010, 2012).

The Lower Cambrian Gog Group is a thick sandstone-dominated succession in Western Laurentia (North America) that records the transition from continental to shallow marine deposition (Deiss, 1940). It regionally and unconformably overlies deep-water turbidites of the Upper Proterozoic Miette Group (Windermere Supergroup) (Figure 5.1A). Outcrops of the Gog Group are widespread in the Main Ranges of the Rocky Mountains, extending from Mount Assiniboine to Pine Pass, British Columbia (Mountjoy, 1962; Mountjoy and Aitken, 1963; Slind and Perkins, 1966; Campbell et al., 1972). The present study was conducted near the Kootenay Plains Ecological Reserve, approximately 60 km southwest of Nordegg, Alberta (Figure 5.1B). In this area, the continental and shallow marine strata of the Gog Group are equivalent to the Mahto and McNaughton formations, respectively. The focus here is on the bioturbated intervals of the Mahto Formation. These strata are well-suited for this study owing to the morphological simplicity of *Skolithos*. Furthermore, the variability in piperock expressions in the area allows for the examination of seven distinct occurrences from both bedding plane and cross-sectional perspectives.

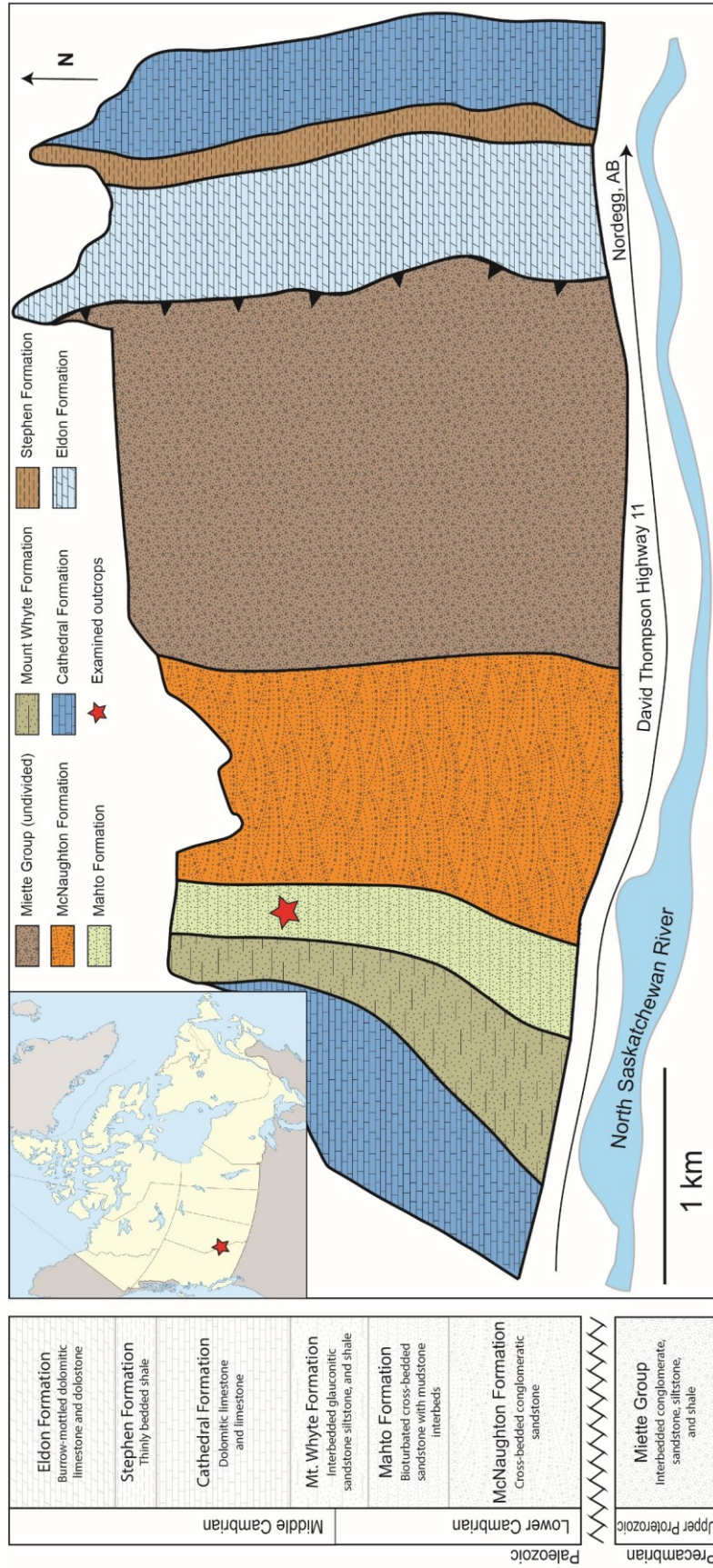


Figure 5.1. Schematic stratigraphic column and geologic map of the study area. The base of the studied section is located approximately at 52.012859°N, 116.512644°W. The upper boundary is located at 52.01341°N, 116.51645°W.

5.3 Methods

5.3.1 Monte Carlo Methods

Monte Carlo simulations are computational techniques used to solve complex mathematical and statistical problems through random sampling and probabilistic methods (e.g., Mooney et al., 1997). In the context of this study, these simulations are used to assess the variability observed in elevation view bioturbation intensity (hereafter EVBI) for a given plan view bioturbation intensity (hereafter PVBI). A range of 2% to 50% PVBI was chosen for analysis as it reflects the full range of bioturbation intensities observed in the study area. Moreover, overlap was not permitted and thus attempts to model PVBI values over 50% posed significant challenges in locating unoccupied spaces large enough for new burrow placements.

The relationship between PVBI and EVBI was evaluated using theoretical block models representing a portion of a sedimentary bed with a volume of 500,000 cubic units. These models featured bedding planes measuring 100 by 100 units (equivalent to 10,000 square units) and had a bed thickness of 50 units. Within the models, vertically-oriented cylinders with a diameter of 0.5 units were positioned at random. These cylinders were assigned random lengths ranging from 40 to 50 units, with an established mean of 45 units. These specific parameters were chosen for their similarities to the field data, emulating a 1 m² bedding plane occupied by vertical burrows with a 5 mm diameter and lengths exceeding 40 cm.

For each examined PVBI value, the bedding plane was partitioned into 100 square domains. Within these domains, 10,000 vertical planes were placed at random, resulting in a total of 1,000,000 cross-sections available for scrutiny. Each plane measured 50 units in length and spanned the full depth of 50 units within their respective domains. Monte

Carlo simulations were then performed on all planes to determine the total area of burrows intersected (EVBI), the number of burrows observed along the plane (burrow counts), and the mean length of burrow intersection (apparent burrow diameter).

5.3.2 Field Methods

Well-exposed outcrops of the Mahto Formation enable detailed comparisons of various piperock ichnofabrics from both bedding plane and elevation views. Seven outcrops were selected to represent the full range of piperock expressions observed. Field observations included physical sedimentary structures, grain size, ichnogenera, burrow diameters, and the presence and width of burrow linings. The bioturbated areas of each outcrop were manually traced using the drafting software Adobe Illustrator. Bioturbation intensity percentages were then calculated using ImageJ, an open-source software increasingly popular in ichnological studies (e.g., Miguez-Salas et al., 2019; Rodríguez-Tovar et al., 2020; Melnyk et al., 2021). The analyzed areas typically span tens of square centimeters, with overly oblique rock faces being omitted from analysis. One example, Piperock 7, was selected for further examination due to its extensive outcropping and closely associated exposures of bedding planes and elevation views.

5.4 Results

5.4.1 Monte Carlo Results

One million vertical cross-sections, each measuring 50 by 50 units, were examined from each PVBI block model to determine EVBI, burrow counts and apparent burrow diameters (Table 5.1). Figure 5.2 illustrates the theoretical bedding planes used in analysis and includes a randomly selected example of a vertical cross-section for visual

comparison. The probability distributions show a nearly perfect correlation between PVBI and EVBI, with the dispersion of EVBI values generally decreasing with increasing bioturbation intensity (Table 5.1; Figure 5.4). Mean EVBI values reflect the product of PVBI and mean burrow length, where burrow length is expressed as a proportion of bed thickness. The modeled parameters include a mean burrow length of 45 units and bed thickness of 50 units, thus mean EVBI values are approximately 10% lower than their corresponding PVBI (Figure 5.4). For instance, a PVBI of 20% yields a mean EVBI of 18%. The burrow counts exhibit a similar trend to that of EVBI, varying from 3 ± 2 at 2% PVBI to 64 ± 4 at 50% PVBI (Table 1). For all PVBI values, the mean apparent burrow diameter was 1.6 units, or 31% of the true burrow diameter.

5.4.2 Piperock Descriptions

Seven distinct piperock ichnofabrics (P1-P7) were analyzed for 2D bioturbation intensity from both plan and elevation views (Table 5.2). Piperocks 1-6, though limited in extent, show bedding planes and elevation views in close association (Figure 5.4). Piperock 7 resembles P6 but has a lower bioturbation intensity and offers a larger area for analysis (Figure 5.5 and Figure 5.6). Vertical shafts referable to *Skolithos* are the predominant structure in all ichnofabrics, with *Cylindrichnus* and *Rosselia* occurring locally in Piperock 3. Some examples of *Skolithos* display sand linings that are difficult to distinguish from the causative burrow. Observed causative burrow diameters range from 1 to 10 mm, with burrow linings reaching a maximum of 5 mm. Individual burrows are often delineated by variations in iron staining and sometimes exhibit differences in weathering. This natural variance leads to subtle differences in how much each burrow contributes to the apparent bioturbation intensity (most salient in P7; Figure 5.5 Figure 5.6). Similar to the model data, the relationship between PVBI and EVBI exhibits a nearly

direct relationship between the two perspectives, with an R-squared value of 0.94 (Figure 5.7). The PVBI ranged from 5% to 45%, and the EVBI varied from 6% to 42% (Table 5.2).

5.5 Discussion

This study highlights the strong correlation between bioturbation intensities observed in plan view (PVBI) and elevation view (EVBI) for *Skolithos*-dominated assemblages, with EVBI increasing in direct proportion to PVBI. This rate of increase is predominantly determined by the average length of burrows in relation to the bed thickness. In the Monte Carlo simulations, the comparably low EVBI values are attributed to the average burrow length being shorter than the bed thickness. In contrast, the examined piperock outcrops exhibit burrows that extend through the entire bed. Model predictions suggest this condition results in a near-perfect alignment between EVBI and PVBI measurements. Field data substantiate this relationship, showing that mean EVBI values vary by no more than 4% compared to their respective PVBI (Figure 5.7).

The literature on bedding plane bioturbation intensity primarily focuses on applications to horizontal burrows owing to their prevalence and prominence in this view (Marenco and Hagadorn, 2019). Nonetheless, bedding planes that display vertical burrows play an important role in paleoecological evaluations, including examinations of mutual avoidance behaviors or the recognition of palimpsest trace fossil assemblages (Allport et al., 2021). They also offer a more accurate depiction of bioturbation intensity, as horizontal burrows can intermittently come in and out of view, thus skewing the apparent intensity. However, this is notwithstanding the challenges imposed by vertical burrows, which sometimes present a marked visual prominence when observed on bedding planes. This can inadvertently give rise to a perception of a higher bioturbation intensity than is

empirically justified. Indeed, thorough examination reveals that bioturbation intensities exceeding 50% are likely uncommon in piperock ichnofabrics (cf. Droser and Bottjer, 1989; Droser, 1991; Desjardins et al., 2010).

Existing frameworks for measuring bedding plane bioturbation intensity, while effective for analyzing the spatial distribution of traces across large areas (Marenco and Hagadorn, 2019), do not provide a reliable means of estimating true bioturbation intensity. To ensure accurate interpretations of bioturbation intensity from bedding planes, further investigation is needed into the relationship between PVBI and EVBI and how they relate to true bioturbation intensity. This study contributes to this effort by supporting a long-standing but rarely tested assumption that bioturbation intensities on piperock bedding planes correspond closely to those observed in elevation view (MacCulloch, 1814). Investigating how this relationship compares with different vertical burrow shapes, like J-, Y-, or U-shaped burrows, would broaden the scope of relevance for the modeled outcomes. Horizontal burrows pose a more significant challenge because of their diverse sizes, shapes, and distributions, which can result in inaccuracies when assessing bioturbation intensity from a two-dimensional plane (Eltom et al., 2022). Despite these challenges, ongoing research has the potential to enhance our ability to integrate bedding plane analyses into established frameworks for quantifying bioturbation intensity.

Table 5.1. Summary of Monte Carlo results for examined Plan View Bioturbation Intensities (PVI).

PVI [%]	Burrow counts			Elevation view bioturbation intensity		
	Mean [burrows]	Std [burrows]	Std [units ²]	Mean [units ²]	Std [%]	Std [%]
2	3	2	45	29	2	1
5	6	2	113	44	5	2
10	13	3	227	58	9	2
20	26	4	453	72	18	3
30	39	4	679	76	27	3
40	52	4	904	75	36	3
50	64	4	1129	71	45	3

Std = standard deviation; Std [%] is absolute uncertainty, expressed as a percentage of the total cross-sectional area.

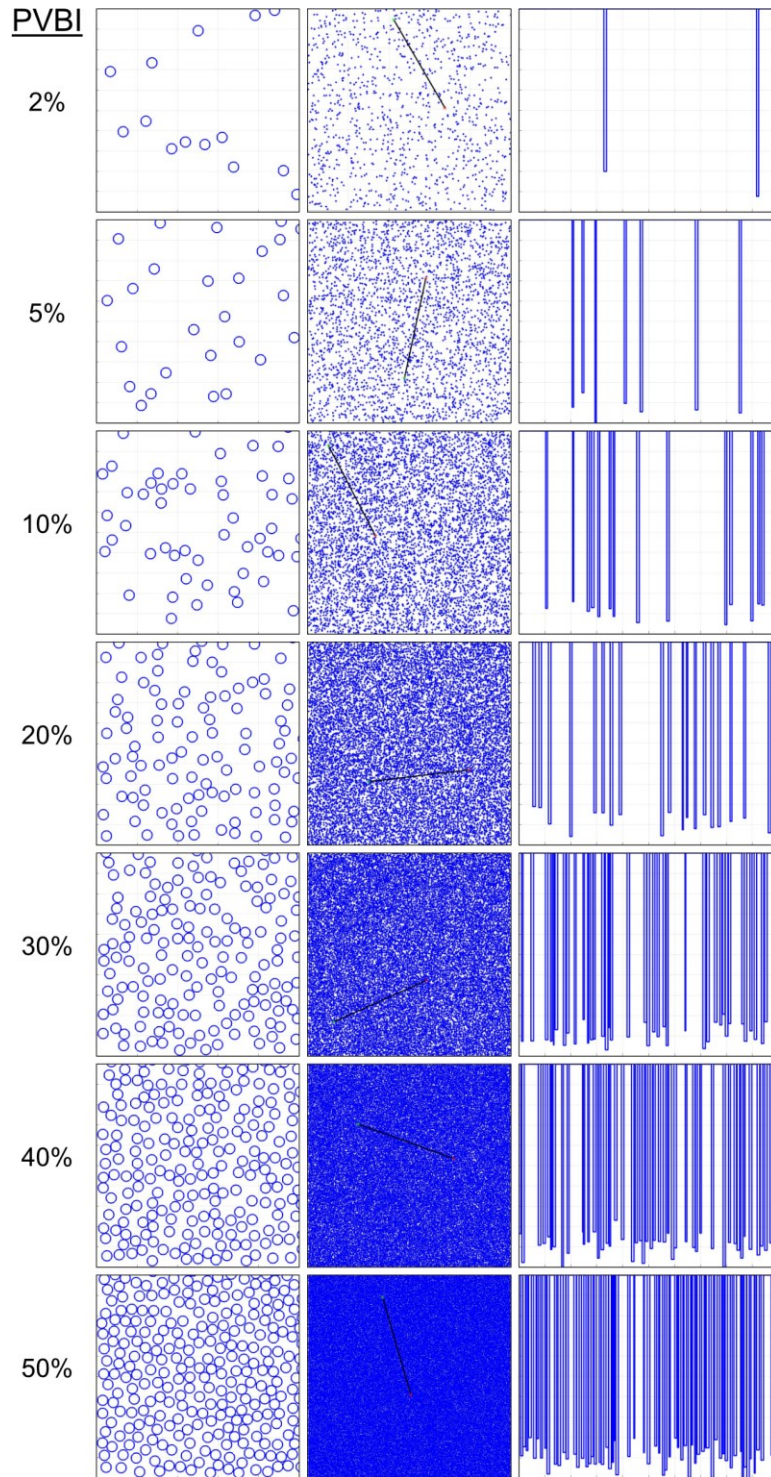


Figure 5.2. Two-dimensional representations of the models for each plan view bioturbation intensity (PVBI). The left column shows a 10 by 10 unit (representing 1% of the total model domain) example of burrow distributions in plan view and the middle column depicts the entire 100 by 100 unit bedding plane. The right column displays an elevation view of a randomly selected cross-section, with its location indicated by the black line on the bedding plane.

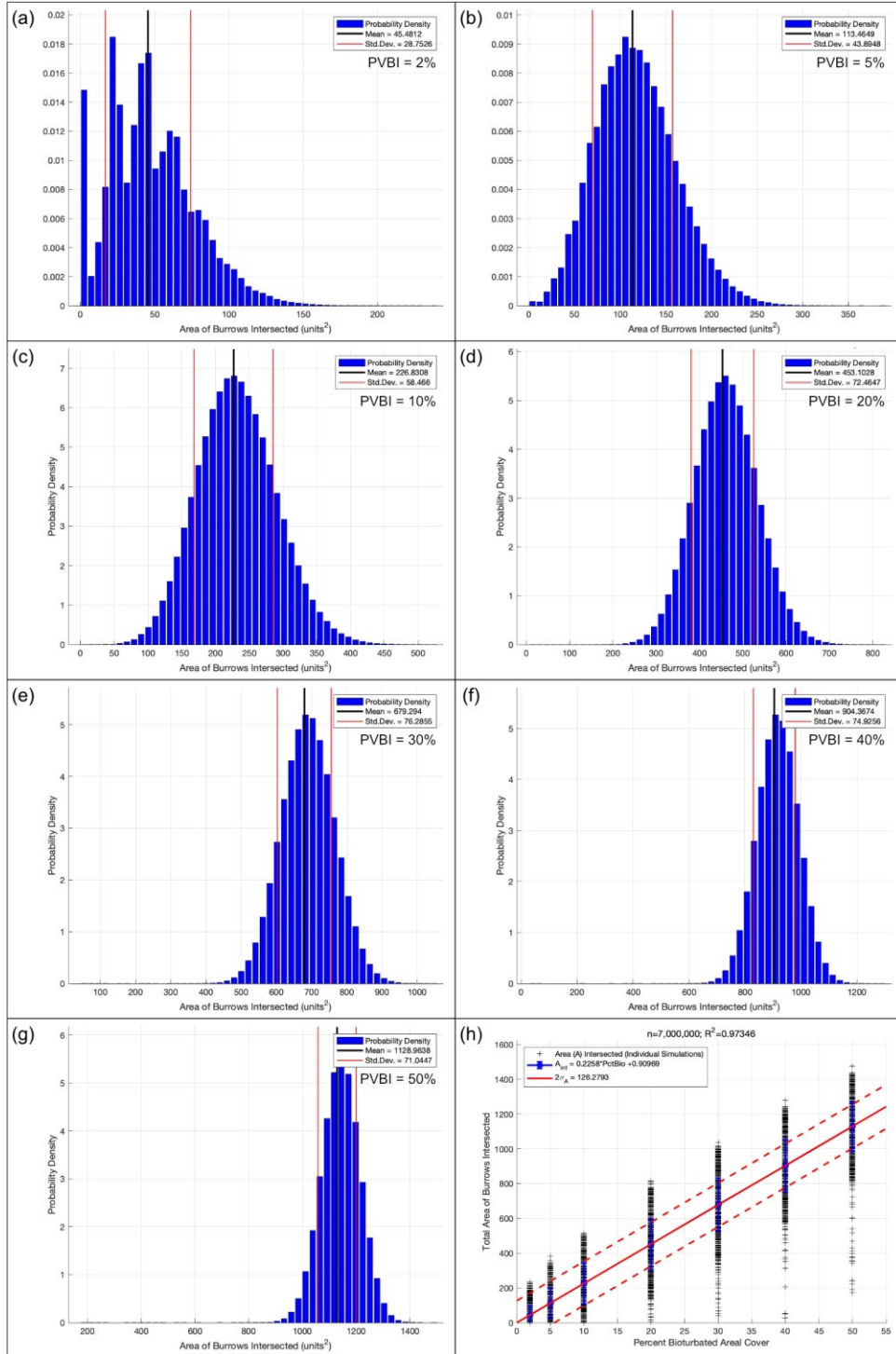


Figure 5.3. Summary of the seven probability distributions of Elevation View Bioturbation Intensity (EVBI) for each Plane View Bioturbation Intensity (PVBI). (A-G) Histograms illustrating the distribution of EVBI values derived from one million 2,500 square unit cross-sections for each modeled PVBI. (H) Plot showing individual data points and the linear relationship between PVBI and EVBI with dashed line indicating the 95% confidence interval.

Table 5.2. Description of the sedimentological and ichnological characteristics of each piperock ichnofabric.

Piperock	Sedimentological Description	Average grain size	Ichno genera	Causative burrow diameter	Burrow lining width
P1	Cross-bedded sandstone with bladed pebbles	Upper medium sand	Unlined <i>Skolithos</i>	3-5 mm	None observed
P2	Planar to low angle cross-laminated silty sandstone	Lower coarse sand	Unlined <i>Skolithos</i>	3-7 mm	None observed
P3	Cross-bedded silty sandstone	Upper coarse sand	Lined and unlined <i>Skolithos</i> , <i>Cylindrichnus</i> , <i>Rosselia</i>	1-10 mm	None observed
P4	Low-angle planar laminated silty sandstone with scattered pebbles	Lower coarse sand	Lined and unlined <i>Skolithos</i>	3-5 mm	0-3mm
P5	Well-sorted cross-bedded sandstone	Lower coarse sand	Lined and unlined <i>Skolithos</i>	2-4 mm	0-4mm
P6	Moderately sorted cross-bedded sandstone	Lower very coarse sand	Lined and unlined <i>Skolithos</i>	2-4 mm	1-4mm
P7	Moderately sorted cross-bedded sandstone	Lower very coarse sand	Lined and unlined <i>Skolithos</i>	1-4 mm	1-5mm

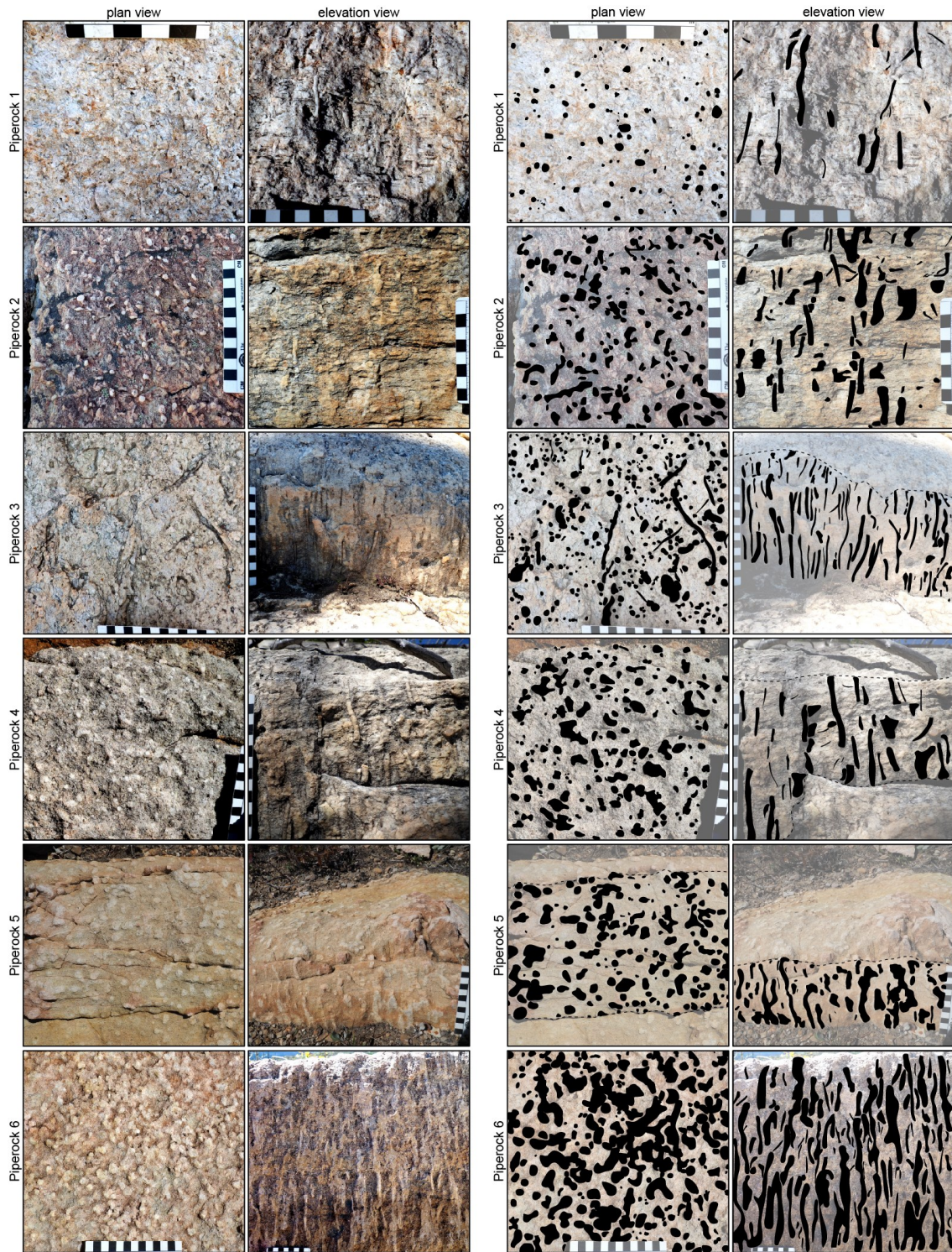


Figure 5.4. Photographs of both plan and elevation views of piperocks 1 to 6 (left) and their corresponding interpreted bioturbation intensity as depicted by the black polygons (right).



Figure 5.5. Outcrop occurrence of Piperock 7. (A,B) Overview of the examined section with plan and elevation views being fortuitously exposed in close association. (C) Plan view showing the spatial distribution of vertical burrows along the bedding plane. (D) Elevation view oriented roughly perpendicular to depositional dip. (E) Elevation view oriented roughly parallel to depositional dip.

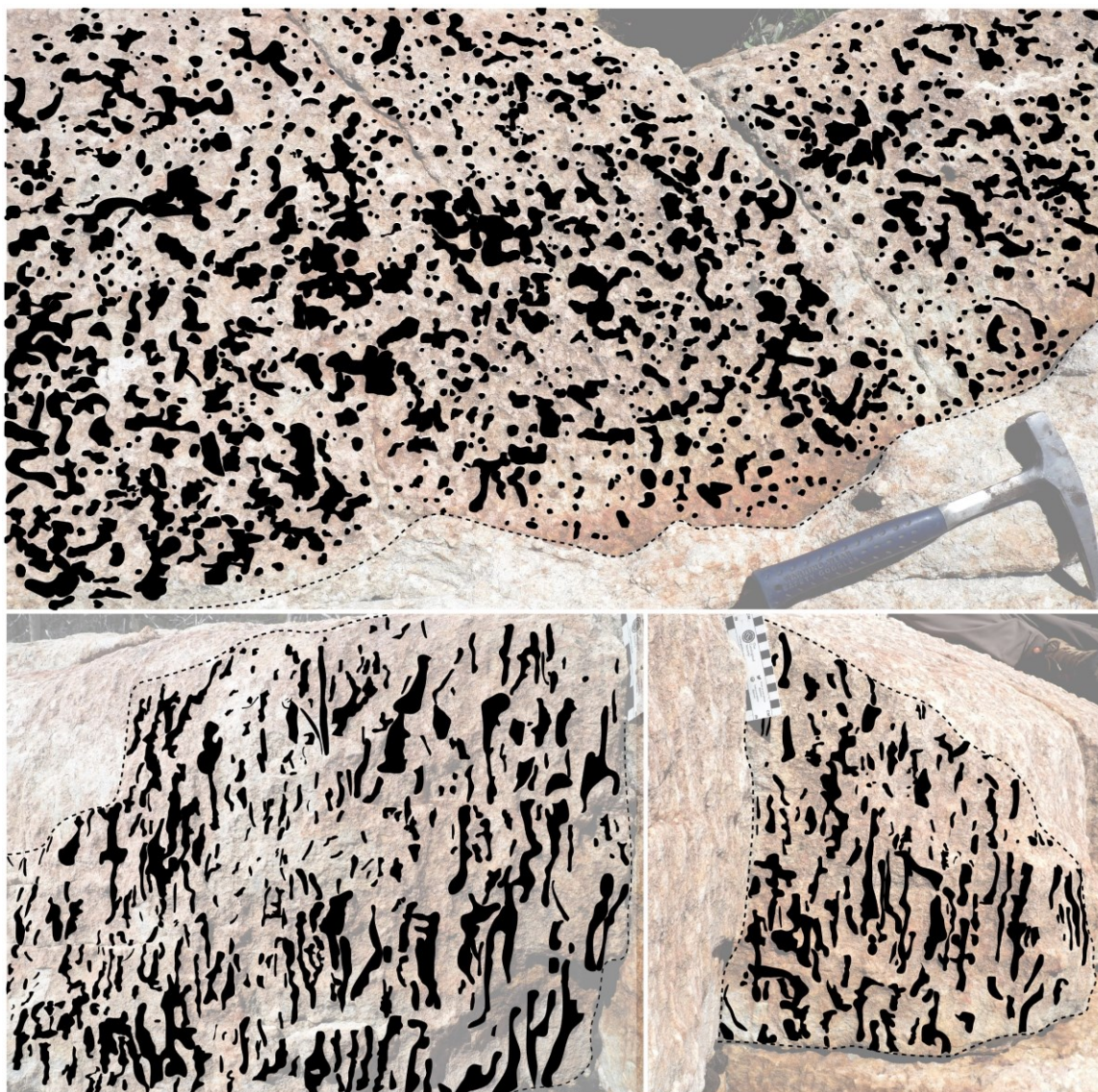


Figure 5.6. Interpretations of two-dimensional bioturbation intensity for Piperock 7. (A) Plan view corresponding to Figure 5.5C. (B) Elevation view corresponding to Figure 5D. (C) Elevation view corresponding to Figure 5.5E.

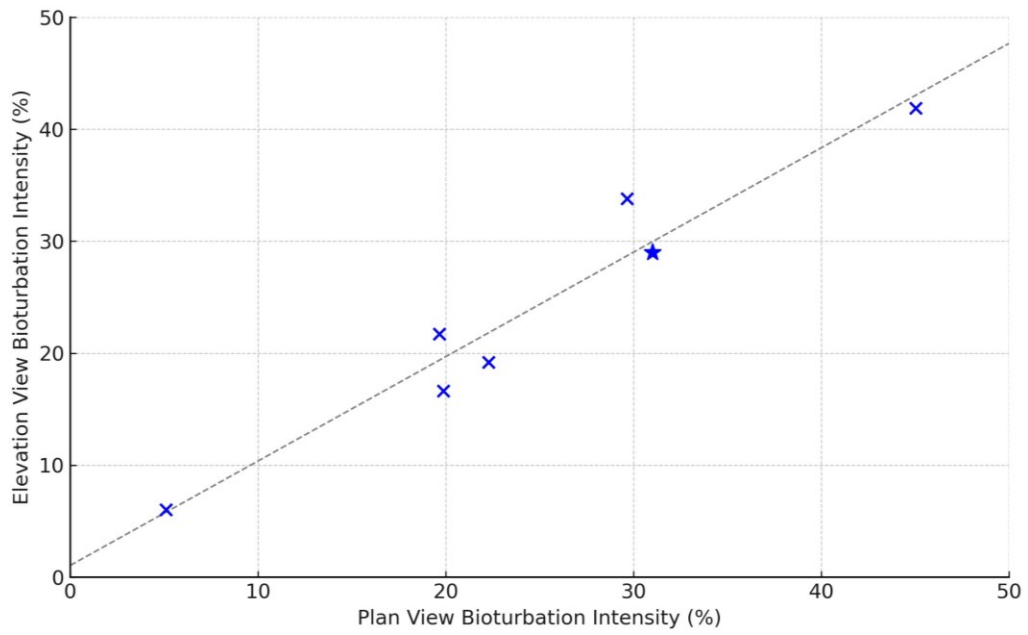


Figure 5.7. Plot showing a strong correlation between plan view and elevation view bioturbation intensities for all examined piperock. The star indicates Piperock 7.

5.6 Summary

Bedding planes hold significant value in ichnological analysis as they improve the recognition of ichnotaxa and yield important insights into the distribution and morphology of burrows. However, a significant limitation lies in the challenge of accurately estimating bioturbation intensity from bedding plane view. This is in part because current approaches do not establish a connection between bioturbation intensity as seen on bedding planes (plan view) and in cross-section (elevation view). This disconnect complicates the integration of bedding plane assessments into more conventional datasets collected from elevation view. This study employs Monte Carlo simulations to explore the relationship between plan and elevation view bioturbation intensities, using *Skolithos*-dominated trace fossils (piperock) from the Lower Cambrian Gog Group for comparison. The findings reveal a strong correlation between plan and elevation view bioturbation intensities. Specifically, elevation view bioturbation intensity can be approximated by multiplying plan view bioturbation intensity by the average burrow length relative to the bed thickness. Observations from the piperock indicate that burrow lengths often surpass bed thickness, suggesting a nearly 1:1 correlation between the bioturbation intensities in both views, confirmed by outcrop analysis.

5.7 References

- Allport, H. A., Davies, N. S., Shillito, A. P., Mitchell, E. G., & Herron, S. T. (2022). Non-palimpsested crowded *Skolithos* ichnofabrics in a Carboniferous tidal rhythmite: Disentangling ecological signatures from the spatio-temporal bias of outcrop. *Sedimentology*, *69*, 1028–1050.
- Bhattacharya, J. P., Howell, C. D., MacEachern, J. A., & Walsh, J. P. (2020). Bioturbation, sedimentation rates, and preservation of flood events in deltas. *Palaeogeography, Palaeoclimatology, Palaeoecology*, *560*, 110049.
- Campbell, R. B. (1973). Structural cross-section and tectonic model of the southeastern Canadian Cordillera. *Canadian Journal of Earth Sciences*, *10*, 1607–1620.
- Deiss, C. (1940). Lower and Middle Cambrian stratigraphy of southwestern Alberta and southeastern British Columbia. *GSA Bulletin*, *51*, 731–793.
- Desjardins, P. R., Buatois, L. A., Pratt, B. R., & Mángano, G., M. (2012). Sedimentological-ichnological model for tide-dominated shelf sandbodies: Lower Cambrian Gog Group of western Canada: Subtidal compound cross-stratified sandstone architecture. *Sedimentology*, *59*, 1452–1477.
- Desjardins, P. R., Mángano, M. G., Buatois, L. A., & Pratt, B. R. (2010). *Skolithos* pipe rock and associated ichnofabrics from the southern Rocky Mountains, Canada: Colonization trends and environmental controls in an early Cambrian sand-sheet complex. *Lethaia*, *43*, 507–528.
- Dorador, J., & Rodríguez-Tovar, F. J. (2018). High-resolution image treatment in ichnological core analysis: Initial steps, advances and prospects. *Earth-Science Reviews*, *177*, 226–237.
- Droser, M. L., & Bottjer, D. J. (1986). A semiquantitative field classification of ichnofabric.

- Journal of Sedimentary Research*, 56, 558–559.
- Droser, Mary L. (1991). Ichnofabric of the Paleozoic *Skolithos* ichnofacies and the nature and distribution of *Skolithos* piperock. *Palaios*, 6, 316–325.
- Droser, Mary L., & Bottjer, D. J. (1989). Ichnofabric of Sandstones Deposited in High-Energy Nearshore Environments: Measurement and Utilization. *PALAIOS*, 4, 598–604.
- Ekdale, A. A., & Lewis, D. W. (1993). Sabellariid reefs in Ruby Bay, New Zealand; a modern analogue of *Skolithos* “piperock” that is not produced by burrowing activity. *Palaios*, 8, 614–620.
- Eltom, H. A., Alqubalee, A. M., & Babalola, L. O. (2022). Understanding the two-dimensional quantification of bioturbation intensity through computer modeling and statistical analysis. *International Journal of Earth Sciences*, 111, 127–143.
- Hauck, T. E., Dashtgard, S. E., Pemberton, S. G., & Gingras, M. K. (2009). Brackish-water ichnological trends in a microtidal barrier island–embayment system, Kouchibouguac National Park, New Brunswick, Canada. *Palaios*, 24, 478–496.
- Howard, J. D. (1975). The sedimentological significance of trace fossils. In R. W. Frey (Ed.), *The Study of Trace Fossils: A Synthesis of Principles, Problems, and Procedures in Ichnology* (pp. 131–146). Berlin, Heidelberg: Springer.
- La Croix, A. D., Dashtgard, S. E., & MacEachern, J. A. (2019). Using a modern analogue to interpret depositional position in ancient fluvial-tidal channels: Example from the McMurray Formation, Canada. *Geoscience Frontiers*, 10, 2219–2238.
- Lapworth, C. (1883). The Secret of the Highlands. *Geological Magazine*, 10, 120–128.
- MacCulloch, J. (1814). Remarks on several parts of Scotland which exhibit quartz rock, and on the nature and connecions, of this Rock in general. *Transactions of the Geological Society of London*, 2, 450–486.

- Marenco, K. N., & Bottjer, D. J. (2010). The intersection grid technique for quantifying the extent of bioturbation on bedding planes. *Palaios*, *25*, 457–462.
- Marenco, Katherine N., & Hagadorn, J. W. (2019). Big bedding planes: Outcrop size and spatial heterogeneity influence trace fossil analyses. *Palaeogeography, Palaeoclimatology, Palaeoecology*, *513*, 14–24.
- McIlroy, D., & Garton, M. (2010). Realistic interpretation of ichnofabrics and palaeoecology of the pipe-rock biotope. *Lethaia*, *43*, 420–426.
- Melnyk, S., Cowper, A., Zonneveld, J.-P., & Gingras, M. K. (2022). Applications of photogrammetry to neoichnological studies: The significance of shorebird trackway distributions at the bay of fundy. *Palaios*, *37*, 606–621.
- Melnyk, S., & Gingras, M. (2020). Using ichnological relationships to interpret heterolithic fabrics in fluvio-tidal settings. *Sedimentology*, *67*.
- Miguez-Salas, O., Dorador, J., & Rodríguez-Tovar, F. J. (2019). Introducing Fiji and ICY image processing techniques in ichnological research as a tool for sedimentary basin analysis. *Marine Geology*, *413*, 1–9.
- Miguez-Salas, O., Löwemark, L., Pan, Y.-Y., & Rodríguez-Tovar, F. J. (2022). Selective colonization after storm events in a delta environment: Applied ichnology from the early Miocene of Taiwan. *Ichnos*, *29*, 27–39.
- Miller, M. F., & Smail, S. E. (1997). A semiquantitative field method for evaluating bioturbation on bedding planes. *PALAIOS*, *12*, 391–396.
- Mooney, C. Z. (1997). *Monte Carlo Simulation*. SAGE.
- Mountjoy, E. W. (1962). *Mount Robson (southeast) map-area, Rocky Mountains of Alberta and British Columbia*. Geological Survey of Canada.
- Mountjoy, E. W., & Aitken, J. D. (1963). Early Cambrian and late Precambrian paleocurrents, Banff and Jasper National Parks. *Bulletin of Canadian Petroleum*

Geology, 11, 161–168.

- Nicol, J. (1857). On the red sandstone and conglomerate, and the superposed quartz-rocks, limestones, and gneiss of the northwest coast of Scotland. *Quarterly Journal of the Geological Society of London*, 13, 17–39.
- Peach, B. N., Horne, J., Gunn, W., Clough, C. T., & Hinxman, L. W. (1907). *The geological structure of the north-west highlands of Scotland*. London, England: The Stationary Office.
- Piper, D. J. W., & Marshall, N. F. (1969). Bioturbation of Holocene sediments on La Jolla deep sea fan, California. *Journal of Sedimentary Research*, 39, 601–606.
- Reineck, H.-E. (1963). Sedimentgefüge im Bereich der südlichen Nordsee. *Abhandlungen der senckenbergische naturforschende Gesellschaft*, 505, 1–138.
- Rodríguez-Tovar, F. J., Miguez-Salas, O., & Dorador, J. (2020). Image processing techniques to improve characterization of composite ichnofabrics. *Ichnos*, 27, 258–267.
- Savrda, C. E., & Bottjer, D. J. (1986). Trace-fossil model for reconstruction of paleo-oxygenation in bottom waters. *Geology*, 14, 3.
- Savrda, C. E., & Bottjer, D. J. (1987). *The exaerobic zone, a new oxygen-deficient marine biofacies*.
- Savrda, C. E., & Bottjer, D. J. (1989). Trace-fossil model for reconstructing oxygenation histories of ancient marine bottom waters: Application to upper cretaceous niobrara formation, Colorado. *Palaeogeography, Palaeoclimatology, Palaeoecology*, 74, 49–74.
- Savrda, C. E., Bottjer, D. J., & Gorsline, D. S. (1984). Development of a Comprehensive Oxygen-Deficient Marine Biofacies Model: Evidence from Santa Monica, San Pedro, and Santa Barbara Basins, California Continental Borderland¹. *AAPG*

Bulletin, 68, 1179–1192.

Slind, O. L., & Perkins, G. D. (1966). Lower Paleozoic and Proterozoic sediments of the Rocky Mountains between Jasper, Alberta and Pine River, British Columbia.

Bulletin of Canadian Petroleum Geology, 14, 442–468.

Taylor, A. M., & Goldring, R. (1993). Description and analysis of bioturbation and ichnofabric. *Journal of the Geological Society*, 150, 141–148.

Timmer, E. R., Gingras, M. K., & Zonneveld, J.-P. (2016). Pychno: A core-image quantitative ichnology logging software. *Palaios*, 31, 525–532.

CHAPTER 6 – USING ICHNOLOGICAL RELATIONSHIPS TO INTERPRET HETEROLITHIC FABRICS IN FLUVIO-TIDAL SETTINGS

6.1 Introduction

The term “Inclined Heterolithic Stratification” (IHS) was proposed by Thomas et al. (1987) to classify laterally accreting, lithologically heterogeneous deposits that display coherent depositional dips. A large proportion of these deposits record the lateral accretion of point bars within meandering channels (Thomas et al., 1987). In addition, IHS can form with elements of downstream accretion and counter point-bars (Smith et al., 2011). Based on the examination of both modern (de Mowbray, 1983; Smith, 1988; Allen, 1991; Choi et al., 2004; Choi, 2010; Sisulak and Dashtgard, 2012; La Croix and Dashtgard, 2015; Shchepetkina et al., 2016a) and ancient settings (Rahmani, 1988; Ranger and Pemberton, 1992; Räsänen et al., 1995; Eberth, 1996; Falcon-Lang, 1998; Gingras et al., 2002; Rebata et al., 2006; Shchepetkina et al., 2016b), the majority of reported IHS has been attributed to the deposition of tidally influenced point bars. The development of IHS is most prominent in meandering channels of estuaries (Thomas et al., 1987) where deposition is influenced by fluvial and tidal processes in varying proportions and the overall hydraulic energy is at a minimum (Dalrymple et al., 1992). The IHS deposits of the McMurray Formation have been variably ascribed to deltas (Carrigy, 1971; Nelson and Glaister, 1978), fluvially dominated point bars (Mossop, 1980; Mossop and Flach, 1983; Flach and Mossop, 1985; Smith et al., 2009; Hubbard et al., 2011; Labrecque et al., 2011; Durkin et al., 2017), and tidally influenced (estuarine) point bars (Stewart and MacCallum, 1978; Pemberton et al., 1982; Wightman et al., 1987; Smith, 1987, 1988; Beynon et al.,

1988; Keith et al., 1988; Ranger and Pemberton, 1988, 1992; Wightman and Pemberton, 1997; Langenberg et al., 2002; Crerar and Arnott, 2007; Musial et al., 2012; Gingras et al., 2016; Shchepetkina et al., 2016a,b).

Ichnological data is becoming increasingly relied upon to assess the degree of marine influence and the landward extent of brackish-water incursion in ancient fluvio-tidal settings (Gingras et al., 2002; La Croix et al., 2015, 2019). Pemberton et al. (1982) first demonstrated that the ichnological characteristics observed throughout the McMurray Formation, and particularly in IHS deposits, indicate a brackish-water depositional setting. Interpreted brackish-water suites comprise low-diversity trace fossil assemblages which display a locally high intensity of bioturbation. Constituent structures are morphologically simple and resemble the domiciles of infaunal trophic generalists recruited from marine communities (Pemberton and Wightman, 1992). Similar characteristics have since been recognized in fluvio-tidal IHS globally in both modern and ancient settings (e.g., Gingras et al., 1999, 2002; Rebata et al., 2006; Sisulak and Dashtgard, 2012; La Croix et al., 2015).

Although the rhythmicity of IHS is often associated with semidiurnal or diurnal tidal cycles, Gingras et al. (2002, 2011) suggested that the presence of burrowing implies that the sedimentation rates must have been sufficiently low to allow organisms to colonize the substrate. As such, the deposition of bioturbated IHS packages is more likely linked to seasonal or annual variations in river discharge. In addition, it has been quantitatively demonstrated that the cyclicity of physical and chemical paleoecological stresses at the estuary scale is linked to climatic variation periods (possibly El Niño–Southern Oscillation cycles) (Timmer et al., 2016b). Nevertheless, examples from the McMurray Formation (Timmer et al., 2016a) and Amazon Basin (Hovikoski et al., 2008) have shown that the

interlaminated portions of IHS can be consistent with tidal periodicities. These examples were dominantly unburrowed, suggesting more rapid sedimentation rates.

Since IHS was defined more than 3 decades ago, it has been recognized as a volumetrically important constituent of tidally influenced sedimentary systems (Dalrymple and Choi, 2007). Apart from identifying the temporal nature of regularly bedded IHS as semi-diurnal or annual using ancillary features such as bioturbation (Gingras et al., 2002, 2011; Sisulak and Dashtgard, 2012) and frequency analyses (Hovikoski et al. 2008; Labrecque et al., 2011; Timmer et al., 2016b), the concept of IHS has evolved little since its introduction. Using examples from fluvio-tidal parts of the McMurray Formation in Alberta, Canada, this paper presents a framework – using detailed ichnological analysis – to determine the relative depositional position that IHS accumulated within the fluvio-tidal system. This study demonstrates how the ichnological relationships of these bioturbated IHS deposits can be related to fluvio-tidal processes to determine the relative importance of tidal *versus* fluvial processes where sediment deposition occurred.

6.2 Study Area and Dataset

This study is based on core data from the Lower Cretaceous (Aptian) McMurray Formation in the Western Canadian Sedimentary Basin. The McMurray Formation unconformably overlies Devonian-aged carbonates of the Beaverhill Lake Group and is unconformably overlain by the Wabiskaw Member of the Clearwater Formation. The study area is located 20 km northeast of Fort McMurray, Alberta, encompassing Township 92 and Range 8W4 (Figure 6.1). A detailed core analysis was conducted on 24 cores with a total cumulative thickness of more than 1,500 m. The dataset consists of

Table 6.1. Summary of studied well bore locations.

UWI	McMurray Formation Total Depth (m)
AA/13-02-092-08W4/0	189.5 - 133.5
AA/11-03-092-08W4/0	178.7 - 123.0
AA/11-04-092-08W4/0	152.3 - 101.9
AA/04-06-092-08W4/0	154.9 - 98.0
AA/15-09-092-08W4/0	169.4 - 108.9
AA/06-10-092-08W4/0	175.7 - 121.8
AA/12-11-092-08W4/0	187.9 - 128.7
AA/12-12-092-08W4/0	186.5 - 142.4
AA/05-13-092-08W4/0	187.1 - 136.5
S0/03-14-092-08W4/0	189.7 - 127.0
AA/10-15-092-08W4/0	176.4 - 113.6
AA/16-16-092-08W4/0	164.5 - 115.3
AB/16-19-092-08W4/0	135.2 - 75.8
AA/16-21-092-08W4/0	165.1 - 110.0
AA/10-22-092-08W4/0	175.2 - 110.2
AA/10-23-092-08W4/0	181.5 - 122.5
AA/07-24-092-08W4/0	192.8 - 136.3
AA/03-25-092-08W4/0	198.7 - 138.9
AA/07-27-092-08W4/0	173.6 - 115.4
AB/12-30-092-08W4/0	121.8 - 73.9
AA/11-33-092-08W4/0	163.0 - 106.6
AA/04-34-092-08W4/0	165.2 - 110.8
AA/10-35-092-08W4/0	190.3 - 134.7
AA/10-36-092-08W4/0	219.8 - 149.6

sedimentological and ichnological observations collected through systematic core analysis. The dataset consists of sedimentological and ichnological observations collected through systematic core analysis. All cores used in this study are available at the Alberta Energy Regulators Core Research Centre. Individual cores were selected based on the presence of dipmeter data, inter-well proximity and vintage (preference was given to more recently cored wells).

The most common facies within the study area is IHS containing interbedded sandstone and siltstone in varying proportions. In this paper, the ichnological variation of these heterolithic deposits is demonstrated by examining two endmember fabrics: A) sand-dominated IHS with bioturbation associated exclusively with silt deposition; and B) silt-dominated IHS with bioturbation associated exclusively with sand deposition.

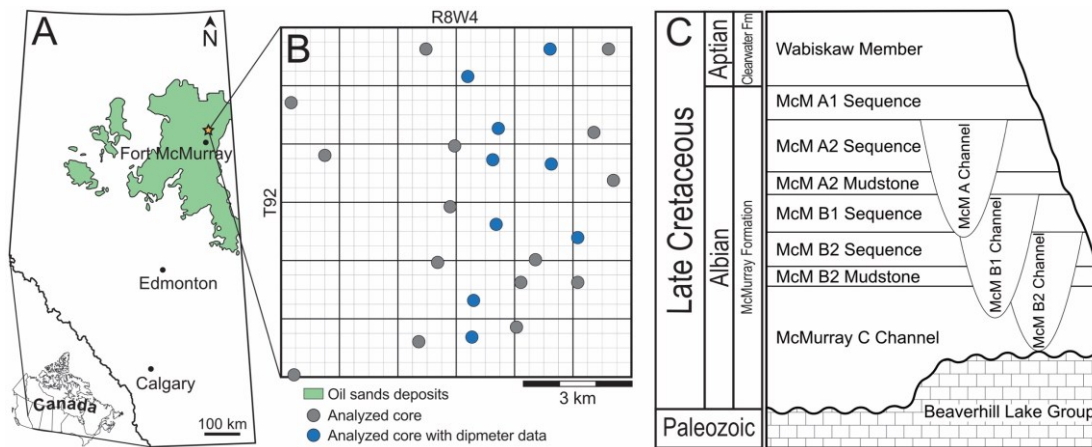


Figure 6.1. (A) Map of Alberta, Canada, outlining the distribution of oil sands deposits. (B) Location of the 24 cores logged for this study. (C) Schematic stratigraphy of the study area.

6.3 Methods

Each core selected for this study was logged in detail using the software AppleCore. Sedimentological analysis focused on characterizing the lithology, grain size, bed thickness, bedding contacts, primary physical sedimentary structures and lithologic accessories (e.g., coal fragments, organic detritus, mud rip-up clasts). Ichnological observations concentrated on the identification and relative abundance of ichnogenera, bioturbation intensity (*sensu* Reineck, 1963; Taylor and Goldring, 1993), trace-fossil size and diversity, and the distribution of bioturbation between beds and bedsets.

Dipmeter data from various wells (Figure 6.1) aided in the identification of continuous point-bar deposits (Muwais and Smith, 1990; Brekke and Couch, 2011). Additionally, point-bar deposits were delineated by the presence of mud breccia at the base of a succession; the disruption of an overall upwards-fining succession; an abrupt change in mud abundance or heterolithic character; and an abrupt change in bioturbate texture (Crerar and Arnott, 2007).

6.4 Results

Two endmember IHS fabrics are recognized based on their sedimentologic and ichnologic character: these are assigned to Fabric A (sand-dominated IHS with bioturbated siltstone) and B (silt-dominated IHS with bioturbated sandstone). Examples of these fabrics chosen for this study are bound above and below by discontinuities, with contiguous strata displaying a variety of expressions consisting of cross-bedded sandstone, IHS or heavily bioturbated heterolithic deposits. A list of occurrences for each endmember fabric is included in the supporting information (

Table 6.3).

Table 6.1. Summary of studied well bore locations.

UWI	McMurray Formation Total Depth (m)
AA/13-02-092-08W4/0	189.5 - 133.5
AA/11-03-092-08W4/0	178.7 - 123.0
AA/11-04-092-08W4/0	152.3 - 101.9
AA/04-06-092-08W4/0	154.9 - 98.0
AA/15-09-092-08W4/0	169.4 - 108.9
AA/06-10-092-08W4/0	175.7 - 121.8
AA/12-11-092-08W4/0	187.9 - 128.7
AA/12-12-092-08W4/0	186.5 - 142.4
AA/05-13-092-08W4/0	187.1 - 136.5
S0/03-14-092-08W4/0	189.7 - 127.0
AA/10-15-092-08W4/0	176.4 - 113.6
AA/16-16-092-08W4/0	164.5 - 115.3
AB/16-19-092-08W4/0	135.2 - 75.8
AA/16-21-092-08W4/0	165.1 - 110.0
AA/10-22-092-08W4/0	175.2 - 110.2
AA/10-23-092-08W4/0	181.5 - 122.5
AA/07-24-092-08W4/0	192.8 - 136.3
AA/03-25-092-08W4/0	198.7 - 138.9
AA/07-27-092-08W4/0	173.6 - 115.4
AB/12-30-092-08W4/0	121.8 - 73.9
AA/11-33-092-08W4/0	163.0 - 106.6
AA/04-34-092-08W4/0	165.2 - 110.8
AA/10-35-092-08W4/0	190.3 - 134.7
AA/10-36-092-08W4/0	219.8 - 149.6

Table 6.1. Summary of studied well bore locations.

UWI	McMurray Formation Total Depth (m)
AA/13-02-092-08W4/0	189.5 - 133.5
AA/11-03-092-08W4/0	178.7 - 123.0
AA/11-04-092-08W4/0	152.3 - 101.9
AA/04-06-092-08W4/0	154.9 - 98.0
AA/15-09-092-08W4/0	169.4 - 108.9
AA/06-10-092-08W4/0	175.7 - 121.8
AA/12-11-092-08W4/0	187.9 - 128.7
AA/12-12-092-08W4/0	186.5 - 142.4
AA/05-13-092-08W4/0	187.1 - 136.5
S0/03-14-092-08W4/0	189.7 - 127.0
AA/10-15-092-08W4/0	176.4 - 113.6
AA/16-16-092-08W4/0	164.5 - 115.3
AB/16-19-092-08W4/0	135.2 - 75.8
AA/16-21-092-08W4/0	165.1 - 110.0
AA/10-22-092-08W4/0	175.2 - 110.2
AA/10-23-092-08W4/0	181.5 - 122.5
AA/07-24-092-08W4/0	192.8 - 136.3
AA/03-25-092-08W4/0	198.7 - 138.9
AA/07-27-092-08W4/0	173.6 - 115.4
AB/12-30-092-08W4/0	121.8 - 73.9
AA/11-33-092-08W4/0	163.0 - 106.6
AA/04-34-092-08W4/0	165.2 - 110.8
AA/10-35-092-08W4/0	190.3 - 134.7
AA/10-36-092-08W4/0	219.8 - 149.6

6.4.1 Sand-Dominated IHS with Bioturbated Siltstone

The sand-dominated Fabric A (Figure 6.3) consists of IHS with very fine-grained sandstone and siltstone. Bedding contacts are typically sharp or bioturbated with gradational contacts observed locally. The thickness of the sandstone lithosomes is highly variable, ranging from 12 mm to 82 cm. Bedding planes record the original depositional dip (ranging from 3° to 19°) and are normally dipping in a channelward direction. Local current ripples preserved. Isolated mud rip-up clasts are common. Mudstone lithosomes range from 2 mm to 6 cm in thickness and commonly occur as double mud drapes (Figure 6.3C). Where preserved, bedding is planar laminated. Soft sediment deformation is abundant. Internal stratification is observed locally with alternations of more silt-rich and more clay-rich laminae. Disseminated organic detritus occurs in varying amounts (0-20% by volume). Mudstone lithosomes may also contain minor sandstone interlaminae (Figure 6.3B).

Table 6.2. Summary of results for fabrics A and B.

Lithosome	Grain size	Bedding contacts	Bed thickness	Sedimentary structures	Accessories	BI	Trace fossils
<u>Fabric A</u>							
Sandstone	Lower very fine to lower fine sand	Sharp	12 mm to 82 cm	Low to high angle planar cross-stratification, current ripples	Mud rip-up clasts, pyrite	0-1	Fugichnia
Mudstone	Clay to silt	Sharp to bioturbated, rarely gradational	2 mm to 62 mm	Planar lamination	Organic detritus, pyrite	1-5	<i>Cylindrichnus</i> , <i>Planolites</i> , <i>Arenicolites</i> , <i>Gyrolithes</i> , <i>Skolithos</i> , <i>Teichichnus</i>
<u>Fabric B</u>							
Sandstone	Lower very fine to upper fine sand	Bioturbated	4 mm to 8 cm	Structureless	None observed	3-6	<i>Planolites</i> , <i>Gyrolithes</i> , <i>Arenicolites</i> , <i>Cylindrichnus</i> , <i>Skolithos</i> , <i>Thalassinoides</i>
Mudstone	Clay to silt	Sharp	2 cm to 15 cm	Planar lamination	Soft sediment deformation, pyrite, organic detritus	0-1	<i>Planolites</i>

Table 6.3. List of occurrences for each endmember fabric.

UWI	Total Depth (m)
<u>Fabric A</u>	
AA/15-09-092-08W4/0	150.5 - 121.7
AA/06-10-092-08W4/0	150.3 - 130.0
AA/10-23-092-08W4/0	147.8 - 127.7
<u>Fabric B</u>	
AA/11-03-092-08W4/0	170.3 - 165.7
AA/07-27-092-08W4/0	166.3 - 151.8
AA/11-33-092-08W4/0	170.3 - 165.7
AA/04-34-092-08W4/0	156.0 - 148.5

Bioturbation is found almost exclusively within mudstone lithosomes and sandstone tops with mud from the overlying bed infilling or lining the burrows (Figure 6.3D), although escape traces (fugichnia) are sometimes observed near the base of sandstone lithosomes (Figure 6.3B). Mudstone lithosomes display a highly variable Bioturbation Index (BI 1-5), although BI values of 2-4 predominate. Burrows are characterized by sporadically distributed, impoverished trace-fossil assemblages. Diminutive structures display a maximum burrow diameter of 9 mm. Individual forms include *Planolites*, *Cylindrichnus*, *Arenicolites*, and *Gyrolithes* with lesser *Skolithos* and *Teichichnus*. *Cylindrichnus* may be found in monospecific assemblages originating from the mudstone and subtending into the underlying sandstone lithosome. Heavily

bioturbated mudstone beds are common, precluding the identification of ichnogenera. Locally occurring, structureless, unburrowed mudstone beds are thicker than their bioturbated counterparts (Figure 6.3A).

6.4.2 Mud-Dominated IHS with Bioturbated Sandstone

Fabric B (Figure 6.2) consists of IHS that is either silt-dominated or has approximately equal proportions of sandstone and siltstone. The coarse members are composed of fine-grained sandstone. Sandstone lithosomes range in thickness from 4 mm to 8 cm and are sometimes discontinuous. Basal sandstone contacts are commonly bioturbated. The sandstone is massive and contains rare mudstone interlaminae. Sharp-based mudstone lithosomes range from 1 to 15 cm in thickness. Mudstones are structureless to planar laminated and contain local sandstone interlaminae. Soft sediment deformation is common.

Bioturbation is present exclusively within sandstone beds and mudstone tops, with sand from the overlying bed infilling the burrows. Burrows within sandstone lithosomes are commonly delineated by silty burrow linings. Sandstones are commonly heavily bioturbated to biogenically homogenized (BI 4-6); beds that have lower bioturbation intensities (BI 3) display sporadic trace fossil distributions. Trace-fossil suites consist predominantly of structures resembling *Planolites*. Present ichnogenera include *Gyrolithes*, *Cylindrichnus*, *Arenicolites*, *Skolithos*. *Gyrolithes* commonly occurs in monospecific abundance (Figure 6.2D). Individual forms are generally diminutive (burrow diameters less than 7 mm), although larger traces (up to 16 mm in diameter) such as *Thalassinoides* occur locally in sandstone lithosomes.

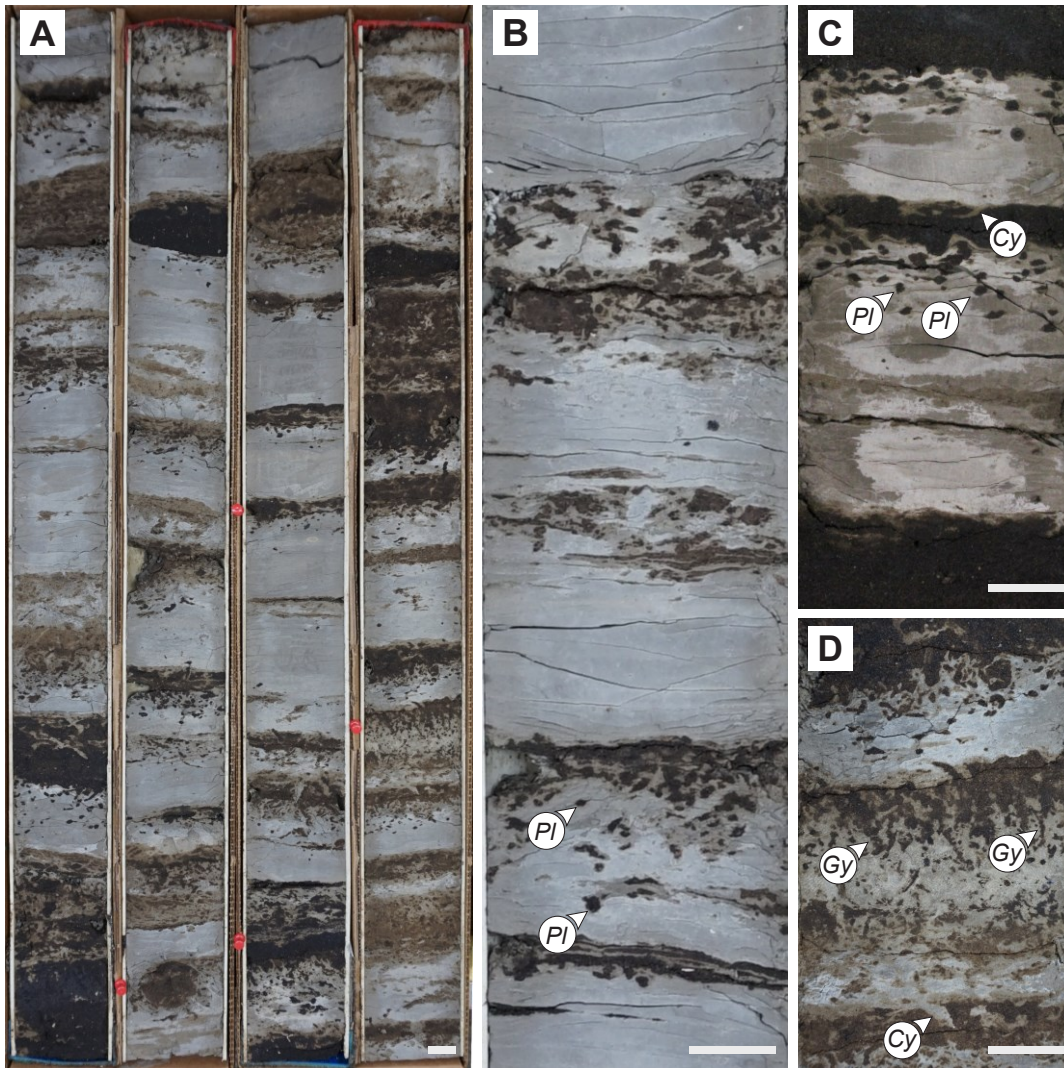


Figure 6.2. Examples of Fabric B from various core. The darker portions consist of bitumen saturated sandstone and the lighter portions comprise siltstone. Scale bars = 3 cm. (A) Cored succession from 57.01928°, 111.20736°. Bottom is lower left and top is upper right. Shown is silt-dominated IHS with bioturbation largely confined to sandstone lithosomes and morphologically simple burrows subtending into underlying mudstones. (B) Typical expression of Fabric B with *Planolites* (*Pl*) sporadically distributed throughout the sandstone lithosomes. 57.01928°, 111.20736°. (C) Example of a bioturbated sandstone lithosome with *Planolites* (*Pl*) subtending into the underlying mudstone. Overlying fluid mud bed cross-cuts mud-lined *Cylindrichnus* (*Cy*) associated with sand deposition. 56.99345°, 111.14190°. (D) Example of a heavily bioturbated sandstone lithosome containing a monospecific assemblage of *Gyrolithes* (*Gy*). Many burrows originate from the mudstone beds, representing a departure from the archetypal Fabric B (*i.e.* deposition occurred seaward of Fabric B). 57.01928°, 111.20736°.

Table 6.4. Summary of interpretations for fabrics A and B.

IHS Fabric	Summary	Interpretation
Fabric A: Unburrowed cross-bedded sandstone and bioturbated mudstone	Sandstone represents deposition during high river discharge. Bioturbated mudstone is associated with low river discharge and a landward shift of the turbidity maximum zone. Mudstone is colonized by brackish-tolerant animals during times of low river discharge.	Fluvially dominated deposition within the (1) outermost inner to middle estuary (<i>sensu</i> Shchepetkina et al. 2016b); or (2) mixed fluvial-tidal to turbidity maximum zone of distributary channel systems (<i>sensu</i> La Croix et al. 2019).
Fabric B: Bioturbated sandstone and unburrowed laminated mudstone	Mudstone represents mud sedimentation associated with low river discharge. Bioturbated sandstone represents tidally transported and winnowed sand that is colonized by brackish-tolerant animals during times of low river discharge.	Tidally dominated deposition within the (1) middle estuary (<i>sensu</i> Shchepetkina et al. 2016a); or (2) outermost mixed fluvial-tidal zone (<i>sensu</i> La Croix et al. 2019).

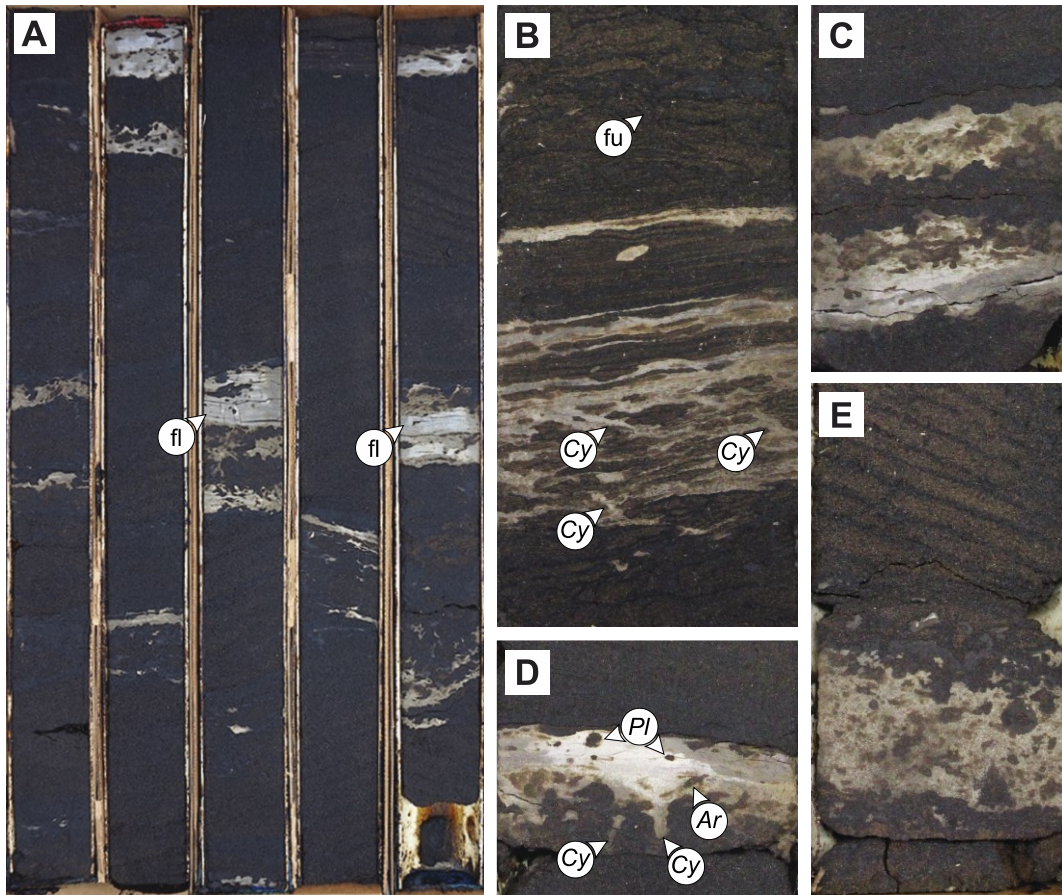


Figure 6.3. Examples of Fabric A from various core. The darker portions consist of bitumen saturated sandstone and the lighter portions comprise siltstone. Scale bars = 3 cm. (A) Cored succession from 56.96332°, 111.20534°. Bottom is lower left and top is upper right. Shown is sand-dominated IHS consisting of cross-bedded sandstone and bioturbated mudstone with locally occurring fluid mud beds (fi) that are largely unburrowed except for bed tops. (B) Example of a mudstone lithosome containing sandstone interlaminae with monospecific *Cylindrichnus* (Cy) and less common fugichnia (fu) present near the base of the overlying sandstone. 57.01928°, 111.20736°. (C) Heavily bioturbated double mud drape within unburrowed sandstone. 56.97955°, 111.15788°. (D) Burrowed mudstone lithosome with a trace-fossil assemblage of *Planolites* (Pl), *Arenicolites* (Ar) and *Cylindrichnus* (Cy). 56.96332°, 111.20534°. (E) Heavily bioturbated mudstone lithosome overlain by cross-bedded sandstone. 56.97352°, 111.17681°.

6.5 Interpretation and Discussion

In both fabrics studied, the heterolithic beds are interpreted to represent seasonal variations in river discharge and record the lateral accretion of fluvio-tidal point bars, an interpretation that is consistent with previous research (de Mowbray, 1983; Thomas et al., 1987; Smith, 1988; Gingras et al., 2002; Rebata et al., 2006; Musial et al., 2012; Sisulak and Dashtgard, 2012; Jablonski and Dalrymple, 2016). This interpretation is supported by the presence of bioturbated fabrics that would require weeks to months to develop (Gingras et al., 2008). Previous studies relate the deposition of the IHS couplets as a record of high river discharge (*i.e.* the sandstone lithosome) *versus* times of low river discharge and increased tidal influence (*i.e.* the mudstone lithosome) (e.g., Gingras et al., 2002; Sisulak and Dashtgard, 2012). This study contends that many examples of IHS—in this case Fabric B—preserve a record of increased fluvial discharge being associated with mud deposition and periods of tidal influence associated with sand deposition in more seaward positions from the fluvio-tidal settings.

6.5.1 Fabric A Interpretation

Fabric A comprises unburrowed cross-bedded sandstone and thinner beds of bioturbated mudstone. The cross-bedded sandstone is interpreted to represent episodes of high river discharge due to the overall lack of bioturbation, the absence of mudstone interlaminae and the preservation of comparatively thick ripple-laminated to cross-bedded sandstone beds. During high river discharge, a large portion of the fluvio-tidal system is fluvially dominated resulting in a net seaward transport of sediment (Dalrymple et al., 1992) (Figure 6.4). Under these conditions the turbidity maximum and saltwater wedge are flushed seaward and sand deposition records high-energy dune migration in dominantly freshwater (cf. La Croix and Dashtgard, 2014). Occasional escape traces

(fugichnia) present near the base of sandstone lithosomes are associated with an increase in sedimentation rates during sand deposition (Figure 6.3B).

The bioturbated mudstone is interpreted to represent periods of brackish-water, tidally facilitated larval recruitment and thereby a dominance of tidal processes (Lettley et al., 2007; Gingras et al., 2016). The landward shift of brackish water is owing to a reduction or cessation of river discharge. Concomitant with this shift, the mixing-zone associated turbidity maximum also shifts landward accompanied by increased flocculation and mud deposition (Kranck, 1981; Dyer, 1986; La Croix and Dashtgard, 2014). The overall lowered sedimentation rates, and most importantly the presence of brackish water and marine-derived larvae, promote colonization of the mud during periods of low river discharge.

6.5.2 Fabric B Interpretation

Fabric B comprises unburrowed, structureless to planar laminated mudstone with bioturbated sandstone interbeds or interlaminae. The mudstone is interpreted to have been deposited during high river discharge due to the absence of bioturbation and comparably greater bed thicknesses. Current strength increases during high river discharge, causing mud to be transported seaward into the outermost mixed fluvial tidal zone (Figure 6.4). An increase in river discharge reduces the already low salinity of the water (perhaps even to being completely fresh; 0 psu), significantly stressing brackish-intolerant marine infauna inhabiting the substrates (Schubel and Pritchard, 1986). Mud is deposited rapidly owing to the increase in sediment budget that results from an increase in river discharge. These depositional conditions preclude animal colonization and subsequent bioturbation.

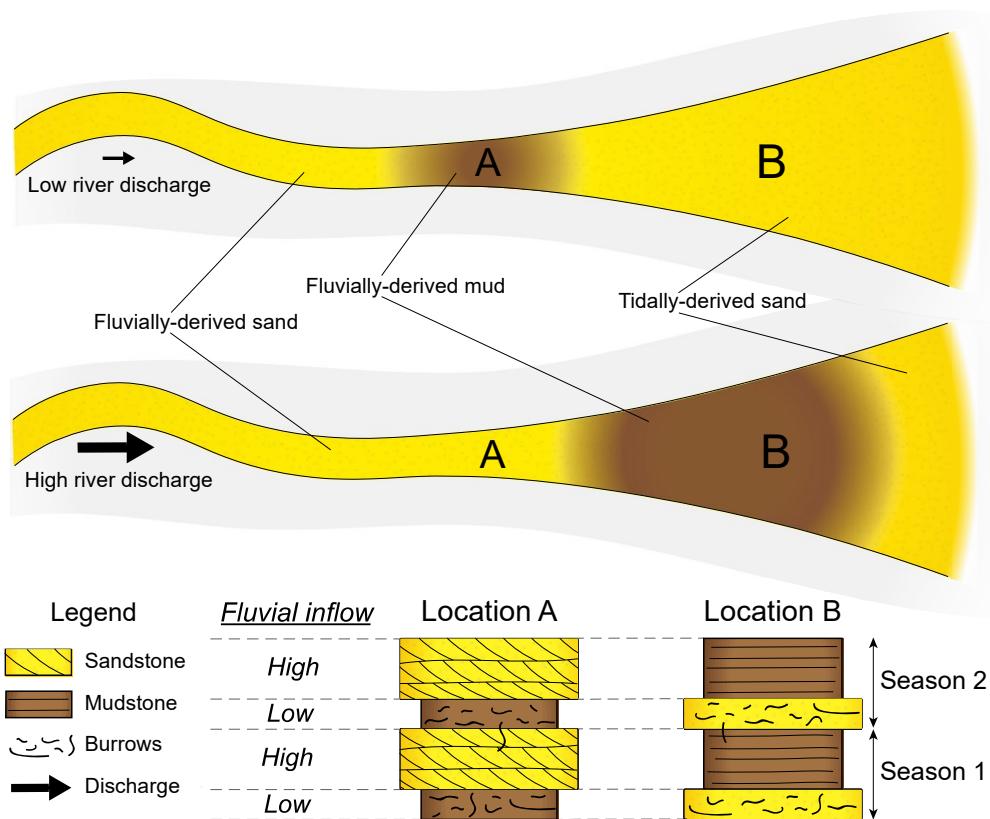


Figure 6.4. Schematic distribution of sediments in a tide-dominated estuary as a function of fluvial flux. Seasonal variations in river discharge result in an alternating dominance of tidal processes during periods low river discharge and fluvial processes during periods of high river discharge. Mud deposition is most prominent near the turbidity maximum, which shifts in response to the variations in river discharge. Locations A and B correspond to fabrics A and B, respectively. During low river discharge, small amounts of mud are delivered to the estuary and mud is deposited in the inner estuary (Location A). Lithosomes deposited during these times are associated with brackish water colonization windows and thus will be bioturbated. During high river discharge, increased amounts of mud are delivered to the estuary and mud is deposited seaward into the middle estuary (Location B). Periods of heightened river discharge record the deposition of comparably thick, unburrowed lithosomes, owing to the increase in sediment supply and freshwater conditions.

The bioturbated sandstone is interpreted to be tidally-derived and deposited under brackish-water conditions. This is owing to the presence of abundant bioturbation and the preservation of comparably thinner beds. Periods of low river discharge are associated with the return of the tidally dominated regime, especially in the outer reaches of the system. The turbidity maximum zone and associated mud sedimentation shift landwards and sand becomes the most abundant sediment type (Dalrymple et al., 1992) (Figure 6.4). As with the mudstone lithosome in Fabric A, in Fabric B it is the sandstone lithosome that is afforded colonization windows under conditions of brackish water and tidal-current facilitated larval advection (Lettley et al., 2007). The increase in overall bioturbation intensity and the inclusion of marine-associated *Thalassinoides* in the trace fossil suite can be explained by the more seaward position of Fabric B with respect to Fabric A. However, in both cases lowered (i.e. brackish) and fluctuating salinity is the dominant stress, giving rise to a similar ichnological expression that is shared between the two fabrics.

6.5.3 Depositional Setting

The IHS deposits that occur in this study are interpreted as fluvio-tidal to estuarine in origin, owing to the notable tidal influence and at least seasonal brackish-water conditions. Indeed, Bhattacharya (1992) suggested that increasingly tide-dominated systems do not show shoreline protuberances and therefore should be considered estuaries. Nevertheless the IHS in this study may constitute an abandoned delta that transitioned into an estuary following avulsion, abandonment and transgression. Sedimentological evidence of tidal influence includes the well-developed heterolithic nature of the deposits as well as the presence of bidirectional cross-stratification, tidal rhythmites and double mud drapes. In addition, trace fossils within the bioturbated

lithosomes indicate that deposition occurred under at least brackish-water conditions (cf. Pemberton et al., 1982; Wightman and Pemberton, 1987; Pemberton and Wightman, 1992; Lettley et al., 2007; Hubbard et al., 2011; Gingras et al., 2016; La Croix et al., 2019).

The distribution of each fabric is a function of seasonal fluvio-tidal hydrodynamics. The inferred hydrodynamic conditions responsible for the deposition of Fabric A are consistent with sedimentary processes in the outermost inner to middle estuary or distributary channels, whereas Fabric B is interpreted to develop in more distal settings (Table 6.4). The predominance of sharp-based bedding contacts indicates an abrupt change in depositional dynamics. In many examples, the top of the fluvially dominated bed is burrowed from the overlying bioturbated brackish-water-associated unit.

6.5.4 Refinement of the Sedimentary Environment

In fluvio-tidal settings, sand deposition is characteristically associated with high river discharge and mud deposition is associated with low river discharge. However, trace fossil distributions can be used to show when the opposite is true. Sandstones in fluvio-tidal through to estuary settings are best associated with the fluvially dominated inner reaches and the tidally dominated outer reaches: the area between the extreme reaches is more prone to sedimentation and preservation of IHS (Thomas et al., 1987) (Figure 6.4). Importantly, sand in the fluvial reaches is delivered from the river, but sand in the tide-dominated zone commonly includes remobilized fluvial sediments and inlet-associated sources (Dalrymple et al., 1990). Fluvially- and tidally-derived sandstones are separated by meandering zone containing the zone of bedload convergence (BLC), in which net landward tidal transport and net seaward fluvial transport are equal (Dalrymple et al., 1992) (Figure 6.4). In short, sand seaward of the BLC is normally sourced from the seaward direction.

The distributions of mud layers are in large part dictated by the range of positions of the turbidity maximum, whereby mud layers are thickest and most abundant near the turbidity maximum and mud content decreases in both a landward and seaward direction (Dalrymple and Choi, 2007; Lettley et al., 2007; La Croix and Dashtgard, 2014). The position and breadth of the turbidity maximum is also affected by river discharge and therefore varies seasonally (Figure 6.4).

In both fabrics discussed above, the bioturbated lithosome is interpreted to have been deposited during low river discharge, as bioturbation must be associated with brackish-water colonization windows and tidally facilitated larvae recruitment (Lettley et al., 2007; Staton et al., 2014; Gingras et al., 2016). During low river discharge, 1) smaller volumes of mud are delivered to the system, 2) the salinity limit extends landwards, and 3) the turbidity maximum zone contracts and shifts landwards. This results in comparatively thin, burrowed mud layers that are thickest and most abundant near the turbidity maximum (Fabric A) (Figure 6.4). Tidally delivered (bioturbated) sand deposition occurs seaward and, in more distal locales, constitute the low river discharge lithosome of Fabric B. The thicker, unburrowed lithosome of each fabric is associated with freshwater conditions (*i.e.* the unburrowed sandstone beds of Fabric A, and the unburrowed / fluid mud beds [e.g., MacKay and Dalrymple, 2011] of Fabric B).

Non-endmember bioturbated heterolithic fabrics (e.g., both sandstone and mudstone lithosomes are bioturbated) develop in conditions where the alternating dominance between fluvial and tidal processes is less significant. In estuaries that experience minor fluvial influence, but some seasonal variation in mud flux, both lithosomes may be associated with brackish-water colonization windows and thus will be bioturbated (Figure 6.3D). A similar fabric may develop in the outer reaches of estuaries where the volume of river discharge is greatly exceeded by the tidal prism. In contrast, IHS

that develops landward of the salinity limit (*i.e.* the tidal backwater zone) will be unburrowed since neither lithosome is associated with a brackish-water colonization window.

Although this paper focuses on estuaries, the interpretations can be applied to deltaic settings (Figure 6.5). Distributary channel systems are normally fluvially dominated, therefore the sedimentological record of distributary channels would be Fabric A (sand-dominated IHS with bioturbated mudstone). Similarly, bioturbated sandstone lithosomes that characterize Fabric B are less common in deltaic settings and we predict that Fabric B would be common only seawards of distributary mouth bars.

Ichnological relationships observed in modern IHS confirm that detailed burrow distributions can be used as a unique indicator of the importance of either tidal- or fluvial-processes (Figure 6.6). La Croix et al. (2019) provide excellent examples of bioturbated IHS of Fraser River fluvio-tidal to distributary channel IHS that nearly exclusively represent Fabric A (Figure 6.6A and B). By comparison, examples of Fabric B are observed in the inner-middle estuary portions of Willapa Bay (Figure 6.6C and D), where the bioturbation originates from the coarser lithosomes that are deposited and redistributed by tides during periods of decreased river discharge (Gingras et al., 1999).

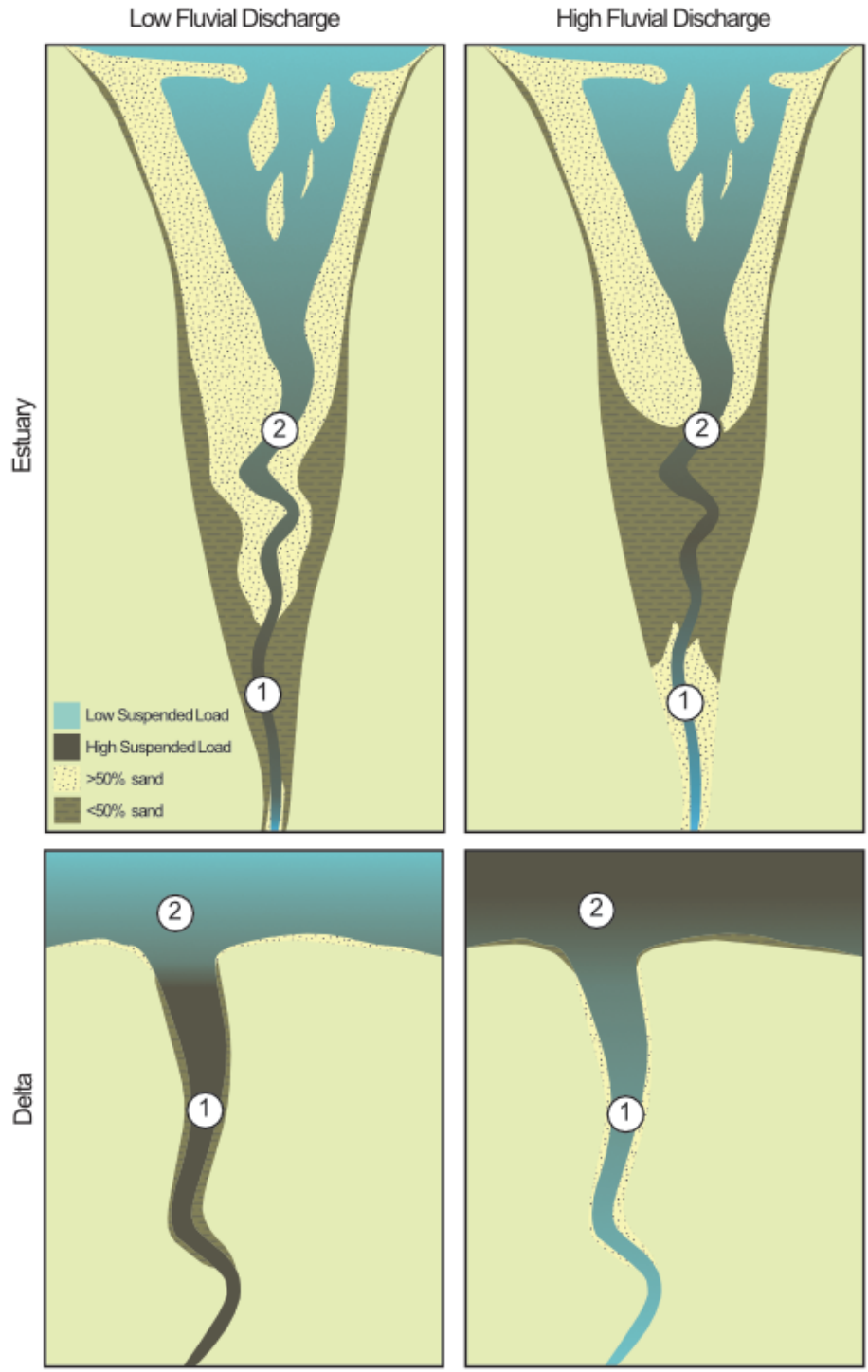


Figure 6.5. Comparison of suspended load concentration in estuary *versus* delta settings as a function of river discharge. Fabric A develops near the locations indicated as 1, while Fabric B develops near the locations indicated as 2.

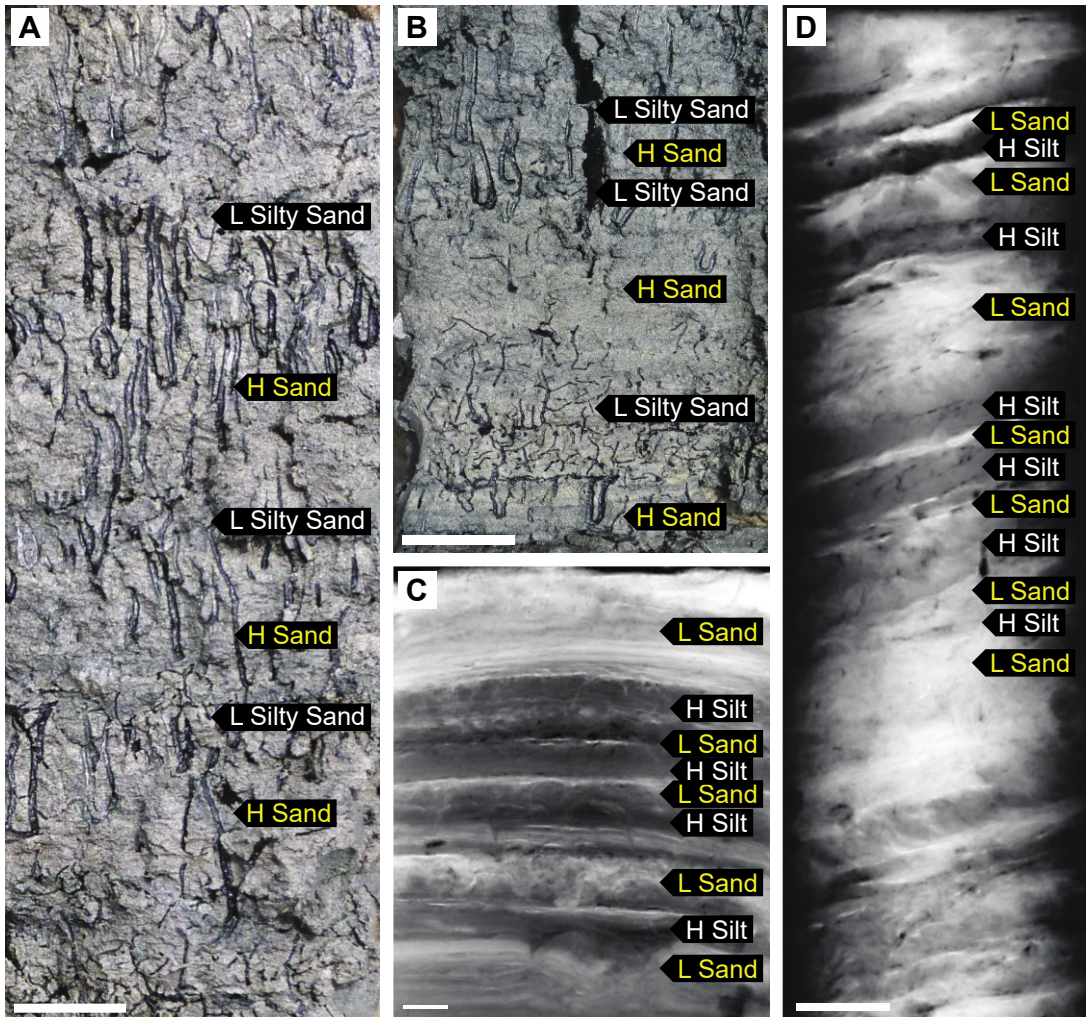


Figure 6.6. Modern examples bioturbated IHS. H = high river discharge; L = low river discharge. Scale bars = 3 cm. (A–B) Photographs of IHS from Fraser River, British Columbia that resemble Fabric A. Here the bioturbation is associated with the silty sand lithosomes, with the burrows commonly descending from the base of the silty sand into the underlying sand lithosome. This core was taken from one of the distributary channels of the Fraser River Delta, approximately 10 km landward of the distributary mouth bar complex. (C–D) Radiographs of IHS from Willapa Bay, Washington that resemble Fabric B. Notice that the mud lithosomes (dark grey on X-ray) are generally unburrowed and that the sands (white on X-ray) display most of the bioturbation. The annual nature of the IHS is demonstrated in Gingras et al. (2014) and the importance of burrow distributions is discussed in Gingras and MacEachern (2012). Location maps for both examples are included in Figure 6.7.

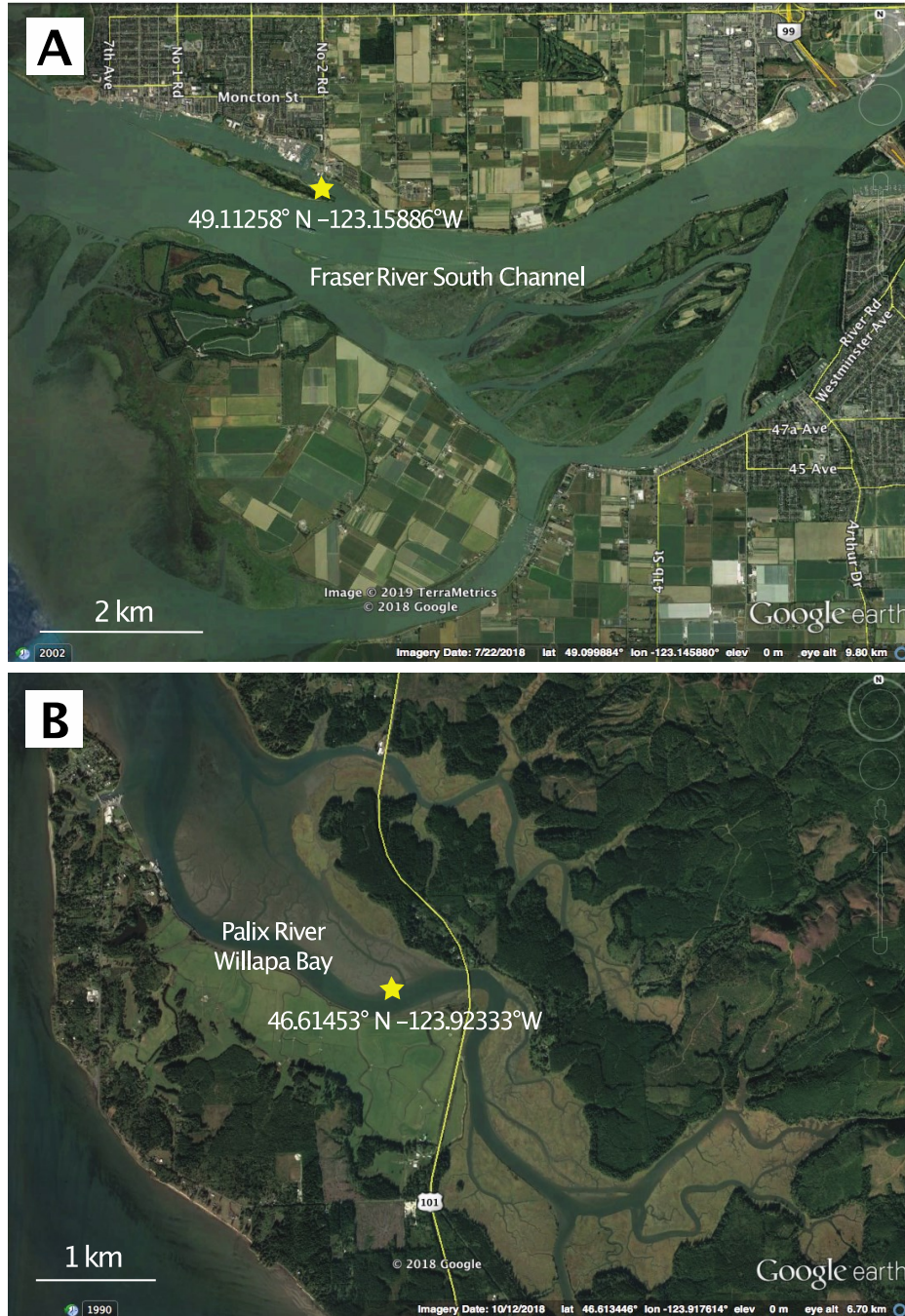


Figure 6.7. Location map for examples from (A) the Fraser River (Figure 6.6A and B) and (B) Willapa Bay (Figure 6.6C and D). Both images taken from Google Earth.

6.6 Summary

The distribution of sand and mud in fluvio-tidal settings is a function of seasonal variations in river discharge, giving rise to seasonally-influenced heterolithic fabrics with distinct ichnological expressions. During times of high river discharge the fluvio-tidal system is flushed with fresh water and mud is deposited in more seaward depositional positions, due to a shift in the zone of mixing between fresh and marine water. Heightened river discharge leads to freshwater conditions that are associated with the deposition of unburrowed sediment layers. During times of low river discharge mud is deposited further landward due to an increase in tidal influence (relative to periods of high river discharge), and correspondingly the zone of mixing between fresh and marine water shifts landward. A brackish-water colonization window is established during low river discharge resulting in the deposition of bioturbated lithosomes.

A conceptual framework for applying ichnological relationships in fluvio-tidal settings is proposed using two endmember heterolithic fabrics: A) sand-dominated IHS with burrows originating from the mudstone lithosomes and subtending into underlying mudstone lithosomes. In estuaries, Fabric A is found in the outermost inner to middle estuary and Fabric B is found further seaward in the middle estuary. In deltaic settings, Fabric A is deposited within fluvially-dominated distributary channels, whereas Fabric B is interpreted to develop in the outermost mixed fluvial-tidal zone. These fabrics and their distributions demonstrate the usefulness of interpreting burrow distributions in the context of colonization windows to refine interpretations of sedimentary environments.

6.7 References

- Carrigy, M. A. (1971). Deltaic Sedimentation in Athabasca Tar Sands. *AAPG Bulletin*, *55*, 1155–1169.
- Choi, K. (2010). Rhythmic Climbing-Ripple Cross-Lamination in Inclined Heterolithic Stratification (IHS) of a Macrotidal Estuarine Channel, Gomso Bay, West Coast of Korea. *Journal of Sedimentary Research*, *80*, 550–561.
- Choi, K. S., Dalrymple, R. W., Chun, S. S., & Kim, S.-P. (2004). Sedimentology of Modern, Inclined Heterolithic Stratification (IHS) in the Macrotidal Han River Delta, Korea. *Journal of Sedimentary Research*, *74*, 677–689.
- Crerar, E. E., & Arnott, R. W. C. (2007). Facies distribution and stratigraphic architecture of the Lower Cretaceous McMurray Formation, Lewis Property, northeastern Alberta. *Bulletin of Canadian Petroleum Geology*, *55*, 99–124.
- Dalrymple, R. W., Knight, R. J., Zaitlin, B. A., & Middleton, G. V. (1990). Dynamics and facies model of a macrotidal sand-bar complex, Cobequid Bay-Salmon River Estuary (Bay of Fundy). *Sedimentology*, *37*, 577–612.
- Dalrymple, R. W., Zaitlin, B. A., & Boyd, R. (n.d.). Estuarine facies models: Conceptual basis and stratigraphic implications I. *Journal of Sedimentary Research*, *62*, 1130–1146.
- de Mowbray, T. (1983). The genesis of lateral accretion deposits in recent intertidal mudflat channels, Solway Firth, Scotland. *Sedimentology*, *30*, 425–435.
- Durkin, P. R., Boyd, R. L., Hubbard, S. M., Shultz, A. W., & Blum, M. D. (2017). Three-Dimensional Reconstruction of Meander-Belt Evolution, Cretaceous McMurray Formation, Alberta Foreland Basin, Canada. *Journal of Sedimentary Research*, *87*, 1075–1099.
- Eberth, D. (1996). Origin and significance of mud-filled incised valleys (Upper Cretaceous)

- in southern Alberta, Canada. *Sedimentology*, *43*, 459–477.
- Falcon-Lang, H. (1998). The impact of wildfire on an Early Carboniferous coastal environment, North Mayo, Ireland. *Palaeogeography, Palaeoclimatology, Palaeoecology*, *139*, 121–138.
- Flach, P. D., & Mossop, G. D. (1985). Depositional Environments of Lower Cretaceous McMurray Formation, Athabasca OU Sands, Alberta. *AAPG Bulletin*, *69*, 1195–1207.
- Gingras, M. K., MacEachern, J. A., & Dashtgard, S. E. (2011). Process ichnology and the elucidation of physico-chemical stress. *Sedimentary Geology*, *237*, 115–134.
- Gingras, M. K., MacEachern, J. A., Dashtgard, S. E., Ranger, M. J., Pemberton, S. G., & Hein, F. (2016). The significance of trace fossils in the McMurray Formation, Alberta, Canada. *Bulletin of Canadian Petroleum Geology*, *64*, 233–250.
- Gingras, M. K., Pemberton, S. G., Dashtgard, S., & Dafoe, L. (2008). How fast do marine invertebrates burrow? *Palaeogeography, Palaeoclimatology, Palaeoecology*, *270*, 280–286.
- Gingras, M. K., Pemberton, S. G., Saunders, T., & Clifton, H. E. (1999). The Ichnology of Modern and Pleistocene Brackish-Water Deposits at Willapa Bay, Washington: Variability in Estuarine Settings. *Palaios*, *14*, 352.
- Gingras, M. K., Räsänen, M., & Ranzi, A. (2002). The Significance of Bioturbated Inclined Heterolithic Stratification in the Southern Part of the Miocene Solimoes Formation, Rio Acre, Amazonia Brazil. *Palaios*, *17*, 591–601.
- Hovikoski, J., Räsänen, M., Gingras, M., Ranzi, A., & Melo, J. (2008). Tidal and seasonal controls in the formation of Late Miocene inclined heterolithic stratification deposits, western Amazonian foreland basin. *Sedimentology*, *55*, 499–530.
- Hubbard, S. M., Smith, D. G., Nielsen, H., Leckie, D. A., Fustic, M., Spencer, R. J., & Bloom,

- L. (2011). Seismic geomorphology and sedimentology of a tidally influenced river deposit, Lower Cretaceous Athabasca oil sands, Alberta, Canada. *AAPG Bulletin*, *95*, 1123–1145.
- Jablonski, B. V. J., & Dalrymple, R. W. (2016). Recognition of strong seasonality and climatic cyclicity in an ancient, fluvially dominated, tidally influenced point bar: Middle McMurray Formation, Lower Steepbank River, north-eastern Alberta, Canada. *Sedimentology*, *63*, 552–585.
- Kranck, K. (1981). Particulate matter grain-size characteristics and flocculation in a partially mixed estuary. *Sedimentology*, *28*, 107–114.
- La Croix, A. D., & Dashtgard, S. E. (2014). Of sand and mud: Sedimentological criteria for identifying the turbidity maximum zone in a tidally influenced river. *Sedimentology*, *61*, 1961–1981.
- La Croix, A. D., & Dashtgard, S. E. (2015). A Synthesis of Depositional Trends In Intertidal and Upper Subtidal Sediments Across the Tidal–Fluvial Transition In the Fraser River, Canada. *Journal of Sedimentary Research*, *85*, 683–698.
- La Croix, A. D., Dashtgard, S. E., Gingras, M. K., Hauck, T. E., & MacEachern, J. A. (2015). Bioturbation trends across the freshwater to brackish-water transition in rivers. *Palaeogeography, Palaeoclimatology, Palaeoecology*, *440*, 66–77.
- La Croix, A. D., Dashtgard, S. E., & MacEachern, J. A. (2019). Using a modern analogue to interpret depositional position in ancient fluvial-tidal channels: Example from the McMurray Formation, Canada. *Geoscience Frontiers*, *10*, 2219–2238.
- Labrecque, P. A., Jensen, J. L., Hubbard, S. M., & Nielsen, H. (2011). Sedimentology and stratigraphic architecture of a point bar deposit, Lower Cretaceous McMurray Formation, Alberta, Canada. *Bulletin of Canadian Petroleum Geology*, *59*, 147–171.
- Langenberg, C. W. (2002). Seismic modeling of fluvial-estuarine deposits in the Athabasca

- oil sands using ray-tracing techniques, Steepbank River area, northeastern Alberta. *Bulletin of Canadian Petroleum Geology*, 50, 178–204.
- Mackay, D. A., & Dalrymple, R. W. (2011). Dynamic Mud Deposition In A Tidal Environment: The Record of Fluid-Mud Deposition In the Cretaceous Bluesky Formation, Alberta, Canada. *Journal of Sedimentary Research*, 81, 901–920.
- Mossop, G. D. (1980). Geology of the Athabasca Oil Sands. *Science*, 207, 145–152.
- Mossop, G. D., & Flach, P. D. (1983). Deep channel sedimentation in the Lower Cretaceous McMurray Formation, Athabasca Oil Sands, Alberta. *Sedimentology*, 30, 493–509.
- Musial, G., Reynaud, J.-Y., Gingras, M. K., Féliès, H., Labourdette, R., & Parize, O. (2012). Subsurface and outcrop characterization of large tidally influenced point bars of the Cretaceous McMurray Formation (Alberta, Canada). *Sedimentary Geology*, 279, 156–172.
- Muwais, W., & Smith, D. G. (1990). Types of channel-fills interpreted from dipmeter logs in the McMurray Formation, northeast Alberta. *Bulletin of Canadian Petroleum Geology*, 38, 53–63.
- Pemberton, S. G., Flach, P. D., & Mossop, G. D. (1982). Trace Fossils from the Athabasca Oil Sands, Alberta, Canada. *Science*, 217, 825–827.
- Rasanen, M. E., Linna, A. M., Santos, J. C. R., & Negri, F. R. (1995). Late Miocene Tidal Deposits in the Amazonian Foreland Basin. *Science*, 269, 386–390.
- Rebata., L. A., Gingras, M. K., Räsänen, M. E., & Barberi, M. (2006). Tidal-channel deposits on a delta plain from the Upper Miocene Nauta Formation, Marañón Foreland Sub-basin, Peru. *Sedimentology*, 53, 971–1013.
- Reineck, H.-E. (1963). Sedimentgefüge im Bereich der südlichen Nordsee. *Abhandlungen der senckenbergische naturforschende Gesellschaft*, 505, 1–138.
- Schubel, J. R., & Pritchard, D. W. (n.d.). *Responses of upper Chesapeake Bay to variations*

in discharge of the Susquehanna River. 14.

Shchepetkina, A., Gingras, M. K., Pemberton, S. G., MacEachern, J. A., & Plint, G. (2016).

What does the ichnological content of the Middle McMurray Formation tell us?

Bulletin of Canadian Petroleum Geology, 64, 24–46.

Shchepetkina, Alina, Gingras, M. K., & Pemberton, S. G. (2016). Sedimentology and

ichnology of the fluvial reach to inner estuary of the Ogeechee River estuary,

Georgia, USA. *Sedimentary Geology*, 342, 202–217.

Sisulak, C. F., & Dashtgard, S. E. (2012). Seasonal Controls On the Development And

Character of Inclined Heterolithic Stratification In A Tide-Influenced, Fluvially

Dominated Channel: Fraser River, Canada. *Journal of Sedimentary Research*, 82,

244–257.

Smith, D. G., Hubbard, S. M., Leckie, D. A., & Fustic, M. (2009). Counter point bar deposits:

Lithofacies and reservoir significance in the meandering modern Peace River and

ancient McMurray Formation, Alberta, Canada. *Sedimentology*, 56, 1655–1669.

Staton, J., Borgianini, S., Gibson, I., Brodie, R., & Greig, T. (2013). Limited gene flow in *Uca*

minax (LeConte 1855) along a tidally influenced river system. *Open Life Sciences*,

9, 28–36.

Taylor, A. M., & Goldring, R. (1993). Description and analysis of bioturbation and

ichnofabric. *Journal of the Geological Society*, 150, 141–148.

Thomas, R. G., Smith, D. G., Wood, J. M., Visser, J., Calverley-Range, E. A., & Koster, E. H.

(1987). Inclined heterolithic stratification—Terminology, description, interpretation

and significance. *Sedimentary Geology*, 53, 123–179.

Timmer, E.R., Gingras, M. K., Morin, M. L., Ranger, M. J., Zonneveld, J.-P., & Plint, G. (2016).

Laminae-scale rhythmicity of inclined heterolithic stratification, Lower Cretaceous

McMurray Formation, NE Alberta, Canada. *Bulletin of Canadian Petroleum*

Geology, 64, 199–217.

Timmer, Eric R., Gingras, M. K., & Zonneveld, J.-P. (2016). Spatial and temporal significance of process ichnology data from silty-mudstone beds of inclined heterolithic stratification, Lower Cretaceous McMurray Formation, NE Alberta, Canada. *Palaios*, 31, 533–548.

CHAPTER 7 – CONCLUSIONS

This thesis explores concepts and approaches for using bioturbation intensity and distribution to interpret tidally-influenced depositional environments. While established ichnological frameworks have proven to be conceptually useful, they have not been subject to significant scrutiny and thus remain a largely untested framework. The case studies presented here offer a context in which bioturbation distributions and intensities can be better interpreted in the rock record.

7.1 Contributions to Process Ichnology

Process ichnology permits the use of trace fossils as biogenic sedimentary structures, resulting in refined depositional interpretations for a wide range of sedimentary environments (Gingras et al., 2011). This framework offers unique insight into the physico-chemical stresses present during sediment deposition. In marginal marine environments, common stresses include salinity, oxygen, water turbidity, sedimentation rates, and substrate consistency. This thesis focuses on the latter two, representing modest contribution to the nascent process ichnology framework. Particularly significant were the measures taken to better understand how these stresses can be interpreted in the context of bioturbation intensity. This was accomplished through case studies from both modern environments and the stratigraphic record, providing analogs for future research. While the findings presented here do not establish a unified framework for interpreting bioturbation intensity, they lay the groundwork for future research endeavors that, when integrated with existing literature, may bring us closer to achieving this overarching goal.

7.2 Research Horizons

Looking beyond the confines of this thesis, a vast domain of scientific inquiry comes into view. This includes but is not limited to 1) expanding neoichnological investigations in fully marine environments, 2) refining sedimentation rate parameters to better understand the temporal nature of the stratigraphic record, 3) incorporating oceanographic data into ichnological frameworks, and 4) developing a new method of classifying bioturbation intensity that is rooted in sedimentological principles.

The process ichnology framework relies on insights gained from modern depositional environments, offering snapshots of infaunal communities and their ecological interactions. The field of ichnology has greatly benefited from comprehensive studies of renowned areas such as the Wadden Sea (Schafer, 1962; Reineck, 1963), Georgia Coast (Howard and Frey, 1975), Willapa Bay (Gingras et al., 1999, 2001), and the Fraser River Delta (Swinbanks and Murray, 1981; Dashtgard et al., 2011a,b). The future of neoichnology therefore requires new sites to be established to encompass the full range of environmental variability, considering major environmental factors such as tidal range, fluvial input, and latitude. Expanding the scope of available data will allow for more robust inferences on how sedimentation and other physico-chemical stressors can be assessed and quantified from the stratigraphic record.

The spatial distribution of bioturbation in a sedimentary succession offers a means of discerning the relative rates of sedimentation (Howard, 1975). This framework employs the concept of the colonization window to relate low bioturbation intensities with periods of high sedimentation rate, and high bioturbation intensities with periods of low sedimentation rate. However, there has been limited ichnological effort in quantifying the timescales associated with these events (Wheatcroft, 1990; Bentley et al., 2006). Further

work is therefore required to better understand how bioturbation intensity can be used to make inferences about the temporal aspects of the sedimentary record.

As alluded to above, there is a prevailing bias in neoichnological research towards intertidal zones, primarily due to their accessibility. Neoichnological frameworks for fully marine environments are thus less refined than their marginal marine counterparts. Overcoming the accessibility hurdles in marine environments is best accomplished through the utilization of ocean cores obtained from drilling expeditions (e.g., Rodríguez-Tovar and Dorador, 2014). These assessments of oceanic bioturbation can be achieved through imaging techniques (Solan and Kennedy, 2002; Solan et al., 2004) and the application of time tracers for quantifying biogenic sediment mixing in marine sediments (Bentley et al., 2006). These investigations, if effectively incorporated into ichnological frameworks, have the capacity to enhance paleoenvironmental interpretations of fully marine settings much like they have for the marginal marine.

Despite our most earnest efforts, it may remain a considerable challenge to fully understand the temporal nature of the stratigraphic record owing to the intricacies involved in reconstructing and quantifying events related to sedimentation, bioturbation, and erosion, even in modern settings. An appropriate first step is to establish a global context by comparing predictive models of sedimentation rates with data on bioturbation intensity (Teal et al., 2008; Solan et al., 2019; Restrepo et al., 2020). Although these global databases are framed in an oceanographic context, they offer insights that ichnologists should not overlook. Indeed, the integration of oceanographic data into ichnological frameworks presents an opportunity to accelerate research related to bioturbation intensity and distribution.

The culmination of the aforementioned research may prompt a reassessment of the classification schemes currently used for measuring bioturbation intensity. These

schemes rely on semi-quantitative methods in which values are delineated by specified percentage intervals (Droser and Bottjer, 1986; Taylor and Goldring, 1993). While they are conceptually and practically useful, the divisions are somewhat arbitrary. Indeed, consensus has yet to be reached regarding the most suitable scheme (Knaust, 2012). An increase in understanding how various sedimentation patterns impact bioturbation intensities and distributions may render it possible to develop a new classification system specifically tailored to effectively interpret the range of bioturbation intensities observed in the stratigraphic record.

7.3 References

- Bentley, S. J., Sheremet, A., & Jaeger, J. M. (2006). Event sedimentation, bioturbation, and preserved sedimentary fabric: Field and model comparisons in three contrasting marine settings. *Continental Shelf Research*, *26*, 2108–2124.
- Dashtgard, S. E. (2011a). Linking invertebrate burrow distributions (neoichnology) to physicochemical stresses on a sandy tidal flat: Implications for the rock record: Tidal-flat ichnology. *Sedimentology*, *58*, 1303–1325.
- Dashtgard, S. E. (2011b). Neoichnology of the lower delta plain: Fraser River Delta, British Columbia, Canada: Implications for the ichnology of deltas. *Palaeogeography, Palaeoclimatology, Palaeoecology*, *307*, 98–108.
- Droser, M. L., & Bottjer, D. J. (1986). A semiquantitative field classification of ichnofabric. *Journal of Sedimentary Research*, *56*, 558–559.
- Gingras, M. K., George Pemberton, S., & Saunders, T. (2001). Bathymetry, sediment texture, and substrate cohesiveness; their impact on modern Glossifungites trace assemblages at Willapa Bay, Washington. *Palaeogeography, Palaeoclimatology, Palaeoecology*, *169*, 1–21.
- Gingras, M. K., MacEachern, J. A., & Dashtgard, S. E. (2011). Process ichnology and the elucidation of physico-chemical stress. *Sedimentary Geology*, *237*, 115–134.
- Gingras, M. K., Pemberton, S. G., Saunders, T., & Clifton, H. E. (1999). The Ichnology of Modern and Pleistocene Brackish-Water Deposits at Willapa Bay, Washington: Variability in Estuarine Settings. *Palaios*, *14*, 352.
- Howard, J. D. (1975). The sedimentological significance of trace fossils. In R. W. Frey (Ed.), *The Study of Trace Fossils: A Synthesis of Principles, Problems, and*

- Procedures in Ichnology* (pp. 131–146). Berlin, Heidelberg: Springer.
- Knaust, D. (2012). Chapter 9—Methodology and Techniques. In D. Knaust & R. G. Bromley (Eds.), *Developments in Sedimentology* (pp. 245–271). Elsevier.
- Miller, M. F., & Smail, S. E. (1997). A semiquantitative field method for evaluating bioturbation on bedding planes. *PALAIOS*, *12*, 391–396.
- Reineck, H.-E. (1963). Sedimentgefüge im Bereich der südlichen Nordsee. *Abhandlungen der senckenbergische naturforschende Gesellschaft*, *505*, 1–138.
- Restrepo, G. A., Wood, W. T., & Phrampus, B. J. (2020). Oceanic sediment accumulation rates predicted via machine learning algorithm: Towards sediment characterization on a global scale. *Geo-Marine Letters*, *40*, 755–763.
- Rodríguez-Tovar, F. J., & Dorador, J. (2014). Ichnological analysis of Pleistocene sediments from the IODP Site U1385 “Shackleton Site” on the Iberian margin: Approaching paleoenvironmental conditions. *Palaeogeography, Palaeoclimatology, Palaeoecology*, *409*, 24–32.
- Schafer, W. (1962). *Aktuo-Palaontologie nach Studien in der Nordsee*. Frankfurt am Main: Kramer.
- Solan, M., & Kennedy, R. (2002). Observation and quantification of in situ animal-sediment relations using time-lapse sediment profile imagery (t-SPI). *Marine Ecology Progress Series*, *228*, 179–191.
- Solan, M., Ward, E. R., White, E. L., Hibberd, E. E., Cassidy, C., Schuster, J. M., ... Godbold, J. A. (2019). Worldwide measurements of bioturbation intensity, ventilation rate, and the mixing depth of marine sediments. *Scientific Data*, *6*, 58.
- Solan, M., Wigham, B. D., Hudson, I. R., Kennedy, R., Coulon, C. H., Norling, K., ... Rosenberg, R. (2004). *In situ* quantification of bioturbation using time lapse fluorescent sediment profile imaging (f SPI), luminophore tracers and model simulation.

Marine Ecology Progress Series, 271, 1–12.

Swinbanks, D. D., & Murray, J. W. (1981). Biosedimentological zonation of Boundary Bay tidal flats, Fraser River Delta, British Columbia. *Sedimentology, 28*, 201–237.

Taylor, A. M., & Goldring, R. (1993). Description and analysis of bioturbation and ichnofabric. *Journal of the Geological Society, 150*, 141–148.

Teal, L. R., Bulling, M. T., Parker, E. R., & Solan, M. (2008). Global patterns of bioturbation intensity and mixed depth of marine soft sediments. *Aquatic Biology, 2*, 207–218.

Wheatcroft, R. A. (1990). Preservation potential of sedimentary event layers. *Geology, 18*, 843–845.

BIBLIOGRAPHY

- Anderson, J. W., & Reish, D. J. (1967). The effects of varied dissolved oxygen concentrations and temperature on the wood-boring isopod genus *Limnoria*. *Marine Biology*, 1, 56–59.
- Anderson, R. Y., Gardner, J. V., & Hemphill-Haley, E. (1989). Variability of the Late Pleistocene-Early Holocene oxygen-minimum zone off northern California. In D. H. Peterson (Ed.), *Geophysical Monograph Series* (pp. 75–84). Washington, D. C.: American Geophysical Union.
- Anfinson, O. A., Lockley, M. G., Kim, S. H., Kim, K. S., & Kim, J. Y. (2009). First report of the small bird track *Koreanaornis* from the Cretaceous of North America: Implications for avian ichnotaxonomy and paleoecology. *Cretaceous Research*, 30, 885–894.
- Bann, K. L., MacEachern, J. A., & Gingras, M. K. (2004). Early Permian Snapper Point Formation of southeastern Australia. In K. A. Campbell & M. R. Gregory (Eds.), *8th International Ichnofabric Workshop* (pp. 13–15). Auckland, New Zealand.
- Beauchamp, G. (2007). Competition in foraging flocks of migrating semipalmated sandpipers. *Oecologia*, 154, 403–409.
- Beauchamp, G. (2009). Functional response of staging semipalmated sandpipers feeding on burrowing amphipods. *Oecologia*, 161, 651–655.
- Beauchamp, G. (2012). Foraging speed in staging flocks of semipalmated sandpipers: Evidence for scramble competition. *Oecologia*, 169, 975–980.
- Beuck, L., Vertino, A., Stepina, E., Karolczak, M., & Pfannkuche, O. (2007). Skeletal response of *Lophelia pertusa* (Scleractinia) to bioeroding sponge infestation visualised with micro-computed tomography. *Facies*, 53, 157–176.

- Beuck, L., Wisshak, M., Munnecke, A., & Freiwald, A. (2008). A giant boring in a Silurian stromatoporoid analysed by computer tomography. *Acta Palaeontologica Polonica*, *53*, 149–160.
- Beukema, J. J. (1979). Biomass and species richness of the macrobenthic animals living on a tidal flat area in the dutch wadden sea: Effects of a severe winter. *Netherlands Journal of Sea Research*, *13*, 21.
- Bolam, S. G. (2011). Burial survival of benthic macrofauna following deposition of simulated dredged material. *Environmental Monitoring and Assessment*, *181*, 13–27.
- Bolam, S. G., Barry, J., Schratzberger, M., Whomersley, P., & Dearnaley, M. (2010). Macrofaunal recolonisation following the intertidal placement of fine-grained dredged material. *Environmental Monitoring and Assessment*, *168*, 499–510.
- Borges, L. M. S., Cragg, S. M., & Busch, S. (2009). A laboratory assay for measuring feeding and mortality of the marine wood borer *Limnoria* under forced feeding conditions: A basis for a standard test method. *International Biodeterioration & Biodegradation*, *63*, 289–296.
- Borges, Luísa M. S., Merckelbach, L. M., & Cragg, S. M. (2014). Biogeography of wood-boring crustaceans (Isopoda: Limnoriidae) established in European coastal waters. *PLoS ONE*, *9*, e109593.
- Brand, L. R. (1996). Variations in salamander trackways resulting from substrate differences. *Journal of Paleontology*, *70*, 1004–1010.
- Brekke, H., & Couch, A. (2011a). *Use of Image Logs in Differentiating Point Bar and Tidal Bar Deposits in the Leismer Area: Implications for SAGD Reservoir Definition in the Athabasca Oilsands*. 12.
- Bromley, R. G., Pemberton, S. G., & Rahmani, R. A. (1984). A Cretaceous woodground: The

- Teredolites* ichnofacies. *Journal of Paleontology*, 58, 488–498.
- Buatois, L. A. (2005). Colonization of brackish-water systems through time: Evidence from the trace-fossil record. *PALAIOS*, 20, 321–347.
- Buatois, Luis A., Wisshak, M., Wilson, M. A., & Mángano, M. G. (2017). Categories of architectural designs in trace fossils: A measure of ichnodisparity. *Earth-Science Reviews*, 164, 102–181.
- Carrigy, M. A. (1971). Deltaic Sedimentation in Athabasca Tar Sands. *AAPG Bulletin*, 55, 1155–1169.
- Choi, K. (2010). Rhythmic Climbing-Ripple Cross-Lamination in Inclined Heterolithic Stratification (IHS) of a Macrotidal Estuarine Channel, Gomso Bay, West Coast of Korea. *Journal of Sedimentary Research*, 80, 550–561.
- Choi, K. S., Dalrymple, R. W., Chun, S. S., & Kim, S.-P. (2004). Sedimentology of Modern, Inclined Heterolithic Stratification (IHS) in the Macrotidal Han River Delta, Korea. *Journal of Sedimentary Research*, 74, 677–689.
- Cohen, A., Lockley, M. G., Halfpenny, J., & Michel, A. E. (1991). Modern vertebrate track taphonomy at Lake Manyara, Tanzania. *Palaios*, 6, 371–389.
- Colwell, M. A., & Landrum, S. L. (1993). Nonrandom shorebird distribution and fine-scale variation in prey abundance. *The Condor*, 95, 94–103.
- Contessi, M., & Fanti, F. (2012). First record of bird tracks in the Late Cretaceous (Cenomanian) of Tunisia. *Palaios*, 27, 455–464.
- Crerar, E. E., & Arnott, R. W. C. (2007). Facies distribution and stratigraphic architecture of the Lower Cretaceous McMurray Formation, Lewis Property, northeastern Alberta. *Bulletin of Canadian Petroleum Geology*, 55, 99–124.
- Dalrymple, R. W., Knight, R. J., Zaitlin, B. A., & Middleton, G. V. (1990). Dynamics and facies model of a macrotidal sand-bar complex, Cobequid Bay-Salmon River Estuary (Bay

- of Fundy). *Sedimentology*, *37*, 577–612.
- Dalrymple, R. W., Zaitlin, B. A., & Boyd, R. (n.d.). Estuarine facies models: Conceptual basis and stratigraphic implications I. *Journal of Sedimentary Research*, *62*, 1130–1146.
- Dashtgard, S. E., Pearson, N. J., & Gingras, M. K. (2014). Sedimentology, ichnology, ecology and anthropogenic modification of muddy tidal flats in a cold-temperate environment: Chignecto Bay, Canada. *Geological Society, London, Special Publications*, *388*, 229–245.
- Dashtgard, S. E., Venditti, J. G., Hill, P. R., Sisulak, C. F., Johnson, S. M., & La Croix, A. D. (2012). Sedimentation across the tidal-fluvial transition in the Lower Fraser River, Canada. *The Sedimentary Record*, *10*, 4–9.
- de Mowbray, T. (1983). The genesis of lateral accretion deposits in recent intertidal mudflat channels, Solway Firth, Scotland. *Sedimentology*, *30*, 425–435.
- Desjardins, P. R., Buatois, L. A., Pratt, B. R., & Mángano, G., M. (2012). Sedimentological-ichnological model for tide-dominated shelf sandbodies: Lower Cambrian Gog Group of western Canada: Subtidal compound cross-stratified sandstone architecture. *Sedimentology*, *59*, 1452–1477.
- Desjardins, P. R., Gabriela Mángano, M., Buatois, L. A., & Pratt, B. R. (2010). *Skolithos* pipe rock and associated ichnofabrics from the southern Rocky Mountains, Canada: Colonization trends and environmental controls in an early Cambrian sand-sheet complex: Early Cambrian *skolithos* pipe rock. *Lethaia*, *43*, 507–528.
- Diaz-Martinez, I., Suarez-Hernando, O., Martinez-Garcia, B., Hernandez, J. M., Fernandez, S. G., Perez-Lorente, F., & Murelaga, X. (2015). Early Miocene shorebird-like footprints from the Ebro Basin, La Rioja, Spain: Paleoecological and paleoenvironmental significance. *Palaios*, *30*, 424–431.
- Donovan, S. K. (2018). A new ichnogenus for *Teredolites longissimus* Kelly and Bromley.

- Swiss Journal of Palaeontology*, 137, 95–98.
- Donovan, S. K., & Ewin, T. A. M. (2018). Substrate is a poor ichnotaxobase: A new demonstration. *Swiss Journal of Palaeontology*, 137, 103–107.
- Donovan, S. K., & Portell, R. W. (2019). Invertebrate borings from the Eocene of Seven Rivers, parish of St. James, western Jamaica. *Swiss Journal of Palaeontology*, 138, 277–283.
- Dorgan, K. M. (2015). The biomechanics of burrowing and boring. *Journal of Experimental Biology*, 218, 176–183.
- Droser, M. L., & Bottjer, D. J. (1986). A semiquantitative field classification of ichnofabric. *Journal of Sedimentary Research*, 56, 558–559.
- Durkin, P. R., Boyd, R. L., Hubbard, S. M., Shultz, A. W., & Blum, M. D. (2017). Three-Dimensional Reconstruction of Meander-Belt Evolution, Cretaceous McMurray Formation, Alberta Foreland Basin, Canada. *Journal of Sedimentary Research*, 87, 1075–1099.
- Eberth, D. (1996). Origin and significance of mud-filled incised valleys (Upper Cretaceous) in southern Alberta, Canada. *Sedimentology*, 43, 459–477.
- Eltringham, S. K. (1961). The effect of salinity upon the boring activity and survival of *Limnoria* (Isopoda). *Journal of the Marine Biological Association of the United Kingdom*, 41, 785–797.
- Eltringham, S. K. (1965). The effect of temperature upon the boring activity and survival of *Limnoria* (Isopoda). *Journal of Applied Ecology*, 2, 149–157.
- Essink, K. (1999). Ecological effects of dumping of dredged sediments; options for management. *Journal of Coastal Conservation*, 5, 69–80.
- Fabricius, J. C. (1775). *Systema entomologiae, sistens insectorum classes, ordines, genera, species, adjectis synonymis, locis, descriptionibus, observationibus*.

- Flensbvirgi et Lipsiae, In officina libraria Kortii.
- Falcon-Lang, H. (1998). The impact of wildfire on an Early Carboniferous coastal environment, North Mayo, Ireland. *Palaeogeography, Palaeoclimatology, Palaeoecology*, *139*, 121–138.
- Falk, A. R., Lim, J.-D., & Hasiotis, S. T. (2014). A behavioral analysis of fossil bird tracks from the Haman Formation (Republic of Korea) shows a nearly modern avian ecosystem. *Vertebrata Palasiatica*, *52*, 129–152.
- Falkingham, P. L. (2014). Interpreting ecology and behaviour from the vertebrate fossil track record: Ecology and behaviour from fossil track record. *Journal of Zoology*, *292*, 222–228.
- Feng, Z., Wang, J., Rößler, R., Ślipiński, A., & Labandeira, C. (2017). Late Permian wood-borings reveal an intricate network of ecological relationships. *Nature Communications*, *8*, 556.
- Finn, P. G., Catterall, C. P., & Driscoll, P. V. (2008). Prey versus substrate as determinants of habitat choice in a feeding shorebird. *Estuarine, Coastal and Shelf Science*, *80*, 381–390.
- Flach, P. D., & Mossop, G. D. (1985). Depositional Environments of Lower Cretaceous McMurray Formation, Athabasca OU Sands, Alberta. *AAPG Bulletin*, *69*, 1195–1207.
- Föllmi, K. B., & Grimm, K. A. (1990). Doomed pioneers: Gravity-flow deposition and bioturbation in marine oxygen-deficient environments. *Geology*, *18*, 1069–1072.
- Gatesy, S. M., & Falkingham, P. L. (2017). Neither bones nor feet: Track morphological variation and ‘preservation quality.’ *Journal of Vertebrate Paleontology*, *37*, e1314298.
- Gatesy, S. M., Middleton, K. M., Jenkins Jr, F. A., & Shubin, N. H. (1999). Three-dimensional

- preservation of foot movements in Triassic theropod dinosaurs. *Nature*, *399*, 141–144.
- Genise, J. F. (1995). Upper Cretaceous trace fossils in permineralized plant remains from Patagonia, Argentina. *Ichnos*, *3*, 287–299.
- Genise, J. F. (2017). *Ichnoentomology*. Cham: Springer International Publishing.
- Genise, J. F., & Hazeldine, P. L. (1995). A new insect trace fossil in Jurassic wood from Patagonia, Argentina. *Ichnos*, *4*, 1–5.
- Genise, Jorge. F., Garrouste, R., Nel, P., Grandcolas, P., Maurizot, P., Cluzel, D., ... Nel, A. (2012). *Asthenopodichnium* in fossil wood: Different trace makers as indicators of different terrestrial palaeoenvironments. *Palaeogeography, Palaeoclimatology, Palaeoecology*, *365–366*, 184–191.
- Gingras, M. K., MacEachern, J. A., & Dashtgard, S. E. (2011). Process ichnology and the elucidation of physico-chemical stress. *Sedimentary Geology*, *237*, 115–134.
- Gingras, M. K., MacEachern, J. A., & Dashtgard, S. E. (2012). The potential of trace fossils as tidal indicators in bays and estuaries. *Sedimentary Geology*, *279*, 97–106.
- Gingras, M. K., MacEachern, J. A., Dashtgard, S. E., Ranger, M. J., Pemberton, S. G., & Hein, F. (2016). The significance of trace fossils in the McMurray Formation, Alberta, Canada. *Bulletin of Canadian Petroleum Geology*, *64*, 233–250.
- Gingras, M. K., MacEachern, J. A., & Pickerill, R. K. (2004). Modern perspectives on the *Teredolites* ichnofacies: Observations from Willapa Bay, Washington. *Palaios*, *79–88*, 10.
- Gingras, M. K., Pemberton, S. G., Dashtgard, S., & Dafoe, L. (2008). How fast do marine invertebrates burrow? *Palaeogeography, Palaeoclimatology, Palaeoecology*, *270*, 280–286.
- Gingras, M. K., Pemberton, S. G., Saunders, T., & Clifton, H. E. (1999). The Ichnology of

- Modern and Pleistocene Brackish-Water Deposits at Willapa Bay, Washington: Variability in Estuarine Settings. *Palaios*, 14, 352.
- Gingras, M. K., Räsänen, M., & Ranzi, A. (2002). The Significance of Bioturbated Inclined Heterolithic Stratification in the Southern Part of the Miocene Solimoes Formation, Rio Acre, Amazonia Brazil. *Palaios*, 17, 591–601.
- Gingras, M. K., Räsänen, Matti, & Ranzi, Alceu. (2002). The Significance of bioturbated Inclined Heterolithic Stratification in the southern part of the Miocene Solimoes Formation, Rio Acre, Amazonia Brazil. *PALAIOS*, 17, 591–601.
- Gingras, M. K., & Zonneveld, J.-P. (2015). Tubular tidalites: A biogenic sedimentary structure indicative of tidally influenced sedimentation. *Journal of Sedimentary Research*, 85, 845–854.
- Goss-Custard, J. D. (1984). Intake rates and food supply in migrating and wintering shorebirds. In J. Burger & B. L. Olla (Eds.), *Behavior of Marine Animals: Current Perspectives in Research* (pp. 233–270).
- Gregory, I. (1968). The fossil woods near Holley in the Sweet Home petrified forest, Linn County, Oregon. In M. L. Steere (Ed.), *Fossils in Oregon* (p. 227). State of Oregon Department of Geology and Mineral Industries.
- Grimm, K. A., & Föllmi, K. B. (1990). Doomed pioneers: Event deposition and bioturbation in anaerobic marine environments. *AAPG Bulletin*, 74. Retrieved from <https://www.osti.gov/biblio/6712799>
- Grimm, K. A., & Föllmi, K. B. (1994). Doomed pioneers: Allochthonous Crustacean tracemakers in aerobic basinal strata, Oligo-Miocene San Gregorio Formation, Baja California Sur, Mexico. *PALAIOS*, 9, 313–334.
- Guo, S. (1991). A Miocene trace fossil of insect from Shanwang Formation in Linqu, Shandong. *Acta Palaeontologica Sinica*, 30, 739–742.

- Hendrick, V. J., Hutchison, Z. L., & Last, K. S. (2016). Sediment burial intolerance of marine macroinvertebrates. *PLoS ONE*, *11*, e0149114.
- Hicklin, P. W., & Smith, P. C. (1984). Selection of foraging sites and invertebrate prey by migrant Semipalmated Sandpipers, *Calidris pusilla* (Pallas), in Minas Basin, Bay of Fundy. *Canadian Journal of Zoology*, *62*, 2201–2210.
- Hinchey, E. K., Schaffner, L. C., Hoar, C. C., Vogt, B. W., & Batte, L. P. (2006). Responses of estuarine benthic invertebrates to sediment burial: The importance of mobility and adaptation. *Hydrobiologia*, *556*, 85–98.
- Holthuis, L. B. (1949). The Isopoda and Tanaidacea of the Netherlands, including the description of a new species of *Limnoria*. *Zoologische Mededelingen Reiksmuseum Van Natuurlijke Historie Te Leiden*, *30*, 163–190.
- Hovikoski, J., Räsänen, M., Gingras, M., Ranzi, A., & Melo, J. (2008a). Tidal and seasonal controls in the formation of Late Miocene inclined heterolithic stratification deposits, western Amazonian foreland basin. *Sedimentology*, *55*, 499–530.
- Hovikoski, J., Räsänen, M., Gingras, M., Ranzi, A., & Melo, J. (2008b). Tidal and seasonal controls in the formation of Late Miocene inclined heterolithic stratification deposits, western Amazonian foreland basin. *Sedimentology*, *55*, 499–530.
- Howard, J. D. (1966). Characteristic trace fossils in Upper Cretaceous sandstones of the Book Cliffs and Wasatch Plateau. *Utah Geological and Mineralogical Survey Bulletin*, *80*, 35–53.
- Howard, J. D. (1975). The sedimentological significance of trace fossils. In R. W. Frey (Ed.), *The Study of Trace Fossils: A Synthesis of Principles, Problems, and Procedures in Ichnology* (pp. 131–146). Berlin, Heidelberg: Springer.
- Hubbard, S. M., Smith, D. G., Nielsen, H., Leckie, D. A., Fustic, M., Spencer, R. J., & Bloom, L. (2011). Seismic geomorphology and sedimentology of a tidally influenced river

- deposit, Lower Cretaceous Athabasca oil sands, Alberta, Canada. *AAPG Bulletin*, 95, 1123–1145.
- Huston, H. A. (1994). *Biological Diversity: The Coexistence of Species on Changing Landscapes*. Cambridge: Cambridge University Press.
- Jablonski, B. V. J., & Dalrymple, R. W. (2016). Recognition of strong seasonality and climatic cyclicity in an ancient, fluvially dominated, tidally influenced point bar: Middle McMurray Formation, Lower Steepbank River, north-eastern Alberta, Canada. *Sedimentology*, 63, 552–585.
- James, M. R., & Robson, S. (2012). Straightforward reconstruction of 3D surfaces and topography with a camera: Accuracy and geoscience application. *Journal of Geophysical Research: Earth Surface*, 117. Retrieved from <http://agupubs.onlinelibrary.wiley.com/doi/abs/10.1029/2011JF002289>
- Jarzemowski, E. A. (1990). A boring beetle from the Wealden Sea of the Weald. In J. Boucot (Ed.), *Evolutionary paleobiology of behaviour and coevolution* (pp. 373–376). Elsevier, Amsterdam.
- Javernick, L., Brasington, J., & Caruso, B. (2014a). Modeling the topography of shallow braided rivers using Structure-from-Motion photogrammetry. *Geomorphology*, 213, 166–182.
- Javernick, L., Brasington, J., & Caruso, B. (2014b). Modeling the topography of shallow braided rivers using Structure-from-Motion photogrammetry. *Geomorphology*, 213, 166–182.
- Jones, L. T. (1963). The geographical and vertical distribution of British *Limnoria* [Crustacea: Isopoda]. *Journal of the Marine Biological Association of the United Kingdom*, 43, 589–603.
- Kalejta, B., & Hockey, P. A. R. (1991). Distribution, abundance and productivity of benthic

- invertebrates at the Berg River Estuary, South Africa. *Estuarine, Coastal and Shelf Science*, 175–191, 17.
- Karpiński, J. J. (1962). Cast of the brood galleries of fossil beetle of the Scolytidae family from Oligocene/Miocene Sandstone at Osieczów (Lower Silesia). *Prace Instytut Geologiczny*, 30, 237–239.
- Kelly, S. R., & Bromley, R. G. (1984). Ichnological nomenclature of clavate borings. *Palaeontology*, 27, 793–807.
- Ketcham, R. A., & Carlson, W. D. (2001). Acquisition, optimization and interpretation of X-ray computed tomographic imagery: Applications to the geosciences. *Computers & Geosciences*, 27, 381–400.
- Kim, J. Y., Lockley, M. G., Seo, S. J., Kim, K. S., Kim, S. H., & Baek, K. S. (2012). A paradise of Mesozoic birds: The world's richest and most diverse Cretaceous bird track assemblage from the Early Cretaceous Haman Formation of the Gajin Tracksite, Jinju, Korea. *Ichnos*, 19, 28–42.
- Kiteley, L. W., & Field, M. E. (1984). Shallow marine depositional environments in the Upper Cretaceous of northern Colorado. In R. W. Tillman & C. T. Siemers (Eds.), *Siliciclastic Shelf Sediments* (pp. 179–204). Society of Economic Paleontologists and Mineralogists Special Publication 34.
- Kranck, K. (1981). Particulate matter grain-size characteristics and flocculation in a partially mixed estuary. *Sedimentology*, 28, 107–114.
- Kranz, P. M. (1974). The anastrophic burial of bivalves and its paleoecological significance. *The Journal of Geology*, 82, 237–265.
- La Croix, A. D., & Dashtgard, S. E. (2014). Of sand and mud: Sedimentological criteria for identifying the turbidity maximum zone in a tidally influenced river. *Sedimentology*, 61, 1961–1981.

- La Croix, A. D., & Dashtgard, S. E. (2015). A Synthesis of Depositional Trends In Intertidal and Upper Subtidal Sediments Across the Tidal–Fluvial Transition In the Fraser River, Canada. *Journal of Sedimentary Research*, *85*, 683–698.
- La Croix, A. D., Dashtgard, S. E., Gingras, M. K., Hauck, T. E., & MacEachern, J. A. (2015). Bioturbation trends across the freshwater to brackish-water transition in rivers. *Palaeogeography, Palaeoclimatology, Palaeoecology*, *440*, 66–77.
- La Croix, A. D., Dashtgard, S. E., & MacEachern, J. A. (2019). Using a modern analogue to interpret depositional position in ancient fluvial-tidal channels: Example from the McMurray Formation, Canada. *Geoscience Frontiers*, *10*, 2219–2238.
- Labrecque, P. A., Jensen, J. L., Hubbard, S. M., & Nielsen, H. (2011). Sedimentology and stratigraphic architecture of a point bar deposit, Lower Cretaceous McMurray Formation, Alberta, Canada. *Bulletin of Canadian Petroleum Geology*, *59*, 147–171.
- Langenberg, C. W. (2002). Seismic modeling of fluvial-estuarine deposits in the Athabasca oil sands using ray-tracing techniques, Steepbank River area, northeastern Alberta. *Bulletin of Canadian Petroleum Geology*, *50*, 178–204.
- Leymerie, A. (1842). Suite de mémoire sur le terrain Crétacé du département de l'Albe. *Mémoires de La Société Géologique de France 1(Série 4)*, 1–34.
- Linck, O. (1949). Fossile Bohrgänge (*Anobichnium simile* n.g. N.sp.) an einen Keuperholz. *Neues Jahrbuch Für Mineralogie, Geognosie, Geologie Und Petrefaktenkunde*, 180–185.
- Lockley, M., Chin, K., Houck, K., Matsukawa, M., & Kukiwara, R. (2009). New interpretations of Ignotornis, the first-reported Mesozoic avian footprints: Implications for the paleoecology and behavior of an enigmatic Cretaceous bird. *Cretaceous Research*, *30*, 1041–1061.
- Lockley, M. G. (1986). The paleobiological and paleoenvironmental importance of

- dinosaur footprints. *Palaios*, 1, 37–47.
- Lockley, M. G., Yang, S. Y., Matsukawa, M., Fleming, F., & Lim, S. K. (1992). The track record of Mesozoic birds: Evidence and implications. *Philosophical Transactions of the Royal Society of London. Series B: Biological Sciences*, 336, 113–134.
- Longhitano, S. G., & Nemeč, W. (2005). Statistical analysis of bed-thickness variation in a Tortonian succession of biocalcarenitic tidal dunes, Amantea Basin, Calabria, southern Italy. *Sedimentary Geology*, 179, 195–224.
- MacEachern, J. A., Burton, J. A., Pemberton, S. G., Bann, K. L., & Gingras, M. K. (2007). Departures from the archetypal ichnofacies: Effective recognition of physiochemical stresses in the rock record. In J. A. MacEachern, K. L. Bann, M. K. Gingras, & S. G. Pemberton (Eds.), *Applied Ichnology* (Vol. 52, pp. 65–93). SEPM Short Course Notes.
- MacKay, D. A., & Dalrymple, R. W. (2011). Dynamic Mud Deposition In A Tidal Environment: The Record of Fluid-Mud Deposition In the Cretaceous Bluesky Formation, Alberta, Canada. *Journal of Sedimentary Research*, 81, 901–920.
- Marchetti, L., Belvedere, M., Voigt, S., Klein, H., Castanera, D., Díaz-Martínez, I., ... Farlow, J. O. (2019). Defining the morphological quality of fossil footprints. Problems and principles of preservation in tetrapod ichnology with examples from the Palaeozoic to the present. *Earth-Science Reviews*, 193, 109–145.
- Marty, D., Strasser, A., & Meyer, C. A. (2009). Formation and taphonomy of human footprints in microbial mats of present-day tidal-flat environments: Implications for the study of fossil footprints. *Ichnos*, 16, 127–142.
- Mayoral, E., Santos, A., Vintaned, J. A. G., Wisshak, M., Neumann, C., Uchman, A., & Nel, A. (2020). Bivalve bioerosion in Cretaceous-Neogene amber around the globe, with implications for the ichnogenera *Teredolites* and *Apectoichnus*. *Palaeogeography*,

- Palaeoclimatology, Palaeoecology*, 538, 109410.
- Melchor, R. N. (2015). Application of vertebrate trace fossils to palaeoenvironmental analysis. *Palaeogeography, Palaeoclimatology, Palaeoecology*, 439, 79–96.
- Melnyk, S., Cowper, A., Zonneveld, J.-P., & Gingras, M. K. (2022). Applications of Photogrammetry to Neoichnological Studies: The Significance of Shorebird Trackway Distributions at the Bay of Fundy. *PALAIOS*, 37, 606–621.
- Melnyk, S., & Gingras, M. (2020). Using ichnological relationships to interpret heterolithic fabrics in fluvio-tidal settings. *Sedimentology*, 67.
- Melnyk, S., Lazowski, C. N., & Gingras, M. K. (2022). Sedimentological and ecological significance of a biodeformational structure associated with an unusual feeding behavior in gulls (*Larus* sp.). *Ichnos*, 29, 84–92.
- Melnyk, S., Packer, S., Zonneveld, J.-P., & Gingras, M. K. (2020). A new marine woodground ichnotaxon from the Lower Cretaceous Mannville Group, Saskatchewan, Canada. *Journal of Paleontology*, (in press), 1–8.
- Menzies, R. J. (1951). A new species of Limnoria (Crustacea: Isopoda) from southern California. *Bulletin of the Southern California Academy of Sciences*, 50, 86–88.
- Menzies, R. J. (1957). The marine borer family Limnoriidae (Crustacea, Isopoda). Part I: Northern and central North America: Systematics, distribution, and ecology. *Bulletin of Marine Science of the Gulf and Caribbean*, 7, 101–200.
- Menzies, R. J., & Turner, R. (1957). The distribution and importance of marine wood borers in the United States. In *Symposium on Wood for Marine Use and Its Protection from Marine Organisms* (pp. 3-3–19). Philadelphia: American Society for Testing Materials.
- Mikuláš, R., Pek, I., & Zimák, J. (1995). Teredolites clavatus from the Cenomanian near Maletín (Bohemian Cretaceous Basin), Moravia, Czech Republic. *Věstník Českého*

Geologického Ústavu, 70, 51–58.

Mikuláš, Radek, & Dvůrák, Z. (2002). Borings in xylic tissues of the tree fern *Tempskya* in the Bohemian Cretaceous Basin, Czech Republic. *Zprávy o Geologických Výzkumech, 36, 129–131.*

Milan, J. (2006). Variations in the morphology of emu (*dromaius novaehollandiae*) tracks reflecting differences in walking pattern and substrate consistency: Ichnotaxonomic implications. *Palaeontology, 49, 405–420.*

Milà, J., & Bromley, R. G. (2007). True tracks, undertracks and eroded tracks, experimental work with tetrapod tracks in laboratory and field. *Palaeogeography, Palaeoclimatology, Palaeoecology, 231, 253–264.*

Miller, D., Muir, C., & Hauser, O. (2002). Detrimental effects of sedimentation on marine benthos: What can be learned from natural processes and rates? *Ecological Engineering, 19, 211–232.*

Miller, M. F., & Smail, S. E. (1997). A semiquantitative field method for evaluating bioturbation on bedding planes. *PALAIOS, 12, 391–396.*

Moore, D. G., & Scrutton, P. C. (1957). Minor internal structures of some recent unconsolidated sediments. *Bulletin of the American Association of Petroleum Geologists, 41, 2723–2751.*

Morshedian, A., MacEachern, J. A., & Dashtgard, S. E. (2012). Stratigraphic framework for the Lower Cretaceous Upper Mannville Group (Sparky, Waseca, and McLaren alloformations) in the Lloydminster area, west-central Saskatchewan. In *Summary of Investigations 2011* (Vol. 1, p. 17). Saskatchewan Geological Survey, Sask. Ministry of Resources.

Mossop, G. D. (1980). Geology of the Athabasca Oil Sands. *Science, 207, 145–152.*

Mossop, G. D., & Flach, P. D. (1983). Deep channel sedimentation in the Lower Cretaceous

- McMurray Formation, Athabasca Oil Sands, Alberta. *Sedimentology*, 30, 493–509.
- Musial, G., Reynaud, J.-Y., Gingras, M. K., Féliès, H., Labourdette, R., & Parize, O. (2012). Subsurface and outcrop characterization of large tidally influenced point bars of the Cretaceous McMurray Formation (Alberta, Canada). *Sedimentary Geology*, 279, 156–172.
- Muszer, J., & Uglik, M. (2013). Palaeoenvironmental reconstruction of the Upper Viséan Paprotnia Beds (Bardo Unit, Polish Sudetes) deposition on the ichnological and palaeontological investigations. *Geological Quarterly*, 57, 365–384.
- Muwais, W. (n.d.). *Types of channel-fills interpreted from dipmeter logs in the McMurray Formation, northeast Alberta*. 11.
- Nichols, J. A., Rowe, G. T., Clifford, C. H., & Young, R. A. (1978). *In situ experiments on the burial of marine invertebrates*. 48, 419–425.
- Nicholson, H. A. (1873). Contributions to the study of the errant annelides of the older Palaeozoic rocks. *Proceedings of the Royal Society of London*, 21, 288–290.
- Norkko, A., Thrush, S., Hewitt, J., Cummings, V., Norkko, J., Ellis, J., ... MacDonald, I. (2002). Smothering of estuarine sandflats by terrigenous clay: The role of wind-wave disturbance and bioturbation in site-dependent macrofaunal recovery. *Marine Ecology Progress Series*, 234, 23–42.
- Padian, K., & Olsen, P. K. (1984). The fossil trackway *Pteraichnus*: Not pterosaurian, but crocodylian. *Journal of Paleontology*, 58, 178–184.
- Panos, V., & Skacel, J. (1966). Zur Frage der Entstehung der Steinsaeulen 'Pobitite Kameni' und anderer eigenartiger Formen zwischen Varna und Beloslav in Nordost-Bulgarien. *Zeitschrift Für Geomorphologie*, 10, 105–118.
- Pearson, N. J., & Gingras, M. K. (2006). An ichnological and sedimentological facies model for muddy point-bar deposits. *Journal of Sedimentary Research*, 76, 771–782.

- Pemberton, S. G., Flach, P. D., & Mossop, G. D. (1982). Trace Fossils from the Athabasca Oil Sands, Alberta, Canada. *Science*, *217*, 825–827.
- Pérez-Vargas, A. D., Bernal, M., Delgadillo, C. S., González-Navarro, E. F., & Landaeta, M. F. (2016). Benthic food distribution as a predictor of the spatial distribution for shorebirds in a wetland of central Chile. *Revista de Biología Marina y Oceanografía*, *51*, 147–159.
- Petrov, A. V. (2013). New ichnotaxon *Megascolytinus zherikhini* (Coleoptera: Curculionidae: Scolytinae) from Upper Cretaceous deposits of Mongolia. *Paleontological Journal*, *47*, 597–600.
- Pickerill, R. K., Donovan, S. K., & Portell, R. W. (2003). *Teredolites longissimus* Kelly & Bromley from the Miocene Grand Bay Formation of Carriacou, the Grenadines, Lesser Antilles. *Scripta Geologica*, *125*, 1–9.
- Pirrie, D., Marshall, J. D., & Crame, J. A. (1998). Marine high Mg calcite cements in *Teredolites*-bored fossil wood; evidence for cool paleoclimates in the Eocene La Meseta Formation, Seymour Island, Antarctica. *Palaios*, *13*, 276.
- Plint, A. G., & Pickerill, R. K. (1985). Non-marine *Teredolites* from the Middle Eocene of southern England. *Lethaia*, *18*, 341–347.
- Pollard, J. E., Goldring, R., & Buck, S. G. (1993). Ichnofabrics containing *Ophiomorpha*: significance in shallow-water facies interpretation. *Journal of the Geological Society*, *150*, 149–164.
- Rasanen, M. E., Linna, A. M., Santos, J. C. R., & Negri, F. R. (1995). Late Miocene Tidal Deposits in the Amazonian Foreland Basin. *Science*, *269*, 386–390.
- Rathke, J. (1799). Observations concerning the natural history of helminths and molluscs. *Skriver Af Naturhist-Selskabet (København)*, *5*, 61–148.
- Razzolini, N. L., & Klein, H. (2018). Crossing slopes: Unusual trackways of recent birds and

- implications for tetrapod footprint preservation. *Ichnos*, 25, 252–259.
- Rebata, L. A., Gingras, M. K., Rasanen, M. E., & Barberi, M. (2006). Tidal-channel deposits on a delta plain from the Upper Miocene Nauta Formation, Marañon Foreland Sub-basin, Peru. *Sedimentology*, 0, 060707053311001-???
- Reineck, H.-E. (1963). Sedimentgefüge im Bereich der südlichen Nordsee. *Abhandlungen der senckenbergische naturforschende Gesellschaft*, 505, 1–138.
- Rhoads, D. C. (1967). Biogenic reworking of intertidal and subtidal sediments in Barnstable Harbor and Buzzards Bay, Massachusetts. *The Journal of Geology*, 75, 461–476.
- Rhoads, D. C., Boesch, D. F., Zhican, T., Fengshan, X., Liqiang, H., & Nilsen, K. J. (1985). Macrobenthos and sedimentary facies on the Changjiang delta platform and adjacent continental shelf, East China Sea. *Continental Shelf Research*, 4, 189–213.
- Robusto, C. C. (1957). The Cosine-Haversine Formula. *The American Mathematical Monthly*, 64, 38–40.
- Savrda, C. E. (1991). *Teredolites*, wood substrates, and sea-level dynamics. *Geology*, 19, 905–908.
- Savrda, C. E., & King, D. T. (1993). Log-ground and *Teredolites* lagerstätte in a Transgressive Sequence, Upper Cretaceous (Lower Campanian) Mooreville Chalk, central Alabama. *Ichnos*, 3, 69–77.
- Savrda, C. E., Ozalas, K., Demko, T. H., Huchison, R. A., & Scheiwe, T. D. (1993). Log-Grounds and the Ichnofossil *Teredolites* in Transgressive Deposits of the Clayton Formation (Lower Paleocene), Western Alabama. *Palaios*, 8, 311.
- Schafer, W. (1962). *Aktuo-Palaontologie nach Studien in der Nordsee*. Frankfurt am Main: Kramer.

- Scharstein, D., & Szeliski, R. (2002). A taxonomy and evaluation of dense two-frame stereo correspondence algorithms. *International Journal of Computer Vision*, 47, 7–42.
- Schlirf, M. (2006). *Linkichnus Terebrans* new ichnogenus et ichnospecies, an insect boring from the Late Triassic of the Germanic Basin, Southern Germany. *Ichnos*, 13, 277–280.
- Schönberg, C. H. L., & Shields, G. (2008). Micro-computed tomography for studies on Entobia: Transparent substrate versus modern technology. In M. Wisshak & L. Tapanila (Eds.), *Current Developments in Bioerosion* (pp. 147–164). Berlin, Heidelberg: Springer.
- Schubel, J. R., & Pritchard, D. W. (n.d.). *Responses of upper Chesapeake Bay to variations in discharge of the Susquehanna River*. 14.
- Scott, J. J., Renaut, R. W., & Owen, R. B. (2010). Taphonomic controls on animal tracks at Saline, Alkaline Lake Bogoria, Kenya Rift Valley: Impact of salt efflorescence and clay mineralogy. *Journal of Sedimentary Research*, 80, 639–665.
- Seilacher, A. (1955). Spuren und Fazies im Unterkambrium. In O. H. Schindewolf & A. Seilacher (Eds.), *Beiträge zur Kenntnis des Kambriums in der Salt Range (Pakistan)* (pp. 373–399). Akademie der Wissenschaften und der Literatur zu Mainz, Abhandlung Mathematisch-Naturwissenschaftliche Klasse.
- Seilacher, A. (1964). Biogenic sedimentary structures. *Approaches to Paleoecology*, 296–316.
- Seitz, S. M., Curless, B., Diebel, J., Scharstein, D., & Szeliski, R. (2006). *A comparison and evaluation of multi-view stereo reconstruction algorithms*. 1, 519–528.
- Shanley, K. W., McCabe, P. J., & Hettinger, R. D. (1992). Tidal influence in Cretaceous fluvial strata from Utah, USA: A key to sequence stratigraphic interpretation. *Sedimentology*, 39, 905–930.

- Shchepetkina, A., Gingras, M. K., Pemberton, S. G., MacEachern, J. A., & Plint, G. (2016). What does the ichnological content of the Middle McMurray Formation tell us? *Bulletin of Canadian Petroleum Geology*, *64*, 24–46.
- Shchepetkina, Alina, Gingras, M. K., & Pemberton, S. G. (2016). Sedimentology and ichnology of the fluvial reach to inner estuary of the Ogeechee River estuary, Georgia, USA. *Sedimentary Geology*, *342*, 202–217.
- Shipway, J. R., Altamia, M. A., Rosenberg, G., Concepcion, G. P., Haygood, M. G., & Distel, D. L. (2019). A rock-boring and rock-ingesting freshwater bivalve (shipworm) from the Philippines. *Proceedings of the Royal Society B: Biological Sciences*, *286*, 20190434.
- Sisulak, C. F., & Dashtgard, S. E. (2012). Seasonal Controls On the Development And Character of Inclined Heterolithic Stratification In A Tide-Influenced, Fluvially Dominated Channel: Fraser River, Canada. *Journal of Sedimentary Research*, *82*, 244–257.
- Smith, D. G., Hubbard, S. M., Leckie, D. A., & Fustic, M. (2009). Counter point bar deposits: Lithofacies and reservoir significance in the meandering modern Peace River and ancient McMurray Formation, Alberta, Canada. *Sedimentology*, *56*, 1655–1669.
- Staton, J., Borgianini, S., Gibson, I., Brodie, R., & Greig, T. (2013). Limited gene flow in *Uca minax* (LeConte 1855) along a tidally influenced river system. *Open Life Sciences*, *9*, 28–36.
- Szeliski, R. (2010). *Computer Vision: Algorithms and Applications*. Springer Science & Business Media.
- Tapanila, L. (2008). The medium is the message: Imaging a complex microboring (*Pyrodendrina cupra* igen. n., isp. n.) from the early Paleozoic of Anticosti Island, Canada. In M. Wisshak & L. Tapanila (Eds.), *Current Developments in Bioerosion*

- (pp. 123–145). Berlin, Heidelberg: Springer Berlin Heidelberg.
- Tapanila, L., & Roberts, E. M. (2012). The earliest evidence of holometabolan insect pupation in conifer wood. *PLoS ONE*, *7*, e31668.
- Tarhan, L. G., Droser, M. L., Planavsky, N. J., & Johnston, D. T. (2015). Protracted development of bioturbation through the early Palaeozoic Era. *Nature Geoscience*, *8*, 865–869.
- Tavani, S., Granado, P., Corradetti, A., Girundo, M., Iannace, A., Arbués, P., ... Mazzoli, S. (2014). Building a virtual outcrop, extracting geological information from it, and sharing the results in Google Earth via OpenPlot and Photoscan: An example from the Khaviz Anticline (Iran). *Computers & Geosciences*, *63*, 44–53.
- Taylor, A. M., & Goldring, R. (1993). Description and analysis of bioturbation and ichnofabric. *Journal of the Geological Society*, *150*, 141–148.
- Thayer, C. W. (1979). Biological bulldozers and the evolution of marine benthic communities. *Science*, *203*, 458–461.
- Thayer, Charles W. (1983). Sediment-mediated biological disturbance and the evolution of marine benthos. In M. J. S. Tevesz & P. L. McCall (Eds.), *Biotic Interactions in Recent and Fossil Benthic Communities* (pp. 479–625). Boston, MA: Springer US.
- Thenius, E. (1979). Lebensspuren von Ephemeropteren-Larven aus dem Jung-Tertiär des Wiener Beckens. *Annalen Des Naturhistorischen Museums in Wien*, *82*, 177–188.
- Thomas, R. G., Smith, D. G., Calverley-Range, E. A., & Koster, E. H. (1987). *Inclined heterolithic stratification-terminology, description, interpretation and significance*. 123–179.
- Thompson, R. K., & Pritchard, A. W. (1969). Respiratory adaptations of two burrowing crustaceans, *Callianassa californiensis* and *Upogebia pugettensis* (decapoda, thalassinidea). *The Biological Bulletin*, *136*, 274–287.

- Timmer, E.R., Gingras, M. K., Morin, M. L., Ranger, M. J., Zonneveld, J.-P., & Plint, G. (2016). Laminae-scale rhythmicity of inclined heterolithic stratification, Lower Cretaceous McMurray Formation, NE Alberta, Canada. *Bulletin of Canadian Petroleum Geology*, *64*, 199–217.
- Timmer, Eric R., Gingras, M. K., & Zonneveld, J.-P. (2016). Spatial and temporal significance of process ichnology data from silty-mudstone beds of inclined heterolithic stratification, Lower Cretaceous McMurray Formation, NE Alberta, Canada. *Palaios*, *31*, 533–548.
- Torell, O. (1870). Petrificata suecana formationis cambricae. *Acta Universitatis Lundensis, Afdelning Matematik Och Naturvetenskap Arsskrift*, *6*, 1–14.
- Uchman, A. (2011). Recent freshwater wood borings from the Vistula River in Poland. In M. Carreiro-Silva & S. P. Ávila (Eds.), *7th international bioerosion workshop* (pp. 18–23). Faial Island, Azores.
- Ullman, S. (1979). The interpretation of motion from structure. *Proceedings of the Royal Society of London Series B, Biological Sciences*, *203*, 405–426.
- Verhoeven, G. (2011). Taking computer vision aloft – archaeological three-dimensional reconstructions from aerial photographs with photostan. *Archaeological Prospection*, *18*, 67–73.
- Walker, M. V. (1938). Evidence of Triassic insects in the Petrified Forest National Monument, Arizona. *Proceedings of the United States National Museum*, *85*, 137–141.
- Wheatcroft, R. A. (1990). Preservation potential of sedimentary event layers. *Geology*, *18*, 843–845.
- Wildenschild, D., & Sheppard, A. P. (2013). X-ray imaging and analysis techniques for quantifying pore-scale structure and processes in subsurface porous medium

- systems. *Advances in Water Resources*, 51, 217–246.
- Wilson, W. H., Jr. (1990). Relationship between prey abundance and foraging site selection by semipalmated sandpipers on a bay of fundy mudflat. *Journal of Field Ornithology*, 61, 9–19.
- Wisshak, M., Knaust, D., & Bertling, M. (2019). Bioerosion ichnotaxa: Review and annotated list. *Facies*, 65, 24.
- Yates, M. G., Goss-Custard, J. D., McGrortry, S., Lakhani, K. H., Durell, S. E. A., Clarke, R. T., ... Frost, A. J. (1993). Sediment characteristics, invertebrate densities and shorebird densities on the inner banks of the wash. *The Journal of Applied Ecology*, 30, 599–614.
- Zenker, J. C. (1836). *Historisch-topographisches Taschenbuch von Jena und seiner Umgebung besonders in seiner naturwissenschaftlicher und medicinischer Bezieh.* Jena: Wackenholder.
- Zonneveld, J. P., Bartels, W. S., Gunnell, G. F., & McHugh, L. P. (2015). Borings in early Eocene turtle shell from the Wasatch Formation, South Pass, Wyoming. *Journal of Paleontology*, 89, 802–820.
- Zonneveld, J.-P., Zaim, Y., Rizal, Y., Ciochon, R. L., Bettis, E. A., Aswan, & Gunnell, G. F. (2011). Oligocene shorebird footprints, Kandi, Ombilin Basin, Sumatra. *Ichnos*, 18, 221–227.

APPENDIX 1 – A NEW MARINE WOODGROUND ICHNOTAXON FROM THE LOWER CRETACEOUS MANNVILLE GROUP, SASKATCHEWAN, CANADA

S1.1 Introduction

Woodground ichnofossils show a range of morphologies that reflect a variety of living strategies. The diversity of these strategies is more apparent in modern than fossil ichnocoenoses. Fossil suites from marginal marine environments are exemplified by clasts and surfaces that exhibit putative bivalve borings (e.g., Kelly and Bromley, 1984; Plint and Pickerill, 1985; Savrda and King, 1993; Savrda et al., 1993; Mikulás et al., 1995; Pirrie et al., 1998; Pickerill et al., 2003). Modern intertidal settings may show additional borings into the xylic substrates, including those of shrimp, isopods, barnacles and even sponges (Gingras et al., 2004; Bann et al., 2004). The bivalve borings, referable to *Apectoichnus longissimus* Kelly and Bromley, 1984 and *Teredolites clavatus*, Leymerie, 1842, are almost exclusively associated with woody substrates and marginal to shallow marine environments (Bromley et al., 1984; Kiteley and Field, 1984; Savrda, 1991; Savrda et al., 1993; Pirrie et al., 1998; Pickerill et al., 2003; Mayoral et al., 2020; among others). However, Shipway et al. (2019) described a new freshwater species of teredinid bivalve that bores into a carbonate substrate. *Apectoichnus* Donovan, 2018 and *Teredolites* Leymerie, 1842 are both characterized as elongate tunnels with approximately circular cross sections, but *Teredolites* differs

from *Apectoichnus* in its overall turbinate morphology (Leyremie, 1842; Kelly and Bromley, 1984; Pickerill et al., 2003; Donovan, 2018).

S1.2 Geologic Setting

Apectoichnus lignummasticans occurs within the Lower Cretaceous (early Albian stage) Sparky Formation of the Mannville Group in the Western Canadian Sedimentary Basin. The Mannville group was deposited during an overall transgression of the Boreal Sea. The Sparky Formation has bounding discontinuities that correspond to marine flooding surfaces, which separate it from the underlying General Petroleum and overlying Waseca formations (Morshedian et al., 2012; Figure S1.1). The trace fossils are present in a wood clast in a coal bed within a cored well bore from west central Saskatchewan. The coal bed in which *A. lignummasticans* is found was truncated during a marine incursion and is demarcated by a Transgressive Surface of Erosion. Locally bioturbated, shallow marine sandstone and mudstone units overlay the bored surface (Figure S1.1).

S1.3 Materials and Methods

S1.3.1 Specimens

The specimens examined in this study, UAI0179 (Figure S1.2A,C) and UAI0180 (Figure S1.2B and Figure S1.3), comprise a single piece of gregariously bored wood that is 98 mm x 67 mm x 15 mm at its maximum. They were observed in core from a wellbore near Bushy Lake, west-central Saskatchewan, Canada (Figure S1.1). The

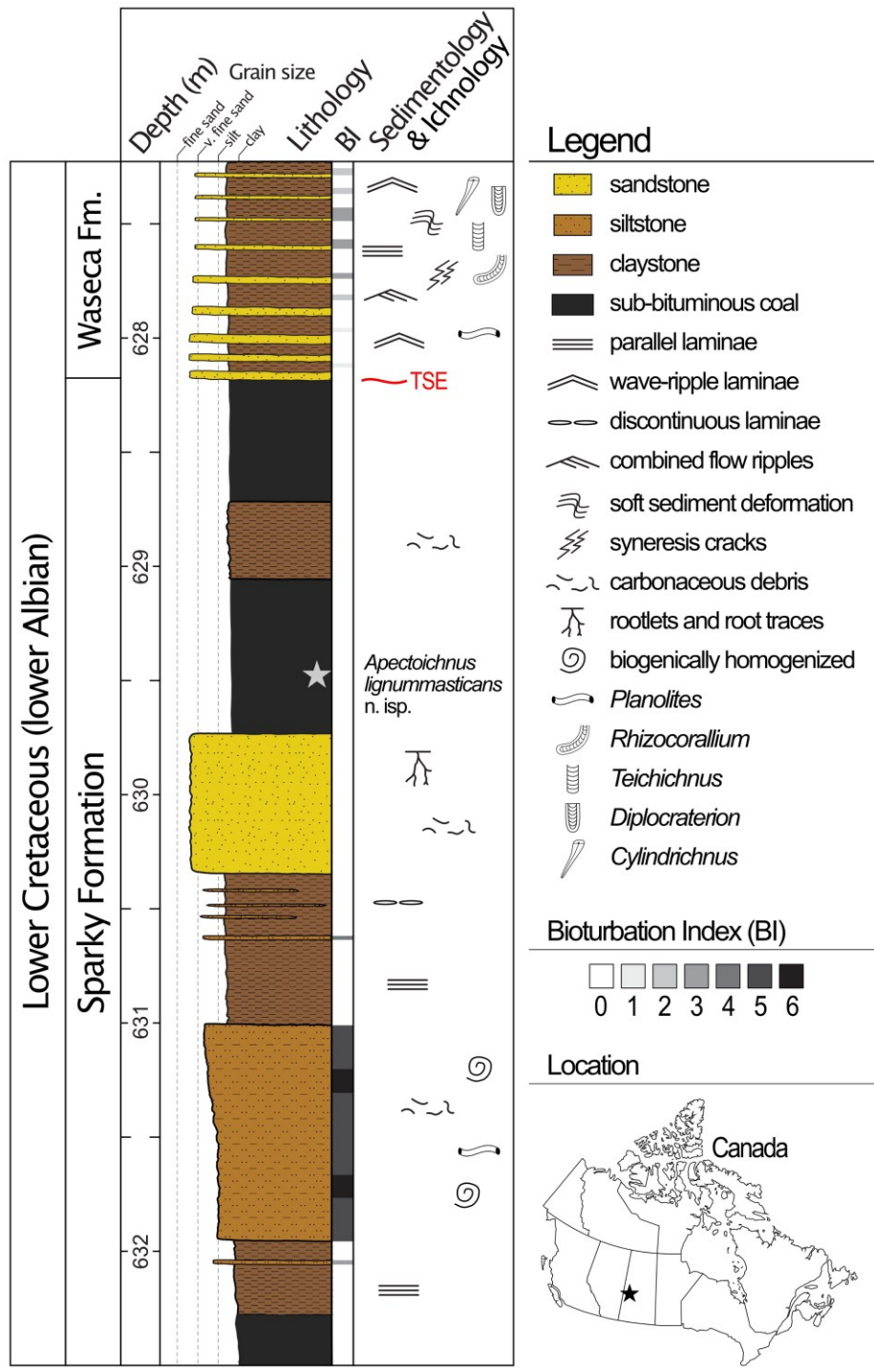


Figure S1.1. Stratigraphic occurrence of the holotype and hypodigm of *Apectoichnus lignumasticans* in west-central Saskatchewan, Canada, from well-bore 16-15-44-20W3M. 52°47'45.0"N, 108°48'55.6"W (NAD83). Other ichnotaxa: *Planolites* Nicholson, 1873, *Rhizocorallium* Zenker, 1836, *Teichichnus* Seilacher, 1955, *Diplocraterion* Torell, 1870, *Cylindrichnus* Toots in Howard, 1966. TSE = transgressive surface of erosion.

trace fossils occur within the Lower Cretaceous Mannville Group (Sparky Formation) and in association with a transgressive surface of marine erosion. The specimens are currently housed in the Ichnology Research Group Trace Fossil Collection in the Department of Earth and Atmospheric Sciences, University of Alberta (UAI), Alberta, Canada.

S1.3.2 Computed Tomography

Computed Tomography (CT) is a non-destructive method whereby X-rays are directed through a rotating sample. X-ray attenuation that occurs at each angle is recorded and used for tomographic reconstruction (see Wildenschild and Sheppard, 2013 for detailed discussion). Previous studies have used similar techniques quite effectively in analyzing various bioerosion features (e.g., Beuck et al., 2007, 2008; Tapanila, 2008; Schönberg and Shields, 2008). Computed Tomography scanning is particularly suitable for substrates with empty borings due to the low attenuation of the tunnels relative to the substrate. This results in images with burrows that are easy to visualize and can be analyzed spatially across multiple dimensions. Although the specimens cannot be viewed directly in full relief, Micro-CT imaging allows observation of additional detail, trace morphology, and overall trace length.

Scanning was performed on a Skyscan 1172 Micro-CT. The x-ray source was set to 92 kV, and 106 μ A and an Al+Cu filter was used to mitigate beam hardening. Data acquisition occurred at a resolution of 17 μ m, with images taken at 0.5° increments over a 180° rotation. Tomographic reconstruction was performed using ©NRecon software, which includes procedures to reduce ring and beam hardening artifacts, which are the most prominent noise features when CT-scanning (Ketcham

and Carlson, 2001). Reconstructed scans were rendered and analyzed using ©CTvox software (Figure S1.3).

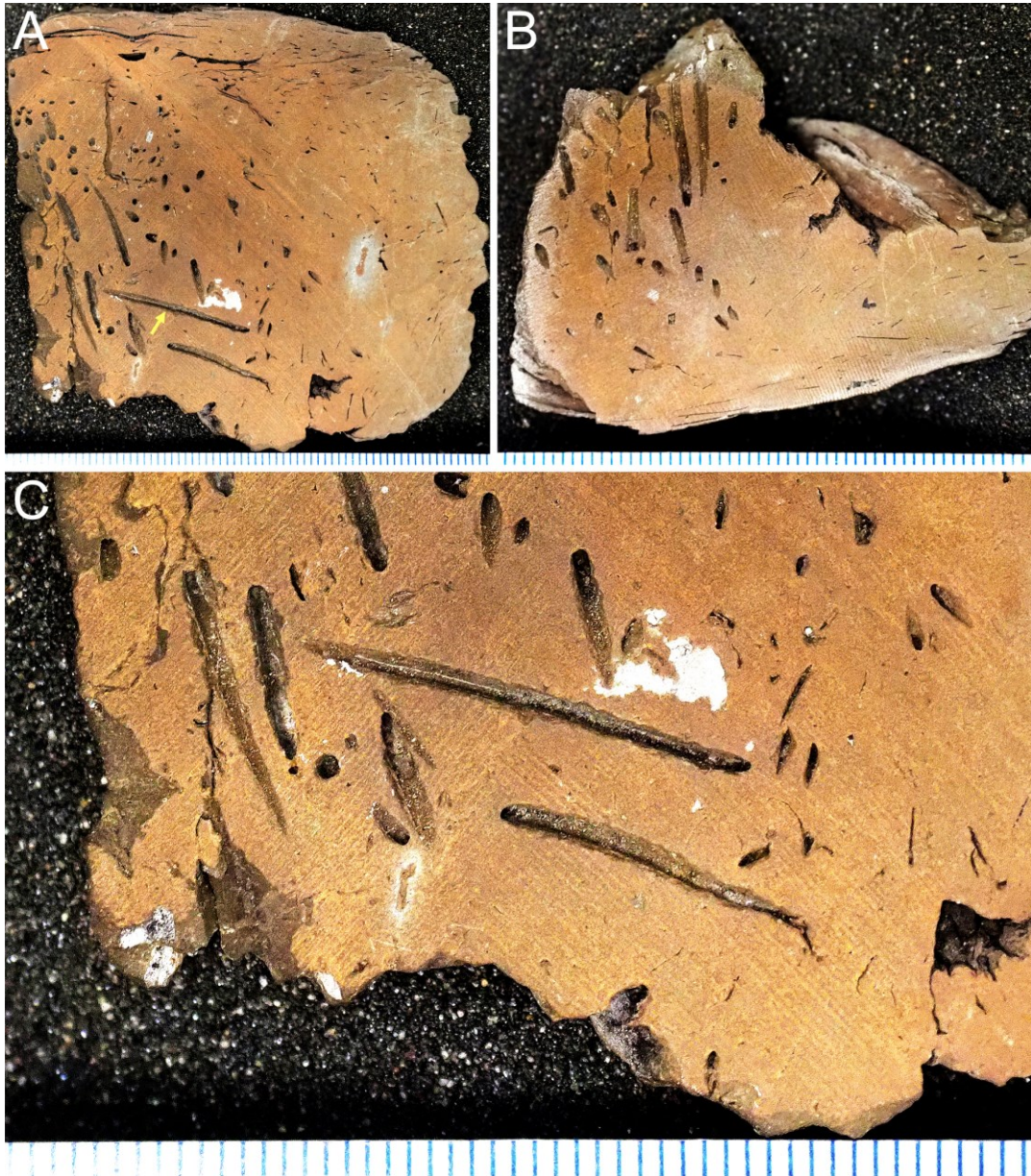


Figure S1.2. *Apectoichnus lignumasticans* assemblage in fossil wood. Scale bars show 1 mm divisions. (A) Sample UAI079 (the arrow indicates the holotype). (B) Sample UAI080. (C) Close-up photograph of UAI079 showing the holotype and surrounding forms.

S1.3.3 Institutional Abbreviations

Specimens examined in this study are housed in the Ichnology Research Group Trace Fossil Collection in the Department of Earth and Atmospheric Sciences, University of Alberta (UAI), Alberta, Canada. BM(NH) = The Natural History Museum, London.

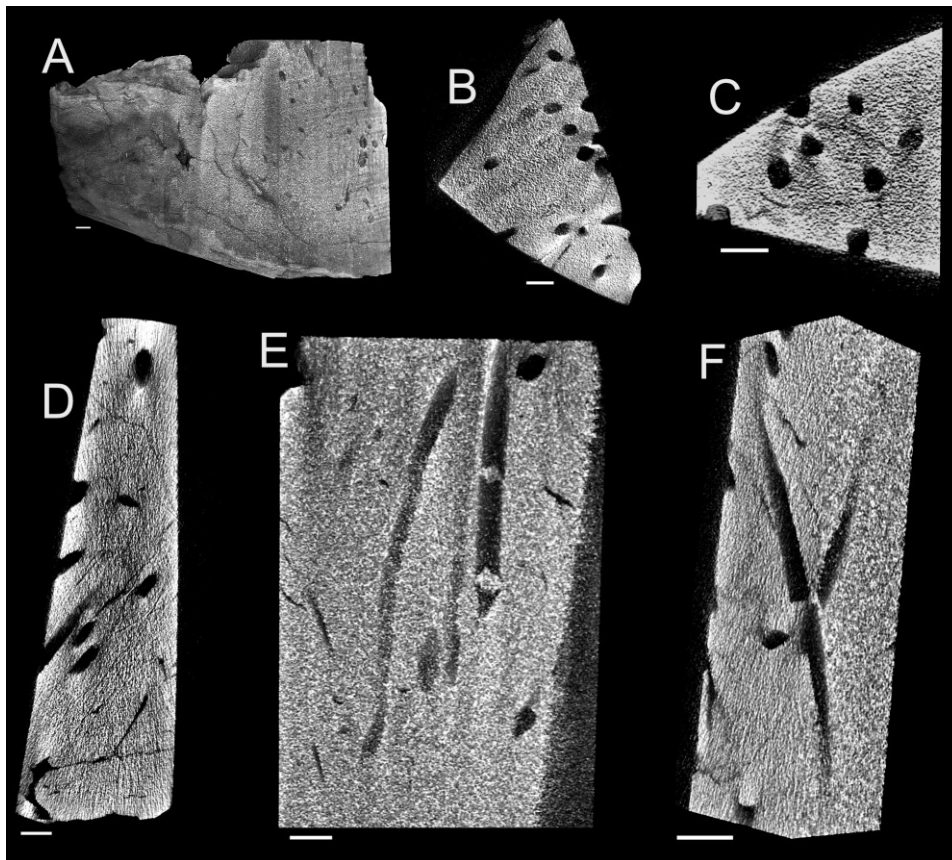


Figure S1.3. Micro-CT images of UAI080. (A) Overview of the scanned specimen. (B, C) Aligned tunnels displaying circular cross sections. (D) Oblique expression of the tunnels. (E) Longitudinal view of the tunnels showing an approximately constant diameter. (F) Three randomly oriented and closely spaced tunnels that do not interpenetrate. Scale bars = 2 mm.

S1.4 Systematic Ichnology

Borehole excavation in different substrates requires different behaviours and abilities (e.g., Dorgan, 2015). Thus, although ichnotaxa differ markedly from biological taxa, no paleontological, paleoecological or taphonomic goal is achieved by lumping together traces excavated in lithic, osteic and xylic substrates. This view was contested by Donovan and Ewin (2018), who considered *Teredolites clavatus* (xylic substrate) and *Gastrochaenolites turbinatus* Kelly and Bromley, 1984 (lithic substrate) to be synonyms because they are morphologically comparable. For the reasons discussed above, we consider substrate to be useful in taxonomic differentiation and advocate to retain both ichnotaxa (see also Zonneveld et al., 2015; Wisshak et al., 2019).

Ichnogenus *Apectoichnus* Donovan, 2018

Type ichnospecies. -- *Apectoichnus longissimus* Kelly and Bromley, 1984.

Emended Diagnosis. -- Elongate borings in xylic substrates and associated resins, nearly circular in cross-section, with an approximately constant diameter. Borings are straight to sinuous or contorted and intertwined and predominantly occur parallel to the fibres of xylic substrates (modified from Donovan, 2018; Mayoral et al., 2020).

Emended Diagnosis. -- Elongate borings in xylic substrates and associated resins, nearly circular in cross-section, with an approximately constant diameter.

Borings are straight to sinuous or contorted and intertwined and predominantly occur parallel to the fibres of xylic substrates (modified from Donovan, 2018; Mayoral et al., 2020).

Remarks.—Kelly and Bromley (1984) proposed *longissimus* as a new ichnospecies of *Teredolites* commonly associated with boring bivalves. This combination was recently challenged by Donovan (2018) who proposed the ichnogenus *Apectoichnus* to describe wood borings that lack the clavate morphology of *Teredolites clavatus*. Donovan (2018) retained the species-level taxonomy of *A. longissimus* and thus, prior to the present work, *Apectoichnus* has been a monospecific ichnogenus. Subsequent contributions have validated the ichnotaxon *Apectoichnus* (e.g., Donovan and Ewin, 2018; Donovan and Portell, 2019; Wisshak et al., 2019). Mayoral et al. (2020) revised the diagnosis of *Apectoichnus* to include amber and other solid resins as possible host substrates. We further emend the genus-level diagnosis to recognize that the trace fossils are generally aligned wood fibre-parallel, which was previously considered diagnostic at the ichnospecies level (Mayoral et al., 2020).

Apectoichnus longissimus (Kelly and Bromley, 1984)

Holotype.—BM(NH) Bensted Collection 38019, Kentish Rag, Lower Cretaceous (Aptian), Hythe, Kent, England (Kelly and Bromley, 1984, Figs. 9B, 11A–B).

Emended Diagnosis.—*Apectoichnus* with a large (>2 mm) diameter and relatively small length-to-width ratio.

Remarks.—Previous ichnospecific ichnotaxobases include a length-to-width ratio greater than 5 and the tendency for the borings to align parallel to the wood fibres (see Mayoral et al., 2020). These characteristics are observed in the non-molluscan borings examined herein and are therefore considered diagnostic at the ichnogenus level.

Apectoichnus lignummasticans new ichnospecies (Figure S1.2 and Figure S1.3).

Holotype.—UAI0179 (Figure S1.2A,C).

Diagnosis.—Straight to gently curved *Apectoichnus* with a small (<2 mm) diameter and relatively large length-to-width ratio, usually greater than 10.

Occurrence.—Lower Cretaceous (early Albian stage) Mannville Group (Sparky Formation), near Bushy Lake, west-central Saskatchewan, Canada (Dominion Land Survey 16-15-44-20W3M; 52°47'45.0"N, 108°48'55.6"W [NAD83]; 630.0 m depth).

Description.—The holotype and associated borings comprise an assemblage of *Apectoichnus lignummasticans* emplaced in fossil wood. The gently curved holotype is displayed in the elevation view of sample UAI0179 (Figure S1.2A,C). It has a preserved length of 22.8 mm, which is the longest of the assemblage, and a diameter of 0.9 mm (length-to-width ratio of ~25). An additional 20 borings were measured. Although the specimens cannot be viewed directly in full relief, Micro-CT imaging allows observation of additional detail, trace morphology, and overall trace length

(Figure S1.3). The preserved lengths vary considerably, averaging about 12 mm. The assemblage displays a range in diameters from 0.4 to 1.2 mm (mean = 0.9 mm, N = 21). The length-to-width ratio ranges from 7 to 38 (mean = 15, N = 21); seventeen of the ratios are between 10 and 25.

Etymology. --From the Latin *lignum masticando* ("wood chew").

Remarks. --Although size alone is not normally an ichnotaxonomic character, the small diameters of *A. lignummasticans* paired with large length to width ratios make it readily discernible from *A. longissimus*. The small diameters and the large length-to-width ratios of *Apectoichnus lignummasticans* are not ascribable to the teredinid bivalves that make *A. longissimus*. The absence of radial bioglyphs that are sometimes associated with teredinid borings, and the lack of space available for a calcareous boring linings or anterior caps further suggest a non-bivalve trace maker. The morphology of the structure is more consistent with mobile wood-boring marine arthropods (e.g., isopods, discussed below).

S1.5 Discussion

Above we ascribe the occurrence of *Apectoichnus lignummasticans* to marine and marginal-marine animals, and this is owing to its similarity to borings made by the extant limnoiid isopod genus *Limnoria* Rathke, 1799 (Figure S1.4). Nevertheless, it is worth emphasizing that *A. lignummasticans* is morphologically different from terrestrial wood-boring ichnofossils (*cf.* Table S1.1) The most common wood-boring species of *Limnoria* are *L. lignorum* Rathke, 1799; *L. tripunctata* Menzies, 1951; and *L.*

quadripunctata Holthuis, 1949 (e.g., Menzies and Turner, 1957; Jones, 1963; Borges et al., 2014). *Limnoria lignorum* has a particularly widespread distribution due to its broad environmental tolerance (Borges et al., 2014). Environmental factors such as temperature, salinity and oxygen are directly related to the survival, distribution and boring activity (*i.e.*, egestion rate) of *Limnoria*; however, the most important constraint is the presence of an adequate food supply (*i.e.* wood) (Menzies, 1957). Mortality rates of *Limnoria* increase rapidly from 10 to 20°C, but boring activity is optimized in warmer water temperatures (20°C) and is significantly reduced below 10°C (Menzies, 1957; Eltringham, 1965). The limiting salinity for boring activity varies inversely with water temperature and ceases altogether in salinities below 10 ppt (Eltringham, 1961); the optimal salinity at 20°C ranges from 30–34 ppt (Borges et al., 2009). The amount of boring activity may also be directly related to dissolved oxygen content and is significantly reduced at levels below 3.0 ppm (Anderson and Reish, 1967).

The presence of bored woodgrounds in the rock record is associated with transgressive coastal settings (Panos and Skacel, 1966; Bromley et al., 1984; Savrda, 1991; Shanley et al., 1992; Savrda et al., 1993; Gingras et al., 2004). Indeed, the colonization of *in situ* woodgrounds by marginal marine and marine organisms requires a rise in relative sea level (e.g., Gingras, et al., 2004). Importantly, *Limnoria* can survive for approximately 24 hours without water and thus commonly inhabits the intertidal zone (Menzies, 1957); populations are generally highest at low tide level where log-ground and woodground substrates are readily available.

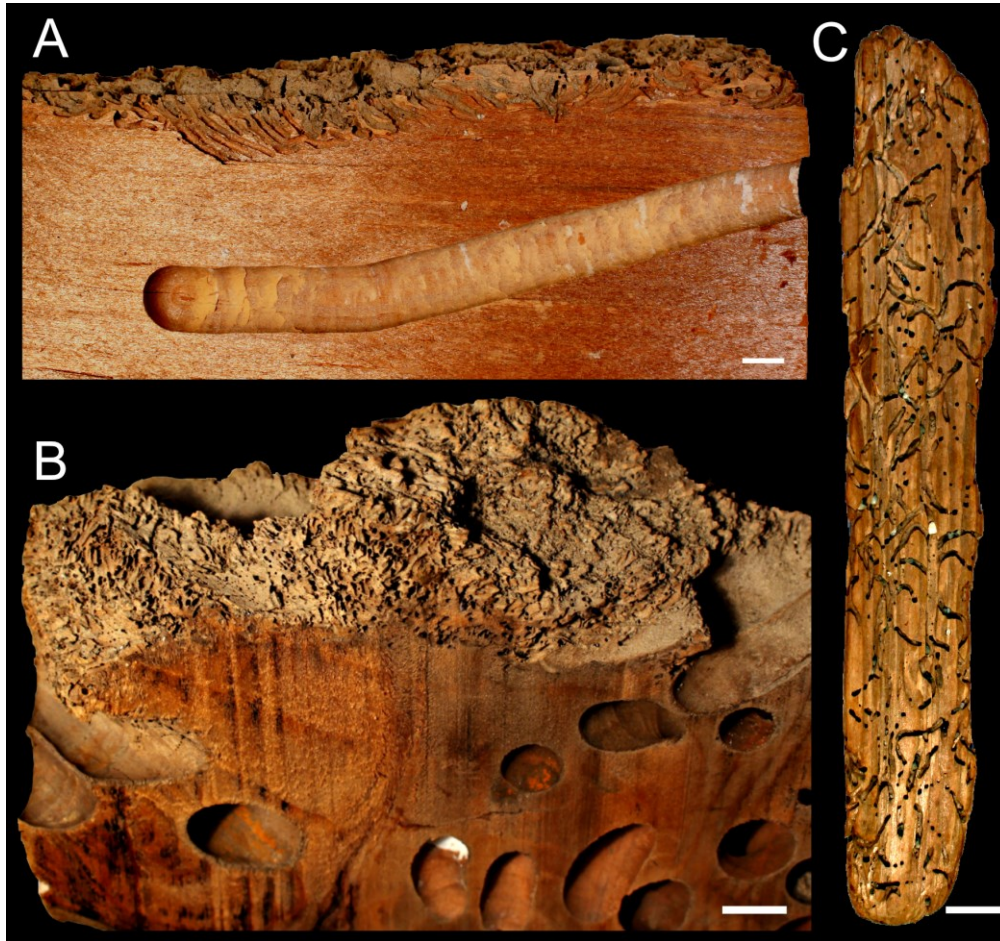


Figure S1.4. Extant *Limnoria lignorum* borings. Scale bars = 1 cm. (A, B) Teredinid-bored wood with *L. lignorum* borings on the exterior. Note that the borings generally follow the grain of the wood. (C) Example of branching *L. lignorum* borings.

Table S1.1. Summary of formally recognized woodground ichnospecies.

Ichnospecies	Inferred tracemaker	Diagnosis/description
Continental woodground ichnospecies		
<i>Anobichnium simile</i> Linck, 1949*	Family Ptinidae	1-1.5 mm wide, smooth cylindrical tunnels with a circular cross section.
<i>Asthenopodichnium xylobiontum</i> Thenius, 1979*	Family Gammeridea (scud) ¹	U-shaped spreiten or pouch-like tunnels with a 1.5-3 mm diameter; aligned perpendicular to the substrate and penetrate up to 20 mm into the wood.
<i>Asthenopodichnium lignorum</i> Genise et al., 2012	Kingdom Fungi	Shallow, elongate, ellipsoidal to almond-shaped scoops; oriented parallel to the wood grain and commonly occurring in clusters.
<i>Cycalichnus garciorum</i> Genise, 1995*	Family Kalotermitidae (drywood termite)	Boxwork of anastomosed longitudinal borings; interconnected by short tangential tunnels; lacks an outer layer but is filled with hexagonal fecal pellets.
<i>Linckichnus terebrans</i> Schlirf, 2006*	Class Insecta	2-4 mm wide, smooth, unbranched, slightly kink-bent, cylindrical borings with a circular cross section and hemispherical terminations; aligned perpendicular to the wood grain; fill massive.
<i>Paleobuprestis maxima</i> Walker, 1938*	Family Buprestidae (jewel beetle)	10 mm wide channels occurring just under the bark and aligned perpendicular to the wood grain; cuttings are visible the borings are filled with castings.
<i>Paleobuprestis minima</i> Walker, 1938	Family Buprestidae (jewel beetle)	2 mm wide channels aligned perpendicular to the wood grain; variably filled with castings.
<i>Paleobuprestis sudeticus</i> Muszer and Uglik, 2013	Family Buprestidae (jewel beetle)	Straight to gently curved, shallow and narrow, randomly oriented channels with a 2-4 mm diameter; unfilled.
<i>Paleoipidius perforatus</i> Walker, 1938*	Subfamily Scolytinae (bark beetle)	5 mm wide tunnels with a square to rectangular outline and oval cross section with one flat side; penetrate deeply into the wood; unfilled.
<i>Paleoipidius marginatus</i> Walker, 1938	Subfamily Scolytinae (bark beetle)	2-3 mm wide tunnels with an oval cross section; filled with castings.
<i>Paleoscolytus divergus</i> Walker, 1938	Subfamily Scolytinae (bark beetle)	5 mm wide channels occurring just under the bark and lacking a preferred orientation; lacks cuttings and castings.
<i>Pecinolites boreki</i> Mikuláš and Dvořák, 2002*	None	Large, straight to gently curved, tubular borings with a reasonably constant diameter, finger-like terminations and rare branching at 60-90°; unfilled.
<i>Scolytolarvariumichnus sussexensis</i> Jarzembowski, 1990	Subfamily Scolytinae (bark beetle)	1.5 mm wide borings that diverge from a central chamber; apparently filled with cuttings and castings.
<i>Scolytolarvariumichnus radiatus</i> Guo, 1991*	Subfamily Scolytinae (bark beetle)	Subround plate with a longitudinal-cylindrical mater tunnel with foveae on both sides and radiating larval tunnels.
<i>Scolytolarvariumichnus zherikhini</i> Petrov, 2013	Subfamily Scolytinae (bark beetle)	Strongly entangled galleries, at least 13 mm wide, branching from a parent gallery; unfilled.
<i>Stiptichnus koppae</i> Genise, 1995*	<i>Rhina barbirostris</i> (bearded weevil)	Unbranched longitudinal borings with circular cross sections; lack an outer layer and are unfilled.
<i>Xylokrypta durossi</i> Tapanila and Roberts, 2012*	Suborder Archostemata	Kidney-shaped borings with apertures oriented perpendicular to the wood surface.
<i>Xylonichnus trypetus</i> Genise, 1995*	Family Buprestidae (jewel beetle)	Longitudinal borings with a rectangular cross section and rounded corners (H:W = 1:4); interconnected by tangential tunnels; have an outer layer and are filled with frass, or has meniscus structure.
<i>Xylonichnus meniscatus</i> Genise and Hazeldine, 1995	Family Cerambycidae (longhorn beetle)	Longitudinal borings with an oval cross section and a H:W of 1:3; interconnected by tangential tunnels, with radial tunnels of different sizes connecting it to the exterior; contains frass that is sometimes packed in backfill meniscae.
<i>Ipites bobrowskianus</i> Karpinski, 1962	Genus <i>Ips</i> (bark beetle: engraver beetle)	Regularly branched borings with a larger central tunnel and smaller radiating tunnels; aligned parallel to the substrate.
Marine woodground ichnospecies		
<i>Apctoichnus longissimus</i> * Kelly and Bromley, 1984	Family Teredinidae (shipworm)	Elongate, curved to contorted borings with a circular cross-section and relatively constant diameter.
<i>Apctoichnus lignumasticans</i> Melnik et al., herein	Family Limnoriidae (gribble)	Small, straight to gently curved borings with a circular cross-section and uniform diameter.
<i>Teredolites clavatus</i> * Leymerie, 1842	Family Pholadidae (piddock)	Clavate borings with a more or less circular cross-section, evenly tapered from aperture to base.

*type ichnospecies; ¹Uchman, 2011.

S1.6 Summary

A new wood-boring ichnospecies is described from transgressive (lagoonal) deposits of the Lower Cretaceous Sparky Formation (Mannville Group) in west-central Saskatchewan, Canada. *Apectoichnus lignummasticans* isp. nov. is a trace fossil that occurs in a thin coal bed and which was emplaced in an *in situ* xylic substrate (woodground). The ichnofossil is thin, elongate, unbranched, and straight to gently curved with a circular cross section and uniform diameter. *Apectoichnus lignummasticans* is similar in many respects to modern borings in wood that are produced by marine isopods, such as *Limnoria lignorum* Rathke, 1799, for feeding and refugium. The recognition of *A. lignummasticans* in the rock record aligns with the modern observation that fossilized wood-boring assemblages should display higher ichnofossil diversities than commonly reported. Additionally, the stratigraphic occurrence of *A. lignummasticans* in association with other evidence of marine deposition reaffirms that certain wood boring morphologies (*i.e.* ichnotaxa) are useful as indicators of marine transgressions.

S1.7 References

- Anderson, J. W., & Reish, D. J. (1967). The effects of varied dissolved oxygen concentrations and temperature on the wood-boring isopod genus *Limnoria*. *Marine Biology*, 1, 56–59.
- Bann, K. L., MacEachern, J. A., & Gingras, M. K. (2004). Early Permian Snapper Point Formation of southeastern Australia. In K. A. Campbell & M. R. Gregory (Eds.), *8th International Ichnofabric Workshop* (pp. 13–15). Auckland, New Zealand.
- Beuck, L., Vertino, A., Stepina, E., Karolczak, M., & Pfannkuche, O. (2007). Skeletal response of *Lophelia pertusa* (Scleractinia) to bioeroding sponge infestation visualised with micro-computed tomography. *Facies*, 53, 157–176.
- Beuck, L., Wisshak, M., Munnecke, A., & Freiwald, A. (2008). A giant boring in a Silurian stromatoporoid analysed by computer tomography. *Acta Palaeontologica Polonica*, 53, 149–160.
- Borges, L. M. S., Cragg, S. M., & Busch, S. (2009). A laboratory assay for measuring feeding and mortality of the marine wood borer *Limnoria* under forced feeding conditions: A basis for a standard test method. *International Biodeterioration & Biodegradation*, 63, 289–296.
- Borges, Luísa M. S., Merckelbach, L. M., & Cragg, S. M. (2014). Biogeography of wood-boring crustaceans (Isopoda: Limnoriidae) established in European coastal waters. *PLoS ONE*, 9, e109593.
- Bromley, R. G., Pemberton, S. G., & Rahmani, R. A. (1984). A Cretaceous woodground: The *Teredolites* ichnofacies. *Journal of Paleontology*, 58, 488–498.
- Donovan, S. K. (2018). A new ichnogenus for *Teredolites longissimus* Kelly and

- Bromley. *Swiss Journal of Palaeontology*, 137, 95–98.
- Donovan, S. K., & Ewin, T. A. M. (2018). Substrate is a poor ichnotaxobase: A new demonstration. *Swiss Journal of Palaeontology*, 137, 103–107.
- Donovan, S. K., & Portell, R. W. (2019). Invertebrate borings from the Eocene of Seven Rivers, parish of St. James, western Jamaica. *Swiss Journal of Palaeontology*, 138, 277–283.
- Dorgan, K. M. (2015). The biomechanics of burrowing and boring. *Journal of Experimental Biology*, 218, 176–183.
- Eltringham, S. K. (1965). The effect of temperature upon the boring activity and survival of *Limnoria* (Isopoda). *Journal of Applied Ecology*, 2, 149–157.
- Genise, J. F. (1995). Upper Cretaceous trace fossils in permineralized plant remains from Patagonia, Argentina. *Ichnos*, 3, 287–299.
- Genise, J. F., & Hazeldine, P. L. (1995). A new insect trace fossil in Jurassic wood from Patagonia, Argentina. *Ichnos*, 4, 1–5.
- Genise, Jorge. F., Garrouste, R., Nel, P., Grandcolas, P., Maurizot, P., Cluzel, D., ... Nel, A. (2012). *Asthenopodichnium* in fossil wood: Different trace makers as indicators of different terrestrial palaeoenvironments. *Palaeogeography, Palaeoclimatology, Palaeoecology*, 365–366, 184–191.
- Gingras, M. K., MacEachern, J. A., & Pickerill, R. K. (2004). Modern perspectives on the *Teredolites* ichnofacies: Observations from Willapa Bay, Washington. *Palaios*, 79–88, 10.
- Guo, S. (1991). A Miocene trace fossil of insect from Shanwang Formation in Linqu, Shandong. *Acta Palaeontologica Sinica*, 30, 739–742.
- Holthuis, L. B. (1949). The Isopoda and Tanaidacea of the Netherlands, including the description of a new species of *Limnoria*. *Zoologische Mededelingen*

- Reiksmuseum Van Natuurlijke Historie Te Leiden, 30, 163–190.*
- Jarzewowski, E. A. (1990). A boring beetle from the Wealden Sea of the Weald. In J. Boucot (Ed.), *Evolutionary paleobiology of behaviour and coevolution* (pp. 373–376). Elsevier, Amsterdam.
- Jones, L. T. (1963). The geographical and vertical distribution of British *Limnoria* [Crustacea: Isopoda]. *Journal of the Marine Biological Association of the United Kingdom, 43, 589–603.*
- Karpiński, J. J. (1962). Cast of the brood galleries of fossil beetle of the Scolytidae family from Oligocene/Miocene Sandstone at Osieczów (Lower Silesia). *Prace Instytut Geologiczny, 30, 237–239.*
- Kelly, S. R., & Bromley, R. G. (1984). Ichnological nomenclature of clavate borings. *Palaeontology, 27, 793–807.*
- Ketcham, R. A., & Carlson, W. D. (2001). Acquisition, optimization and interpretation of X-ray computed tomographic imagery: Applications to the geosciences. *Computers & Geosciences, 27, 381–400.*
- Kiteley, L. W., & Field, M. E. (1984). Shallow marine depositional environments in the Upper Cretaceous of northern Colorado. In R. W. Tillman & C. T. Siemers (Eds.), *Siliciclastic Shelf Sediments* (pp. 179–204). Society of Economic Paleontologists and Mineralogists Special Publication 34.
- Leymerie, A. (1842). Suite de mémoire sur le terrain Crétacé du département de l'Albe. *Mémoires de La Société Géologique de France 1(Série 4), 1–34.*
- Linck, O. (1949). Fossile Bohrgänge (*Anobichnium simile* n.g. N.sp.) an einen Keuperholz. *Neues Jahrbuch Für Mineralogie, Geognosie, Geologie Und Petrefaktenkunde, 180–185.*
- Mayoral, E., Santos, A., Vintaned, J. A. G., Wisshak, M., Neumann, C., Uchman, A., & Nel,

- A. (2020). Bivalve bioerosion in Cretaceous-Neogene amber around the globe, with implications for the ichnogenera *Teredolites* and *Apectoichnus*. *Palaeogeography, Palaeoclimatology, Palaeoecology*, 538, 109410.
- Menzies, R. J. (1951). A new species of *Limnoria* (Crustacea: Isopoda) from southern California. *Bulletin of the Southern California Academy of Sciences*, 50, 86–88.
- Menzies, R. J. (1957). The marine borer family Limnoriidae (Crustacea, Isopoda). Part I: Northern and central North America: Systematics, distribution, and ecology. *Bulletin of Marine Science of the Gulf and Caribbean*, 7, 101–200.
- Menzies, R. J., & Turner, R. (1957). The distribution and importance of marine wood borers in the United States. In *Symposium on Wood for Marine Use and Its Protection from Marine Organisms* (pp. 3-3–19). Philadelphia: American Society for Testing Materials.
- Mikuláš, R., Pek, I., & Zimák, J. (1995). *Teredolites clavatus* from the Cenomanian near Maletín (Bohemian Cretaceous Basin), Moravia, Czech Republic. *Věstník Českého Geologického Ústavu*, 70, 51–58.
- Mikuláš, R., Radek, & Dvorák, Z. (2002). Borings in xylic tissues of the tree fern *Tempskya* in the Bohemian Cretaceous Basin, Czech Republic. *Zprávy o Geologických Výzkumech*, 36, 129–131.
- Morshedian, A., MacEachern, J. A., & Dashtgard, S. E. (2012). Stratigraphic framework for the Lower Cretaceous Upper Mannville Group (Sparky, Waseca, and McLaren alloformations) in the Lloydminster area, west-central Saskatchewan. In *Summary of Investigations 2011* (Vol. 1, p. 17). Saskatchewan Geological Survey, Sask. Ministry of Resources.
- Muszer, J., & Uglik, M. (2013). Palaeoenvironmental reconstruction of the Upper Viséan Paprotnia Beds (Bardo Unit, Polish Sudetes) deposition on the

- ichnological and palaeontological investigations. *Geological Quarterly*, *57*, 365–384.
- Panos, V., & Skacel, J. (1966). Zur Frage der Entstehung der Steinsaeulen 'Pobitite Kameni' und anderer eigenartiger Formen zwischen Varna und Beloslav in Nordost-Bulgarien. *Zeitschrift Für Geomorphologie*, *10*, 105–118.
- Petrov, A. V. (2013). New ichnotaxon *Megascolytinus zherikhini* (Coleoptera: Curculionidae: Scolytinae) from Upper Cretaceous deposits of Mongolia. *Paleontological Journal*, *47*, 597–600.
- Pickerill, R. K., Donovan, S. K., & Portell, R. W. (2003). *Teredolites longissimus* Kelly & Bromley from the Miocene Grand Bay Formation of Carriacou, the Grenadines, Lesser Antilles. *Scripta Geologica*, *125*, 1–9.
- Pirrie, D., Marshall, J. D., & Crame, J. A. (1998). Marine high Mg calcite cements in *Teredolites*-bored fossil wood; evidence for cool paleoclimates in the Eocene La Meseta Formation, Seymour Island, Antarctica. *Palaios*, *13*, 276.
- Plint, A. G., & Pickerill, R. K. (1985). Non-marine *Teredolites* from the Middle Eocene of southern England. *Lethaia*, *18*, 341–347.
- Rathke, J. (1799). Observations concerning the natural history of helminths and molluscs. *Skrivter Af Naturhist-Selskabet (København)*, *5*, 61–148.
- Savrda, C. E. (1991). *Teredolites*, wood substrates, and sea-level dynamics. *Geology*, *19*, 905–908.
- Savrda, C. E., & King, D. T. (1993). Log-ground and *Teredolites* lagerstätte in a Transgressive Sequence, Upper Cretaceous (Lower Campanian) Mooreville Chalk, central Alabama. *Ichnos*, *3*, 69–77.
- Savrda, C. E., Ozalas, K., Demko, T. H., Huchison, R. A., & Scheiwe, T. D. (1993). Log-Grounds and the Ichnofossil *Teredolites* in Transgressive Deposits of the

- Clayton Formation (Lower Paleocene), Western Alabama. *Palaios*, 8, 311.
- Schlirf, M. (2006). *Linkichnus Terebrans* new ichnogenus et ichnospecies, an insect boring from the Late Triassic of the Germanic Basin, Southern Germany. *Ichnos*, 13, 277–280.
- Schönberg, C. H. L., & Shields, G. (2008). Micro-computed tomography for studies on Entobia: Transparent substrate versus modern technology. In M. Wisshak & L. Tapanila (Eds.), *Current Developments in Bioerosion* (pp. 147–164). Berlin, Heidelberg: Springer.
- Shanley, K. W., McCabe, P. J., & Hettinger, R. D. (1992). Tidal influence in Cretaceous fluvial strata from Utah, USA: A key to sequence stratigraphic interpretation. *Sedimentology*, 39, 905–930.
- Shipway, J. R., Altamia, M. A., Rosenberg, G., Concepcion, G. P., Haygood, M. G., & Distel, D. L. (2019). A rock-boring and rock-ingesting freshwater bivalve (shipworm) from the Philippines. *Proceedings of the Royal Society B: Biological Sciences*, 286, 20190434.
- Tapanila, L. (2008). The medium is the message: Imaging a complex microboring (*Pyrodendrina cupra* igen. n., isp. n.) from the early Paleozoic of Anticosti Island, Canada. In M. Wisshak & L. Tapanila (Eds.), *Current Developments in Bioerosion* (pp. 123–145). Berlin, Heidelberg: Springer Berlin Heidelberg.
- Tapanila, L., & Roberts, E. M. (2012). The earliest evidence of holometabolan insect pupation in conifer wood. *PLoS ONE*, 7, e31668.
- Thenius, E. (1979). Lebensspuren von Ephemeropteren-Larven aus dem Jung-Tertiär des Wiener Beckens. *Annalen Des Naturhistorischen Museums in Wien*, 82, 177–188.
- Uchman, A. (2011). Recent freshwater wood borings from the Vistula River in Poland.

- In M. Carreiro-Silva & S. P. Ávila (Eds.), *7th international bioerosion workshop* (pp. 18–23). Faial Island, Azores.
- Walker, M. V. (1938). Evidence of Triassic insects in the Petrified Forest National Monument, Arizona. *Proceedings of the United States National Museum*, *85*, 137–141.
- Wildenschild, D., & Sheppard, A. P. (2013). X-ray imaging and analysis techniques for quantifying pore-scale structure and processes in subsurface porous medium systems. *Advances in Water Resources*, *51*, 217–246.
- Wisshak, M., Knaust, D., & Bertling, M. (2019). Bioerosion ichnotaxa: Review and annotated list. *Facies*, *65*, 24.
- Zonneveld, J. P., Bartels, W. S., Gunnell, G. F., & McHugh, L. P. (2015). Borings in early Eocene turtle shell from the Wasatch Formation, South Pass, Wyoming. *Journal of Paleontology*, *89*, 802–820.

APPENDIX 2 – SUPPLEMENTAL MATERIAL FOR CHAPTER 6

LITHOLOGY	PHYSICAL STRUCTURES	LITHOLOGIC ACCESSORIES	ICHTHOFOSSILS
breccia	Current Ripples	".,.,." Silt Beds	Rootlets
SAND/SANDSTONE	Climbing Ripples	- - - - Shale Beds	Skolithos
silty sand	Low Angle Bedding	o o o o Pebbles/granule lag	Planolites
shaly sand	Flaser Bedding	▲▲▲▲ Breccia Horizon	Palaeophycus
Sandy silt	Wavy Parallel Bedding	Gl Glauconitic	Gyrolithes
Silt with clay	Biogenically Homogenized	Py Pyrite	Arenicolites
SHALE/MUDSTONE	Graded Bedding	Rip Up Clasts	Fugichnia
Silty shale	Reverse Graded Bedding	Coal Fragments	Cylindrichnus
Sandy shale	Synaeresis Cracks	Wood Fragments	Conichnus
Organic shale	Double Mud Drapes	Grain Striping	Asterosoma
LIMESTONE	Massive Appearance	Carbonaceous Laminae	Thalassinoides
Lost Core	Preserved Ripple Foresets Sand Lamina	Chondrites
	Variably oriented current ripples	- - - - Shale Lamina	Schaubcylindrichnus
	Wavy lamination	Organic detritus	Teichichnus
	Dewatering structure	= = = = Inclined mud drapes	Zoophycos
	Parallel lamination	- - - - Inclined mud lamina	Helminthopsis
	Fault		Scolicia
	Soft Sediment Deformation		
	Parallel lamination		
	Combined flow ripples		

Figure S2.1. Legend of symbols used in figures S2.2 to S2.25.

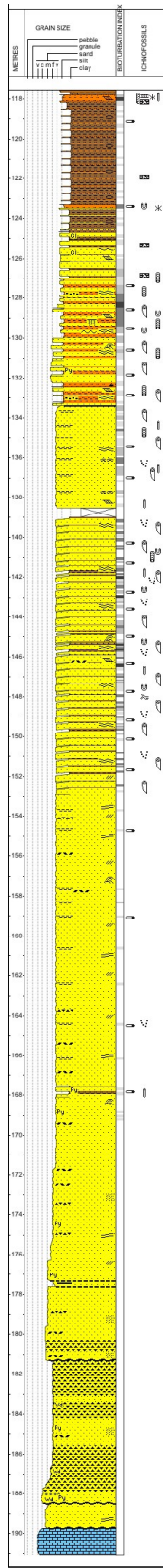


Figure S2.2. Litholog for UWI AA-03-14-092-08W4.

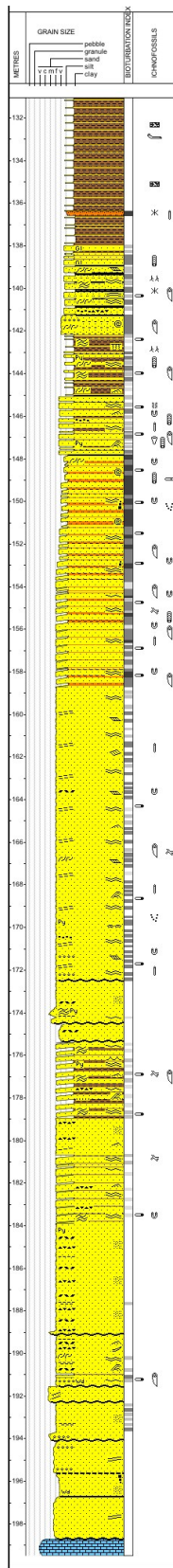


Figure S2.3. Litholog for UWI AA-03-25-092-08W4.

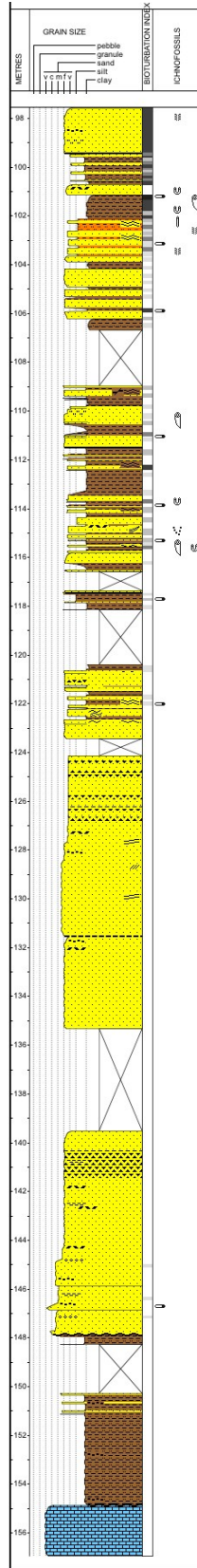


Figure S2.4. Litholog for UWI AA-04-06-092-08W4.

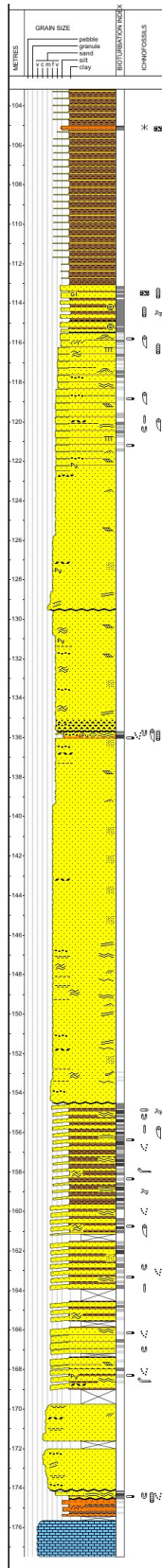


Figure S2.5. Litholog for UWI AA-04-34-092-08W4.

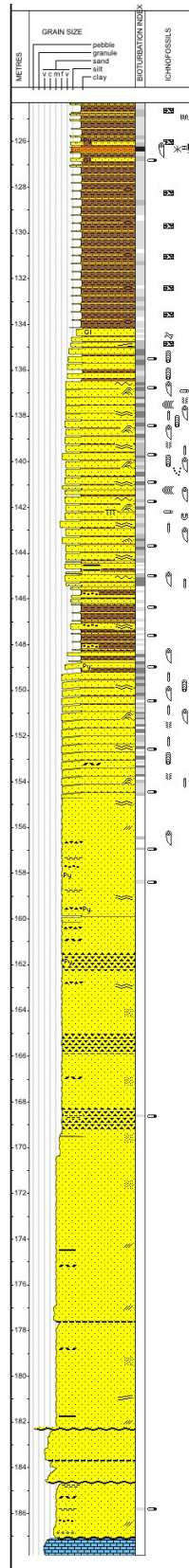


Figure S2.6. Litholog for UWI AA-05-13-092-08W4.

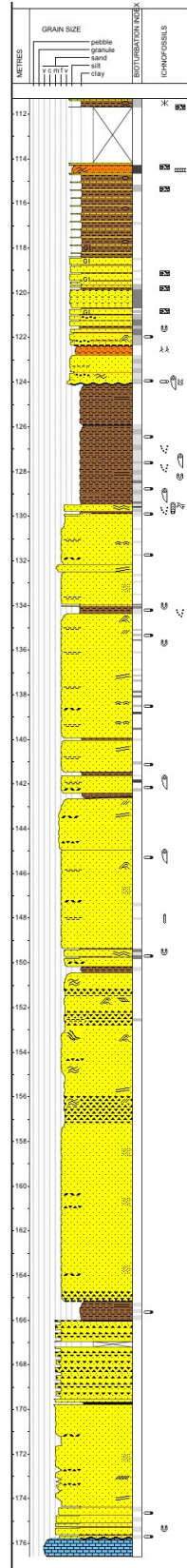


Figure S2.7. Litholog for UWI AA-06-10-092-08W4.

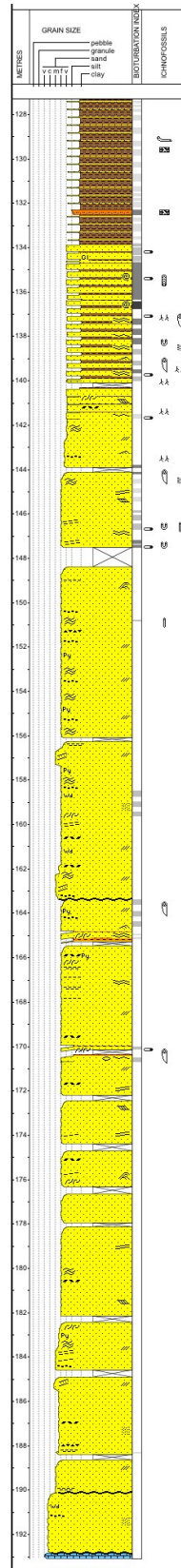


Figure S2.8. Litholog for UWI AA-07-24-092-08W4.

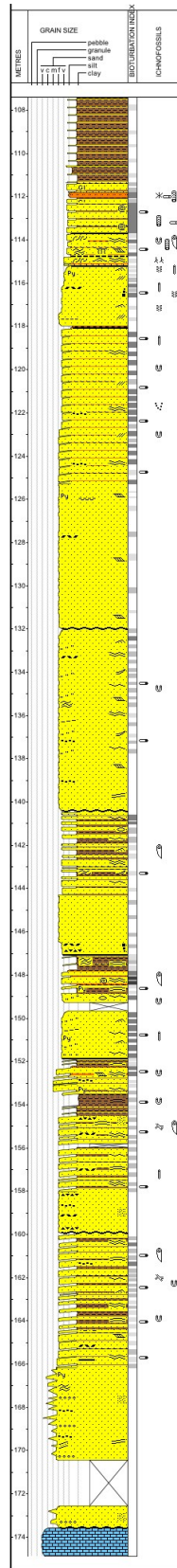


Figure S2.9. Litholog for UWI AA-07-27-092-08W4.

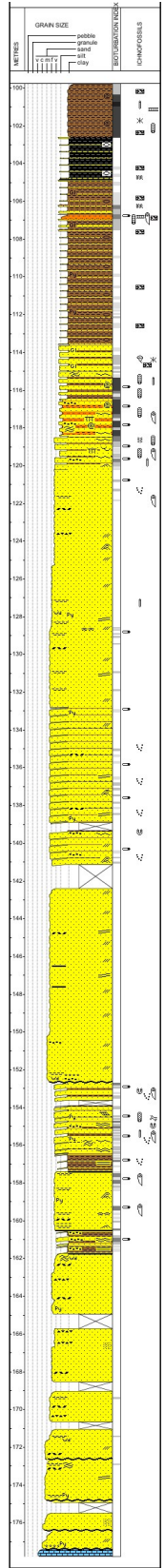


Figure S2.10. Litholog for UWI AA-10-15-092-08W4.

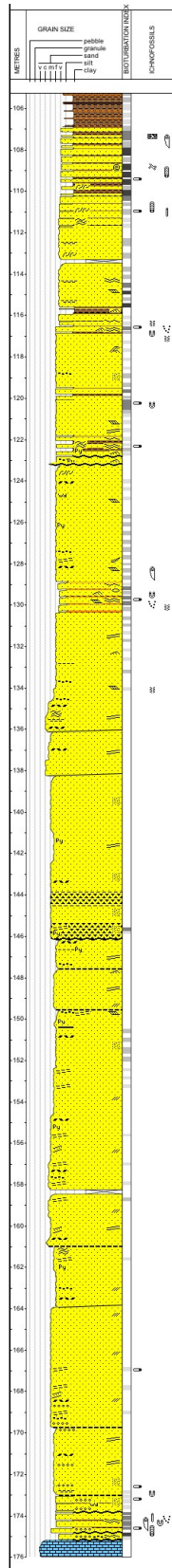


Figure S2.11. Litholog for UWI AA-10-22-092-08W4.

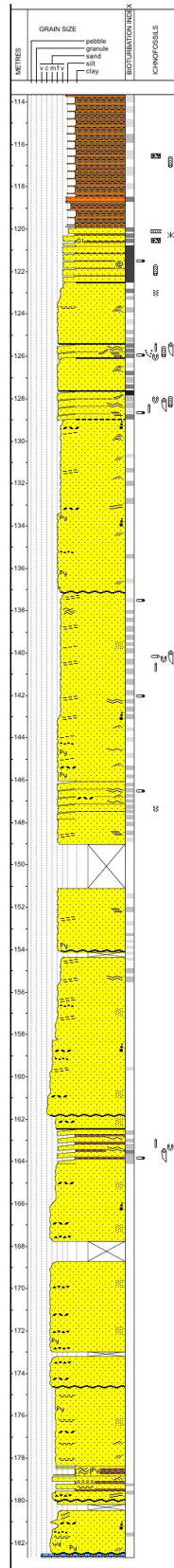


Figure S2.12. Litholog for UWI AA-10-23-092-08W4.

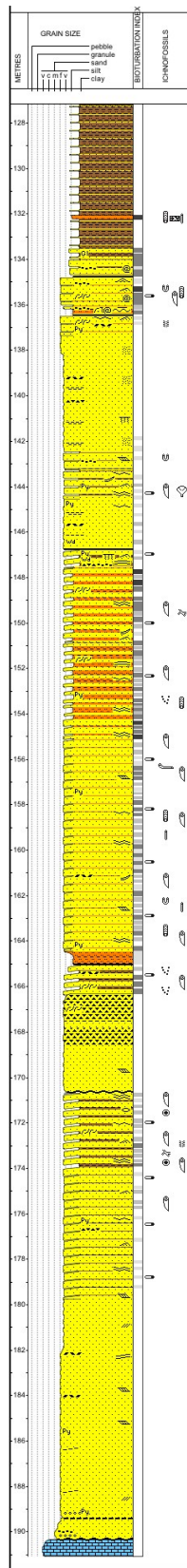


Figure S2.13. Litholog for UWI AA-10-35-092-8W4.

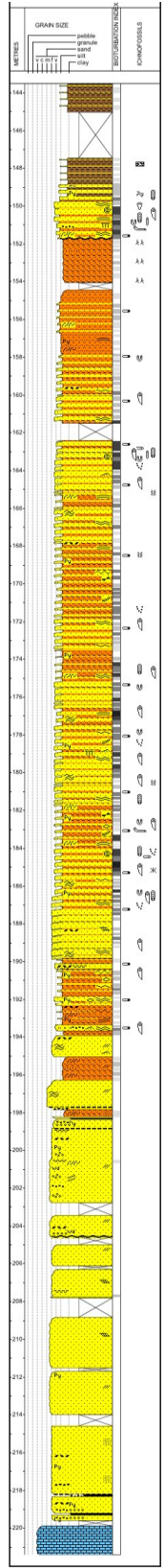


Figure S2.14. Litholog for UWI AA-10-36-092-08W4.

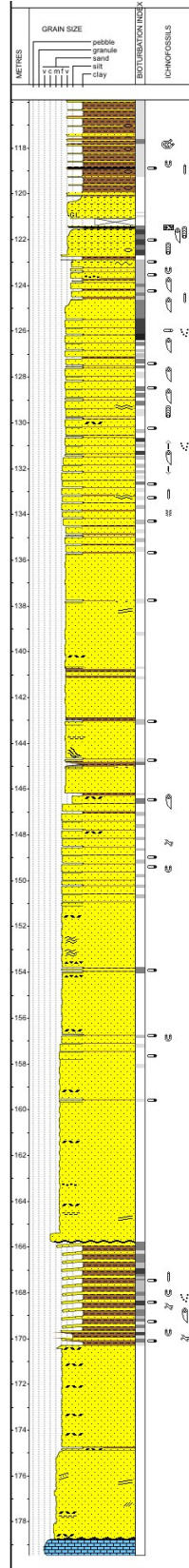


Figure S2.15. Litholog for UWI AA-11-03-092-08W4.

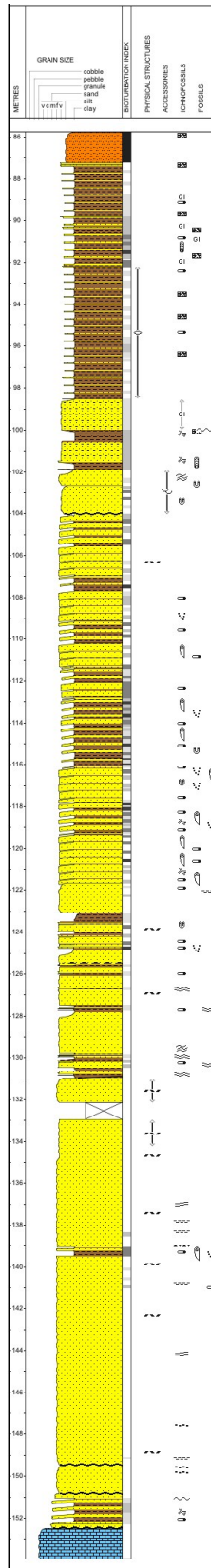


Figure S2.16. Litholog for UWI AA-11-04-092-08W4.

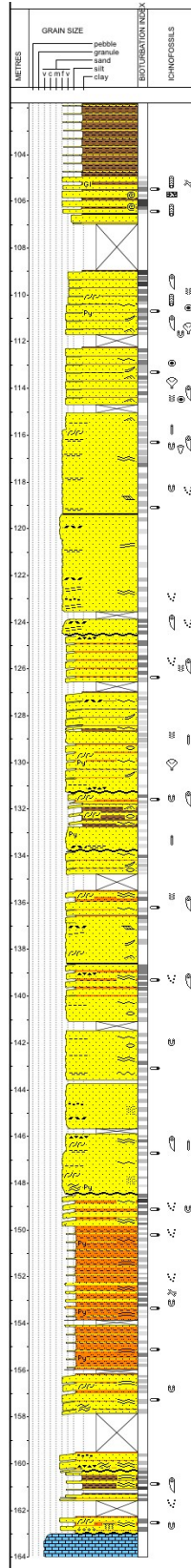


Figure S2.17. Litholog for UWI AA-11-33-092-08W4.

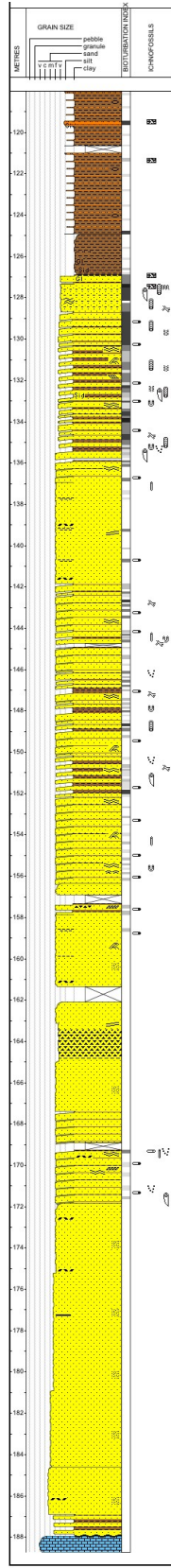


Figure S2.18. Litholog for UWI AA-12-11-092-08W4.

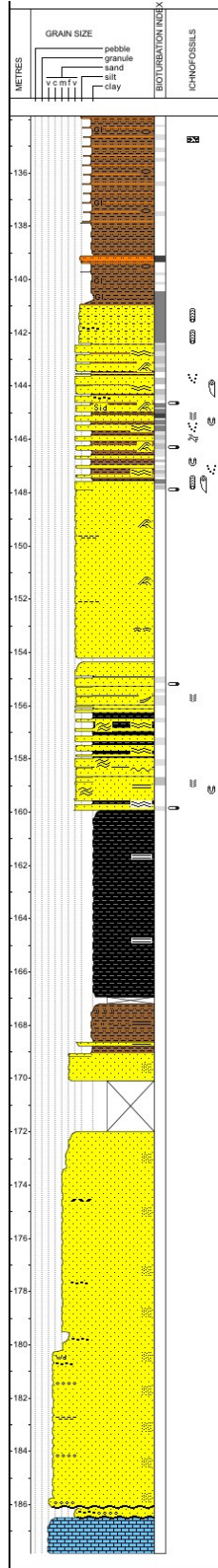


Figure S2.19. Litholog for UWI AA-12-12-092-08W4.

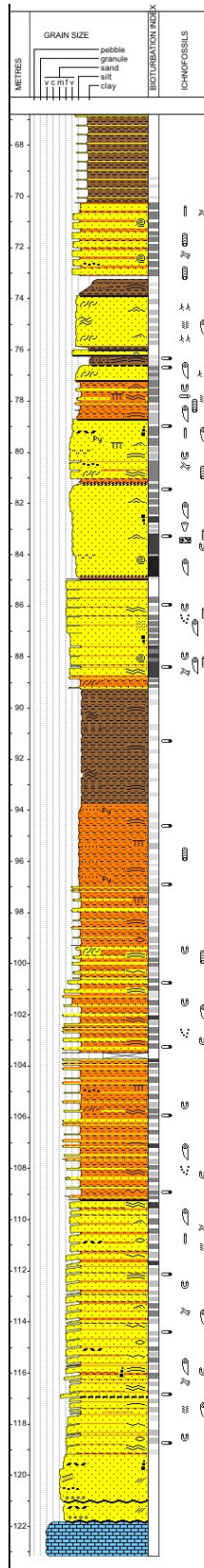


Figure S2.20. Litholog for UWI AA-12-30-092-08W4.

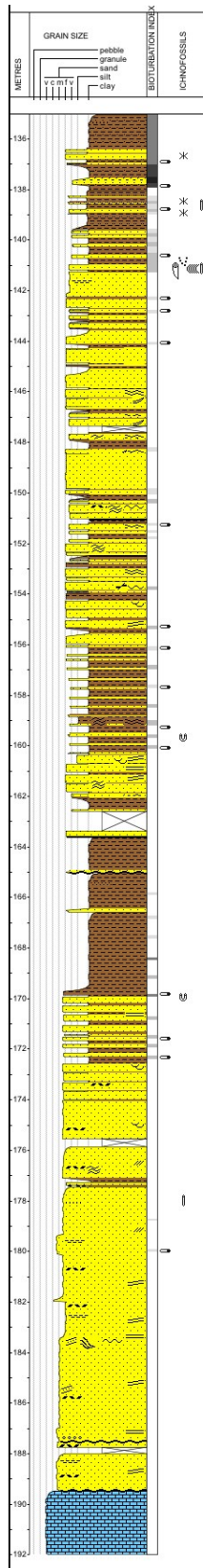


Figure S2.21. Litholog for UWI AA-13-02-092-08W4.

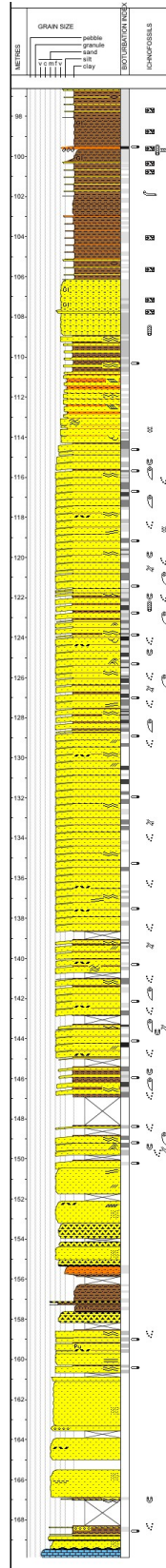


Figure S2.22. Litholog for UWI AA-15-09-092-08W4.

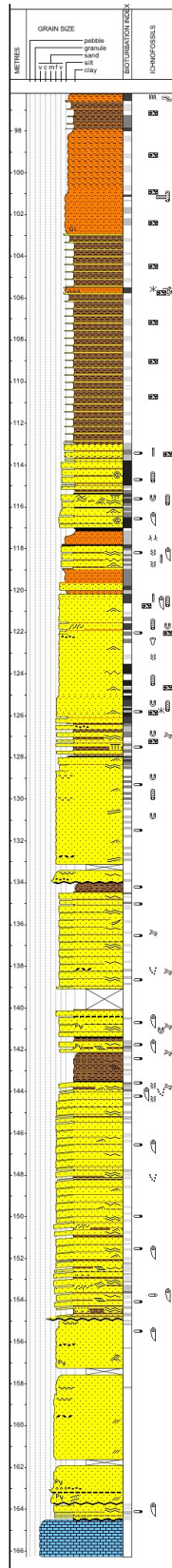


Figure S2.23. Litholog for UWI AA-16-16-092-08W4.

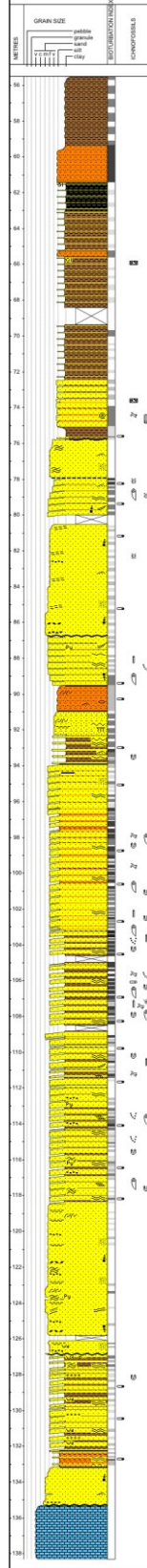


Figure S2.24. Litholog for UWI AA-16-19-092-08W4.

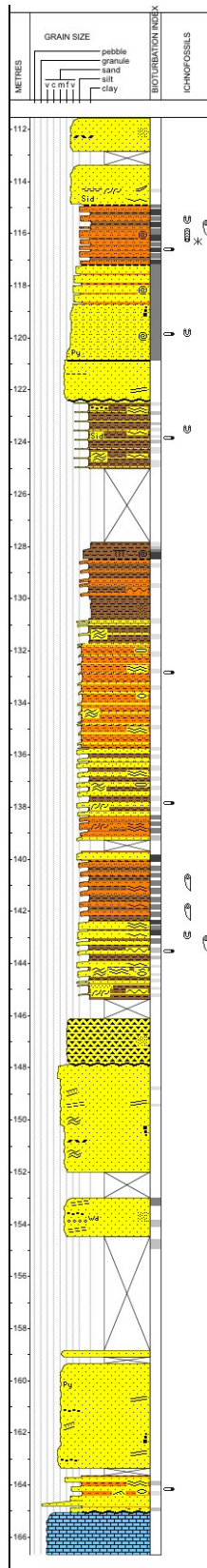


Figure S2.25. Litholog for UWI AA-16-21-092-08W4.